10.1 INTRODUCTION

The performance of a feedback control system is of primary importance. This subject was discussed at length in Chapter 5 and quantitative measures of performance were developed. We have found that a suitable control system is stable and that it results in an acceptable response to input commands, is less sensitive to system parameter changes, results in a minimum steady-state error for input commands, and, finally, is able to reduce the effect of undesirable disturbances. A feedback control system that provides an optimum performance without any necessary adjustments is rare indeed. Usually, we find it necessary to compromise among the many conflicting and demanding specifications and to adjust the system parameters to provide a suitable and acceptable performance when it is not possible to obtain all the desired optimum specifications.

At several points in the preceding chapters, we have considered the question of design and adjustment of the system parameters in order to provide a desirable response and performance. In Chapter 5, we defined and established several suitable measures of performance. In Chapter 6, we determined a method of investigating the stability of a control system, recognizing that a system is unacceptable unless it is stable. In Chapter 7, we used the root locus method to design a self-balancing scale and illustrated a method of parameter design by using the root locus method. Furthermore, in Chapters 8 and 9, we developed suitable measures of performance in terms of the frequency variable ω and used them to design several suitable control systems. Thus, we have been considering the problems of the design of feedback control systems as an integral part of the subjects of the preceding chapters. It is now our purpose to study the question further and to point out several significant design and compensation methods.

The preceding chapters have shown that it is often possible to adjust the system parameters in order to provide the desired system response. However, we often find that it is not sufficient to adjust a system parameter and thus obtain the desired performance. Rather, we are required to consider the structure of the system and redesign the system in order to obtain a suitable one. That is, we must examine the scheme or plan of the system and obtain a new design or plan that results in a suitable system. Thus, **the design of a control system is concerned with the arrangement, or the plan, of the system structure and the selection of suitable components and parameters**. For example, if we desire a set of performance measures to be less than some specified values, we often encounter a conflicting set of requirements. Hence, if we wish a system to have a percent overshoot less than 20% and $\omega_n T_p = 3.3$, we obtain a conflicting requirement on the system damping ratio ζ, as can be seen by examining Figure 5.8 again. If we are unable to relax these two performance requirements, we must alter the system in some way. The alteration or adjustment of a control system in order to provide a suitable performance is called **compensation**; that is, compensation is the adjustment of a system in order to make up for deficiencies or inadequacies.

In redesigning a control system to alter the system response, an additional component is inserted within the structure of the feedback system. It is this additional component or device that equalizes or compensates for the performance deficiency. The compensating device may be electric, mechanical, hydraulic, pneumatic, or some other type of device or network and is often called a **compensator**. Commonly, an electric circuit serves as a compensator in many control systems.

CHAPTER

10 The Design of Feedback Control Systems

PREVIEW

In this chapter, we address the central issue of the design of compensators. Using the methods of the previous chapters, we develop several design techniques in the frequency domain that enable us to achieve the desired system performance. The powerful lead and lag controllers are introduced and used in several design examples. Phase-lead and phase-lag control design approaches using both root locus plots and Bode diagrams are presented. The proportional-integral (PI) controller is revisited in the context of achieving high steady-state tracking accuracies. The chapter concludes with a proportional-derivative (PD) controller design with prefiltering for the Sequential Design Example: Disk Drive Read System.

DESIRED OUTCOMES

Upon completion of Chapter 10, students should:

- Be familiar with the design of lead and lag compensators using root locus and Bode plot methods.
- Understand the value of prefilters and how to design for deadbeat response.
- Have a greater appreciation for the varied approaches available for control system design.

Therefore, we can use the root locus method and determine a suitable compensator network transfer function so that the resultant root locus yields the desired closed-loop root configuration.

Alternatively, we can describe the performance of a feedback control system in terms of frequency performance measures. Then a system can be described in terms of the peak of the closed-loop frequency response M_{pwr}, the resonant frequency ω_r, the bandwidth, and the phase margin of the system. We can add a suitable compensation network, if necessary, in order to satisfy the system specifications. The design of the network, represented by $G_c(s)$, is developed in terms of the frequency response as portrayed on the polar plane, the Bode diagram, or the Nichols chart. Because a cascade transfer function is readily accounted for on a Bode plot by adding the frequency response of the network, we usually prefer to approach the frequency response methods by utilizing the Bode diagram.

Thus, the design of a system is concerned with the alteration of the frequency response or the root locus of the system in order to obtain a suitable system performance. For frequency response methods, we are concerned with altering the system so that the frequency response of the compensated system will satisfy the system specifications. Hence, in the frequency response approach, we use compensation networks to alter and reshape the system characteristics represented on the Bode diagram and Nichols chart.

Alternatively, the design of a control system can be accomplished in the s-plane by root locus methods. For the case of the s-plane, the designer wishes to alter and reshape the root locus so that the roots of the system will lie in the desired position in the s-plane.

We have illustrated several of these approaches in the preceding chapters. In Chapter 7, we used the root locus method in considering the design of a feedback network in order to obtain a satisfactory performance. In Chapters 8 and 9, we considered the selection of the gain in order to obtain a suitable phase margin and therefore a satisfactory relative stability.

Quite often, in practice, the best and easiest way to improve the performance of a control system is to alter, if possible, the process itself. That is, if the system designer is able to specify and alter the design of the process that is represented by the transfer function $G(s)$, then the performance of the system may be readily improved. For example, to improve the transient behavior of a servomechanism position controller, we often can choose a better motor for the system. In the case of an airplane control system, we might be able to alter the aerodynamic design of the airplane and thus improve the flight transient characteristics. Thus, a control system designer should recognize that an alteration of the process may result in an improved system. However, the process is often unalterable or has been altered as much as possible and still results in unsatisfactory performance. Then the addition of compensation networks becomes useful for improving the performance of the system.

In the following sections, we will assume that the process has been improved as much as possible and that the $G(s)$ representing the process is unalterable. First, we shall consider the addition of a so-called phase-lead compensation network and describe the design of the network by root locus and frequency response techniques. Then, using both the root locus and frequency response techniques, we will describe the design of the integration compensation networks in order to obtain a suitable system performance.

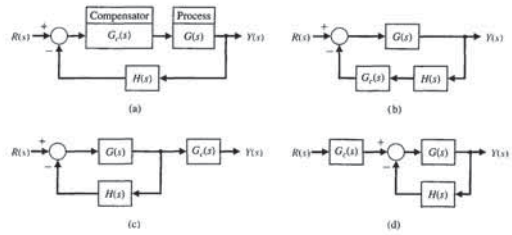

FIGURE 10.1
Types of compensation. (a) Cascade compensation. (b) Feedback compensation. (c) Output, or load, compensation. (d) Input compensation.

A compensator is an additional component or circuit that is inserted into a control system to compensate for a deficient performance.

The transfer function of a compensator is designated as $G_c(s) = E_o(s)/E_{in}(s)$, and the compensator can be placed in a suitable location within the structure of the system. Several types of compensation are shown in Figure 10.1 for a simple, single-loop feedback control system. The compensator placed in the feedforward path is called a **cascade**, or series, compensator (Figure 10.1a). Similarly, the other compensation schemes are called feedback, output (or load), and input compensation, as shown in Figures 10.1(b), (c), and (d), respectively. The selection of the compensation scheme depends upon a consideration of the specifications, the power levels at various signal nodes in the system, and the networks available for use. Usually, the output $Y(s)$ is a direct output of the process $G(s)$ and the output compensation of Figure 10.1(c) is not physically realizable. We cannot consider all the possibilities in this chapter; Chapters 11 and 12 will provide further information.

10.2 APPROACHES TO SYSTEM DESIGN

The performance of a control system can be described in terms of the time-domain performance measures or the frequency-domain performance measures. The performance of a system can be specified by requiring a certain peak time T_p, maximum overshoot, and settling-time for a step input. Furthermore, it is usually necessary to specify the maximum allowable steady-state error for several test signal inputs and disturbance inputs. These performance specifications can be defined in terms of the desirable location of the poles and zeros of the closed-loop system transfer function $T(s)$. Thus, the location of the s-plane poles and zeros of $T(s)$ can be specified. As we found in Chapter 7, the locus of the roots of the closed-loop system can be readily obtained for the variation of one system parameter. However, when the locus of roots does not result in a suitable root configuration, we must add a compensating network (Figure 10.1) to alter the locus of the roots as the parameter is varied.

Thus, a compensation network of the form of Equation (10.2) is a differentiator-type network. The differentiator network of Equation (10.3) has the frequency characteristic

$$G_c(j\omega) = j\frac{K}{p}\omega = \left(\frac{K}{p}\omega\right)e^{+j90^\circ} \tag{10.4}$$

and a phase angle of +90°. Similarly, the frequency response of the differentiating network of Equation (10.2) is

$$G_c(j\omega) = \frac{K(j\omega + z)}{j\omega + p} = \frac{(Kz/p)[j(\omega/z) + 1]}{j(\omega/p) + 1} = \frac{K_1(1 + j\omega\alpha\tau)}{1 + j\omega\tau}, \tag{10.5}$$

where $\tau = 1/p$, $p = \alpha z$, and $K_1 = K/\alpha$. The frequency response of this phase-lead network is shown in Figure 10.3. The angle of the frequency characteristic is

$$\phi(\omega) = \tan^{-1}(\alpha\omega\tau) - \tan^{-1}(\omega\tau). \tag{10.6}$$

Because the zero occurs first on the frequency axis, we obtain a phase-lead characteristic, as shown in Figure 10.3. The slope of the asymptotic magnitude curve is +20 dB/decade.

The phase-lead compensation transfer function can be obtained with the network shown in Figure 10.4. The transfer function of this network is

$$G_c(s) = \frac{V_2(s)}{V_1(s)} = \frac{R_2}{R_2 + \dfrac{R_1/(Cs)}{R_1 + 1/(Cs)}}$$

$$= \frac{R_2}{R_1 + R_2}\frac{R_1Cs + 1}{[R_1R_2/(R_1 + R_2)]Cs + 1}. \tag{10.7}$$

Therefore, we let

$$\tau = \frac{R_1R_2}{R_1 + R_2}C \quad \text{and} \quad \alpha = \frac{R_1 + R_2}{R_2}.$$

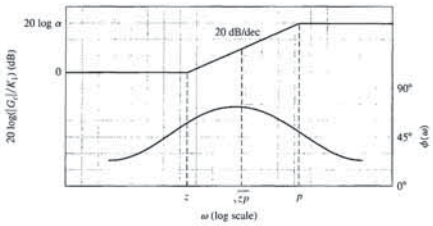

FIGURE 10.3
Bode diagram of the phase-lead network.

10.3 CASCADE COMPENSATION NETWORKS

In this section, we will consider the design of a cascade or feedback network, as shown in Figures 10.1(a) and (b), respectively. The compensation network function $G_c(s)$ is cascaded with the specified process $G(s)$ in order to provide a suitable loop transfer function $L(s) = G_c(s)G(s)H(s)$. The compensator $G_c(s)$ can be chosen to alter either the shape of the root locus or the frequency response. In either case, the network may be chosen to have a transfer function

$$G_c(s) = \frac{K\prod_{i=1}^{M}(s + z_i)}{\prod_{j=1}^{n}(s + p_j)}. \tag{10.1}$$

Then the problem reduces to the judicious selection of the poles and zeros of the compensator. To illustrate the properties of the compensation network, we will consider a first-order compensator. The compensation approach developed on the basis of a first-order compensator can then be extended to higher-order compensators, for example, by cascading several first-order compensators.

A compensator $G_c(s)$ is used with a process $G(s)$ so that the overall loop gain can be set to satisfy the steady-state error requirement, and then $G_c(s)$ is used to adjust the system dynamics favorably without affecting the steady-state error.

Consider the first-order compensator with the transfer function

$$\boxed{G_c(s) = \frac{K(s + z)}{s + p}.} \tag{10.2}$$

The design problem then becomes the selection of z, p, and K in order to provide a suitable performance. When $|z| < |p|$, the network is called a **phase-lead network** and has a pole–zero s-plane configuration, as shown in Figure 10.2. If the pole was negligible, that is, $|p| \gg |z|$, and the zero occurred at the origin of the s-plane, we would have a differentiator so that

$$G_c(s) \approx \frac{K}{p}s. \tag{10.3}$$

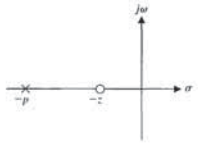

FIGURE 10.2
Pole–zero diagram of the phase-lead network.

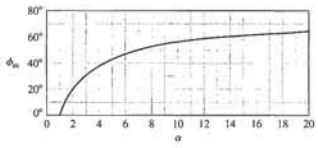

FIGURE 10.5
Maximum phase angle ϕ_m versus α for a phase-lead network.

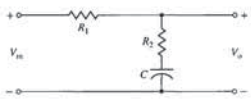

FIGURE 10.6
Phase-lag network.

It is often useful to add a cascade compensation network that provides a phase-lag characteristic. The **phase-lag network** is shown in Figure 10.6. The transfer function of the phase-lag network is

$$G_c(s) = \frac{V_o(s)}{V_{in}(s)} = \frac{R_2 + 1/(Cs)}{R_1 + R_2 + 1/(Cs)} = \frac{R_2Cs + 1}{(R_1 + R_2)Cs + 1}. \tag{10.12}$$

When $\tau = R_2C$ and $\alpha = (R_1 + R_2)/R_2$, we have the **phase-lag compensation** transfer function

$$\boxed{G_c(s) = \frac{1 + \tau s}{1 + \alpha\tau s} = \frac{1}{\alpha}\frac{s + z}{s + p},} \tag{10.13}$$

where $z = 1/\tau$ and $p = 1/(\alpha\tau)$. In this case, because $\alpha > 1$, the pole lies closest to the origin of the s-plane, as shown in Figure 10.7. This type of compensation network is often called an integrating network because it has a frequency response like an integrator over a finite range of frequencies. The Bode diagram of the phase-lag network is obtained from the transfer function

$$G_c(j\omega) = \frac{1 + j\omega\tau}{1 + j\omega\alpha\tau} \tag{10.14}$$

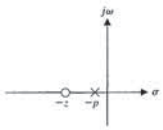

FIGURE 10.7
Pole–zero diagram of the phase-lag network.

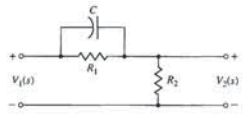

FIGURE 10.4
Phase-lead network.

and we obtain the **phase-lead compensation** transfer function

$$\boxed{G_c(s) = \frac{1 + \alpha\tau s}{\alpha(1 + \tau s)}.} \tag{10.8}$$

which is equal to Equation (10.5) when an additional cascade gain K is inserted.

The maximum value of the phase lead occurs at a frequency ω_m, where ω_m is the geometric mean of $p = 1/\tau$ and $z = 1/(\alpha\tau)$; that is, the maximum phase lead occurs halfway between the pole and zero frequencies on the logarithmic frequency scale. Therefore,

$$\boxed{\omega_m = \sqrt{zp} = \frac{1}{\tau\sqrt{\alpha}}.}$$

To obtain an equation for the maximum phase-lead angle, we rewrite the phase angle of Equation (10.5) as

$$\boxed{\phi = \tan^{-1}\frac{\alpha\omega\tau - \omega\tau}{1 + (\omega\tau)^2\alpha}.} \tag{10.9}$$

Then, substituting the frequency for the maximum phase angle, $\omega_m = 1/(\tau\sqrt{\alpha})$, we have

$$\tan\phi_m = \frac{\alpha/\sqrt{\alpha} - 1/\sqrt{\alpha}}{1 + 1} = \frac{\alpha - 1}{2\sqrt{\alpha}}. \tag{10.10}$$

We use the trigonometric relationship $\sin\phi = \tan\phi/\sqrt{1 + \tan^2\phi}$ and obtain

$$\boxed{\sin\phi_m = \frac{\alpha - 1}{\alpha + 1}.} \tag{10.11}$$

Equation (10.11) is very useful for calculating a necessary α ratio between the pole and zero of a compensator in order to provide a required maximum phase lead. A plot of ϕ_m versus α is shown in Figure 10.5. The phase angle readily obtainable from this network is not much greater than 70°. Also, since $\alpha = (R_1 + R_2)/R_2$, there are practical limitations on the maximum value of α that we should attempt to obtain. Therefore, if we required a maximum angle greater than 70°, two cascade compensation networks would be used. Then the equivalent compensation transfer function would be $G_{c_1}(s)G_{c_2}(s)$ when the loading effect of $G_{c_2}(s)$ on $G_{c_1}(s)$ is negligible.

$G(j\omega)H(j\omega)$ and determine a suitable location for p and z of $G_c(j\omega)$ in order to satisfactorily reshape the frequency response. The uncompensated $G(j\omega)H(j\omega)$ is plotted with the desired gain to allow an acceptable steady-state error. Then the phase margin and the expected M_{pw} are examined to find whether they satisfy the specifications. If the phase margin is not sufficient, phase lead can be added to the phase-angle curve of the system by placing the $G_c(j\omega)$ in a suitable location. To obtain maximum additional phase lead, we adjust the network so that the frequency ω_m is located at the frequency where the magnitude of the compensated magnitude curve crosses the 0-dB axis. (Recall the definition of phase margin.) The value of the added phase lead required allows us to determine the necessary value for α from Equation (10.11) or Figure 10.5. The zero $z = 1/(\alpha\tau)$ is located by noting that the maximum phase lead should occur at $\omega_m = \sqrt{zp}$, halfway between the pole and the zero. Because the total magnitude gain for the network is 20 log α, we expect a gain of 10 log α at ω_m. Thus, we determine the compensation network by completing the following steps:

1. Evaluate the uncompensated system phase margin when the error constants are satisfied.
2. Allowing for a small amount of safety, determine the necessary additional phase lead ϕ_m.
3. Evaluate α from Equation (10.11).
4. Evaluate 10 log α and determine the frequency where the uncompensated magnitude curve is equal to $-10 \log \alpha$ dB. Because the compensation network provides a gain of 10 log α at ω_m, this frequency is the new 0-dB crossover frequency and ω_m simultaneously.
5. Calculate the pole $p = \omega_m\sqrt{\alpha}$ and $z = p/\alpha$.
6. Draw the compensated frequency response, check the resulting phase margin, and repeat the steps if necessary. Finally, for an acceptable design, raise the gain of the amplifier in order to account for the attenuation $(1/\alpha)$.

EXAMPLE 10.1 **A lead compensator for a type-two system**

Let us consider a single-loop feedback control system as shown in Figure 10.1(a), where

$$G(s) = \frac{K_1}{s^2} \tag{10.15}$$

and $H(s) = 1$. The uncompensated system is a type-two system and at first appears to possess a satisfactory steady-state error for both step and ramp input signals. However, the response of the uncompensated system is an undamped oscillation because

$$T(s) = \frac{Y(s)}{R(s)} = \frac{K_1}{s^2 + K_1}. \tag{10.16}$$

Therefore, the compensation network is added so that the loop transfer function is $L(s) = G_c(s)G(s)$. The specifications for the system are

$$\text{Settling time, } T_s \le 4 \text{ s;}$$
$$\text{System damping constant } \zeta \ge 0.45.$$

The settling time (with a 2% criterion) requirement is

$$T_s = \frac{4}{\zeta\omega_n} = 4;$$

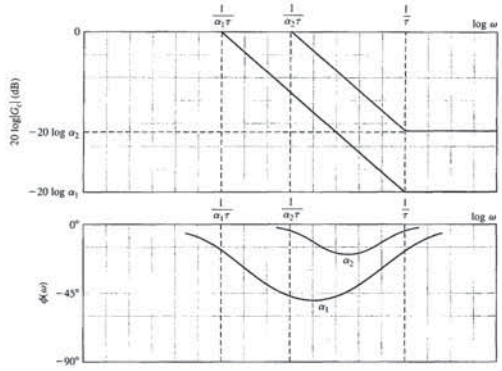

FIGURE 10.8 Bode diagram of the phase-lag network.

and is shown in Figure 10.8. The form of the Bode diagram of the **lag network** is similar to that of the phase-lead network; the difference is the resulting attenuation and phase-lag angle instead of amplification and phase-lead angle. However, note that the shapes of the diagrams of Figures 10.3 and 10.8 are similar. Therefore, we can show that the maximum phase lag occurs at $\omega_m = \sqrt{zp}$.

In the succeeding sections, we wish to utilize these compensation networks to obtain a desired system frequency response or s-plane root location. The **lead network** can provide a phase-lead angle and thus a satisfactory phase margin for a system. Alternatively, the phase-lead network can enable us to reshape the root locus and thus provide the desired root locations. The phase-lag network is used, not to provide a phase-lag angle, which is normally a destabilizing influence, but rather to provide an attenuation and to increase the steady-state error constant [3]. The following six sections discuss these approaches to design utilizing the phase-lead and phase-lag networks.

10.4 PHASE-LEAD DESIGN USING THE BODE DIAGRAM

The Bode diagram is used to design a suitable phase-lead network in preference to other frequency response plots. The frequency response of the cascade compensation network is added to the frequency response of the uncompensated system. That is, because the total loop transfer function of Figure 10.1(a) is $L(j\omega) = G_c(j\omega)G(j\omega)H(j\omega)$, we will first plot the Bode diagram for $G(j\omega)H(j\omega)$. Then we can examine the plot for

and thus $\alpha = 5.8$. To provide a margin of safety, we will use $\alpha = 6$. The value of 10 log α is then equal to 7.78 dB. Then the lead network will add an additional gain of 7.78 dB at the frequency ω_m, and we want to have ω_m equal to the compensated slope near the 0-dB axis (the dashed line) so that the new crossover is ω_m and the dashed magnitude curve is 7.78 dB above the uncompensated curve at the crossover frequency. Thus, the compensated crossover frequency is located by evaluating the frequency where the uncompensated magnitude curve is equal to −7.78 dB, which in this case is $\omega = 4.95$. Then the maximum phase-lead angle is added to $\omega = \omega_m = 4.95$, as shown in Figure 10.9. Using step 5, we determine the pole $p = \omega_m\sqrt{\alpha} = 12.0$ and the zero $z = p/\alpha = 2.0$.

The bandwidth of the compensated system can be obtained from the Nichols chart. For estimating the bandwidth, we can simply examine Figure 9.26 and note that the −3-dB line for the closed-loop system occurs when the magnitude of $G(j\omega)$ is −6 dB and the phase shift of $G(j\omega)$ is approximately −140°. Therefore, to estimate the bandwidth from the open-loop diagram, we will approximate the bandwidth as the frequency for which $20 \times \log|G|$ is equal to −6 dB. Thus, the bandwidth of the uncompensated system is approximately equal to $\omega_B = 4.4$, while the bandwidth of the compensated system is equal to $\omega_B = 8.4$. The lead compensation doubles the bandwidth in this case, and satisfies the specification that $\omega_B > 3.00$. Therefore, the compensation of the system is completed, and the system specifications are satisfied. The total compensated loop transfer function is

$$L(j\omega) = G_c(j\omega)G(j\omega) = \frac{10[j\omega/2.0 + 1]}{(j\omega)^2[j\omega/12.0 + 1]}. \tag{10.19}$$

The transfer function of the compensator is

$$G_c(s) = \frac{1 + \alpha\tau s}{\alpha(1 + \tau s)} = \frac{1}{6}\frac{1 + s/2.0}{1 + s/12.0}, \tag{10.20}$$

in the form of Equation (10.8). Because an attenuation of $\frac{1}{6}$ results from the passive RC network, the gain of the amplifier in the loop must be raised by a factor of 6 so that the total DC loop gain is still equal to 10, as required in Equation (10.19). When we add the compensation network Bode diagram to the uncompensated Bode diagram, as in Figure 10.9, we assume that we can raise the amplifier gain to account for this $1/\alpha$ attenuation. The pole and zero values can be read from Figure 10.9, noting that $p = \alpha z$.

The total loop transfer function is (recall that $H(s) = 1$)

$$L(s) = \frac{10(1 + s/2)}{s^2(1 + s/12)} = \frac{60(s + 2)}{s^2(s + 12)}.$$

The closed-loop transfer function is

$$T(s) = \frac{60(s + 2)}{s^3 + 12s^2 + 60s + 120} \approx \frac{60(s + 2)}{(s^2 + 6s + 20)(s + 6)},$$

and the effects of the zero at $s = -2$ and the third pole at $s = -6$ will affect the transient response. Plotting the step response, we find an overshoot of 34% and a settling time of 1.4 seconds. ■

therefore,

$$\omega_n = \frac{1}{\zeta} = \frac{1}{0.45} = 2.22.$$

Perhaps the easiest way to check the value of ω_n for the frequency response is to relate ω_n to the bandwidth ω_B, and evaluate the −3-dB bandwidth of the closed-loop system. For a closed-loop system with $\zeta = 0.45$, we estimate from Figure 8.26 that $\omega_B = 1.33\omega_n$. Therefore, we require a closed-loop bandwidth $\omega_B = 1.33(2.22) = 3.00$. The bandwidth can be checked following compensation by utilizing the Nichols chart. For the uncompensated system, the bandwidth of the system is $\omega_B = 1.33\omega_n$ and $\omega_n = \sqrt{K}$. Therefore, a loop gain equal to $K = \omega_n^2 \approx 5$ would be sufficient. To provide a suitable margin for the settling time, we will select $K = 10$ in order to draw the Bode diagram of

$$G(j\omega) = \frac{K}{(j\omega)^2}.$$

The Bode diagram of the uncompensated system is shown as solid lines in Figure 10.9.

By using Equation (9.58), the phase margin of the system is required to be approximately

$$\phi_{pm} = \frac{\zeta}{0.01} = \frac{0.45}{0.01} = 45°. \tag{10.17}$$

The phase margin of the uncompensated system is 0° because the double integration results in a constant 180° phase lag. Therefore, we must add a 45° phase-lead angle at the crossover (0-dB) frequency of the compensated magnitude curve. Evaluating the value of α, we have

$$\frac{\alpha - 1}{\alpha + 1} = \sin\phi_m = \sin 45°, \tag{10.18}$$

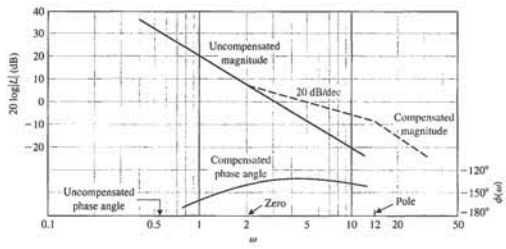

FIGURE 10.9 Bode diagram for Example 10.1.

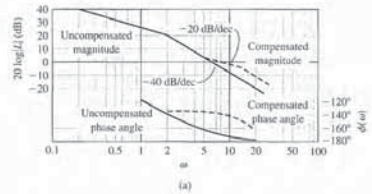

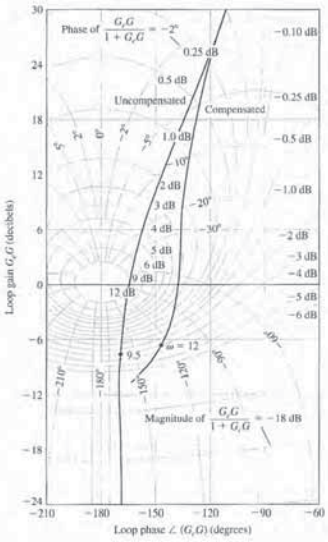

FIGURE 10.10
(a) Bode diagram for Example 10.2. (b) Nichols diagram for Example 10.2.

EXAMPLE 10.2 **A lead compensator for a second-order system**

A unity feedback control system has a loop transfer function

$$L(s) = \frac{K}{s(s+2)}, \tag{10.21}$$

where $L(s) = G_c(s)G(s)$ and $H(s) = 1$. We want to have a steady-state error for a ramp input equal to 5% of the velocity of the ramp. Therefore, we require that

$$K_v = \frac{A}{e_{ss}} = \frac{A}{0.05A} = 20. \tag{10.22}$$

Furthermore, we desire that the phase margin of the system be at least 45°. The first step is to plot the Bode diagram of the uncompensated transfer function

$$G(j\omega) = \frac{K_v}{j\omega(0.5j\omega + 1)} = \frac{20}{j\omega(0.5j\omega + 1)}, \tag{10.23}$$

as shown in Figure 10.10(a). The frequency at which the magnitude curve crosses the 0-dB line is 6.2 rad/s, and the phase margin at this frequency is determined readily from the equation of the phase of $G(j\omega)$, which is

$$\underline{/G(j\omega)} = \phi(\omega) = -90° - \tan^{-1}(0.5\omega). \tag{10.24}$$

At the crossover frequency $\omega = \omega_c = 6.2$ rad/s, we have

$$\phi(\omega) = -162°, \tag{10.25}$$

and therefore the phase margin is 18°. Using Equation (10.24) to evaluate the phase margin is often easier than drawing the complete phase-angle curve, which is shown in Figure 10.10(a). Thus, we need to add a phase-lead network so that the phase margin is raised to 45° at the new crossover (0-dB) frequency. Because the compensation crossover frequency is greater than the uncompensated crossover frequency, the phase lag of the uncompensated system is also greater. We shall account for this additional phase lag by attempting to obtain a maximum phase lead of 45° − 18° = 27°, plus a small increment (10%) of phase lead to account for the added lag. Thus, we will design a compensation network with a maximum phase lead equal to 27° + 3° = 30°. Then, calculating α, we obtain

$$\frac{\alpha - 1}{\alpha + 1} = \sin 30° = 0.5, \tag{10.26}$$

and therefore $\alpha = 3$.

The maximum phase lead occurs at ω_m, and this frequency will be selected so that the new crossover frequency and ω_m coincide. The magnitude of the lead network at ω_m is $10 \log \alpha = 10 \log 3 = 4.8$ dB. The compensated crossover frequency is then evaluated where the magnitude of $G(j\omega)$ is −4.8 dB, and thus $\omega_m = \omega_c = 8.4$. Drawing the compensated magnitude line so that it intersects the

where α and τ are defined for the *RC* network in Equation (10.7). The locations of the zero and pole are selected so as to result in a satisfactory root locus for the compensated system. The specifications of the system are used to specify the desired location of the dominant roots of the system. The *s*-plane root locus method is as follows:

1. List the system specifications and translate them into a desired root location for the dominant roots.
2. Sketch the uncompensated root locus, and determine whether the desired root locations can be realized with an uncompensated system.
3. If a compensator is necessary, place the zero of the phase-lead network directly below the desired root location (or to the left of the first two real poles).
4. Determine the pole location so that the total angle at the desired root location is 180° and therefore is on the compensated root locus.
5. Evaluate the total system gain at the desired root location and then calculate the error constant.
6. Repeat the steps if the error constant is not satisfactory.

Therefore, we first locate our desired dominant root locations so that the dominant roots satisfy the specifications in terms of ζ and ω_n, as shown in Figure 10.11(a). The root locus of the uncompensated system is sketched as illustrated in Figure 10.11(b).

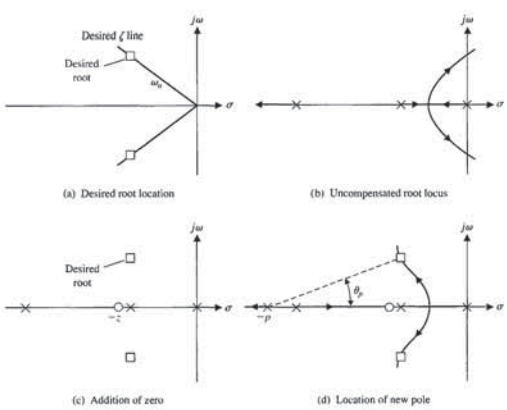

FIGURE 10.11
Compensation on the *s*-plane using a phase-lead network.

0-dB axis at $\omega = \omega_c = 8.4$, we find that $z = \omega_m/\sqrt{\alpha} = 4.8$ and $p = \alpha z = 14.4$. Therefore, the compensation network is

$$G_c(s) = \frac{1}{3}\frac{1 + s/4.8}{1 + s/14.4}. \tag{10.27}$$

The total DC loop gain must be raised by a factor of three in order to account for the factor $1/\alpha = \frac{1}{3}$. Then the compensated loop transfer function is

$$L(s) = G_c(s)G(s) = \frac{20(s/4.8 + 1)}{s(0.5s + 1)(s/14.4 + 1)}. \tag{10.28}$$

To verify the final phase margin, we can evaluate the phase of $G_c(j\omega)G(j\omega)$ at $\omega = \omega_c = 8.4$ and thus obtain the phase margin. The phase angle is then

$$\begin{aligned}\phi(\omega_c) &= -90° - \tan^{-1} 0.5\omega_c - \tan^{-1}\frac{\omega_c}{14.4} + \tan^{-1}\frac{\omega_c}{4.8} \\ &= -90° - 76.5° - 30.0° + 60.2° \\ &= -136.3°. \end{aligned} \tag{10.29}$$

Therefore, the phase margin for the compensated system is 43.7°. If we desire to have exactly a 45° phase margin, we would repeat the steps with an increased value of α—for example, with $\alpha = 3.5$. In this case, the phase lag increased by 7° between $\omega = 6.2$ and $\omega = 8.4$, and therefore the allowance of 3° in the calculation of α was not sufficient. The step response of this system yields a 28% overshoot with a settling time of 0.75 second.

The Nichols diagram for the compensated and uncompensated system is shown in Figure 10.10(b). The reshaping of the frequency response locus is clear on this diagram. Note the increased phase margin for the compensated system as well as the reduced magnitude of M_{pw}, the maximum magnitude of the closed-loop frequency response. In this case, M_{pw} has been reduced from an uncompensated value of +12 dB to a compensated value of approximately +3.2 dB. Also, we note that the closed-loop 3-dB bandwidth of the compensated system is equal to 12 rad/s compared with 9.5 rad/s for the uncompensated system. ■

Looking again at Examples 10.1 and 10.2, we note that the system design is satisfactory when the asymptotic curve for the magnitude $20 \log|GG_c|$ crosses the 0-dB line with a slope of −20 dB/decade.

10.5 PHASE-LEAD DESIGN USING THE ROOT LOCUS

The design of the phase-lead compensation network can also be readily accomplished using the root locus. The phase-lead network has a transfer function

$$G_c(s) = \frac{s + 1/\alpha\tau}{s + 1/\tau} = \frac{s + z}{s + p}, \tag{10.30}$$

Therefore, the damping ratio should be $\zeta \geq 0.32$. The settling time requirement is

$$T_s = \frac{4}{\zeta\omega_n} = 4,$$

so $\zeta\omega_n = 1$. Thus, we will choose a desired dominant root location as

$$r_1, \bar{r}_1 = -1 \pm j2, \tag{10.34}$$

as shown in Figure 10.12 (hence, $\zeta = 0.45$).

Now we place the zero of the compensator directly below the desired location at $s = -z = -1$, as shown in Figure 10.12. Measuring the angle at the desired root, we have

$$\phi = -2(116°) + 90° = -142°.$$

Therefore, to have a total of 180° at the desired root, we evaluate the angle from the undetermined pole, θ_p, as

$$-180° = -142° - \theta_p, \tag{10.35}$$

or $\theta_p = 38°$. Then a line is drawn at an angle $\theta_p = 38°$ intersecting the desired root location and the real axis, as shown in Figure 10.12. The point of intersection with the real axis is then $s = -p = -3.6$. Therefore, the compensator is

$$G_c(s) = \frac{s + 1}{s + 3.6}, \tag{10.36}$$

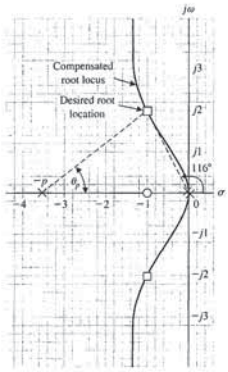

FIGURE 10.12
Phase-lead design for Example 10.3.

Then the zero is added to provide a phase lead by placing it to the left of the first two real poles. Some caution is necessary because the zero must not alter the dominance of the desired roots; that is, the zero should not be placed closer to the origin than the second pole on the real axis, or a real root near the origin will result and will dominate the system response. Thus, in Figure 10.11(c), we note that the desired root is directly above the second pole, and we place the zero z somewhat to the left of the second real pole.

Consequently, the real root may be near the real zero, and the coefficient of this term of the partial fraction expansion may be relatively small. Hence, the response due to this real root may have very little effect on the overall system response. Nevertheless, the designer must be continually aware that the compensated system response will be influenced by the roots and zeros of the system and that the dominant roots will not by themselves dictate the response. It is usually wise to allow for some margin of error in the design and to test the compensated system using a computer simulation.

Because the desired root is a point on the root locus when the final compensation is accomplished, we expect the algebraic sum of the vector angles to be 180° at that point. Thus, we calculate the angle θ_p from the pole of the compensator in order to result in a total angle of 180°. Then, locating a line at an angle θ_p intersecting the desired root, we are able to evaluate the compensator pole p, as shown in Figure 10.11(d).

The advantage of the root locus method is the ability of the designer to specify the location of the dominant roots and therefore the dominant transient response. The disadvantage of the method is that we cannot directly specify an error constant (for example, K_v) as in the Bode diagram approach. After the design is complete, we evaluate the gain of the system at the root location, which depends on p and z, and then calculate the error constant for the compensated system. If the error constant is not satisfactory, we must repeat the design steps and alter the location of the desired root as well as the location of the compensator pole and zero. We shall consider again Examples 10.1 and 10.2 and design a compensation network using the root locus (s-plane) approach.

EXAMPLE 10.3 **Lead compensator using the root locus**

Let us consider again the system of Example 10.1 where the uncompensated loop transfer function is

$$L(s) = \frac{K_1}{s^2}. \tag{10.31}$$

The characteristic equation of the uncompensated system is

$$1 + L(s) = 1 + \frac{K_1}{s^2} = 0, \tag{10.32}$$

and the root locus is the $j\omega$-axis. Therefore, we propose to compensate this system with a network

$$G_c(s) = \frac{s + z}{s + p}, \tag{10.33}$$

where $|z| < |p|$. The specifications for the system are

Settling time (with a 2% criterion), $T_s \leq 4$ s;
Percent overshoot for a step input $P.O. \leq 35\%$.

EXAMPLE 10.4 **Lead compensator for a type-one system**

Now, let us consider again the system of Example 10.2 and design a compensator based on the root locus approach. The system loop transfer function is

$$L(s) = \frac{K}{s(s + 2)}. \tag{10.40}$$

We want the damping ratio of the dominant roots of the system to be $\zeta = 0.45$ and the velocity error constant to be equal to 20. To satisfy the error constant requirement, the gain of the uncompensated system must be $K = 40$. When $K = 40$, the roots of the uncompensated system are

$$s^2 + 2s + 40 = (s + 1 + j6.25)(s + 1 - j6.25). \tag{10.41}$$

The damping ratio of the uncompensated roots is approximately 0.16, and therefore a compensation network must be added. To achieve a rapid settling time, we will select the real part of the desired roots as $\zeta\omega_n = 4$, and therefore $T_s = 1$ s. This implies the natural frequency of these roots is fairly large, $\omega_n = 9$; hence, the velocity constant should be reasonably large. The location of the desired roots is shown in Figure 10.13(a) for $\zeta\omega_n = 4$, $\zeta = 0.45$, and $\omega_n = 9$.

The zero of the compensator is placed at $s = -z = -4$, directly below the desired root location. Then the angle at the desired root location is

$$\phi = -116° - 104° + 90° = -130°. \tag{10.42}$$

Therefore, the angle from the undetermined pole is determined from

$$-180° = -130° - \theta_p,$$

and thus $\theta_p = 50°$. This angle is drawn to intersect the desired root location, and p is evaluated as $s = -p = -10.6$, as shown in Figure 10.13(a). The gain of the compensated system is then

$$K = \frac{9(8.25)(10.4)}{8} = 96.5. \tag{10.43}$$

The compensated system loop transfer function is then

$$L(s) = G_c(s)G(s) = \frac{96.5(s + 4)}{s(s + 2)(s + 10.6)}. \tag{10.44}$$

Therefore, the velocity constant of the compensated system is

$$K_v = \lim_{s \to 0} s[G_c(s)G(s)] = \frac{96.5(4)}{2(10.6)} = 18.2. \tag{10.45}$$

The velocity constant of the compensated system is less than the desired value of 20. Accordingly, we must repeat the design procedure for a second choice of a desired root. If we choose $\omega_n = 10$, the process can be repeated, and the resulting gain K will be increased. The compensator pole and zero location will also be altered.

and the compensated loop transfer function for the system is

$$L(s) = G_c(s)G(s) = \frac{K_1(s + 1)}{s^2(s + 3.6)}. \tag{10.37}$$

The gain K_1 is evaluated by measuring the vector lengths from the poles and zeros to the root location. Hence,

$$K_1 = \frac{(2.23)^2(3.25)}{2} = 8.1. \tag{10.38}$$

Finally, the error constants of this system are evaluated. We find that this system with two open-loop integrations will result in a zero steady-state error for a step and ramp input signal. The acceleration constant is

$$K_a = \frac{8.1}{3.6} = 2.25. \tag{10.39}$$

The steady-state performance of this system is quite satisfactory, and therefore the compensation is complete. When we compare the compensation network evaluated by the s-plane method with the network obtained by using the Bode diagram approach, we find that the magnitudes of the poles and zeros are different. However, the resulting system will have the same performance, and we need not be concerned with the difference. In fact, the difference arises from the arbitrary design step (number 3), which places the zero directly below the desired root location. If we placed the zero at $s = -2.0$, we would find that the pole evaluated by the s-plane method is approximately equal to the pole evaluated by the Bode diagram approach.

The specifications for the transient response of this system were originally expressed in terms of the overshoot and the settling time of the system. These specifications were translated, on the basis of an approximation of the system by a second-order system, to an equivalent ζ and ω_n and therefore a desired root location. However, the original specifications will be satisfied only if the selected roots are dominant. The zero of the compensator and the root resulting from the addition of the compensator pole result in a third-order system with a zero. The validity of approximating this system with a second-order system without a zero is dependent upon the validity of the dominance assumption. Often, the designer will simulate the final design by using a digital computer and obtain the actual transient response of the system. In this case, a computer simulation of the system resulted in an overshoot of 46% and a settling time (to within 2% of the final value) of 3.8 seconds for a step input. These values compare moderately well with the specified values of 35% and 4 seconds, and they justify the use of the dominant root specifications. The difference in the overshoot from the specified value is due to the zero, which is not negligible. Thus, again we find that the specification of dominant roots is a useful approach but must be utilized with caution and understanding. A second attempt to obtain a compensated system with an overshoot of 30% would use a **prefilter** to eliminate the effect of the zero in the closed-loop transfer function, as described in Section 10.10. ■

0.8 second, as shown in Figure 10.13(b). As shown here, we may use a computer to verify the actual transient response. ■

The phase-lead compensation network is a useful compensator for altering the performance of a control system. The phase-lead network adds a phase-lead angle to provide an adequate phase margin for feedback systems. Using an s-plane design approach, we can choose the phase-lead network in order to alter the system root locus and place the roots of the system in a desired position in the s-plane. When the design specifications include an error constant requirement, the Bode diagram method is more suitable, because the error constant of a system designed on the s-plane must be ascertained following the choice of a compensator pole and zero. Therefore, the root locus method often results in an iterative design procedure when the error constant is specified. On the other hand, the root locus is a very satisfactory approach when the specifications are given in terms of overshoot and settling time, thus specifying the ζ and ω_n of the desired dominant roots in the s-plane. The use of a lead network compensator always extends the bandwidth of a feedback system, which may be objectionable for systems subjected to large amounts of noise. Also, lead networks are not suitable for providing high steady-state accuracy in systems requiring very high error constants. To provide large error constants, typically K_p and K_v, we must consider the use of integration-type compensation networks. This is the subject of the following section.

10.6 SYSTEM DESIGN USING INTEGRATION NETWORKS

For a large proportion of control systems, the primary objective is obtaining a high steady-state accuracy. Another goal is maintaining the transient performance of these systems within reasonable limits. As we found in Chapters 4 and 5, the steady-state accuracy of many feedback systems can be increased by increasing the amplifier gain in the forward channel. However, the resulting transient response may be totally unacceptable—even unstable. Therefore, it is often necessary to introduce a compensation network in the forward path of a feedback control system in order to provide a sufficient steady-state accuracy.

Consider the single-loop control system shown in Figure 10.14. The compensation network is chosen to provide a large error constant. With $G_p(s) = 1$, the steady-state error of this system is

$$\lim_{t\to\infty} e(t) = \lim_{s\to 0} s\frac{R(s)}{1 + G_c(s)G(s)H(s)}. \tag{10.48}$$

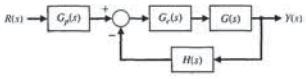

FIGURE 10.14
Single-loop feedback control system.

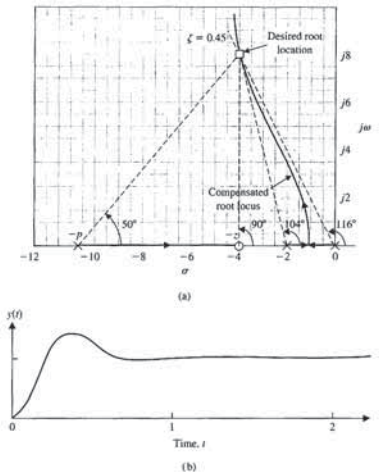

FIGURE 10.13
(a) Design of a phase-lead network on the s-plane for Example 10.4. (b) Step response of the compensated system of Example 10.4.

Then the velocity constant can be again evaluated. We will leave it as an exercise to show that for $\omega_n = 10$, the velocity constant is $K_v = 22.7$ when $z = 4.5$ and $p = 11.6$.

Finally, for the compensation network of Equation (10.44), we have

$$G_c(s) = \frac{s + 4}{s + 10.6} = \frac{s + 1/(\alpha\tau)}{s + 1/\tau}. \tag{10.46}$$

The design of an RC-lead network to implement $G_c(s)$, as shown in Figure 10.4, follows directly from Equations (10.46) and (10.7):

$$G_c(s) = \frac{R_2}{R_1 + R_2}\frac{R_1Cs + 1}{[R_1R_2/(R_1 + R_2)]\,Cs + 1}. \tag{10.47}$$

Thus, in this case, we have

$$\frac{1}{R_1C} = 4 \quad \text{and} \quad \alpha = \frac{R_1 + R_2}{R_2} = \frac{10.6}{4}.$$

Then, choosing $C = 1\ \mu$f, we obtain $R_1 = 250{,}000\ \Omega$ and $R_2 = 152{,}000\ \Omega$. The step response of the compensated system yields a 32% overshoot with a settling time of

The addition of an integration as $G_c(s) = K_P + K_I/s$ can also be used to reduce the steady-state error for a ramp input $r(t) = t$, $t \geq 0$. For example, if the uncompensated system $G(s)$ possessed one integration, the additional integration due to $G_c(s)$ would result in a zero steady-state error for a ramp input. To illustrate the design of this type of integration compensator, we will consider a temperature control system in some detail.

EXAMPLE 10.5 **Temperature control system**

The uncompensated loop transfer function of a unity feedback temperature control system is

$$L(s) = G(s) = \frac{K_1}{(2s + 1)(0.5s + 1)} = \frac{K_1}{(s + .5)(s + 2)}, \tag{10.53}$$

where K_1 can be adjusted. To maintain zero steady-state error for a step input, we will add the PI compensation network

$$G_c(s) = K_P + \frac{K_I}{s} = K_P\frac{s + K_I/K_P}{s}. \tag{10.54}$$

Furthermore, the transient response of the system is required to have an overshoot less than or equal to 10%. Therefore, the dominant complex roots must be on (or below) the $\zeta = 0.6$ line, as shown in Figure 10.15. We will adjust the compensator zero so that the negative real part of the complex roots is $\zeta\omega_n = 0.75$, and thus the settling time (with a 2% criterion) is $T_s = 4/(\zeta\omega_n) = \frac{16}{3}$ s. Now, as in the preceding section, we will determine the location of the zero $z = -K_I/K_P$ by ensuring that the angle at the desired root is $-180°$. Therefore, the sum of the angles at the desired root is

$$-180° = -127° - 104° - 38° + \theta_z,$$

where θ_z is the angle from the undetermined zero. Consequently, we find that $\theta_z = +89°$, and the location of the zero is $z = -0.75$. Finally, to determine the gain at the desired root, we evaluate the vector lengths from the poles and zeros and obtain

$$K = K_1K_P = \frac{1.25(1.03)1.6}{1.0} = 2.08.$$

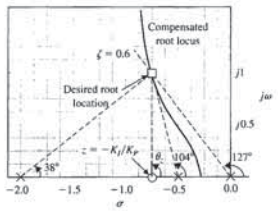

FIGURE 10.15
The s-plane design of an integration compensator.

We found in Section 5.6 that the steady-state error of a system depends on the number of poles at the origin for $L(s) = G_c(s)G(s)H(s)$. A pole at the origin can be considered an integration, and therefore the steady-state accuracy of a system ultimately depends on the number of integrations in the loop transfer function $L(s) = G_c(s)G(s)H(s)$. If the steady-state accuracy is not sufficient, we will introduce an **integration-type network** $G_c(s)$ in order to compensate for the lack of integration in the uncompensated loop transfer function $G(s)H(s)$.

One widely used form of controller is the **proportional plus integral (PI) controller**, which has a transfer function

$$\boxed{G_c(s) = K_p + \frac{K_I}{s}.} \tag{10.49}$$

For an example, let us consider a temperature control system where the transfer function $H(s) = 1$, and the transfer function of the heat process is [28]

$$G(s) = \frac{K_1}{(\tau_1 s + 1)(\tau_2 s + 1)}.$$

The steady-state error of the uncompensated system is then

$$\lim_{t\to\infty} e(t) = \lim_{s\to 0} s\frac{A/s}{1 + G(s)} = \frac{A}{1 + K_1}, \tag{10.50}$$

where $R(s) = A/s$, a step input signal. To obtain a small steady-state error (less than 0.05 A, for example), the magnitude of the gain K_1 must be quite large. However, when K_1 is quite large, the transient performance of the system will very likely be unacceptable. Therefore, we must consider the addition of a compensation transfer function $G_c(s)$, as shown in Figure 10.14. To eliminate the steady-state error of this system, we might choose the compensation as

$$G_c(s) = K_P + \frac{K_I}{s} = \frac{K_Ps + K_I}{s}. \tag{10.51}$$

This PI compensation can be readily constructed by using an integrator and an amplifier and adding their output signals. The steady-state error for a step input of the system is always zero, because

$$\begin{aligned}\lim_{t\to\infty} e(t) &= \lim_{s\to 0} s\frac{A/s}{1 + G_c(s)G(s)} \\ &= \lim_{s\to 0}\frac{A}{1 + (K_Ps + K_I)/s\,K_1/[(\tau_1 s + 1)(\tau_2 s + 1)]} \\ &= 0.\end{aligned} \tag{10.52}$$

The transient performance can be adjusted to satisfy the system specifications by adjusting the constants K_1, K_P, and K_I. The adjustment of the transient response is perhaps best accomplished by using the root locus methods of Chapter 7 and drawing a root locus for the gain K_PK_1 after locating the zero $s = -K_I/K_P$ on the s-plane by the method outlined for the s-plane in the preceding section.

as shown in Section 5.7. In general, if $G(s)$ is written as

$$G(s) = \frac{K\prod_{i=1}^{M}(s + z_i)}{s\prod_{j=1}^{n}(s + p_j)}, \tag{10.60}$$

we obtain the velocity constant

$$K_v = \frac{K\prod_{i=1}^{M} z_i}{\prod_{j=1}^{n} p_j}. \tag{10.61}$$

We will now add the integration-type phase-lag network as a compensator and determine the compensated velocity constant. If the velocity constant of the uncompensated system (Equation 10.61) is designated as $K_{v,\text{unc}}$, we have

$$K_{v,\text{comp}} = \lim_{s\to 0} s\{G_c(s)G(s)\} = \lim_{s\to 0}\{G_c(s)\}K_{v,\text{unc}}$$

$$= \frac{z}{p}\frac{1}{\alpha}K_{v,\text{unc}} = \frac{z}{p}\frac{K}{\alpha}\frac{\prod z_i}{\prod p_j} \tag{10.62}$$

The gain on the compensated root locus at the desired root location will be K/α. Now, if the pole and zero of the compensator are chosen so that $|z| = \alpha|p| < 1$, the resultant K_v will be increased at the desired root location by the ratio $z/p = \alpha$. Then, for example, if $z = 0.1$ and $p = 0.01$, the velocity constant of the desired root location will be increased by a factor of 10. If the compensator pole and zero appear relatively close together on the s-plane, their effect on the location of the desired root will be negligible. Therefore, the compensator pole–zero combination near the origin of the s-plane compared to ω_n can be used to increase the error constant of a feedback system by the factor α while altering the root location very slightly. The factor α does have an upper limit, typically about 100, because the required resistors and capacitors of the network become excessively large for a higher α. For example, when $z = 0.1$ and $\alpha = 100$, we find from Equation (10.57) that

$$z = 0.1 = \frac{1}{R_2C} \quad \text{and} \quad \alpha = 100 = \frac{R_1 + R_2}{R_2}.$$

If we let $C = 10\,\mu\text{f}$, then $R_2 = 1\,\text{M}\Omega$ and $R_1 = 99\,\text{M}\Omega$. As we increase α, we increase the required magnitude of R_1. However, we should note that an attenuation α of 1000 or more may be obtained by utilizing pneumatic process controllers, which approximate a phase-lag characteristic (Figure 10.8).

The steps necessary for the design of a phase-lag network on the s-plane are as follows:

1. Obtain the root locus of the uncompensated system.
2. Determine the transient performance specifications for the system and locate suitable dominant root locations on the uncompensated root locus that will satisfy the specifications.

The compensated root locus and the location of the zero are shown in Figure 10.15. Note that the zero $z = -K_I/K_P$ should be placed to the left of the pole at $s = -0.5$ to ensure that the complex roots dominate the transient response. In fact, the third root of the compensated system of Figure 10.15 can be determined as $s = -1.0$, and therefore this real root is only $\frac{4}{3}$ times the real part of the complex roots. Although complex roots dominate the response of the system, the equivalent damping of the system is somewhat less than $\zeta = 0.60$ due to the real root and zero.

The closed-loop transfer function of the system of Figure 10.14 is

$$T(s) = \frac{G_p(s)G_c(s)G(s)}{1 + G_c(s)G(s)} = \frac{2.08(s + 0.75)G_p(s)}{(s + 1)(s + r_1)(s + \hat{r}_1)}, \tag{10.55}$$

where $r_1 = -0.75 + j1$. The effect of the zero is to increase the overshoot to a step input (see Figure 5.13). If we wish to attain an overshoot of 5%, we may use a prefilter $G_p(s)$, so that the zero is eliminated in $T(s)$ by setting

$$G_p(s) = \frac{0.75}{s + 0.75}. \tag{10.56}$$

Note that the overall DC gain (set $s = 0$) is $T(0) = 1.0$ when $G_p(s) = 1$, as obtained with the prefilter of Equation (10.56). The overshoot without the prefilter is 17.6%; with the prefilter, it is 2%. Further discussion of the use of a prefilter is provided in Section 10.10. ■

10.7 PHASE-LAG DESIGN USING THE ROOT LOCUS

The phase-lag RC network of Figure 10.6 is an integration-type network and can be used to increase the error constant of a feedback control system. We found in Section 10.3 that the transfer function of the RC phase-lag network is of the form

$$G_c(s) = \frac{1}{\alpha}\frac{s + z}{s + p}, \tag{10.57}$$

as given in Equation (10.13), where

$$z = \frac{1}{\tau} = \frac{1}{R_2C}, \qquad \alpha = \frac{R_1 + R_2}{R_2}, \quad \text{and} \quad p = \frac{1}{\alpha\tau}.$$

The steady-state error of an uncompensated unity feedback system is

$$\lim_{t\to\infty} e(t) = \lim_{s\to 0} s\left\{\frac{R(s)}{1 + G(s)}\right\}. \tag{10.58}$$

Then, for example, the velocity constant of a type-one uncompensated system is

$$K_v = \lim_{s\to 0} s\{G(s)\}, \tag{10.59}$$

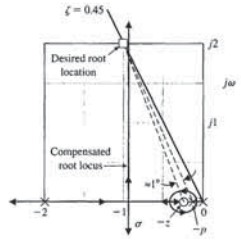

FIGURE 10.17
Root locus of the compensated system of Example 10.6. Note that the actual root will differ from the desired root by a slight amount. The vertical portion of the locus leaves the σ axis at $\sigma = -0.95$.

Thus, the required ratio of the zero to the pole of the compensator is

$$\left|\frac{z}{p}\right| = \alpha = \frac{K_{v,\text{comp}}}{K_{v,\text{unc}}} = \frac{20}{2.5} = 8. \tag{10.64}$$

Examining Figure 10.17, we find that we might set $z = 0.1$ and then $p = 0.1/8$. The difference of the angles from p and z at the desired root is approximately 1°; therefore, $s = -1 \pm j2$ is still the location of the dominant roots. A sketch of the compensated root locus is shown as a heavy line in Figure 10.17. Thus, the compensated system loop transfer function is

$$L(s) = G_c(s)G(s) = \frac{5(s + 0.1)}{s(s + 2)(s + 0.0125)}, \tag{10.65}$$

where $K/\alpha = 5$, so $K = 40$, in order to account for the attenuation of the lag network. ■

EXAMPLE 10.7 **Design of a phase-lag compensator**

Let us now consider a system that is difficult to design using a phase-lead network. The loop transfer function of the uncompensated unity feedback system is

$$L(s) = \frac{K}{s(s + 10)^2}. \tag{10.66}$$

It is specified that the velocity constant of this system be equal to 20, while the damping ratio of the dominant roots is equal to 0.707. The gain necessary for a K_v of 20 is

$$K_v = 20 = \frac{K}{(10)^2},$$

3. Calculate the loop gain at the desired root location and thus the system error constant.
4. Compare the uncompensated error constant with the desired error constant, and calculate the necessary increase that must result from the pole–zero ratio α of the compensator.
5. With the known ratio of the pole–zero combination of the compensator, determine a suitable location of the pole and zero of the compensator so that the compensated root locus will still pass through the desired root location. Locate the pole and zero near the origin of the s-plane in comparison to ω_n.

The fifth requirement can be satisfied if the magnitudes of the pole and zero are significantly less than ω_n of the dominant roots and they appear to merge as measured from the desired root location. The pole and zero will appear to merge at the root location if the angles from the compensator pole and zero are essentially equal as measured to the root location. One method of locating the zero and pole of the compensator is based on the requirement that the difference between the angle of the pole and the angle of the zero as measured at the desired root is less than 2°. An example will illustrate this approach to the design of a phase-lag compensator.

EXAMPLE 10.6 **Design of a phase-lag compensator**

Consider the uncompensated unity feedback system of Example 10.2, where the uncompensated loop transfer function is

$$L(s) = \frac{K}{s(s + 2)}. \tag{10.63}$$

We require the damping ratio of the dominant complex roots to be 0.45, while a system velocity constant equal to 20 is attained. The uncompensated root locus is a vertical line at $s = -1$ and results in a root on the $\zeta = 0.45$ line at $s = -1 \pm j2$, as shown in Figure 10.16. Measuring the gain at this root, we have $K = (2.24)^2 = 5$. Therefore, the velocity constant of the uncompensated system is

$$K_v = \frac{K}{2} = \frac{5}{2} = 2.5.$$

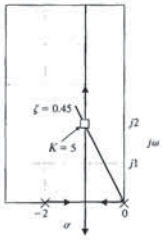

FIGURE 10.16
Root locus of the uncompensated system of Example 10.6.

10.8 PHASE-LAG DESIGN USING THE BODE DIAGRAM

The design of a phase-lag *RC* network suitable for compensating a feedback control system can be readily accomplished on the Bode diagram. The advantage of the Bode diagram is again apparent, for we will simply add the frequency response of the compensator to the Bode diagram of the uncompensated system in order to obtain a satisfactory system frequency response. The transfer function of the phase-lag network, written in Bode diagram form, is

$$G_c(j\omega) = \frac{1 + j\omega\tau}{1 + j\omega\alpha\tau}, \tag{10.68}$$

as we found in Equation (10.14). The Bode diagram of the phase-lag network is shown in Figure 10.8 for two values of α. On the Bode diagram, the pole and the zero of the compensator have a magnitude much smaller than the smallest pole of the uncompensated system. Thus, the phase lag is not the useful effect of the compensator; it is the attenuation $-20 \log \alpha$ that is the useful effect for compensation. The phase-lag network is used to provide an attenuation and therefore to lower the 0-dB (crossover) frequency of the system. However, at lower crossover frequencies, we usually find that the phase margin of the system is increased, and our specifications can be satisfied. The design procedure for a phase-lag network on the Bode diagram is as follows:

1. Obtain the Bode diagram of the uncompensated system with the gain adjusted for the desired error constant.
2. Determine the phase margin of the uncompensated system and, if it is insufficient, proceed with the following steps.
3. Determine the frequency where the phase margin requirement would be satisfied if the magnitude curve crossed the 0-dB line at this frequency, ω_c'. (Allow for 5° phase lag from the phase-lag network when determining the new crossover frequency.)
4. Place the zero of the compensator one decade below the new crossover frequency ω_c', and thus ensure only 5° of additional phase lag at ω_c' (see Figure 10.8) due to the lag network.
5. Measure the necessary attenuation at ω_c' to ensure that the magnitude curve crosses at this frequency.
6. Calculate α by noting that the attenuation introduced by the phase-lag network is $-20 \log \alpha$ at ω_c'.
7. Calculate the pole as $\omega_p = 1/(\alpha\tau) = \omega_z/\alpha$, and the design is completed.

An example of this design procedure will illustrate that the method is simple to carry out in practice.

EXAMPLE 10.8 **Design of a phase-lag network**

Let us consider again the unity feedback system of Example 10.6 and design a phase-lag network so that the desired phase margin is obtained. The uncompensated loop transfer function is

$$L(j\omega) = \frac{K}{j\omega(j\omega + 2)} = \frac{K_v}{j\omega(0.5j\omega + 1)}, \tag{10.69}$$

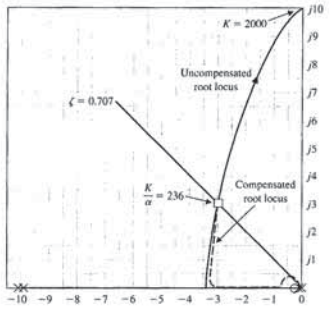

FIGURE 10.18
Design of a phase-lag compensator on the *s*-plane.

or $K = 2000$. However, using Routh's criterion, we find that the roots of the characteristic equation lie on the $j\omega$-axis at $\pm j10$ when $K = 2000$. The roots of the system when the K_v requirement is satisfied are a long way from satisfying the damping ratio specification, and it would be difficult to bring the dominant roots from the $j\omega$-axis to the $\zeta = 0.707$ line by using a phase-lead compensator. Therefore, we will attempt to satisfy the K_v and ζ requirements by using a phase-lag network. The uncompensated root locus of this system is shown in Figure 10.18, and the roots are shown when $\zeta = 0.707$ and $s = -2.9 \pm j2.9$. Measuring the gain at these roots, we find that $K = 236$. Therefore, the necessary ratio of the zero to the pole of the compensator (use Equation 10.64) is

$$\alpha = \left|\frac{z}{p}\right| = \frac{2000}{236} = 8.5.$$

Thus, we will choose $z = 0.1$ and $p = 0.1/9$ in order to allow a small margin of safety. Examining Figure 10.18, we find that the difference between the angle from the pole and zero of $G_c(s)$ is negligible. Therefore, the compensated system is

$$G_c(s)G(s) = \frac{236(s + 0.1)}{s(s + 10)^2(s + 0.0111)}, \tag{10.67}$$

where $K/\alpha = 236$ and $\alpha = 9$. ■

The design of an integration compensator to increase the error constant of an uncompensated control system is particularly illustrative using *s*-plane and root locus methods. We shall now turn to similarly useful methods of designing integration compensation using Bode diagrams.

Then we find that 20 dB = 20 log α, or $\alpha = 10$. Therefore, the zero is one decade below the crossover, or $\omega_z = \omega_c'/10 = 0.15$, and the pole is at $\omega_p = \omega_z/10 = 0.015$. The compensated system is then

$$G_c(j\omega)G(j\omega) = \frac{20(6.66j\omega + 1)}{j\omega(0.5j\omega + 1)(66.6j\omega + 1)}. \tag{10.70}$$

The frequency response of the compensated system is shown in Figure 10.19(a) with dashed lines. It is evident that the phase lag introduces an attenuation that lowers the crossover frequency and therefore increases the phase margin. Note that the phase angle of the lag network has almost totally disappeared at the crossover frequency ω_c'. As a final check, we numerically evaluate the phase margin and find that $\phi_{pm} = 46.8°$ at $\omega_c' = 1.58$ which is the desired result. Using the Nichols chart, we find that the closed-loop bandwidth of the system has been reduced from $\omega = 10$ rad/s for the uncompensated system to $\omega = 2.5$ rad/s for the compensated system. Due to the reduced bandwidth, we expect a slower time response to a step command.

The time response of the system is shown in Figure 10.19(b). Note that the overshoot is 25% and the peak time is 1.85 seconds. Thus, the response is within the specifications. ■

EXAMPLE 10.9 **Design of a phase-lag compensator**

Let us consider again the unity feedback system of Example 10.7, which is

$$L(j\omega) = \frac{K}{j\omega(j\omega + 10)^2} = \frac{K_v}{j\omega(0.1j\omega + 1)^2}, \tag{10.71}$$

where $K_v = K/100$. A velocity constant of K_v equal to 20 is specified. Furthermore, a damping ratio of 0.707 for the dominant roots is required. From Figure 9.21, we estimate that a phase margin of 65° is required. The frequency response of the uncompensated system is shown in Figure 10.20. The phase margin of the uncompensated system is 0°. Allowing 5° for the lag network, we locate the frequency where the phase is −110°. This frequency is equal to 1.74, and therefore we will attempt to locate the new crossover frequency at $\omega_c' = 1.5$. Measuring the necessary attenuation at $\omega = \omega_c'$, we find that 23 dB is required; then $23 = 20 \log \alpha$ gives $\alpha = 14.2$. The zero of the compensator is located one decade below the crossover frequency, and thus

$$\omega_z = \frac{\omega_c'}{10} = 0.15.$$

The pole is then

$$\omega_p = \frac{\omega_z}{\alpha} = \frac{0.15}{14.2}.$$

Therefore, the compensated system is

$$G_c(j\omega)G(j\omega) = \frac{20(6.66j\omega + 1)}{j\omega(0.1j\omega + 1)^2(94.6j\omega + 1)}. \tag{10.72}$$

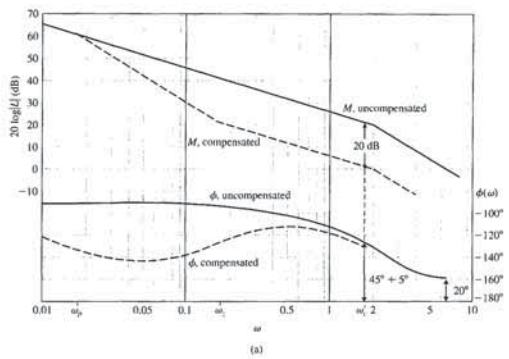

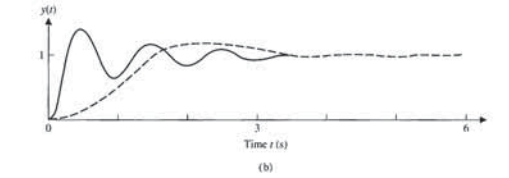

FIGURE 10.19
(a) Design of a phase-lag network on the Bode diagram for Example 10.8.
(b) Time response to a step input for the uncompensated system (solid line) and the compensated system (dashed line) of Example 10.8.

where $K_v = K/2$. We want $K_v = 20$ while a phase margin of 45° is attained. The uncompensated Bode diagram is shown as a solid line in Figure 10.19. The uncompensated system has a phase margin of 20°, and the phase margin must be increased. Allowing 5° for the phase-lag compensator, we locate the frequency ω where $\phi(\omega) = -130°$, which is to be our new crossover frequency ω_c'. In this case, we find that $\omega_c' = 1.5$, which allows for a small margin of safety. The attenuation necessary to cause ω_c' to be the new crossover frequency is equal to 20 dB. Both the compensated and uncompensated magnitude curves are an asymptotic approximation. Both the actual curves are 2 dB lower than shown. Thus, $\omega_c' = 1.5$, and the required attenuation is 20 dB.

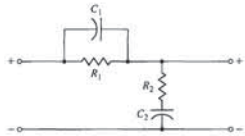

FIGURE 10.21
An *RC* lead-lag network.

The phase-lead compensation network alters the frequency response of a network by adding a positive (leading) phase angle and therefore increases the phase margin at the crossover (0-dB) frequency. It becomes evident that a designer might wish to consider using a compensation network that provides the attenuation of a phase-lag network and the lead-phase angle of a phase-lead network. Such a network does exist. It is called a **lead-lag network** and is shown in Figure 10.21. The transfer function of this network is

$$\frac{V_2(s)}{V_1(s)} = \frac{(R_1C_1s + 1)(R_2C_2s + 1)}{R_1R_2C_1C_2s^2 + (R_1C_1 + R_1C_2 + R_2C_2)s + 1}. \tag{10.73}$$

When $\alpha\tau_1 = R_1C_1$, $\beta\tau_2 = R_2C_2$, $\tau_1 + \tau_2 = R_1C_1 + R_1C_2 + R_2C_2$, and $\tau_1\tau_2 = R_1R_2\,C_1C_2$, we note that $\alpha\beta = 1$, and then Equation (10.73) is

$$\frac{V_2(s)}{V_1(s)} = \frac{(1 + \alpha\tau_1 s)(1 + \beta\tau_2 s)}{(1 + \tau_1 s)(1 + \tau_2 s)}, \tag{10.74}$$

where $\alpha > 1$ and $\beta < 1$. The first factors in the numerator and denominator, which are functions of τ_1, provide the phase-lead portion of the network. The second factors, which are functions of τ_2, provide the phase-lag portion of the compensation network. The parameter β is adjusted to provide suitable attenuation of the low-frequency portion of the frequency response, and the parameter α is adjusted to provide an additional phase lead at the new crossover (0-dB) frequency. Alternatively, the compensation can be designed on the s-plane by placing the lead pole and zero compensation in order to locate the dominant roots in a desired location. Then the phase-lag compensation is used to raise the error constant at the dominant root location by a suitable ratio $1/\beta$. The design of a phase lead-lag compensator follows the procedures already discussed. Other literature will further illustrate the utility of lead-lag compensation [2, 3, 25].

10.9 DESIGN ON THE BODE DIAGRAM USING ANALYTICAL METHODS

We will often use computers, when appropriate, to assist the designer in the selection of the parameters of a compensator. The development of algorithms for computer-aided design is an important alternative approach to the trial-and-error methods considered in earlier sections. Computer programs have been developed for the selection of suitable parameter values for compensators based on satisfaction of frequency response criteria such as the phase margin [3, 4].

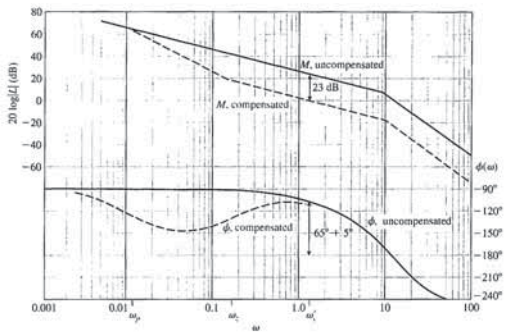

FIGURE 10.20
Design of a phase-lag network on the Bode diagram for Example 10.9.

The compensated frequency response is shown in Figure 10.20. As a final check, we evaluate the phase margin at $\omega_c' = 1.5$ and find that $\phi_{pm} = 67°$, which is within the specifications. ■

We have seen that a phase-lag compensation network can be used to alter the frequency response of a feedback control system in order to attain satisfactory system performance. Examining both Examples 10.8 and 10.9, we note again that the system design is satisfactory when the asymptotic curve for the magnitude of the compensated system crosses the 0-dB line with a slope of −20 dB/decade. The attenuation of the phase-lag network reduces the magnitude of the crossover (0-dB) frequency to a point where the phase margin of the system is satisfactory. Thus, in contrast to the phase-lead network, the phase-lag network reduces the closed-loop bandwidth of the system as it maintains a suitable error constant.

We might ask, why not place the compensator zero more than one decade below the new crossover ω_c' (see step 4 of the design procedure) and thus ensure less than 5° of lag at ω_c' due to the compensator? This question can be answered by considering the requirements placed on the resistors and capacitors of the lag network by the values of the poles and zeros (see Equation 10.12). As the magnitudes of the pole and zero of the lag network are decreased, the magnitudes of the resistors and the capacitor required increase proportionately. The zero of the lag compensator in terms of the circuit components is $z = 1/(R_2C)$, and the α of the network is $\alpha = (R_1 + R_2)/R_2$. Thus, considering Example 10.9, we require a zero at $\omega_z = 0.15$, which can be obtained with $C = 1\,\mu$F and $R_2 = 6.66\,M\Omega$. However, for $\alpha = 14$, we require a resistance R_1 of $R_1 = R_2(\alpha - 1) = 88\,M\Omega$. A designer does not wish to place the zero ω_z further than one decade below ω_c' and thus require larger values of R_1, R_2, and C.

Using c and p, we obtain

$$-4.31\alpha^2 + 12.62\alpha + 73.32 = 0. \tag{10.82}$$

Solving for α, we obtain $\alpha = 5.84$. Solving Equation (10.79), we obtain $\tau = 0.087$. Therefore, the compensator is

$$G_c(s) = \frac{1 + 0.515s}{1 + 0.087s}. \tag{10.83}$$

The pole is equal to 11.5, and the zero is 1.94. This design is similar to that obtained by the graphical technique of Section 10.4. ■

10.10 SYSTEMS WITH A PREFILTER

In the earlier sections of this chapter, we utilized compensators of the form

$$G_c(s) = \frac{s + z}{s + p}$$

that alter the roots of the characteristic equation of the closed-loop system. However, the closed-loop transfer function $T(s)$ will contain the zero of $G_c(s)$ as a zero of $T(s)$. This zero will significantly affect the response of the system $T(s)$.

Let us consider the system shown in Figure 10.22, where

$$G(s) = \frac{1}{s}.$$

We will introduce a PI compensator, so that

$$G_c(s) = K_P + \frac{K_I}{s} = \frac{K_Ps + K_I}{s}.$$

The closed-loop transfer function of the system with a prefilter (Figure 10.22) is

$$T(s) = \frac{(K_Ps + K_I)G_p(s)}{s^2 + K_Ps + K_I}. \tag{10.84}$$

For illustrative purposes, the specifications require a settling time (with a 2% criterion) of 0.5 second and an overshoot of approximately 4%. We use $\zeta = 1/\sqrt{2}$ and note that

$$T_s = \frac{4}{\zeta\omega_n}.$$

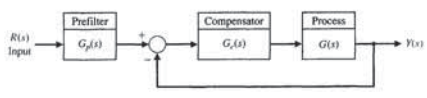

FIGURE 10.22
Control system with a prefilter $G_p(s)$.

An analytical technique of selecting the parameters of a lead or lag network has been developed for the Bode diagram [4, 5]. For a single-stage compensator,

$$G_c(s) = \frac{1 + \alpha\tau s}{1 + \tau s}, \tag{10.75}$$

where $\alpha < 1$ yields a lag compensator and $\alpha > 1$ yields a lead compensator. The phase contribution of the compensator at the desired crossover frequency ω_c (see Equation 10.9) is given by

$$p = \tan\phi = \frac{\alpha\omega_c\tau - \omega_c\tau}{1 + (\omega_c\tau)^2\alpha}. \tag{10.76}$$

The magnitude M (in dB) of the compensator at ω_c is given by

$$c = 10^{M/10} = \frac{1 + (\omega_c\alpha\tau)^2}{1 + (\omega_c\tau)^2}. \tag{10.77}$$

Eliminating $\omega_c\tau$ from Equations (10.76) and (10.77), we obtain the nontrivial solution equation for α as

$$(p^2 - c + 1)\alpha^2 + 2p^2c\alpha + p^2c^2 + c^2 - c = 0. \tag{10.78}$$

For a single-stage compensator, it is necessary that $c > p^2 + 1$. If we solve for α from Equation (10.78), we can obtain τ from

$$\tau = \frac{1}{\omega_c}\sqrt{\frac{1 - c}{c - \alpha^2}}. \tag{10.79}$$

The design steps for a lead compensator are:

1. Select the desired ω_c.
2. Determine the phase margin desired and therefore the required phase ϕ for Equation (10.76).
3. Verify that the phase lead is applicable: $\phi > 0$ and $M > 0$.
4. Determine whether a single stage will be sufficient by testing $c > p^2 + 1$.
5. Determine α from Equation (10.78).
6. Determine τ from Equation (10.79).

If we need to design a single-lag compensator, then $\phi < 0$ and $M < 0$ (step 3). Step 4 will require $c < 1/(1 + p^2)$. Otherwise the method is the same.

EXAMPLE 10.10 **Design using an analytical technique**

Let us consider again the system of Example 10.1 and design a lead network by the analytical technique. Examine the uncompensated curves in Figure 10.9. We select $\omega_c = 5$. Then, as before, we desire a phase margin of 45°. The compensator must yield this phase, so

$$p = \tan 45° = 1. \tag{10.80}$$

The required magnitude contribution is 8 dB, or $M = 8$, so that

$$c = 10^{M/10} = 6.31. \tag{10.81}$$

The closed-loop transfer function is then

$$T(s) = \frac{5(s + 0.1)}{(s^2 + 1.98s + 5.1)(s + 0.095)} \approx \frac{5}{s^2 + 1.98s + 5.1},$$

since the zero at $s = -0.1$ and the pole at $s = -0.095$ approximately cancel. We expect an overshoot of 20% and a settling time (with a 2% criterion) of 4.0 seconds for the design parameters $\zeta = 0.45$ and $\zeta\omega_n = 1$. However, the actual response has an overshoot of 26% and a longer settling time of 5.8 seconds due to the effect of the real pole of $T(s)$ at $s = -0.095$. Thus, we usually do not use a prefilter with systems that utilize lag compensators.

EXAMPLE 10.11 **Design of a third-order system**

Consider a system of the form shown in Figure 10.22 with

$$G(s) = \frac{1}{s(s + 1)(s + 5)}.$$

Let us design a system that will yield a step response with an overshoot less than 2% and a settling time less than 3 seconds by using both $G_c(s)$ and $G_p(s)$ to achieve the desired response.

We use a lead compensation network

$$G_c(s) = \frac{K(s + 1.2)}{s + 10}$$

and select K to find the complex roots with $\zeta = 1/\sqrt{2}$. Then, with $K = 78.7$, the closed-loop transfer function is

$$T(s) = \frac{78.7(s + 1.2)G_p(s)}{(s + 1.71 + j1.71)(s + 1.71 - j1.71)(s + 1.45)(s + 11.1)}$$
$$\approx \frac{7.1(s + 1.2)G_p(s)}{(s^2 + 3.42s + 5.85)(s + 1.45)}.$$

If we choose

$$G_p(s) = \frac{p}{s + p} \tag{10.85}$$

the closed-loop transfer function is

$$T(s) \approx \frac{7.1p(s + 1.2)}{(s^2 + 3.42s + 5.85)(s + 1.45)(s + p)}.$$

If $p = 1.2$, we cancel the effect of the zero. The response of the system with a prefilter is summarized in Table 10.1. We choose the appropriate value for p to achieve the response desired. Note that $p = 2.40$ will provide a response that may be desirable, since it effects a faster rise time than $p = 1.20$. The prefilter provides an additional parameter to select for design purposes. ■

Thus, we require that $\zeta\omega_n = 8$ or $\omega_n = 8\sqrt{2}$. We now obtain

$$K_P = 2\zeta\omega_n = 16 \quad \text{and} \quad K_I = \omega_n^2 = 128.$$

The closed-loop transfer function when $G_p(s) = 1$ is then

$$T(s) = \frac{16(s + 8)}{s^2 + 16s + 128}.$$

The effect of the zero on the step response is significant. Using Figure 5.13(a), we have $a/(\zeta\omega_n) = 1$ and $\zeta = 1/\sqrt{2}$, and the overshoot to a step as predicted from Figure 5.13(a) is 21%.

We use a prefilter $G_p(s)$ to eliminate the zero from $T(s)$ while maintaining the DC gain of 1, thus requiring that

$$G_p(s) = \frac{8}{s + 8}.$$

Then we have

$$T(s) = \frac{128}{s^2 + 16s + 128},$$

and the overshoot of this system is 4.5%, as expected.

Reviewing Figure 5.13(a), we note that the zero at $s = -a$ has a significant effect when $a/\zeta\omega_n < 5$, where $-a$ is the zero and $-\zeta\omega_n$ is the real part of the dominant roots of the characteristic equation of $T(s)$.

Let us now consider again Example 10.3, which includes the design of a lead compensator. The resulting closed-loop transfer function can be determined to be (using Figure 10.22)

$$T(s) = \frac{8.1(s + 1)G_p(s)}{(s + 1 + j2)(s + 1 - j2)(s + 1.62)}.$$

If $G_p(s) = 1$ (no prefilter), then we obtain a response with an overshoot of 46.6% and a settling time of 3.8 seconds. If we use a prefilter,

$$G_p(s) = \frac{1}{s + 1},$$

we obtain an overshoot of 6.7% and a settling time of 3.8 seconds. The real root at $s = -1.62$ helps to damp the step response. The prefilter is very useful in permitting the designer to introduce a compensator with a zero to adjust the root locations (poles) of the closed-loop transfer function while eliminating the effect of the zero incorporated in $T(s)$.

In general, we will add a prefilter for systems with lead networks or PI compensators. We will not use a prefilter for a system with a lag network, since we expect the effect of the zero to be insignificant. To check this assertion, let us consider again the design obtained in Example 10.6. The system with a phase-lag controller is

$$G(s)G_c(s) = \frac{5(s + 0.1)}{s(s + 2)(s + 0.0125)}.$$

We consider the transfer function $T(s)$ of a closed-loop system. To determine the coefficients that yield the optimal deadbeat response, the standard transfer function is first normalized. An example of this for a third-order system is

$$T(s) = \frac{\omega_n^3}{s^3 + \alpha\omega_n s^2 + \beta\omega_n^2 s + \omega_n^3}. \tag{10.86}$$

Dividing the numerator and denominator by ω_n^3 yields

$$T(s) = \frac{1}{\frac{s^3}{\omega_n^3} + \alpha\frac{s^2}{\omega_n^2} + \beta\frac{s}{\omega_n} + 1}. \tag{10.87}$$

Let $\bar{s} = s/\omega_n$ to obtain

$$T(s) = \frac{1}{\bar{s}^3 + \alpha\bar{s}^2 + \beta\bar{s} + 1}. \tag{10.88}$$

Equation (10.88) is the normalized, third-order, closed-loop transfer function. For a higher-order system, the same method is used to derive the normalized equation. The coefficients of the equation—α, β, γ, and so on—are then assigned the values necessary to meet the requirement of deadbeat response. The coefficients recorded in Table 10.2 were selected to achieve deadbeat response and minimize settling time and rise time T_r to 100% of the desired command. The form of Equation (10.88) is normalized since $\bar{s} = s/\omega_n$. Thus, we choose ω_n based on the desired settling time or rise time. Therefore, if we have a third-order system with a required settling time of 1.2 seconds, we note from Table 10.2 that the normalized settling time is

$$\omega_n T_s = 4.04.$$

Therefore, we require that

$$\omega_n = \frac{4.04}{T_s} = \frac{4.04}{1.2} = 3.37.$$

Once ω_n is chosen, the complete closed-loop transfer function is known, having the form of Equation (10.86). When designing a system to obtain a deadbeat response,

Table 10.2 Coefficients and Response Measures of a Deadbeat System

System	Coefficients					Percent Overshoot	Percent Undershoot	90% Rise Time	100% Rise Time	Settling Time
Order	α	β	γ	δ	ϵ	P.O.	P.U.	T_{r90}	T_r	T_s
2nd	1.82					0.10%	0.00%	3.47	6.58	4.82
3rd	1.90	2.20				1.65%	1.36%	3.48	4.32	4.04
4th	2.20	3.50	2.80			0.89%	0.95%	4.16	5.29	4.81
5th	2.70	4.90	5.40	3.40		1.29%	0.37%	4.84	5.73	5.43
6th	3.15	6.50	8.70	7.55	4.05	1.63%	0.94%	5.49	6.31	6.04

Note: All times are normalized.

Table 10.1 Effect of a Prefilter on the Step Response

$G_p(s)$	$p = 1$	$p = 1.20$	$p = 2.4$
Percent overshoot	9.9%	0%	4.8%
90% rise time (seconds)	1.05	2.30	1.60
Settling time (seconds)	2.9	3.0	3.2

10.11 DESIGN FOR DEADBEAT RESPONSE

Often, the goal for a control system is to achieve a fast response to a step command with minimal overshoot. We define a **deadbeat response** as a response that proceeds rapidly to the desired level and holds at that level with minimal overshoot. We use the ±2% band at the desired level as the acceptable range of variation from the desired response. Then, if the response enters the band at time T_s, it has satisfied the settling time T_s upon entry to the band, as illustrated in Figure 10.23. A deadbeat response has the following characteristics:

1. Steady-state error = 0
2. Fast response → minimum rise time and settling time
3. 0.1% ≤ percent overshoot <2%
4. Percent undershoot <2%

Characteristics (3) and (4) require that the response remain within the ±2% band so that the entry to the band occurs at the settling time.

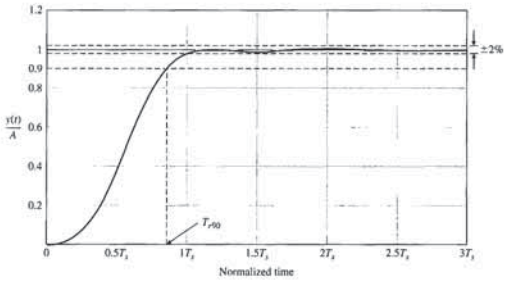

FIGURE 10.23 The deadbeat response. A is the magnitude of the step input.

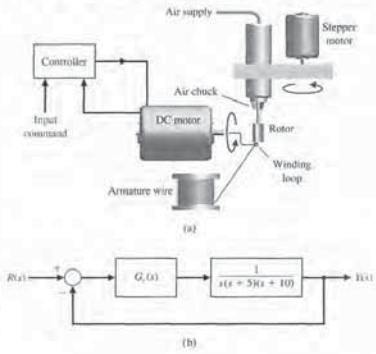

FIGURE 10.24
(a) Rotor winder control system.
(b) Block diagram.

throughput of the process be high. The operator simply inserts an unwound rotor, pushes a start button, and then removes the completely wound rotor. The DC motor is used to achieve accurate rapid windings. Thus, the goal is to achieve high steady-state accuracy for both position and velocity. The control system is shown in Figure 10.24(a) and the block diagram in Figure 10.24(b). This system has zero steady-state error for a step input, and the steady-state error for a ramp input is

$$e_{ss} = A/K_v,$$

where

$$K_v = \lim_{s \to 0} \frac{G_c(s)}{50}.$$

When $G_c(s) = K$, we have $K_v = K/50$. If we select $K = 500$, we will have $K_v = 10$, but the overshoot to a step is 70%, and the settling time is 8 seconds.

We first try a lead compensator so that

$$G_c(s) = \frac{K(s + z_1)}{s + p_1}. \tag{10.89}$$

Selecting $z_1 = 4$ and the pole p_1 so that the complex roots have a ζ of 0.6, we have (see Figure 10.25)

$$G_c(s) = \frac{191.2(s + 4)}{s + 7.3}. \tag{10.90}$$

the compensator is chosen, and the closed-loop transfer function is found. This compensated transfer function is then set equal to Equation (10.86), and the required compensator can be determined.

EXAMPLE 10.12 **Design of a system with a deadbeat response**

Let us consider a unity feedback system with a compensator $G_c(s)$ and a prefilter $G_p(s)$, as shown in Figure 10.22. The process is

$$G(s) = \frac{K}{s(s + 1)},$$

and the compensator is

$$G_c(s) = \frac{s + z}{s + p}.$$

Using the necessary prefilter yields

$$G_p(s) = \frac{z}{s + z}.$$

The closed-loop transfer function is

$$T(s) = \frac{Kz}{s^3 + (1 + p)s^2 + (K + p)s + Kz}.$$

We use Table 10.2 to determine the required coefficients, $\alpha = 1.90$ and $\beta = 2.20$. If we select a settling time (with a 2% criterion) of 2 seconds, then $\omega_n T_s = 4.04$, and thus $\omega_n = 2.02$. The required closed-loop system has the characteristic equation

$$q(s) = s^3 + \alpha\omega_n s^2 + \beta\omega_n^2 s + \omega_n^3 = s^3 + 3.84s^2 + 8.98s + 8.24.$$

Then, we determine that $p = 2.84$, $z = 1.34$, and $K = 6.14$. The response of this system will have $T_s = 2$ s, $T_r = 2.14$ s, and $T_{r90} = 1.72$ s. ■

10.12 DESIGN EXAMPLES

In this section we present three illustrative examples. The first example is a rotor winder control system where both a lead and lag compensator are designed using root locus methods. The second example is an x-y plotter. In this example, three different controllers are designed, including a proportional controller, a lead compensator, and a **PD controller**. In the third example, precise control of a milling machine used in manufacturing is employed to illustrate the design process. A lag compensator is designed using root locus methods to meet steady-state tracking error and percent overshoot specifications.

EXAMPLE 10.13 **Rotor winder control system**

Our goal is to replace a manual operation using a machine to wind copper wire onto the rotors of small motors. Each motor has three separate windings of several hundred turns of wire. It is important that the windings be consistent and that the

Table 10.3 Design Example Results

Controller	Gain, K	Lead Network	Lag Network	Lead-Lag Network
Step overshoot	70%	3%	12%	5%
Settling time (seconds)	8	1.5	2.5	2.0
Steady-state error for ramp	10%	48%	2.6%	4.8%
K_v	10	2.1	38	21

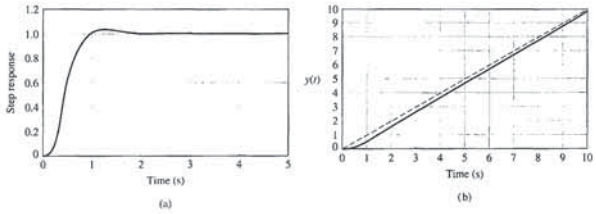

FIGURE 10.26 (a) Step response and (b) ramp response for rotor winder system.

The results for the simple gain, the lead network, and the lag network are summarized in Table 10.3.

Let us return to the lead-network system and add a cascade lag network, so that the compensator is

$$G_c(s) = \frac{K(s + z_1)(s + z_2)}{(s + p_1)(s + p_2)}. \tag{10.91}$$

The lead compensator of Equation (10.90) requires $K = 191.2$, $z_1 = 4$, and $p_1 = 7.3$. The root locus for the system is shown in Figure 10.25. We recall that this lead network resulted in $K_v = 2.1$ (see Table 10.3). To obtain $K_v = 21$, we use $\alpha = 10$ and select $z_2 = 0.1$ and $p_2 = 0.01$. Then the compensated loop transfer function is

$$G(s)G_c(s) = \frac{191.2(s + 4)(s + 0.1)}{s(s + 5)(s + 10)(s + 7.28)(s + 0.01)}. \tag{10.92}$$

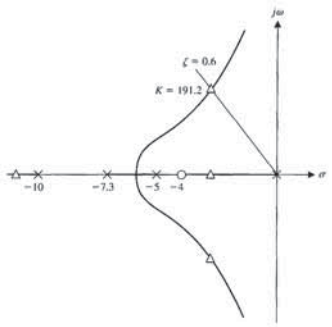

FIGURE 10.25
Root locus for lead compensator.

We find the response to a step input has a 3% overshoot and a settling time of 1.5 seconds. However, the velocity constant is

$$K_v = \frac{191.2(4)}{7.3(50)} = 2.1,$$

which is inadequate.

If we use a phase-lag design, we select

$$G_c(s) = \frac{K(s + z_2)}{s + p_2}$$

in order to achieve $K_v = 38$. Thus, the velocity constant of the lag-compensated system is

$$K_v = \frac{Kz_2}{50p_2}.$$

Using a root locus, we select $K = 105$ in order to achieve a reasonable uncompensated step response with an overshoot of less than or equal to 10%. We select $\alpha = z/p$ to achieve the desired K_v. We then have

$$\alpha = \frac{50K_v}{K} = \frac{50(38)}{105} = 18.1.$$

Selecting $z_2 = 0.1$ to avoid affecting the uncompensated root locus, we have $p_2 = 0.0055$. We then obtain a step response with a 12% overshoot and a settling time of 2.5 seconds.

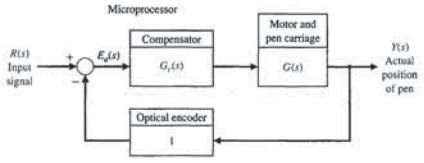

FIGURE 10.27
Model of the pen-plotter control system.

and our initial attempt at a specification of a compensator is to use a simple gain so that

$$G_c(s) = K.$$

In this case, we have only one parameter to adjust: K. To achieve a fast response, we have to adjust K so that it will provide two dominant s-plane roots with a damping ratio of 0.707, which will result in a step response overshoot of about 4.5%. A sketch of the root locus (note the break in the real axis) is shown in Figure 10.28.

Adjusting the gain to $K = 47{,}200$, we obtain a system with an overshoot of 3.6% to a step input and a settling time of 0.8 second. Since the transfer function has a pole at the origin, we have a steady-state error of zero for a step input.

This system does not meet our specifications, so we select a compensator that will reduce the settling time. Let us select a lead compensator so that

$$G_c(s) = \frac{K\alpha(s + z)}{(s + p)}, \tag{10.94}$$

where $p = \alpha z$. Let us use the method of Section 10.5, which selects the phase-lead compensator on the s-plane. Hence, we place the zero at $s = -20$ and determine the location of the pole, p, that will place the dominant roots on the line that has the damping ratio of $1/\sqrt{2}$. Thus, we find that $p = 60$ and $\alpha = 3$, so that

$$G(s)G_c(s) = \frac{142{,}600(s + 20)}{s(s + 10)(s + 60)(s + 1000)}. \tag{10.95}$$

Obtaining the actual step response, we determine that the percent overshoot is 2% and that the settling time is 0.35 second, which meet the specifications. The third design approach is to recognize that the encoder can be used to generate a velocity signal by counting the rate at which encoder lines pass by a fixed point, using the microprocessor. Since the position signal and the velocity signal are available, we can describe the compensator as

$$G_c(s) = K_P + K_D s, \tag{10.96}$$

where K_P is the gain for the error signal and K_D is the gain for the velocity signal.

The step response and ramp response of this system are shown in Figure 10.26 in parts (a) and (b), respectively, and are summarized in Table 10.3. Clearly, the lead-lag design is suitable for satisfaction of the design goals. ■

EXAMPLE 10.14 **X-Y plotter**

Many physical phenomena are characterized by parameters that are transient or slowly varying. If recorded, these changes can be examined at leisure and stored for future reference or comparison. To accomplish such a recording, a number of electromechanical instruments have been developed, among them the x-y recorder. In this instrument, the displacement along the x-axis represents a variable of interest or time and the displacement along the y-axis varies as a function of another variable [6].

Such recorders can be found in many laboratories recording experimental data, such as changes in temperature, variations in transducer output levels, and stress versus applied strain, to name just a few. The x-y plotter produces graphs with ink pens by drawing lines from a graphics file or directly from input data. These output devices offer a resolution superior to a printer since the lines are actually drawn rather than being composed of tiny dots.

The purpose of a plotter is to accurately follow the input signal as it varies. We will consider the design of the movement of one axis, since the movement dynamics of both axes are identical. Thus, we will strive to control the position and the movement of the pen very accurately as it follows the input signal.

To achieve accurate results, our goal is to achieve (1) a step response with an overshoot of less than 5% and a settling time (with a 2% criterion) less than 0.5 second, and (2) a percentage steady-state error for a step equal to zero. If we achieve these specifications, we will have a fast and accurate response.

To move the pen, we select a DC motor as the actuator. The feedback sensor will be a 500-line optical encoder. By detecting all state changes of the two-channel quadrature output of the encoder, 2000 encoder counts per revolution of the motor shaft can be detected. This yields an encoder resolution of 0.001 inch at the pen tip. The encoder is mounted on the shaft of the motor. Since the encoder provides digital data, it is compared with the input signal by using a microprocessor. Next, we propose using the difference signal calculated by the microprocessor as the error signal and then using the microprocessor to calculate the necessary algorithm to obtain the designed compensator. The output of the compensator is then converted to an analog signal that will drive the motor.

The model of the feedback position control system is shown in Figure 10.27. Since the microprocessor calculation speed is very fast compared to the rate of change of the encoder and input signals, we assume that the continuous signal model is very accurate.

The model for the motor and pen carriage is

$$G(s) = \frac{1}{s(s + 10)(s + 1000)}, \tag{10.93}$$

EXAMPLE 10.15 **Milling machine control system**

Smaller, lighter, less costly sensors are being developed by engineers for machining and other manufacturing processes. A milling machine table is depicted in Figure 10.29. This particular machine table has a new sensor that obtains information about the cutting process (that is, the depth-of-cut) from the acoustic emission (AE) signals. Acoustic emissions are low-amplitude, high-frequency stress waves that originate from the rapid release of strain energy in a continuous medium. The AE sensors are commonly piezoelectric amplitude sensitive in the 100 kHz to 1 MHz range; they are cost effective and can be mounted on most machine tools.

There is a relationship between the sensitivity of the AE power signal and small depth-of-cut changes [15, 18, 19]. This relationship can be exploited to obtain a feedback signal or measurement of the depth-of-cut. A simplified block diagram of the feedback system is shown in Figure 10.30. The elements of the design process emphasized in this example are highlighted in Figure 10.31.

Since the acoustic emissions are sensitive to material, tool geometry, tool wear, and cutting parameters such as cutter rotational speed, the measurement of the depth-of-cut is modeled as being corrupted by noise, denoted by $N(s)$ in Figure 10.30. Also disturbances to the process, denoted by $T_d(s)$, are modeled. These could represent external disturbances resulting in unwanted motion of the cutter, fluctuations in the cutter rotation speed, and so forth.

The process model $G(s)$ is given by

$$G(s) = \frac{2}{s(s + 1)(s + 5)}, \tag{10.99}$$

and represents the model of the cutter apparatus and the AE sensor dynamics. The input to $G(s)$ is a control signal to actuate an electromechanical device, which then applies downward pressure on the cutter.

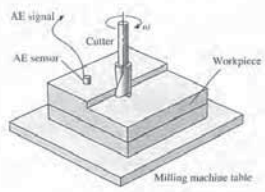

FIGURE 10.29
A depiction of the milling machine.

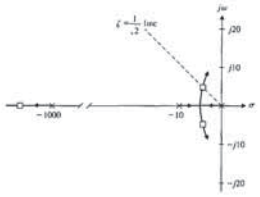

FIGURE 10.28
Root locus for the pen plotter, showing the roots with a damping ratio of $1/\sqrt{2}$. The dominant roots are $s = -4.9 \pm j4.9$.

Then we can write

$$G(s)G_c(s) = \frac{K_D(s + K_P/K_D)}{s(s + 10)(s + 1000)}.$$

If we set $K_P/K_D = 10$, we cancel the pole at $s = -10$ and obtain

$$G(s)G_c(s) = \frac{K_D}{s(s + 1000)}.$$

The characteristic equation for this system is

$$s^2 + 1000s + K_D = 0, \tag{10.97}$$

and we want $\zeta = 1/\sqrt{2}$. Noting that $2\zeta\omega_n = 1000$, we have $\omega_n = 707$ and $K_D = \omega_n^2$. Therefore, we obtain $K_D = 5 \times 10^5$, and the compensated system is

$$G_c(s)G(s) = \frac{5 \times 10^5}{s(s + 1000)}. \tag{10.98}$$

The response of this system will provide an overshoot of 4.3% and a settling time of 8 milliseconds.

The results for the three approaches to system design are compared in Table 10.4. The best design uses the velocity feedback. ■

Table 10.4 Results for Three Designs

	Step Response	
System	Percent Overshoot	Settling Time (milliseconds)
Gain adjustment	3.6	800
Gain and lead compensator	2.0	350
Gain adjustment plus velocity signal multiplied by gain K_D	4.3	8

There are a variety of methods available to obtain the model represented by Equation (10.99). One approach would be to use basic principles to obtain a mathematical model in the form of a nonlinear differential equation, which can then be linearized about an operating point leading to a linear model (or equivalently, a transfer function). The basic principles include Newton's laws, the various conservation laws, and Kirchhoff's laws. Another approach would be to assume a form of the model (such as a second-order system) with unknown parameters (such as ω_n and ζ), and then experimentally obtain good values of the unknown parameters.

A third approach is to conduct a laboratory experiment to obtain the step or impulse response of the system. In other words we can apply an input (in this case, a voltage) to the system and measure the output—the depth-of-cut into the desired workpiece. Suppose, for example, we have the impulse response data shown in Figure 10.32 (the small circles on the graph represent the data). If we had access to the function $C_{\text{imp}}(t)$—the impulse response function of the milling machine—we could take the Laplace transform to obtain the transfer function model. There are many methods available for curve fitting the data to obtain the function $C_{\text{imp}}(t)$. We will not cover curve fitting here, but we can say a few words regarding the basic structure of the function.

From Figure 10.32 we see that the response approaches a steady-state value:

$$C_{\text{imp}}(t) \to C_{\text{imp,ss}} \approx \frac{2}{5} \text{ as } t \to \infty.$$

So we expect that

$$C_{\text{imp}}(t) = \frac{2}{5} + \Delta C_{\text{imp}}(t),$$

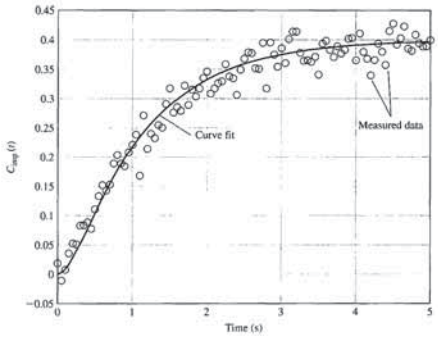

FIGURE 10.32 Hypothetical impulse response of the milling machine.

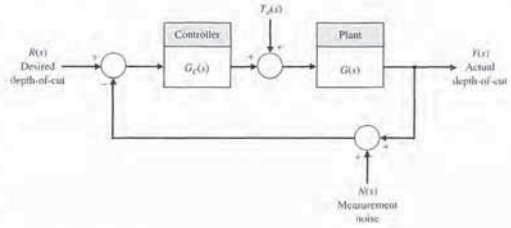

FIGURE 10.30 A simplified block diagram of the milling machine feedback system.

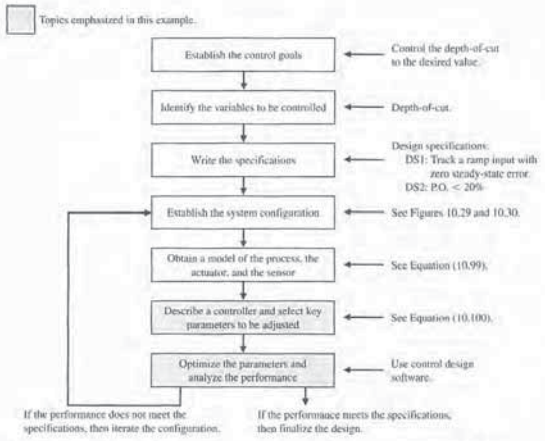

FIGURE 10.31 Elements of the control system design process emphasized in this milling machine control system design example.

Therefore,

$$E(s) = \frac{1}{1 + G_c(s)G(s)}R(s).$$

With $R(s) = a/s^2$ and using the final value theorem, we find that

$$e_{ss} = \lim_{t\to\infty} e(t) = \lim_{s\to 0} sE(s) = \lim_{s\to 0} s\frac{1}{1 + G_c(s)G(s)}\frac{a}{s^2},$$

or equivalently,

$$\lim_{s\to 0} sE(s) = \frac{a}{\lim_{s\to 0} sG_c(s)G(s)}.$$

According to DS1, we require that

$$\frac{a}{\lim_{s\to 0} sG_c(s)G(s)} < \frac{a}{8},$$

or

$$\lim_{s\to 0} sG_c(s)G(s) > 8.$$

Substituting for $G(s)$ and $G_c(s)$ from Equations (10.99) and (10.100), respectively, we obtain the compensated velocity constant

$$K_{\text{ecomp}} = \frac{2}{5}\frac{K}{\alpha}\frac{z}{p} = \frac{2}{5}\hat{K}\frac{z}{p} > 8,$$

where $\hat{K} = K/\alpha$. The compensated velocity constant is the velocity constant of the system when the lag compensator is in the loop.

The loop transfer function is

$$L(s) = G_c(s)G(s) = \frac{s+z}{s+p}\frac{2\hat{K}}{s(s+1)(s+5)}.$$

We separate the lag compensator from the process and obtain the uncompensated root locus by considering the feedback loop with the gain $\hat{K}$, but not the lag compensator zero and pole factors. The uncompensated root locus for the characteristic equation

$$1 + \hat{K}\frac{2}{s(s+1)(s+5)} = 0$$

is shown in Figure 10.33.

From DS2 we determine that the target damping ratio of the dominant roots is $\zeta > 0.45$. We find that $\hat{K} \le 2.48$ at $\zeta \ge 0.45$. Then with $\hat{K} = 2.0$ the uncompensated velocity constant is

$$K_{v,\text{unc}} = \lim_{s\to 0} s\frac{2\hat{K}}{s(s+1)(s+5)} = \frac{2\hat{K}}{5} = 0.8.$$

where $\Delta C_{\text{imp}}(t)$ is a function that goes to zero as t gets large. This leads us to consider $\Delta C_{\text{imp}}(t)$ as a sum of stable exponentials. Since the response does not oscillate, we might expect that the exponentials are, in fact, real exponentials,

$$\Delta C_{\text{imp}}(t) = \sum_i k_i e^{-\tau_i t},$$

where τ_i are positive real numbers. The data in Figure 10.32 can be fitted by the function

$$C_{\text{imp}}(t) = \frac{2}{5} + \frac{1}{10}e^{-5t} - \frac{1}{2}e^{-t},$$

for which the Laplace transform is

$$G(s) = \mathcal{L}\{C_{\text{imp}}(t)\} = \frac{2}{5}\frac{1}{s} + \frac{1}{10}\frac{1}{s+5} - \frac{1}{2}\frac{1}{s+1} = \frac{2}{s(s+1)(s+5)}.$$

Thus we can obtain the transfer function model of the milling machine.

The control goal is to develop a feedback system to track a desired step input. In this case the reference input is the desired depth-of-cut. The control goal is stated as

Control Goal
Control the depth-of-cut to the desired value.

The variable to be controlled is the depth-of-cut, or

Variable to Be Controlled
Depth-of-cut $y(t)$.

Since we are focusing on lead and lag controllers in this chapter, the key tuning parameters are the parameters associated with the compensator given in Equation (10.100).

Select Key Tuning Parameters
Compensator variables: p, z, and K.

The control design specifications are

Control Design Specifications

DS1 Track a ramp input, $R(s) = a/s^2$, with a steady-state tracking error less than $a/8$, where a is the ramp velocity.

DS2 Percent overshoot to a step input less than 20%.

The lag compensator is given by

$$G_c(s) = \frac{K}{\alpha}\frac{s+z}{s+p}, \quad |p| < |z|, \tag{10.100}$$

where $\alpha = z/p$. The tracking error is

$$E(s) = R(s) - Y(s) = (1 - T(s))R(s),$$

where

$$T(s) = \frac{G_c(s)G(s)}{1 + G_c(s)G(s)}.$$

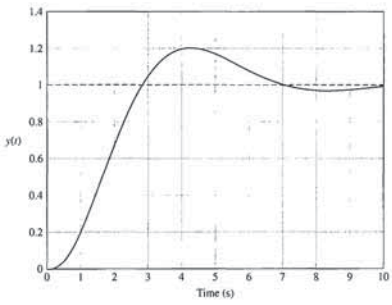

FIGURE 10.34
Step response for the compensated system.

10.13 SYSTEM DESIGN USING CONTROL DESIGN SOFTWARE

We want to use computers, when appropriate, to assist the designer in the selection of the parameters of a compensator. The development of algorithms for computer-aided design is an important alternative approach to the trial-and-error methods considered in earlier sections. Computer programs have been developed for the selection of suitable parameter values for compensators based on satisfaction of frequency response criteria such as the phase margin [3, 4].

In this section, the compensation of control systems is illustrated using frequency response and s-plane methods. We will consider again the rotor winder design example of Section 10.12 to illustrate the use of m-file scripts in designing and developing control systems with good performance characteristics. We examine both the lead and lag compensators for this design example and obtain the system response using computer-based analysis tools.

EXAMPLE 10.16 **Rotor winder control system**

Let us consider again the rotor winder control system shown in Figure 10.24. The design objective is to achieve high steady-state accuracy to a ramp input. The steady-state error to a unit ramp input $R(s) = 1/s^2$ is

$$e_{ss} = \frac{1}{K_v},$$

where

$$K_v = \lim_{s\to 0} \frac{G_c(s)}{50}.$$

The performance specification of overshoot and settling time must be considered, as must the steady-state tracking error. In all likelihood, a simple gain will not be

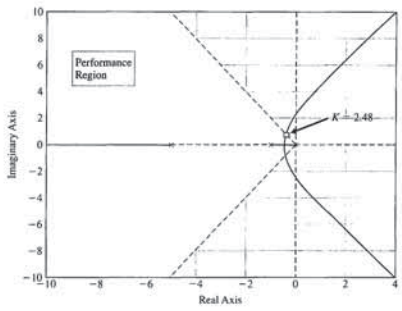

FIGURE 10.33
Root locus for the uncompensated system.

The compensated velocity constant is

$$K_{v,\text{comp}} = \lim_{s\to 0} s\frac{s+z}{s+p}\frac{2\hat{K}}{s(s+1)(s+5)} = \frac{z}{p}K_{v,\text{unc}}.$$

Therefore with $\alpha = z/p$, we obtain the relationship

$$\alpha = \frac{K_{v,\text{comp}}}{K_{v,\text{unc}}}.$$

We require $K_{v,\text{comp}} > 8$. A possible choice is $K_{v,\text{comp}} = 10$ as the desired velocity constant. Then

$$\alpha = \frac{K_{v,\text{comp}}}{K_{v,\text{unc}}} = \frac{10}{0.8} = 12.5.$$

But $\alpha = z/p$, thus our lag compensator should have $p = 0.08z$. If we select $z = 0.01$ then $p \approx 0.0008$.

The compensated loop transfer function is given by

$$G_c(s)G(s) = \hat{K}\frac{s+z}{s+p}\frac{2}{s(s+1)(s+5)}.$$

The lag compensator with z and p as above is determined to be

$$G_c(s) = 2.0\frac{s+0.01}{s+0.0008}. \tag{10.101}$$

The step response is shown in Figure 10.34. The percent overshoot is approximately 20%. The velocity error constant is approximately 10, which satisfies DS1. ■

$$G_c(s) = \frac{K(s+z)}{s+p},$$

where $|z| < |p|$. The lead compensator will give us the capability to improve the transient response. We will use a frequency-domain approach to design the lead compensator.

We want a steady-state error of less than 10% to a ramp input and $K_v = 10$. In addition to the steady-state specifications, we want to meet certain performance specifications: (1) settling time (with a 2% criterion) $T_s \le 3$ s, and (2) percent overshoot for a step input ≤10%. Solving for ζ and ω_n using

$$P.O. = 100\exp^{-\zeta\pi/\sqrt{1-\zeta^2}} = 10 \quad \text{and} \quad T_s = \frac{4}{\zeta\omega_n} = 3$$

yields $\zeta = 0.59$ and $\omega_n = 2.26$. We thus obtain the phase margin requirement:

$$\phi_{\text{pm}} = \frac{\zeta}{0.01} \approx 60°.$$

The steps leading to the final design are as follows:

1. Obtain the uncompensated system Bode diagram with $K = 500$, and compute the phase margin.
2. Determine the amount of necessary phase lead ϕ_m.
3. Evaluate α from $\sin\phi_m = (\alpha - 1)/(\alpha + 1)$.
4. Compute 10 log α and find the frequency ω_m on the uncompensated Bode diagram where the magnitude curve is equal to -10 log α.
5. In the neighborhood of ω_m on the uncompensated Bode diagram, draw a line through the 0-dB point at ω_m with slope equal to the current slope plus 20 dB/decade. Locate the intersection of the line with the uncompensated Bode diagram to determine the lead compensation zero location. Then calculate the lead compensator pole location as $p = \alpha z$.
6. Obtain the compensated Bode diagram and check the phase margin. Repeat any steps if necessary.
7. Raise the gain to account for the attenuation $1/\alpha$.
8. Verify the final design with simulation using step function inputs, and repeat any design steps if necessary.

We use three scripts in the design. The design scripts are shown in Figures 10.36–10.38. The script in Figure 10.36 is for the Bode diagram of the uncompensated system. The script in Figure 10.37 is for the detailed Bode diagram of the compensated system. The script in Figure 10.38 is for the step response analysis. The final lead compensator design is

$$G_c(s) = \frac{1800(s+3.5)}{s+25},$$

where $K = 1800$ was selected after iteratively using the m-file script.

The settling time and overshoot specifications are satisfied, but $K_v = 5$, resulting in a 20% steady-state error to a ramp input. It is possible to continue the design iteration and refine the compensator somewhat, although it should be clear that the lead compensator has added phase margin and improved the transient response as anticipated.

satisfactory, so we will also consider compensation utilizing lead and lag compensators, using both Bode diagram and root locus plot design methods. Our approach is to develop a series of m-file scripts to aid in the compensator designs.

Consider a simple gain controller

$$G_c(s) = K.$$

Then the steady-state error is

$$e_{ss} = \frac{50}{K}.$$

The larger we make K, the smaller is the steady-state error e_{ss}. However, we must consider the effect that increasing K has on the transient response, as shown in Figure 10.35. When $K = 500$, our steady-state error for a ramp is 10%, but the overshoot is 70%, and the settling time is approximately 8 seconds for a step input. We consider this to be unacceptable performance and thus turn to compensation. The two important compensator types that we consider are lead and lag compensators.

First, we try a lead compensator

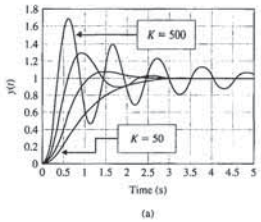

(a)

```
K=[50 100 200 500];          <- Compute response for four gains.
%
numg=[1]; deng=[1 15 50 0];
sysg=tf(numg,deng);
t=[0:0.1:5];
%
for i=1:4                    <- Closed-loop transfer function.
sys=feedback(K(i)*sysg,[1]);
y=step(sys,t);
Ys(:,i)=y;                   <- Store response for ith gain in Ys.
end
%
plot(t,Ys(:,1),t,Ys(:,2),t,Ys(:,3),t,Ys(:,4))
xlabel('Time (s)'), ylabel('y(t)')
```

(b)

FIGURE 10.35
(a) Transient response for simple gain controller.
(b) m-file script.

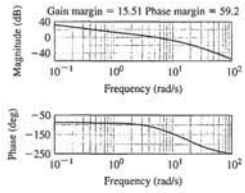

(a)

```
K=1800;
numg=[1]; deng=[1 15 50 0];
numgc=K*[1 3.5]; dengc=[1 25];
sysg=tf(numg,deng);
sysgc=tf(numgc,dengc);
sys=series(sysgc,sysg);
margin(sys)
```

Increase K to account for attenuation of $1/\alpha$.

Lead compensator.

(b)

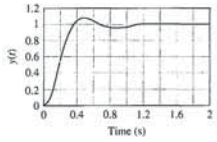

(a)

FIGURE 10.37
Lead compensator: (a) compensated Bode diagram, (b) m-file script.

```
K=1800;
%
numg=[1]; deng=[1 15 50 0]; sysg=tf(numg,deng);
numgc=K*[1 3.5]; dengc=[1 25]; sysgc=tf(numgc,dengc);
%
syso=series(sysgc,sysg);
sys=feedback(syso,[1]);
%
t=[0:0.01:2];
step(sys,t)
ylabel ('y(t)')
```

(b)

FIGURE 10.38
Lead compensator: (a) step response, (b) m-file script.

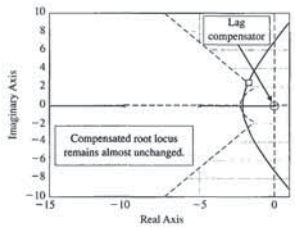

(a)

```
numg=[1]; deng=[1 15 50 0]; sysg=tf(numg,deng);
numgc=[1 0.1]; dengc=[1 0.01]; sysgc=tf(numgc,dengc);
sys=series(sysgc,sysg);
clf; rlocus(sys); hold on
%
zeta=0.5912; wn=2.2555;
x=[-10:0.1:-zeta*wn]; y=-(sqrt(1-zeta^2)/zeta)*x;
xc=[-10:0.1:-zeta*wn];c=sqrt(wn^2-xc.^2);
plot(x,y,':',x,-y,':',xc,c,':',xc,-c,':')
axis([-15,1,-10,10]);
```

(b)

FIGURE 10.40
Lag compensator: (a) compensated root locus, (b) m-file script.

Table 10.5 Compensator Design Results

Controller	Gain, K = 500	Lead	Lag
Step overshoot	70%	8%	13%
Settling time (seconds)	8	1	9
Steady-state error for ramp	10%	20%	10%
K_v	10	5	10

10.14 SEQUENTIAL DESIGN EXAMPLE: DISK DRIVE READ SYSTEM

In this chapter, we design a proportional-derivative controller (PD) to achieve the specified response to a unit step input. The specifications are given in Table 10.6. The closed-loop system is shown in Figure 10.42. A prefilter is used to eliminate any undesired effects of the term $s + z$ introduced in the closed-loop transfer function. We will

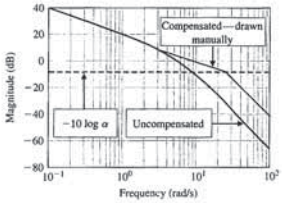

(a)

```
K=500;
numg=[1]; deng=[1 15 50 0]; sysg=tf(numg,deng);
sys=K*sysg;
%
[Gm,Pm,Wcg,Wcp]=margin(sys);
%
Phi=(60-Pm)*pi/180;
alpha=(1+sin(Phi))/(1-sin(Phi))
[mag,phase,w]=bode(sys);
mag_save(1,:)=mag(:,1,:);
%
M=-10*log10(alpha)*ones(length(w),1);
%
semilogx(w,20*log10(mag_save),w,M), grid
xlabel('Frequency (rad/s)'), ylabel('Magnitude (dB)')
```

Compute phase margin.

Additional phase lead.

Compute α.

Plot $-10\log(\alpha)$ line to aid in locating ω_m.

(b)

FIGURE 10.36
(a) Bode diagram. (b) m-file script.

To reduce the steady-state error, we can consider the lag compensator, which has the form

$$G_c(s) = \frac{K(s + z)}{s + p},$$

where $|p| < |z|$. We will use a root locus approach to design the lag compensator, although it can be done using a Bode diagram as well. The desired root location region of the dominant roots is specified by

$$\zeta = 0.59 \quad \text{and} \quad \omega_n = 2.26.$$

The steps in the design are as follows:

1. Obtain the root locus of the uncompensated system.
2. Locate suitable root locations on the uncompensated system that lie in the region defined by $\zeta = 0.59$ and $\omega_n = 2.26$.
3. Calculate the loop gain at the desired root location and the system error constant, $K_{v,\text{uncomp}}$.
4. Compute $\alpha = K_{v,\text{comp}}/K_{v,\text{uncomp}}$, where $K_{v,\text{comp}} = 10$.

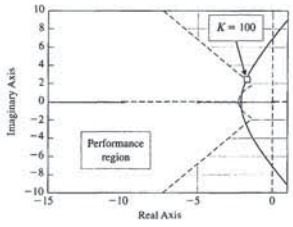

(a)

```
numg=[1]; deng=[1 15 50 0];
sysg=tf(numg,deng);
clf; rlocus(sysg); hold on
%
zeta=0.5912; wn=2.2555;
%
x=[-10:0.1:-zeta*wn]; y=-(sqrt(1-zeta^2)/zeta)*x;
xc=[-10:0.1:-zeta*wn]; c=sqrt(wn^2-xc.^2);
%
plot(x,y,':',x,-y,':',xc,c,':',xc,-c,':')
axis([-15,1,-10,10]);
```

Plot performance regions on locus.

(b)

FIGURE 10.39
Lag compensator: (a) uncompensated root locus, (b) m-file script.

5. With α known, determine suitable locations of the compensator pole and zero so that the compensated root locus still passes through the desired location.
6. Verify with simulation and repeat any steps if necessary.

The design methodology is illustrated in Figures 10.39–10.41. Using the rlocfind function, we can compute the gain K associated with the roots of our choice on the uncompensated root locus that lie in the performance region. We then compute α to ensure that we achieve the desired K_v. We place the lag compensator pole and zero to avoid affecting the uncompensated root locus. In Figure 10.40, the lag compensator pole and zero are very near the origin, at $z = -0.1$ and $p = -0.01$.

The settling time and overshoot specifications are not satisfied, but $K_v = 10$, as desired. It is possible to continue the design iteration and refine the compensator somewhat, although it should be clear that the lag compensator has improved the steady-state errors to a ramp input relative to the lead compensator design. The final lag compensator design is

$$G_c(s) = \frac{100(s + 0.1)}{s + 0.01}.$$

The resulting performance is summarized in Table 10.5. ■

use the deadbeat system of Section 10.11, where the desired closed-loop transfer function (Equation 10.86) is

$$T(s) = \frac{\omega_n^2}{s^2 + \alpha\omega_n s + \omega_n^2}. \tag{10.102}$$

For the second-order model shown in Figure 10.42, we require $\alpha = 1.82$ (see Table 10.2). Then the settling time is

$$\omega_n T_s = 4.82.$$

Since we want a settling time less than 50 ms, we will use $\omega_n = 120$. Then we expect $T_s = 40$ ms. Therefore, the denominator of Equation (10.102) is

$$s^2 + 218.4s + 14400. \tag{10.103}$$

The characteristic equation of the closed-loop system of Figure 10.42 is

$$s^2 + (20 + 5K_D)s + 5K_P = 0. \tag{10.104}$$

Equating Equations (10.103) and (10.104), we have

$$218.4 = 20 + 5K_D$$

and

$$14400 = 5K_P.$$

Therefore, $K_P = 2880$ and $K_D = 39.68$. Then we note that

$$G_c(s) = 39.68(s + 72.58).$$

The prefilter will then be

$$G_p(s) = \frac{72.58}{s + 72.58}.$$

The model neglected the motor field. Nevertheless, this design will be very accurate. The actual response is given in Table 10.6. All the specifications are satisfied.

10.15 SUMMARY

In this chapter, we have considered several alternative approaches to the design of feedback control systems. In the first two sections, we discussed the concepts of design and compensation and noted the several design cases that we completed in the preceding chapters. Then we examined the possibility of introducing cascade compensation networks within the feedback loops of control systems. The cascade compensation networks are useful for altering the shape of the root locus or frequency response of a system. The phase-lead network and the phase-lag

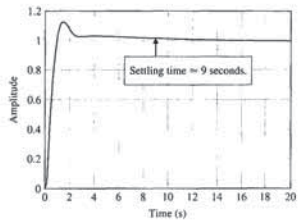

(a)

```
K=100;
%
numg=[1]; deng=[1 15 50 0]; sysg=tf(numg,deng);
numgc=K*[1 0.1]; dengc=[1 0.01]; sysgc=tf(numgc,dengc);
%
syso=series(sysgc,sysg);
sys=feedback(syso,[1]);
%
step(sys)
```

(b)

FIGURE 10.41 Lag compensator: (a) step response, (b) m-file response.

Table 10.6 Disk Drive Control System Specifications and Actual Performance

Performance Measure	Desired Value	Actual Response
Percent overshoot	Less than 5%	0.1%
Settling time	Less than 250 ms	40 ms
Maximum response to a unit disturbance	Less than 5×10^{-3}	6.9×10^{-5}

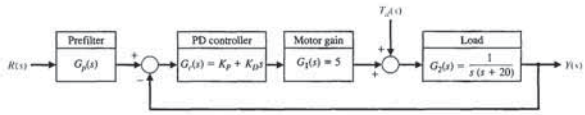

FIGURE 10.42 Disk drive control system with PD controller (second-order model).

Table 10.8 Operational Amplifier Circuits for Compensators

Type of Controller	$G_c(s) = \frac{V_0(s)}{V_i(s)}$	
PD	$G_c = \frac{R_4R_2}{R_3R_1}(R_1C_1s + 1)$	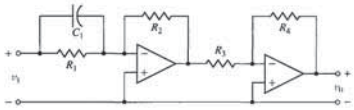
PI	$G_c = \frac{R_4R_2(R_2C_2s + 1)}{R_3R_1(R_2C_2s)}$	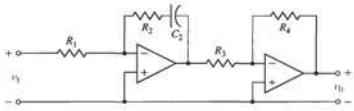
Lead or lag Lead if $R_1C_1 > R_2C_2$ Lag if $R_1C_1 < R_2C_2$	$G_c = \frac{R_4R_2(R_1C_1s + 1)}{R_3R_1(R_2C_2s + 1)}$	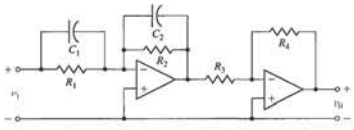

SKILLS CHECK

In this section, we provide three sets of problems to test your knowledge: True or False, Multiple Choice, and Word Match. To obtain direct feedback, check your answers with the answer key provided at the conclusion of the end-of-chapter problems. Use the block diagram in Figure 10.43 as specified in the various problem statements.

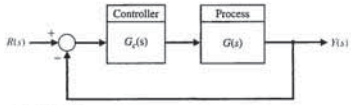

FIGURE 10.43 Block diagram for the Skills Check.

network were considered in detail as candidates for system compensators. Then system compensation was studied by using a phase-lead s-plane network on the Bode diagram and the root locus s-plane. We noted that the phase-lead compensator increases the phase margin of the system and thus provides additional stability. When the design specifications include an error constant, the design of a phase-lead network is more readily accomplished on the Bode diagram. Alternatively, when an error constant is not specified but the settling time and overshoot for a step input are specified, the design of a phase-lead network is more readily carried out on the s-plane. When large error constants are specified for a feedback system, it is usually easier to compensate the system by using integration (phase-lag) networks. We also noted that the phase-lead compensation increases the system bandwidth, whereas the phase-lag compensation decreases the system bandwidth. The bandwidth may often be an important factor when noise is present at the input and generated within the system. Also, we noted that a satisfactory system is obtained when the asymptotic course for magnitude of the compensated system crosses the 0-dB line with a slope of -20 dB/decade. The characteristics of the phase-lead and phase-lag compensation networks are summarized in Table 10.7. Operational amplifier circuits for phase-lead and phase-lag and for PI and PD compensators are summarized in Table 10.8 [1]. The use of these controllers has been widely demonstrated in this and earlier chapters. These operational amplifier circuits are widely used in industrial practice to provide the compensator $G_c(s)$.

Table 10.7 A Summary of the Characteristics of Phase-Lead and Phase-Lag Compensation Networks

	Compensation	
	Phase-Lead	Phase-Lag
Approach	Addition of phase-lead angle near crossover frequency on Bode diagram. Add lead network to yield desired dominant roots in s-plane.	Addition of phase-lag to yield an increased error constant while maintaining desired dominant roots in s-plane or phase margin on Bode diagram
Results	1. Increases system bandwidth 2. Increases gain at higher frequencies	1. Decreases system bandwidth
Advantages	1. Yields desired response 2. Improves dynamic response	1. Suppresses high-frequency noise 2. Reduces steady-state error
Disadvantages	1. Requires additional amplifier gain 2. Increases bandwidth and thus susceptibility to noise 3. May require large values of components for RC network	1. Slows down transient response 2. May require large values of components for RC network
Applications	1. When fast transient response is desired	1. When error constants are specified
Situations not applicable	1. When phase decreases rapidly near crossover frequency	1. When no low-frequency range exists where phase is equal to desired phase margin

9. Consider the feedback system in Figure 10.43, where the plant model is

$$G(s) = \frac{500}{s(s + 50)}$$

and the controller is a proportional-plus-integral (PI) controller given by

$$G_c(s) = K_P + \frac{K_I}{s}.$$

Selecting $K_I = 1$, determine a suitable value of K_P for a percent overshoot of approximately 20%.

a. $K_P = 0.5$

b. $K_P = 1.5$

c. $K_P = 2.5$

d. $K_P = 5.0$

10. Consider the feedback system in Figure 10.43, where

$$G(s) = \frac{1}{s(1 + s/8)(1 + s/20)}.$$

The design specifications are: $K_v \geq 100$, $G.M. \geq 10$ dB, $P.M. \geq 45°$, and the crossover frequency, $\omega_c \geq 10$ rad/s. Which of the following controllers meets these specifications?

a. $G_c(s) = \dfrac{(1 + s)(1 + 20s)}{(1 + s/0.01)(1 + s/50)}$

b. $G_c(s) = \dfrac{100(1 + s)(1 + s/5)}{(1 + s/0.1)(1 + s/50)}$

c. $G_c(s) = \dfrac{1 + 100s}{1 + 120s}$

d. $G_c(s) = 100$

11. Consider a feedback system in which a phase-lead compensator

$$G_c(s) = \frac{1 + 0.4s}{1 + 0.04s}$$

is placed in series with the plant

$$G(s) = \frac{500}{(s + 1)(s + 5)(s + 10)}.$$

The feedback system is a negative unity feedback control system shown in Figure 10.43. Compute the gain and phase margin.

a. $G.M. = \infty$ dB, $P.M. = 60°$

b. $G.M. = 20.5$ dB, $P.M. = 47.8°$

c. $G.M. = 8.6$ dB, $P.M. = 33.6°$

d. Closed-loop system is unstable.

12. Consider the feedback system in Figure 10.43, where

$$G(s) = \frac{1}{s(s + 10)(s + 15)}.$$

Which of the following represents a suitable lag compensator that achieves a steady-state error less than 10% for a ramp input and a damping ratio of the closed-loop system dominant roots of $\zeta \approx 0.707$.

a. $G_c(s) = \dfrac{2850(s + 1)}{(10s + 1)}$

In the following **True or False** and **Multiple Choice** problems, circle the correct answer.

1. A cascade compensator network is a compensator network that is placed in parallel with the system process. *True or False*

2. Generally, a phase-lag network speeds up the transient response. *True or False*

3. The arrangement of the system and the selection of suitable components and parameters is part of the process of control system design. *True or False*

4. A deadbeat response of a system is a rapid response with minimal overshoot and zero steady-state error to a step input. *True or False*

5. A phase-lead network can be used to increase the system bandwidth. *True or False*

6. Consider the feedback system in Figure 10.43, where

$$G(s) = \frac{1000}{s(s + 400)(s + 20)}.$$

A phase lag compensator is designed for the system to give additional attenuation at higher frequencies. The compensator is

$$G_c(s) = \frac{1 + 0.25s}{1 + 2s}.$$

When compared with the uncompensated system (that is, $G_c(s) = 1$), the compensated system utilizing the lag compensator:

a. Increases the phase lag near the cross-over frequency.

b. Decreases the phase margin.

c. Provides additional attenuation at higher frequencies.

d. All of the above.

7. A position control system can be analyzed using the feedback system in Figure 10.43, where the process transfer function is

$$G(s) = \frac{5}{s(s + 1)(0.4s + 1)}.$$

A phase-lag compensator that provides a phase margin of $P.M. \approx 30°$ is:

a. $G_c(s) = \dfrac{1 + s}{1 + 106s}$

b. $G_c(s) = \dfrac{1 + 26s}{1 + 115s}$

c. $G_c(s) = \dfrac{1 + 106s}{1 + 118s}$

d. None of the above

8. Consider a unity feedback system in Figure 10.43, where

$$G(s) = \frac{1450}{s(s + 3)(s + 25)}.$$

A lead compensator is introduced into the feedback loop, where

$$G_c(s) = \frac{1 + 0.3s}{1 + 0.03s}.$$

The peak magnitude and the bandwidth of the closed-loop frequency response are:

a. $M_{p_c} = 1.9$ dB; $\omega_b = 12.1$ rad/s

b. $M_{p_c} = 12.8$ dB; $\omega_b = 14.9$ rad/s

c. $M_{p_c} = 5.3$ dB; $\omega_b = 4.7$ rad/s

d. $M_{p_c} = 4.3$ dB; $\omega_b = 24.2$ rad/s

b. Phase lead compensation	A network that provides a positive phase angle over the frequency range of interest.	_____
c. PI controller	A network that acts, in part, like an integrator.	_____
d. Lead-lag network	A network with the characteristics of both a lead network and a lag network.	_____
e. Design of a control system	A network that provides a negative phase angle and a significant attenuation over the frequency range of interest.	_____
f. Phase lag compensation	An additional component or circuit that is inserted into the system to compensate for a performance deficiency.	_____
g. Integration network	A compensator network placed in cascade or series with the system process.	_____
h. Compensator	Controller with a proportional term and an integral term.	_____
i. Compensation	A transfer function, $G_p(s)$, that filters the input signal $R(s)$ prior to calculating the error signal.	_____
j. Phase-lag network	The arrangement or the plan of the system structure and the selection of suitable components and parameters.	_____
k. Cascade compensation network	The alteration or adjustment of a control system in order to provide a suitable performance.	_____
l. Phase-lead network	A widely-used compensator that possesses one zero and one pole with the pole closer to the origin of the s-plane.	_____
m. Prefilter	A widely-used compensator that possesses one zero and one pole with the zero closer to the origin of the s-plane.	_____

EXERCISES

E10.1 A negative feedback control system has a transfer function

$$G(s) = \frac{K}{s + 2}.$$

We select a compensator

$$G_c(s) = \frac{s + a}{s},$$

in order to achieve zero steady-state error for a step input. Select a and K so that the overshoot to a step is approximately 5% and the settling time (with a 2% criterion) is approximately 1 second.

Answer: $K = 6$, $a = 5.6$

E10.2 A control system with negative unity feedback has a process

$$G(s) = \frac{400}{s(s + 40)},$$

and we wish to use proportional plus integral compensation, where

$$G_c(s) = K_P + \frac{K_I}{s}.$$

Note that the steady-state error of this system for a ramp input is zero. (a) Set $K_I = 1$ and find a suitable value of K_P so the step response will have an overshoot of approximately 20%. (b) What is the expected

b. $G_c(s) = \dfrac{100(s + 1)(s + 5)}{(s + 10)(s + 50)}$

c. $G_c(s) = \dfrac{10}{s + 1}$

d. Closed-loop system cannot track a ramp input for any $G_c(s)$.

13. A viable lag-compensation for a unity negative feedback system with plant transfer function

$$G(s) = \frac{1000}{(s + 8)(s + 14)(s + 20)}$$

that satisfies the design specifications: (i) percent overshoot $P.O. \leq 5\%$; (ii) rise time $T_r \leq 20$ seconds, and (iii) position error constant $K_p > 6$, is which of the following:

a. $G_c(s) = \dfrac{s + 1}{s + 0.074}$

b. $G_c(s) = \dfrac{s + 0.074}{s + 1}$

c. $G_c(s) = \dfrac{20s + 1}{100s + 1}$

d. $G_c(s) = 20$

14. Consider the feedback system depicted in Figure 10.43, where

$$G(s) = \frac{1}{s(s + 4)^2}.$$

A suitable compensation $G_c(s)$ for this system that satisfies the specifications: (i) $P.O. \leq 20\%$, and (ii) velocity error constant $K_v \geq 10$, is which of the following:

a. $G_c(s) = \dfrac{s + 4}{(s + 1)}$

b. $G_c(s) = \dfrac{160(10s + 1)}{200s + 1}$

c. $G_c(s) = \dfrac{24(s + 1)}{s + 4}$

d. None of the above

15. Using a Nichols chart, determine the gain and phase margin of the system in Figure 10.43 with loop gain transfer function

$$L(s) = G_c(s)G(s) = \frac{8s + 1}{s(s^2 + 2s + 4)}.$$

a. $G.M. = 20.4$ dB, $P.M. = 58.1°$

b. $G.M. = \infty$ dB, $P.M. = 47°$

c. $G.M. = 6$ dB, $P.M. = 45°$

d. $G.M. = \infty$ dB, $P.M. = 23°$

In the following **Word Match** problems, match the term with the definition by writing the correct letter in the space provided.

a. Deadbeat response	A system with a rapid response, minimal overshoot, and zero steady-state error for a step input.	_____

E10.8 A negative unity feedback system has a plant

$$G(s) = \frac{2257}{s(\tau s + 1)},$$

where $\tau = 2.8$ ms. Select a compensator

$$G_c(s) = K_P + K_I/s,$$

so that the dominant roots of the characteristic equation have ζ equal to $1/\sqrt{2}$. Plot $y(t)$ for a step input.

E10.9 A control system with a controller is shown in Figure E10.9. Select K_P and K_I so that the overshoot to a step input is equal to 5% and the velocity constant K_v is equal to 5. Verify the results of your design.

E10.10 A control system with a controller is shown in Figure E10.10. We will select $K_I = 2$ in order to provide a reasonable steady-state error to a step [8]. Find K_P to obtain a phase margin of 60°. Find the peak time and percent overshoot of this system.

E10.11 A unity feedback system has

$$G(s) = \frac{1350}{s(s + 2)(s + 30)}.$$

A lead network is selected so that

$$G_c(s) = \frac{1 + 0.25s}{1 + 0.025s}.$$

Determine the peak magnitude and the bandwidth of the closed-loop frequency response using (a) the Nichols chart, and (b) a plot of the closed-loop frequency response.

Answer: $M_{pr} = 2.3$ dB, $\omega_B = 22$

E10.12 The control of an automobile ignition system has unity negative feedback and a loop transfer function $G_c(s)G(s)$, where

$$G(s) = \frac{K}{s(s + 5)} \quad \text{and} \quad G_c(s) = K_P + K_I/s.$$

A designer selects $K_I/K_P = 0.5$ and asks you to determine KK_P so that the complex roots have a ζ of $1/\sqrt{2}$.

E10.13 The design of Example 10.3 determined a lead network in order to obtain desirable dominant root locations using a cascade compensator $G_c(s)$ in the system configuration shown in Figure 10.1(a). The same lead network would be obtained if we used the feedback compensation configuration of Figure 10.1(b). Determine the closed-loop transfer function $T(s) = Y(s)/R(s)$ of both the cascade and feedback configurations, and show how the transfer function of each configuration differs. Explain how the response to a step $R(s)$ will be different for each system.

E10.14 A robot will be operated by NASA to build a permanent lunar station. The position control system for the gripper tool is shown in Figure 10.1(a), where $H(s) = 1$, and

$$G(s) = \frac{5}{s(s + 1)(0.25s + 1)}.$$

Determine a compensator lag network $G_c(s)$ that will provide a phase margin of 45°.

Answer: $G_c(s) = \dfrac{1 + 7.5s}{1 + 110s}$

E10.15 A unity feedback control system has a plant transfer function

$$G(s) = \frac{40}{s(s + 2)}.$$

We desire to attain a steady-state error to a ramp $r(t) = At$ of less than $0.05A$ and a phase margin of 30°. We desire to have a crossover frequency ω_c of 10 rad/s.

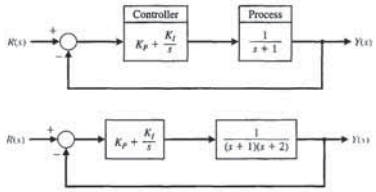

FIGURE E10.9
Design of a controller.

FIGURE E10.10
Design of a PI controller.

settling time (with a 2% criterion) of the compensated system?

Answer: $K_P = 0.5$

E10.3 A unity negative feedback control system in a manufacturing system has a process transfer function

$$G(s) = \frac{e^{-s}}{s + 1},$$

and it is proposed that we use a compensator to achieve a 5% overshoot to a step input. The compensator is [4]

$$G_c(s) = K\left(1 + \frac{1}{\tau s}\right),$$

which provides proportional plus integral control. Show that one solution is $K = 0.5$ and $\tau = 1$.

E10.4 Consider a unity negative feedback system with

$$G(s) = \frac{K}{s(s + 5)(s + 10)},$$

where K is set equal to 100 in order to achieve a specified $K_v = 2$. We wish to add a lead-lag compensator

$$G_c(s) = \frac{(s + 0.15)(s + 0.7)}{(s + 0.015)(s + 7)}.$$

Show that the gain margin of the compensated system is 28.6 dB and that the phase margin is 75.4°.

E10.5 Consider a unity feedback system with the transfer function

$$G(s) = \frac{K}{s(s + 2)(s + 4)}.$$

We desire to obtain the dominant roots with $\omega_n = 3$ and $\zeta = 0.5$. We wish to obtain a $K_v = 2.7$. Show that we require a compensator

$$G_c(s) = \frac{7.53(s + 2.2)}{(s + 16.4)}.$$

Determine the value of K that should be selected.

Answer: $K = 22$

E10.6 Consider again the wind tunnel control system of Problem P7.31. When $K = 326$, find $T(s)$ and estimate the expected overshoot and settling time (with a 2% criterion). Compare your estimates with the actual overshoot of 60% and a settling time of 4 seconds. Explain the discrepancy in your estimates.

E10.7 NASA astronauts retrieved a satellite and brought it into the cargo bay of the space shuttle, as shown in Figure E10.7(a). A model of the feedback control system is shown in Figure. E10.7(b). Determine the value of K that will result in a phase margin of 40° when $T = 0.6$ s.

Answer: $K = 26.93$

(a)

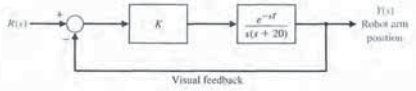

(b)

FIGURE E10.7
Retrieval of a satellite.

PROBLEMS

P10.1 The design of a lunar excursion module (LEM) is an interesting control problem. The attitude control system for the lunar vehicle is shown in Figure P10.1. The vehicle damping is negligible, and the attitude is controlled by gas jets. The torque, as a first approximation, will be considered to be proportional to the signal $V(s)$ so that $T(s) = K_2V(s)$. The loop gain may be selected by the designer in order to provide a suitable damping. A damping ratio of $\zeta = 0.6$ with a settling time (with a 2% criterion) of less than 2.5 seconds is required. Using a lead network compensation, select the necessary compensator $G_c(s)$ by using (a) frequency response techniques and (b) root locus methods.

P10.2 A magnetic tape recorder transport for modern computers requires a high-accuracy, rapid-response control system. The requirements for a specific transport are as follows: (1) The tape must stop or start in 10 ms, and (2) it must be possible to read 45,000 characters per second. This system was discussed in Problem P7.11. We desire to set $J = 5 \times 10^{-3}$, and K_1 is set on the basis of the maximum error allowable for a velocity input. In this case, we desire to maintain a steady-state speed error of less than 5%. We will use a tachometer in this case and set $K_a = 50{,}000$ and $K_2 = 1$. To provide a suitable performance, a compensator $G_c(s)$ is inserted immediately following the photocell transducer. Select a compensator $G_c(s)$ so that the overshoot of the system for a step input is less than 25%. We will assume that $\tau_1 = \tau_a = 0$.

P10.3 A simplified version of the attitude rate control for the F-94 or X-15 type aircraft is shown in Figure P10.3. When the vehicle is flying at four times the speed of sound (Mach 4) at an altitude of 100,000 ft, the parameters are [26]

$$\frac{1}{\tau_a} = 1.0, \qquad K_1 = 1.0,$$

$$\zeta\omega_a = 1.0, \quad \text{and} \quad \omega_a = 4.$$

Design a compensator $G_c(s)$ so that the response to a step input has an overshoot of less than 5% and a settling time (with a 2% criterion) of less than 5 seconds.

P10.4 Magnetic particle clutches are useful actuator devices for high power requirements because they can typically provide a 200-W mechanical power output. The particle clutches provide a high torque-to-inertia ratio and fast time-constant response. A particle clutch positioning system for nuclear reactor rods is shown in Figure P10.4. The motor drives two counter-rotating clutch housings.

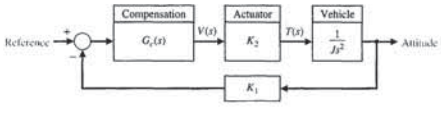

FIGURE P10.1
Attitude control system for a lunar excursion module.

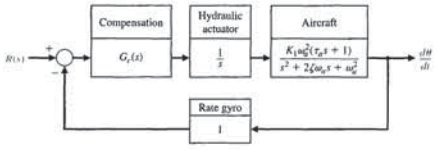

FIGURE P10.3
Aircraft attitude control.

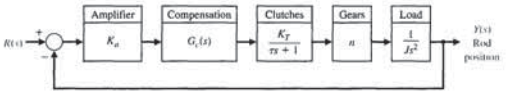

FIGURE P10.4
Nuclear reactor rod control.

Use the methods of Section 10.9 to determine whether a lead or a lag compensator is required.

E10.16 Consider again the system and specifications of Exercise E10.15 when the required crossover frequency is 2 rad/s.

E10.17 Consider again the system of Exercise 10.9. Select K_P and K_I so that the step response is deadbeat and the settling time (with a 2% criterion) is less than 2 seconds.

E10.18 The nonunity feedback control system shown in Figure E10.18 has the transfer functions

$$G(s) = \frac{1}{s - 20} \quad \text{and} \quad H(s) = 10.$$

Design a compensator $G_c(s)$ and prefilter $G_p(s)$ so that the closed-loop system is stable and meets the following specifications: (i) a percent overshoot to a unit step input of less than 10%, (ii) a settling time of less than 2 seconds, and (iii) zero steady-state tracking error to a unit step.

E10.19 A unity feedback control system has the plant transfer function

$$G(s) = \frac{1}{s(s - 5)}.$$

Design a PID controller of the form

$$G_c(s) = K_p + K_D s + \frac{K_I}{s}$$

so that the closed-loop system has a settling time less than 1 second to a unit step input.

E10.20 Consider the system shown in Figure E10.20. Design the proportional-derivative controller $G_c(s) = K_P + K_D s$ such that the system has a phase margin of $40° \leq P.M. \leq 60°$.

E10.21 Consider the unity feedback system shown in Figure E10.21. Design the controller gain, K, such that the maximum value of the output $y(t)$ in response to a unit step disturbance $T_d(s) = 1/s$ is less than 0.1.

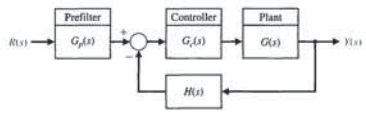

FIGURE E10.18
Nonunity feedback system with a prefilter.

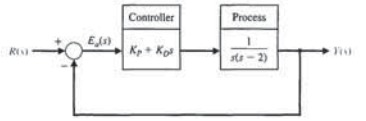

FIGURE E10.20
Unity feedback system with PD controller.

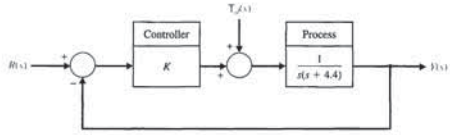

FIGURE E10.21
Closed-loop feedback system with a disturbance input.

(a)

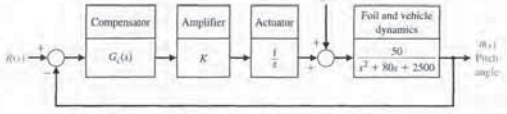

(b)

FIGURE P10.9
(a) The Avernar ferry built for ferry service between Barcelona and the Balearic Islands. (b) A block diagram of the lift control system.

seas with waves up to 8 ft in amplitude at a speed of 40 knots as a result of an automatic stabilization control system. Stabilization is achieved by means of flaps on the main foils and the adjustment of the aft foil. The stabilization control system maintains a level flight through rough seas. Thus, a system that minimizes deviations from a constant lift force or, equivalently, that minimizes the pitch angle θ has been designed. A block diagram of the lift control system is shown in Figure P10.9(b). The desired response of the system to wave disturbance is a constant-level travel of the craft. Establish a set of reasonable specifications and design a compensator $G_c(s)$ so that the performance of the system is suitable. Assume that the disturbance is due to waves with a frequency $\omega = 6$ rad/s.

P10.10 A unity feedback system of the form shown in Figure 10.1(a) has a plant

$$G(s) = \frac{5}{s(s^2 + 6s + 10)}.$$

(a) Determine the step response when $G_c(s) = 1$, and calculate the settling time and steady state for a ramp input $r(t) = t, t > 0$. (b) Design a lag network using the root locus method so that the velocity constant is increased to 10. Determine the settling time (with a 2% criterion) of the compensated system.

P10.11 A unity feedback control system of the form shown in Figure 10.1(a) has a plant

$$G(s) = \frac{160}{s^2}.$$

Select a lead-lag compensator so that the percent overshoot for a step input is less than 5% and the settling time (with a 2% criterion) is less than 1 second. It also is desired that the acceleration constant K_a be greater than 7500 (see Table 5.5).

P10.12 A unity feedback system has a plant

$$G(s) = \frac{20}{s(1 + 0.1s)(1 + 0.05s)}.$$

Select a compensator $G_c(s)$ so that the phase margin is at least 75°. Use a two-stage lead compensator

$$G_c(s) = \frac{K(1 + s/\omega_1)(1 + s/\omega_3)}{(1 + s/\omega_2)(1 + s/\omega_4)}$$

It is required that the error for a ramp input be 0.5% of the magnitude of the ramp input ($K_v = 200$).

P10.13 Materials testing requires the design of control systems that can faithfully reproduce normal specimen operating environments over a range of specimen parameters [23]. From the control system design viewpoint, a materials-testing machine system can be considered a servomechanism in which we want to have the load waveform track the reference signal. The system is shown in Figure P10.13.

(a) Determine the phase margin of the system with $G_c(s) = K$, choosing K so that a phase margin of 50° is achieved. Determine the system bandwidth for this design.

(b) The additional requirement introduced is that the velocity constant K_v be equal to 2.0. Design a lag

The clutch housings are geared through parallel gear trains, and the direction of the servo output is dependent on the clutch that is energized. The time constant of a 200-W clutch is $\tau = 1/40$ s. The constants are such that $K_T n/J = 1$. We want the maximum overshoot for a step input to be in the range of 10% to 20%. Design a compensating network so that the system is adequately stabilized. The settling time (with a 2% criterion) of the system should be less than or equal to 2 seconds.

P10.5 A stabilized precision rate table uses a precision tachometer and a DC direct-drive torque motor, as shown in Figure P10.5. We want to maintain a high steady-state accuracy for the speed control. To obtain a zero steady-state error for a step command design, select a proportional plus integral compensator. Select the appropriate gain constants so that the system has an overshoot of approximately 10% and a settling time (with a 2% criterion) less than 1.5 seconds.

P10.6 Repeat Problem P10.5 by using a lead network compensator, and compare the results.

P10.7 A chemical reactor process whose production rate is a function of catalyst addition is shown in block diagram form in Figure P10.7 [10]. The time delay is $T = 50$ s, and the time constant τ is approximately 40 s. The gain of the process is $K = 1$. Design a compensation by using Bode diagram methods in order to provide a suitable system response. We want to have a steady-state error less than $0.10A$ for a step input $R(s) = A/s$. For the system with the compensation added, estimate the settling time of the system.

P10.8 A numerical path-controlled machine turret lathe is an interesting problem in attaining sufficient accuracy [2, 23]. A block diagram of a turret lathe control system is shown in Figure P10.8. The gear ratio is $n = 0.1$, $J = 10^{-3}$, and $b = 10^{-2}$. It is necessary to attain an accuracy of 5×10^{-4} in., and therefore a steady-state position accuracy of 2.5% is specified for a ramp input. Design a cascade compensator to be inserted before the silicon-controlled rectifiers in order to provide a response to a step command with an overshoot of less than 5%. A suitable damping ratio for this system is 0.7. The gain of the silicon-controlled rectifiers is $K_R = 5$. Design a suitable lag compensator by using the (a) Bode diagram method and (b) s-plane method.

P10.9 The Avernar ferry, shown in Figure P10.9(a), is a large 670-ton ferry hydrofoil built for Mediterranean ferry service. It is capable of 45 knots (52 mph) [29]. The boat's appearance, like its performance, derives from the innovative design of the narrow "wavepiercing" hulls which move through the water like racing shells. Between the hulls is a third quasihull which gives additional buoyancy in rough seas. Loaded with 900 passengers and crew, and a mix of cars, buses, and freight cars trucks, one of the boats can carry almost its own weight. The Avernar is capable of operating in

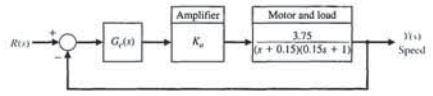

FIGURE P10.5
Stabilized rate table.

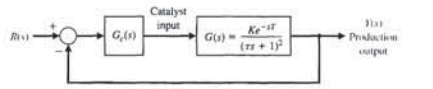

FIGURE P10.7
Chemical reactor control.

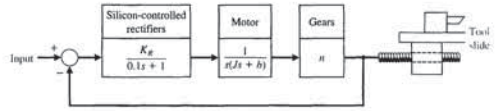

FIGURE P10.8
Path-controlled turret lathe.

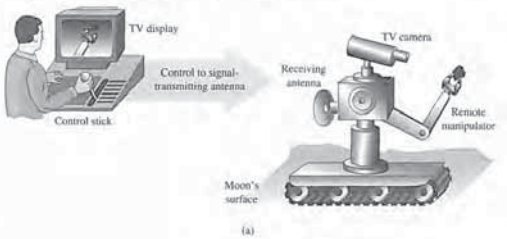

(a)

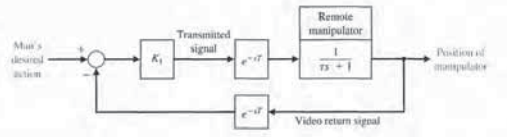

(b)

FIGURE P10.18
(a) Conceptual diagram of a remote manipulator on the Moon controlled by a person on the Earth. (b) Feedback diagram of the remote manipulator control system with τ = transmission time delay of the video signal.

and accident recovery activities. These developments suggest that the application of remotely operated devices can significantly reduce radiation exposure to personnel and improve maintenance-program performance.

Currently, an operational robotic system is under development to address particular operational problems within a nuclear power plant. This device, IRIS (Industrial Remote Inspection System), is a general-purpose surveillance system that conducts particular inspection and handling tasks with the goal of significantly reducing personnel exposure to high radiation fields [12]. The device is shown in Figure P10.19. The open-loop transfer function is

$$G(s) = \frac{Ke^{-sT}}{(s + 1)(s + 3)}.$$

(a) Determine a suitable gain K for the system when $T = 0.5$ s, so that the overshoot to a step input is less than 30%. Determine the steady-state error. (b) Design a compensator

$$G_p(s) = \frac{s + 2}{s + b}$$

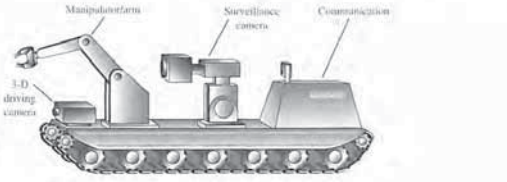

FIGURE P10.19
Remotely controlled robot for nuclear plants.

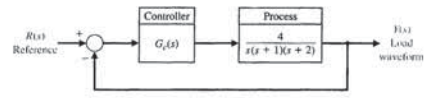

FIGURE P10.13
Materials testing machine system.

network so that the phase margin is 50° and $K_v = 2$.

P10.14 For the system described in Problem P10.13, the goal is to achieve a phase margin of 50° with the additional requirement that the time to settle (to within 2% of the final value) be less than 4 seconds. Design a lead network to meet the specifications. As before, we require $K_v = 2$.

P10.15 A robot with an extended arm has a heavy load, whose effect is a disturbance, as shown in Figure P10.15 [22]. Let $R(s) = 0$ and design $G_p(s)$ so that the effect of the disturbance is less than 20% of the open-loop system effect.

P10.16 A driver and car may be represented by the simplified model shown in Figure P10.16 [17]. The goal is to have the speed adjust to a step input with less than 10% overshoot and a settling time (with a 2% criterion) of 1 second. Select a proportional plus integral (PI) controller to yield these specifications. For the selected controller, determine the actual response (a) for $G_p(s) = 1$ and (b) with a prefilter $G_p(s)$ that removes the zero from the closed-loop transfer function $T(s)$.

P10.17 A unity feedback control system for a robot submarine has a plant with a third-order transfer function [20]:

$$G(s) = \frac{K}{s(s + 10)(s + 50)}.$$

We want the overshoot to be approximately 7.5% for a step input and the settling time (with a 2% criterion) of the system be 400 ms. Find a suitable phase-lead compensator by using root locus methods. Let the zero of the compensator be located at $s = -15$, and determine the compensator pole. Determine the resulting system K_v.

P10.18 NASA is developing remote manipulators that can be used to extend the hand and the power of humankind through space by means of radio. A concept of a remote manipulator is shown in Figure P10.18(a) [11, 22]. The closed-loop control is shown schematically in Figure P10.18(b). Assuming an average distance of 238,855 miles from Earth to the Moon, the time delay T in transmission of a communication signal is 1.28 seconds. The operator uses a control stick to control remotely the manipulator placed on the Moon to assist in geological experiments, and the TV display to access the response of the manipulator. The time constant of the manipulator is $\frac{1}{4}$ second.

(a) Set the gain K_1 so that the system has a phase margin of approximately 30°. Evaluate the percentage steady-state error for this system for a step input. (b) To reduce the steady-state error for a position command input to 5%, add a lag compensation network in cascade with K_1. Plot the step response.

P10.19 There have been significant developments in the application of robotics technology to nuclear power plant maintenance problems. Thus far, robotics technology in the nuclear industry has been used primarily on spent-fuel reprocessing and waste management. Today, the industry is beginning to apply the technology to such areas as primary containment inspection, reactor maintenance, facility decontamination,

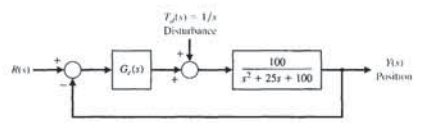

FIGURE P10.15
Robot control.

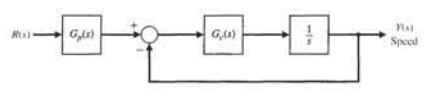

FIGURE P10.16
Speed control of an automobile.

Using root locus methods, select a suitable value for K_1 and b so the system has a damping ratio for the underdamped roots of $\zeta = 0.50$. Assume, if appropriate, that the pole of the air gap feedback loop ($s = -200$) can be neglected.

P10.26 A computer uses a printer as a fast output device. We desire to maintain accurate position control while moving the paper rapidly through the printer. Consider a system with unity feedback and a transfer function for the motor and amplifier of

$$G(s) = \frac{0.15}{s(s + 1)(5s + 1)}.$$

Design a lead network compensator so that the system bandwidth is 0.75 rad/s and the phase margin is 30°. Use a lead network with $\alpha = 10$.

P10.27 An engineering design team is attempting to control a process shown in Figure P10.27. The system has a controller $G_c(s)$, but the design team is unable to select $G_c(s)$ appropriately. It is agreed that a system with a phase margin of 50° is acceptable, but $G_c(s)$ is unknown. Determine $G_c(s)$.

First, let $G_c(s) = K$ and find (a) a value of K that yields a phase margin of 50° and the system's step response for this value of K. (b) Determine the settling time, percent overshoot, and the peak time. (c) Obtain the system's closed-loop frequency response, and determine M_{pw} and the bandwidth.

The team has decided to let

$$G_c(s) = \frac{K(s + 12)}{(s + 20)}$$

and to repeat parts (a), (b), and (c). Determine the gain K that results in a phase margin of 50° and then proceed to evaluate the time response and the closed-loop frequency response. Prepare a table contrasting the results of the two selected controllers for $G_c(s)$ by comparing settling time (with a 2% criterion), percent overshoot, peak time, M_{pw}, and bandwidth.

P10.28 An adaptive suspension vehicle uses a legged locomotion principle. The control of the leg can be represented by a unity feedback system with [12]

$$G(s) = \frac{K}{s(s + 10)(s + 14)}.$$

We desire to achieve a steady-state error for a ramp input of 10% and a damping ratio of the dominant roots of 0.707. Determine a suitable lag compensator, and determine the actual overshoot and the time to settle (to within 2% of the final value).

P10.29 A liquid-level control system (see Figure 9.32) has a loop transfer function

$$L(s) = G_c(s)G(s)H(s),$$

where $H(s) = 1$, $G_c(s)$ is a compensator, and the plant is

$$G(s) = \frac{10e^{-\tau s}}{s^2(s + 10)},$$

where $T = 50$ ms. Design a compensator so that M_{pw} does not exceed 3.5 dB and ω_r is approximately 1.4 rad/s. Predict the overshoot and settling time (with a 2% criterion) of the compensated system when the input is a step. Plot the actual response.

P10.30 An automated guided vehicle (AGV) can be considered as an automated mobile conveyor designed to transport materials. Most AGVs require some type of guide path. The steering stability of the guidance control system has not been fully solved. The slight "snaking" of the AGV about the track generally has been acceptable, although it indicates instability of the steering guidance control system [9].

Most AGVs have a specification of maximum speed of about 1 m/s, although in practice they are usually operated at half that speed. In a fully automated manufacturing environment, there should be few personnel in the production area; therefore, the AGV should be able to be run at full speed. As the speed of the AGV increases, so does the difficulty in designing stable and smooth tracking controls.

A steering system for an AGV is shown in Figure P10.30, where $\tau_1 = 40$ ms and $\tau_2 = 1$ ms. We require that the velocity constant K_v be 100 so that the steady-state error for a ramp input will be 1% of the slope of the ramp. Neglect τ_2 and design a lead compensator so that the phase margin is

$$45° \le P.M. \le 65°.$$

Attempt to obtain the two limiting cases for phase margin, and compare your results for the two designs by determining the actual percent overshoot and settling time for a step input.

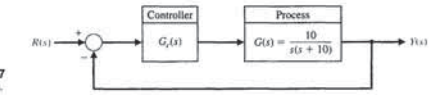

FIGURE P10.27
Controller design.

to improve the step response for the system in part (a) so that the steady-state error is less than 12%. Assume the closed-loop system of Figure 10.1(a).

P10.20 An uncompensated control system with unity feedback has a plant transfer function

$$G(s) = \frac{K}{s(s/2 + 1)(s/6 + 1)}.$$

We want to have a velocity error constant of $K_v = 20$. We also want to have a phase margin of approximately 45° and a closed-loop bandwidth greater than $\omega = 4$ rad/s. Use two identical cascaded phase-lead networks to compensate the system.

P10.21 For the system of Problem P10.20, design a phase-lag network to yield the desired specifications, with the exception that a bandwidth equal to or greater than 2 rad/s will be acceptable.

P10.22 For the system of Problem P10.20, we wish to achieve the same phase margin and K_v, but in addition, we wish to limit the bandwidth to less than 10 rad/s but greater than 2 rad/s. Use a lead-lag compensation network to compensate the system. The lead-lag network could be of the form

$$G_c(s) = \frac{(1 + s/10a)(1 + s/b)}{(1 + s/a)(1 + s/10b)},$$

where a is to be selected for the lag portion of the compensator, and b is to be selected for the lead portion of the compensator. The ratio α is chosen to be 10 for both the lead and lag portions.

P10.23 A system of the form of Figure 10.1(a) with unity feedback has

$$G(s) = \frac{K}{(s + 5)^2}.$$

We desire the steady-state error to a step input to be approximately 5% and the phase margin of the system to be approximately 45°. Design a lag network to meet these specifications.

P10.24 The stability and performance of the rotation of a robot (similar to waist rotation) presents a challenging control problem. The system requires high gains in order to achieve high resolution; yet a large overshoot of the transient response cannot be tolerated. The block diagram of an electrohydraulic system for rotation control is shown in Figure P10.24 [15]. The arm-rotating dynamics are represented by

$$G(s) = \frac{80}{s(s^2/4900 + s/70 + 1)}.$$

We want to have $K_v = 20$ for the compensated system. Design a compensator that results in an overshoot to a step input of less than 10%.

P10.25 The possibility of overcoming wheel friction, wear, and vibration by contactless suspension for passenger-carrying mass-transit vehicles is being investigated throughout the world. One design uses a magnetic suspension with an attraction force between the vehicle and the guideway with an accurately controlled airgap. A system is shown in Figure P10.25, which incorporates feedback compensation.

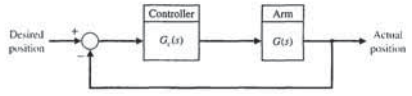

FIGURE P10.24
Robot position control.

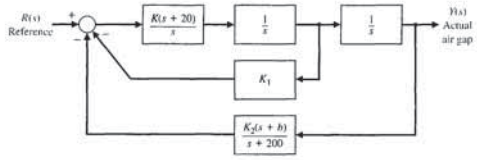

FIGURE P10.25
Airgap control of train.

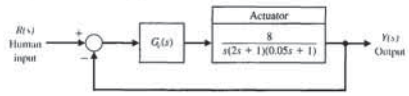

FIGURE P10.33
Extender robot control.

will have a velocity constant K_v equal to 80, so that the settling time (with a 2% criterion) will be 1.6 seconds, and that the overshoot will be 16%, so that the dominant roots have a ζ of 0.5. Determine a lead-lag compensator using root locus methods.

P10.34 A magnetically levitated train is operating in Berlin, Germany. The M-Bahn 1600-m line represents the current state of worldwide systems. Fully automated trains can run at short intervals and operate with excellent energy efficiency. The control system for the levitation of the car is shown in Figure P10.34. Select a compensator so that the phase margin of the system is $45° \le P.M. \le 55°$. Predict the response of the system to a step command, and determine the actual step response for comparison.

P10.35 A unity feedback system has the loop transfer function

$$L(s) = G_c(s)G(s) = \frac{Ks + 0.54}{s(s + 1.76)}e^{-Ts},$$

where T is a time delay and K is the controller proportional gain. The block diagram is illustrated in Figure P10.35. The nominal value of $K = 2$. Plot the phase margin of the system for $0 \le T \le 2$ s when $K = 2$. What happens to the phase margin as the time delay increases? What is the maximum time delay allowed before the system becomes unstable?

P10.36 A system's open-loop transfer function is a pure time delay of 0.5 s, so that $G(s) = e^{-s/2}$. Select a compensator $G_c(s)$ so that the steady-state error for a step input is less than 2% of the magnitude of the step and the phase margin is greater than 30°. Determine the bandwidth of the compensated system and plot the step response.

P10.37 A unity feedback system of the form shown in Figure 10.1(a) has

$$G(s) = \frac{1}{(s + 2)(s + 8)}.$$

Design a compensator $G_c(s)$ so that the overshoot for a step input $R(s)$ is less than 5% and the steady-state error is less than 1%. Determine the bandwidth of the system.

P10.38 A unity feedback system has a plant

$$G(s) = \frac{40}{s(s + 2)}.$$

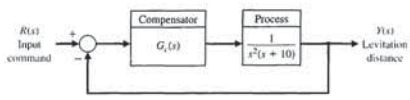

FIGURE P10.34
Magnetically levitated train control.

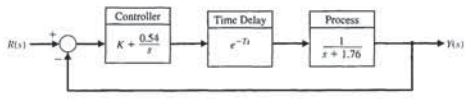

FIGURE P10.35
Unity feedback system with a time delay and PI controller.

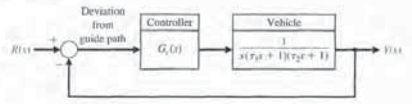

FIGURE P10.30
Steering control for vehicle.

P10.31 For the system of Problem P10.30, use a phase-lag compensator and attempt to achieve a phase margin of approximately 50°. Determine the actual overshoot and peak time for the compensated system.

P10.32 When a motor drives a flexible structure, the structure's natural frequencies, as compared to the bandwidth of the servodrive, determine the contribution of the structural flexibility to the errors of the resulting motion. In current industrial robots, the drives are often relatively slow, and the structures are relatively rigid, so that overshoots and other errors are caused mainly by the servodrive. However, depending on the accuracy required, the structural deflections of the driven members can become significant. Structural flexibility must be considered the major source of motion errors in space structures and manipulators. Because of weight restrictions in space, large arm lengths result in flexible structures. Furthermore, future industrial robots should require lighter and more flexible manipulators.

To investigate the effects of structural flexibility and how different control schemes can reduce unwanted oscillations, an experimental apparatus was constructed consisting of a DC motor driving a slender aluminum beam. The purpose of the experiments was to identify simple and effective control strategies to deal with the motion errors that occur when a servomotor is driving a very flexible structure [13].

The experimental apparatus is shown in Figure P10.32(a), and the control system is shown in Figure P10.32(b). The goal is that the system will have a K_v of 100. (a) When $G_c(s) = K$, determine K and plot the Bode diagram. Find the phase margin and gain margin. (b) Using the Nichols chart, find ω_r, M_{pw}, and ω_B. (c) Select a compensator so that the phase margin is greater than 35° and find ω_r, M_{pw}, and ω_B for the compensated system.

P10.33. Consider the extender robot presented in AP6.7. The block diagram of the system is shown in Figure P10.33 [14]. The goal is that the compensated system

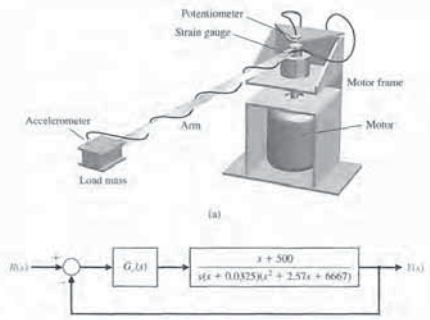

FIGURE P10.32
Flexible arm control.

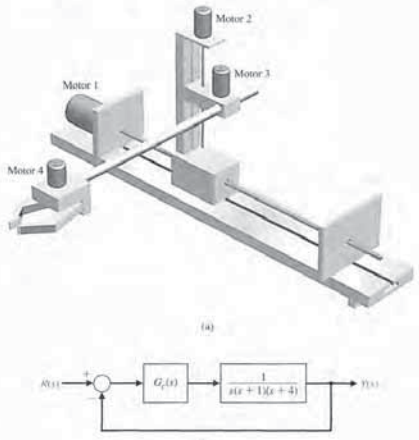

FIGURE AP10.1
Pick-and-place robot.

Design a proportional plus integral (PI) controller to meet the specifications.

AP10.4 A DC motor control system with unity feedback has the form shown in Figure AP10.4. Select K_1 and K_2 so that the system response has a settling time (with a 2% criterion) less than 1 second and an overshoot less than 5% for a step input.

AP10.5 A unity feedback system is shown in Figure AP10.5. We want the step response of the system to have an overshoot of about 10% and a settling time (with a 2% criterion) of about 4 seconds.

(a) Design a lead compensator $G_c(s)$ to achieve the dominant roots desired. (b) Determine the step response of the system when $G_p(s) = 1$. (c) Select a prefilter $G_p(s)$, and determine the step response of the system with the prefilter.

AP10.6 Consider again Example 10.12 when we wish to minimize the settling time of the system while requiring that $K < 52$. Determine the appropriate compensator that will minimize the settling time. Plot the system response.

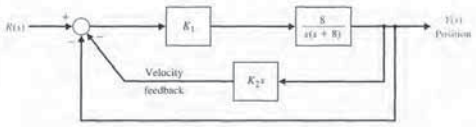

FIGURE AP10.4
Motor control system.

We desire to have a phase margin of 30° and a relatively large bandwidth. Select the crossover frequency $\omega_c = 10$ rad/s, and design a lead compensator. Verify the results.

P10.39 A unity feedback system has a plant

$$G(s) = \frac{40}{s(s+2)}.$$

We desire that the phase margin be equal to 30°. For a ramp input $r(t) = t$, we want the steady-state error to be equal to 0.05. Design a lag compensator to satisfy the requirements. Verify the results.

P10.40 For the system and requirements of Problem P10.39, determine the required compensator when the steady-state error for the ramp input must be equal to 0.02.

P10.41 Repeat Example 10.12 when we want the 100% rise time $T_r = 1$ second.

P10.42 Consider again the design for Example 10.4. Using a system as shown in Figure 10.22 and the compensator determined in Equation (10.46), select an appropriate prefilter. Compare the response of the system with and without the prefilter.

P10.43 Consider the system shown in Figure P10.43 and let $R(s) = 0$ and $T_d(s) = 0$. Design the controller $G_c(s) = K$ such that, in the steady-state, the response of the system $y(t)$ is less than -40 dB when the noise $N(s)$ is a sinusoidal input at a frequency of $\omega \geq 100$ rad/s.

P10.44 A unity feedback system has a loop transfer function

$$L(s) = G_c(s)G(s) = \frac{K(s^2 + 2s + 20)}{s(s+2)(s^2 + 2s + 1)}.$$

Plot the percent overshoot of the closed-loop system response to a unit step input for K in the range $0 < K \leq 100$. Explain the behavior of the system response for K in the range $0.129 < K \leq 69.872$.

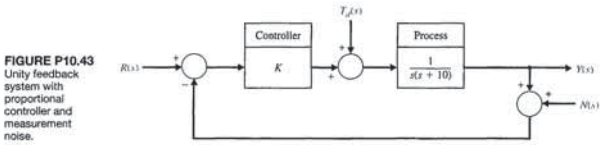

FIGURE P10.43
Unity feedback system with proportional controller and measurement noise.

ADVANCED PROBLEMS

AP10.1 A three-axis pick-and-place application requires the precise movement of a robotic arm in three-dimensional space, as shown in Figure AP10.1 for joint 2. The arm has specific linear paths it must follow to avoid other pieces of machinery. The overshoot for a step input should be less than 13%.
(a) Let $G_c(s) = K$, and determine the gain K that satisfies the requirement. Determine the resulting settling time (with a 2% criterion). (b) Use a lead network and reduce the settling time to less than 3 seconds.

AP10.2 The system of Advanced Problem AP10.1 is to have a percent overshoot less than 13%. In addition, we desire that the steady-state error for a unit ramp input will be less than 0.125 ($K_v = 8$) [24]. Design a lag network to meet the specifications. Check the resulting percent overshoot and settling time (with a 2% criterion) for the design.

AP10.3 The system of Advanced Problem AP 10.1 is required to have a percent overshoot less than 13% with a steady-state error for a unit ramp input less than 0.125 ($K_v = 8$).

DESIGN PROBLEMS

CDP10.1 The capstan-slide system of Figure CDP4.1 uses a PD controller. Determine the necessary values of the gain constants of the PD controller so that the deadbeat response is achieved. Also, we want the settling time (with a 2% criterion) to be less than 250 ms. Verify the results.

DP10.1 In Figure DP10.1, two robots are shown cooperating with each other to manipulate a long shaft to insert it into the hole in the block resting on the table. Long part insertion is a good example of a task that can benefit from cooperative control. The unity feedback control system of one robot joint has the process transfer function

$$G(s) = \frac{20}{s(s+2)}.$$

The specifications require a steady-state error for a unit ramp input of 0.02, and the step response has an overshoot of less than 15% with a settling time (with a 2% criterion) of less than 1 second. Determine a lead-lag compensator that will meet the specifications, and plot the compensated responses for the ramp and step inputs.

FIGURE DP10.1 Two robots cooperate to insert a shaft.

DP10.2 The heading control of the traditional bi-wing aircraft, shown in Figure DP10.2(a), is represented by the block diagram of Figure DP10.2(b).

(a) Determine the minimum value of the gain K when $G_c(s) = K$, so that the steady-state effect of a unit step disturbance $T_d(s) = 1/s$ is less than or equal to 5% of the unit step ($y(\infty) = 0.05$).
(b) Determine whether the system using the gain of part (a) is stable.
(c) Design a compensator using one stage of lead compensation, so that the phase margin is 30°.
(d) Design a two-stage lead compensator so that the phase margin is 55°.
(e) Compare the bandwidth of the systems of parts (c) and (d).
(f) Plot the step response $y(t)$ for the systems of parts (c) and (d) and compare percent overshoot settling time (with a 2% criterion), and peak time.

DP10.3 NASA has identified the need for large deployable space structures, which will be constructed of lightweight materials and will contain large numbers of joints or structural connections. This need is evident for programs such as the space station. These deployable space structures may have precision shape requirements and a need for vibration suppression during in-orbit operations [16].

One such structure is the mast flight system, which is shown in Figure DP10.3(a). The intent of the system is to provide an experimental test bed for controls and dynamics. The basic element in the mast flight system is a 60.7-m-long truss beam structure, which is attached to the shuttle orbiter. Included at the tip of the truss structure are the primary actuators and collocated sensors. A deployment/retraction subsystem, which also secures the stowed beam package during launch and landing, is provided.

The system uses a large motor to move the structure and has the block diagram shown in Figure DP10.3(b). The goal is an overshoot to a step response of less than or equal to 16%; thus, we estimate the system ζ as 0.5 and the required phase margin as 50°. Design for $0.1 < K < 1$ and record overshoot, rise time, and phase margin for selected gains.

DP10.4 A high-speed train is under development in Texas [21] with a design based on the French *Train à Grande Vitesse* (TGV). Train speeds of 186 miles per hour are foreseen. To achieve these speeds on tight curves, the train may use independent axles combined with the ability to tilt the train. Hydraulic cylinders connecting the passenger compartments to their wheeled bogies allow the train to lean into curves like a motorcycle. A pendulum like device on the leading bogie of each car senses when it is entering a curve and feeds this information to the hydraulic system. Tilting does not make the train safer, but it does make passengers more comfortable.

Consider the tilt control shown in Figure DP10.4. Design a compensator $G_c(s)$ for a step-input command so that the overshoot is less than 5% and the settling time (with a 2% criterion) less than

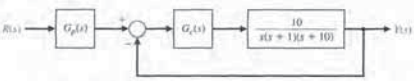

FIGURE AP10.5
Unity feedback with a prefilter.

AP10.7 A system has the form shown in Figure 10.22, with

$$G(s) = \frac{1}{s(s+2)(s+8)}.$$

A lead compensator is used, with

$$G_c(s) = \frac{K(s+3)}{s+28}.$$

Determine K so that the complex roots have $\zeta = 1/\sqrt{2}$. The prefilter is

$$G_p(s) = \frac{p}{s+p}.$$

(a) Determine the overshoot and rise time for $G_p(s) = 1$ and for $p = 3$. (b) Select an appropriate value for p that will give an overshoot of 1% and compare the results.

AP10.8 The Manutec robot has large inertia and arm length resulting in a challenging control problem, as shown in Figure AP10.8(a). The block diagram model of the system is shown in Figure AP10.8(b). The plant dynamics are represented by

$$G(s) = \frac{250}{s(s+2)(s+40)(s+45)}.$$

The percentage overshoot for a step input should be less than 20% with a rise time less than $\frac{1}{2}$ second and a settling time (with a 2% criterion) less than 1.2 seconds. Also, we desire that for a ramp input $K_v \geq 10$. Determine a suitable lead compensator.

AP10.9 The plant dynamics of a chemical process are represented by

$$G(s) = \frac{100}{s(s+5)(s+10)}.$$

We desire that the system have a small steady-state error for a ramp input so that $K_v = 100$. For stability purposes, we desire a gain margin of 10 dB or greater and a phase margin of 40° or greater. Determine a lead-lag compensator that meets these specifications. Assume the system is of the form shown in Figure 10.1(a) with $H(s) = 1$.

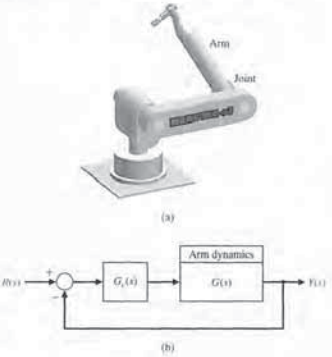

FIGURE AP10.8
(a) Manutec robot.
(b) Block diagram.

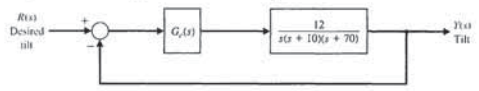

FIGURE DP10.4 High-speed train feedback control system.

0.6 second. We also desire that the steady-state error for a velocity (ramp) input be less than 0.15A, where $r(t) = At$, $t > 0$. Verify the results for the design.

DP10.5 High-performance tape transport systems are designed with a small capstan to pull the tape past the read/write heads and with take-up reels turned by DC motors. The tape is to be controlled at speeds up to 200 inches per second, with start-up as fast as possible, while preventing permanent distortion of the tape. Since we wish to control the speed and the tension of the tape, we will use a DC tachometer for the speed sensor and a potentiometer for the position sensor. We will use a DC motor for the actuator. Then the linear model for the system is a unity feedback system with

$$\frac{Y(s)}{E(s)} = G(s) = \frac{K(s + 4000)}{s(s + 1000)(s + 3000)(s + p_1)(s + \bar{p}_1)},$$

where $p_1 = +2000 + j2000$, and $Y(s)$ is position.

The specifications for the system are (1) settling time of less than 12 ms, (2) an overshoot to a step position command of less than 10%, and (3) a steady-state velocity error of less than .5%. Determine a compensator scheme to achieve these stringent specifications.

DP10.6 The past several years have witnessed a significant engine model-building activity in the automotive industry in a category referred to as "control-oriented" or "control design" models. These models contain representations of the throttle body, engine pumping phenomena, induction process dynamics, fuel system, engine torque generation, and rotating inertia.

The control of the fuel-to-air ratio in an automobile carburetor became of prime importance in the 1980s as automakers worked to reduce exhaust-pollution emissions. Thus, auto engine designers turned to the feedback control of the fuel-to-air ratio. Operation of an engine at or near a particular air-to-fuel ratio requires management of both air and fuel flow into the manifold system. The fuel command is considered the input and the engine speed is considered the output [9, 10].

The block diagram of the system is shown in Figure DP10.6, where $T = 0.066$ second. A compensator is required to yield zero steady-state error for a step input and an overshoot of less than 10%. We also desire that the settling time (with a 2% criterion) not exceed 10 seconds.

DP10.7 A high-performance jet airplane is shown in Figure DP10.7(a), and the roll-angle control system is shown in Figure DP10.7(b). Design a controller $G_c(s)$ so that the step response is well behaved and the steady-state error is zero.

DP10.8 A simple closed-loop control system has been proposed to demonstrate proportional-integral (PI) control of a windmill radiometer [27]. The windmill radiometer is shown in Figure DP10.8(a) and the control system is shown in Figure DP10.8(b). The variable to be controlled is the angular velocity ω of the windmill radiometer whose vanes turn when exposed to infrared radiation. An experimental setup using a reflexive photoelectric sensor and basic electronic circuitry makes possible the design and implementation of a high performance control system.

The transfer function of the light source and radiometer is

$$G(s) = \frac{\tau}{\tau s + 1},$$

where $\tau = 20$ s. Design a PI controller so that the system achieves a deadbeat response with a settling time less than 25 s.

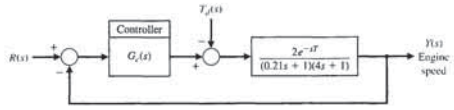

FIGURE DP10.6 Engine control system.

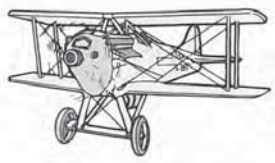

(a)

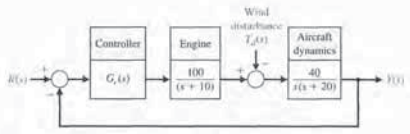

(b)

FIGURE DP10.2 (a) Bi-wing aircraft. (*Source: The Illustrated London News*, October 9, 1920.) (b) Control system.

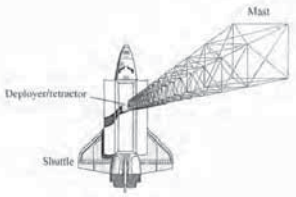

(a)

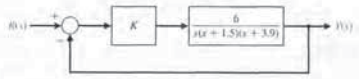

(b)

FIGURE DP10.3 Mast flight system.

DP10.10 A unity feedback system has the process transfer function

$$G(s) = \frac{s + 1.59}{s(s + 3.7)(s^2 + 2.4s + 0.43)}.$$

Design the controller $G_c(s)$ such that the Bode magnitude plot of the loop transfer function $L(s) = G_c(s)G(s)$ is greater than 20 dB for $\omega \leq 0.01$ rad/s and less than -20 dB for $\omega \leq 10$ rad/s. The desired shape of the loop transfer function Bode plot magnitude is illustrated in Figure DP10.10. Explain why we would want the gain to be high at low-frequency and the gain to be low at high-frequency.

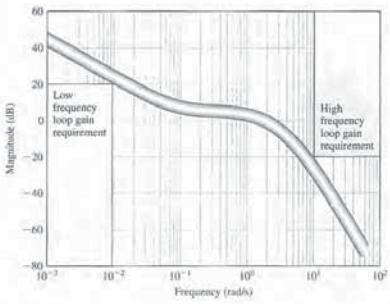

FIGURE DP10.10 Bode plot loop shaping requirements.

DP10.11 Modern micronanalytical systems used for polymerase chain reaction (PCR) requires fast, damped tracking response. The control of the temperature of the PCR reactor can be represented as shown in Figure DP10.11. The controller is chosen to be PID controller, denoted by $G_c(s)$, with a prefilter, denoted by $G_p(s)$. The transfer function is [30]

$$G(s) = \frac{45}{(s + 2.9)(s + 0.14)}.$$

It is required that the percent overshoot $P.O. < 1\%$ and the settling time $T_s < 3$ seconds to a unit step input. Design a controller $G_c(s)$ and prefilter $G_p(s)$ to achieve the control specifications.

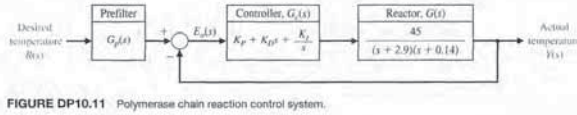

FIGURE DP10.11 Polymerase chain reaction control system.

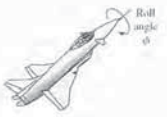

(a)

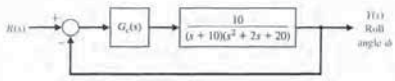

(b)

FIGURE DP10.7 Roll-angle control of a jet airplane.

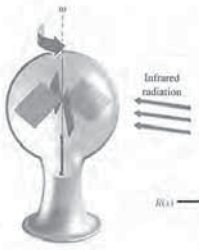

(a)

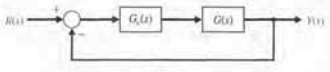

(b)

FIGURE DP10.8 (a) Radiometric windmill. (b) Control system.

DP10.9 The feedback control system shown in Figure DP10.9 has the transfer function

$$G(s) = \frac{60}{(s^2 + 4s + 6)(s + 10)}.$$

Design a PID compensator $G_{c1}(s)$ and a lead-lag compensator $G_{c2}(s)$ such that, in each case, the closed-loop system is stable in the presence of a time-delay $T = 0.1$ s. Discuss the capability of each compensator to insure stability in the presence of an increase in the time-delay uncertainty of up to 0.2 second.

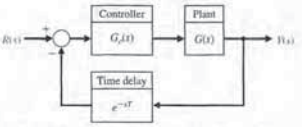

FIGURE DP10.9 Feedback control system with a time-delay.

(1) closed-loop system bandwidth about 10 rad/s, and (2) percent overshoot less than 20% to a 10° step input. Complete the design by developing and using an interactive m-file script. (b) Verify the design by simulating the response to a 10° step input. (c) Include a closed-loop transfer function Bode plot to verify that the bandwidth requirement is satisfied.

CP10.6 Consider the control system shown in Figure CP10.6. Design a lag compensator using root locus methods to meet the following specifications: (1) steady-state error less than 10% for a step input, (2) phase margin greater than 45°, and (3) settling time (with a 2% criterion) less than 5 seconds for a unit step input.

(a) Design a lag compensator utilizing root locus methods to meet the design specifications. Develop a set of m-file scripts to assist in the design process. (b) Test the controller developed in part (a) by simulating the closed-loop system response to unit step input. Provide the time histories of the output $y(t)$. (c) Compute the phase margin using the margin function.

CP10.7 A lateral beam guidance system has an inner loop as shown in Figure CP10.7, where the transfer function for the coordinated aircraft is [26]

$$G(s) = \frac{23}{s + 23}.$$

Consider the PI controller

$$G_c(s) = K_P + \frac{K_I}{s}.$$

(a) Design a control system to meet the following specifications: (1) settling time (with a 2% criterion) to a unit step input of less than 1 second, and (2) steady-state tracking error for a unit ramp input of less than 0.1. (b) Verify the design by simulation.

CP10.8 Consider again the system and the lead compensator designed in Example 10.3. The actual overshoot of the compensated system will be 46%. We want to reduce the overshoot to 32%. Using a m-file script, determine an appropriate value for the zero of $G_c(s)$.

CP10.9 Plot the frequency response of the circuit of AP10.10.

CP10.10 The feedback control system shown in Figure CP10.10 has the transfer function

$$G(s) = \frac{K(s + 0.2)}{s^3 + 6s^2}.$$

The time delay is $T = 0.2$ s. Plot the phase margin for the system versus the gain in the range $0.1 \le K \le 10$. Determine the gain K that maximizes the phase margin.

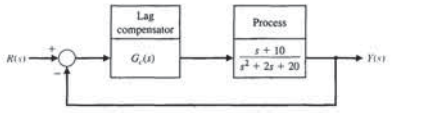

FIGURE CP10.6
A unity feedback control system.

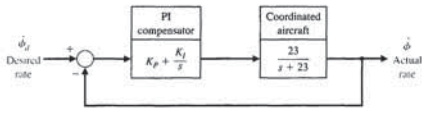

FIGURE CP10.7
A lateral beam guidance system inner loop.

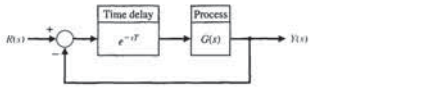

FIGURE CP10.10
Feedback control system with a time delay.

COMPUTER PROBLEMS

CP10.1 Consider the control system in Figure CP10.1, where

$$G(s) = \frac{1}{s + 10} \quad \text{and} \quad G_c(s) = \frac{110}{s}.$$

Develop an m-file to show that the phase margin is approximately 50° and that the percent overshoot to a unit step input is 18%.

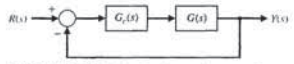

FIGURE CP10.1 A feedback control system with compensation.

CP10.2 A negative feedback control system is shown in Figure CP10.2 Design the proportional controller $G_c(s) = K$ so that the system has a 40° phase margin. Develop an m-file to obtain a Bode plot and verify that the design specification is satisfied.

CP10.3 Consider the system in Figure CP10.1, where

$$G(s) = \frac{1}{s(s + 2)}.$$

Design a compensator $G_c(s)$ so that the steady-state tracking error to a ramp input is zero and the settling time (with a 2% criterion) is less than 5 seconds. Obtain the response of the closed-loop system to the input $R(s) = 1/s^2$ and verify that the settling time requirement has been satisfied and that the steady-state error is zero.

CP10.4 A fighter aircraft has the transfer function

$$\frac{\dot{\theta}}{\delta} = \frac{-10(s + 1)(s + 0.01)}{(s^2 + 2s + 2)(s^2 + 0.02s + 0.0101)},$$

where $\dot{\theta}$ is the pitch rate (rad/s) and δ is the elevator deflection (rad). The four poles represent the phugoid and short-period modes. The phugoid mode has a natural frequency of 0.1 rad/s, and the short period mode is 1.4 rad/s. The block diagram is shown in Figure CP10.4.

(a) Let the lead compensator be

$$G_c = K\frac{s + z}{s + p},$$

where $|z| < |p|$. Using Bode plot methods, design the lead compensator to meet the following specifications: (1) settling time (with a 2% criterion) to a unit step less than 2 seconds, and (2) percent overshoot less than 10%. (b) Simulate the closed-loop system with a step input of 10°/second, and show the time history of $\dot{\theta}$.

CP10.5 The pitch attitude motion of a rigid spacecraft is described by

$$J\ddot{\theta} = u,$$

where J is the principal moment of inertia, and u is the input torque on the vehicle [7]. Consider the PD controller

$$G_c(s) = K_P + K_D s.$$

(a) Obtain a block diagram of the control system. Design a control system to meet the following specifications:

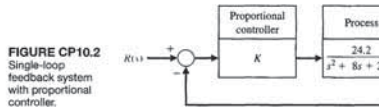

FIGURE CP10.2
Single-loop feedback system with proportional controller.

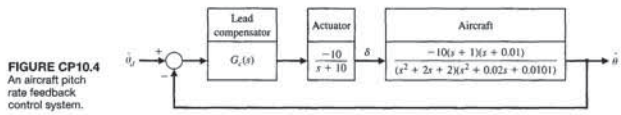

FIGURE CP10.4
An aircraft pitch rate feedback control system.

CHAPTER 11 The Design of State Variable Feedback Systems

PREVIEW

The design of controllers utilizing state feedback is the subject of this chapter. We first present a system test for controllability and observability. Using the powerful notion of state variable feedback, we introduce the pole placement design technique. Ackermann's formula can be used to determine the state variable feedback gain matrix to place the system poles at the desired locations. The closed-loop system pole locations can be arbitrarily placed if and only if the system is controllable. When the full state is not available for feedback, we introduce an observer. The observer design process is described and the applicability of Ackermann's formula is established. The state variable compensator is obtained by connecting the full-state feedback law to the observer. We consider optimal control system design and then describe the use of internal model design to achieve prescribed steady-state response to selected input commands. The chapter concludes by revisiting the Sequential Design Example: Disk Drive Read System.

DESIRED OUTCOMES

Upon completion of Chapter 11, students should:

- ❑ Be familiar with the concepts of controllability and observability.
- ❑ Be able to design full-state feedback controllers and observers.
- ❑ Appreciate pole-placement methods and the application of Ackermann's formula.
- ❑ Understand the separation principle and how to construct state variable compensators.
- ❑ Have a working knowledge of reference inputs, optimal control, and internal model design.

ANSWERS TO SKILLS CHECK

True or False: (1) False; (2) False; (3) True; (4) True; (5) True
Multiple Choice: (6) d; (7) b; (8) d; (9) a; (10) b; (11) c; (12) a; (13) a; (14) b; (15) b
Word Match (in order, top to bottom): a, l, g, d, j, h, k, c, m, e, i, f, b

TERMS AND CONCEPTS

Cascade compensation network A compensator network placed in cascade or series with the system process.

Compensation The alteration or adjustment of a control system in order to provide a suitable performance.

Compensator An additional component or circuit that is inserted into the system to compensate for a performance deficiency.

Deadbeat response A system with a rapid response, minimal overshoot, and zero steady-state error for a step input.

Design of a control system The arrangement or the plan of the system structure and the selection of suitable components and parameters.

Integration network A network that acts, in part, like an integrator.

Lag network *See* Phase-lag network.

Lead-lag network A network with the characteristics of both a lead network and a lag network.

Lead network *See* Phase-lead network.

Phase lag compensation A widely-used compensator that possesses one zero and one pole with the pole closer to the origin of the s-plane. This compensator reduces the steady-state tracking errors.

Phase lead compensation A widely-used compensator that possesses one zero and one pole with the zero closer to the origin of the s-plane. This compensator increases the system bandwidth and improves the dynamic response.

Phase-lag network A network that provides a negative phase angle and a significant attenuation over the frequency range of interest.

Phase-lead network A network that provides a positive phase angle over the frequency range of interest. Thus, phase lead can be used to cause a system to have an adequate phase margin.

PD controller Controller with a proportional term and a derivative term (Proportional-Derivation).

PI controller Controller with a proportional term and an integral term (Proportional-Integral).

Prefilter A transfer function $G_p(s)$ that filters the input signal $R(s)$ prior to calculating the error signal.

11.1 INTRODUCTION

The time-domain method, expressed in terms of state variables, can also be used to design a suitable compensation scheme for a control system. Typically, we are interested in controlling the system with a control signal $\mathbf{u}(t)$ that is a function of several measurable state variables. Then we develop a state variable controller that operates on the information available in measured form. This type of system compensation is quite useful for system optimization and will be considered in this chapter.

State variable design typically comprises *three* steps. In the first step, we assume that all the state variables are measurable and utilize them in a **full-state feedback control law**. Full-state feedback is usually not practical because it is not possible (in general) to measure all the states. In practice, only certain states (or linear combinations thereof) are measured and provided as system outputs. The second step in state variable design is to construct an **observer** to estimate the states that are not directly sensed and available as outputs. Observers can either be full-state observers or reduced-order observers. Reduced-order observers account for the fact that certain states are already available as system outputs; hence they do not need to be estimated [26]. In this chapter, we consider only full-state observers. The final step in the design process is to appropriately connect the observer to the full-state feedback control law. It is common to refer to the state-variable controller (full-state control law plus the observer) as a **compensator**. The state variable design yields a compensator of the form depicted in Figure 11.1. Additionally, it is possible to consider reference inputs to the state variable compensator to complete the design. All three steps in the design process are discussed in the subsequent sections, as well as how to incorporate the reference inputs.

11.2 CONTROLLABILITY AND OBSERVABILITY

A key question that arises in the design of state variable compensators is whether or not all the poles of the closed-loop system can be arbitrarily placed in the complex plane. Recall that the poles of the closed-loop system are equivalent to the eigenvalues of the system matrix in state variable format. As we shall see, if the system is

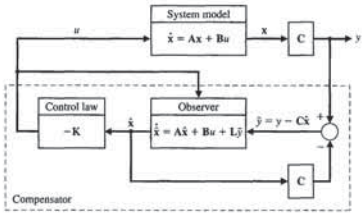

FIGURE 11.1
State variable compensator employing full-state feedback in series with a full-state observer.

controllable and **observable,** then we can accomplish the design objective of placing the poles precisely at the desired locations to meet the performance specifications. Full-state feedback design commonly relies on **pole-placement** techniques [2, 27]. Pole placement is discussed more fully in Section 11.3. It is important to note that a system must be completely controllable and completely observable to allow the flexibility to place *all* the closed-loop system poles arbitrarily. The concepts of controllability and observability (discussed in this section) were introduced by Kalman in the 1960s [28–30]. Rudolph Kalman was a central figure in the development of mathematical systems theory upon which much of the subject of state variable methods rests. Kalman is well known for his role in the development of the so-called Kalman filter, which was instrumental in the successful Apollo moon landings [31, 32].

A system is completely controllable if there exists an unconstrained control $\mathbf{u}(t)$ that can transfer any initial state $\mathbf{x}(t_0)$ to any other desired location $\mathbf{x}(t)$ in a finite time, $t_0 \le t \le T$.

For the system

$$\dot{\mathbf{x}} = \mathbf{A}\mathbf{x} + \mathbf{B}u,$$

we can determine whether the system is controllable by examining the algebraic condition

$$\text{rank}[\mathbf{B} \quad \mathbf{AB} \quad \mathbf{A}^2\mathbf{B} \ \ldots \ \mathbf{A}^{n-1}\mathbf{B}] = n. \tag{11.1}$$

The matrix $\mathbf{A}$ is an $n \times n$ matrix and $\mathbf{B}$ is an $n \times 1$ matrix. For multi-input systems, $\mathbf{B}$ can be $n \times m$, where m is the number of inputs.

For a single-input, single-output system, the **controllability matrix** $\mathbf{P}_c$ is described in terms of $\mathbf{A}$ and $\mathbf{B}$ as

$$\boxed{\mathbf{P}_c = [\mathbf{B} \quad \mathbf{AB} \quad \mathbf{A}^2\mathbf{B} \ \ldots \ \mathbf{A}^{n-1}\mathbf{B}],} \tag{11.2}$$

which is an $n \times n$ matrix. Therefore, if the determinant of $\mathbf{P}_c$ is nonzero, the system is controllable [11].

Advanced state variable design techniques can handle situations wherein the system is not completely controllable, but where the states (or linear combinations thereof) that cannot be controlled are inherently stable. These systems are classified as **stabilizable.** If a system is completely controllable, it is also stabilizable. The **Kalman state-space decomposition** provides a mechanism for partitioning the state-space so that it becomes apparent which states (or state combinations) are controllable and which are not [12, 18]. The controllable subspace is thus exposed, and if the system is stabilizable, the control system design can, in theory, proceed. In this chapter, we consider only completely controllable systems.

EXAMPLE 11.1 **Controllability of a system**

Let us consider the system

$$\dot{\mathbf{x}} = \begin{bmatrix} 0 & 1 & 0 \\ 0 & 0 & 1 \\ -a_0 & -a_1 & -a_2 \end{bmatrix}\mathbf{x} + \begin{bmatrix} 0 \\ 0 \\ 1 \end{bmatrix}u.$$

$$y = [1 \quad 0 \quad 0]\mathbf{x} + [0]u$$

The signal-flow graph and block diagram model are illustrated in Figure 11.2. Then we have

$$\mathbf{A} = \begin{bmatrix} 0 & 1 & 0 \\ 0 & 0 & 1 \\ -a_0 & -a_1 & -a_2 \end{bmatrix}, \quad \mathbf{B} = \begin{bmatrix} 0 \\ 0 \\ 1 \end{bmatrix}, \quad \mathbf{AB} = \begin{bmatrix} 0 \\ 1 \\ -a_2 \end{bmatrix}, \quad \text{and} \quad \mathbf{A}^2\mathbf{B} = \begin{bmatrix} 1 \\ -a_2 \\ a_2^2 - a_1 \end{bmatrix}.$$

Therefore, we obtain

$$\mathbf{P}_c = [\mathbf{B} \quad \mathbf{AB} \quad \mathbf{A}^2\mathbf{B}] = \begin{bmatrix} 0 & 0 & 1 \\ 0 & 1 & -a_2 \\ 1 & -a_2 & a_2^2 - a_1 \end{bmatrix}.$$

The determinant of $\mathbf{P}_c = -1 \neq 0$, hence this system is controllable. ■

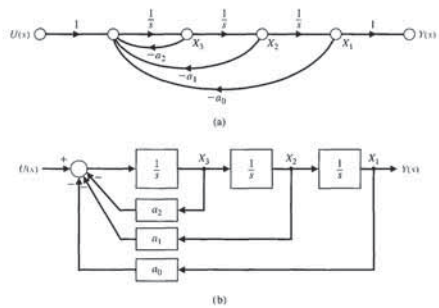

FIGURE 11.2
Third-order system. (a) Signal-flow graph model. (b) Block diagram model.

EXAMPLE 11.2 **Controllability of a two-state system**

Let us consider a system represented by the two state equations

$$\dot{x}_1 = -2x_1 + u, \quad \text{and} \quad \dot{x}_2 = -3x_2 + dx_1$$

and determine the condition for controllability. Also, we have $y = x_2$, as shown in Figure 11.3. The system state variable model is

$$\dot{\mathbf{x}} = \begin{bmatrix} -2 & 0 \\ d & -3 \end{bmatrix}\mathbf{x} + \begin{bmatrix} 1 \\ 0 \end{bmatrix}u,$$

$$y = [0 \quad 1]\mathbf{x} + [0]u.$$

We can determine the requirement on the parameter d by generating the matrix $\mathbf{P}_c$. So, with

$$\mathbf{B} = \begin{bmatrix} 1 \\ 0 \end{bmatrix} \quad \text{and} \quad \mathbf{AB} = \begin{bmatrix} -2 & 0 \\ d & -3 \end{bmatrix}\begin{bmatrix} 1 \\ 0 \end{bmatrix} = \begin{bmatrix} -2 \\ d \end{bmatrix},$$

we have

$$\mathbf{P}_c = \begin{bmatrix} 1 & -2 \\ 0 & d \end{bmatrix}.$$

The determinant of $\mathbf{P}_c$ is equal to d, which is nonzero whenever d is nonzero. ■

All the poles of the closed-loop system can be placed arbitrarily in the complex plane if and only if the system is observable and controllable. Observability refers to the ability to estimate a state variable.

A system is completely observable if and only if there exists a finite time T such that the initial state $\mathbf{x}(0)$ can be determined from the observation history $y(t)$ given the control $u(t)$, $0 \le t \le T$.

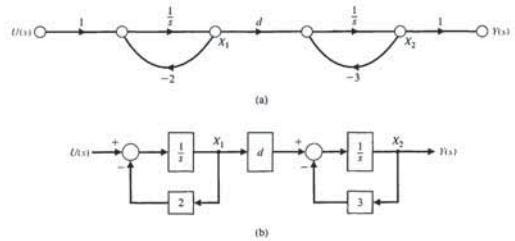

FIGURE 11.3
(a) Flow graph model for Example 11.2. (b) Block diagram model.

EXAMPLE 11.4 **Observability of a two-state system**

Consider the system given by

$$\dot{\mathbf{x}} = \begin{bmatrix} 2 & 0 \\ -1 & 1 \end{bmatrix}\mathbf{x} + \begin{bmatrix} 1 \\ -1 \end{bmatrix}u \quad \text{and} \quad y = [1 \quad 1]\mathbf{x}.$$

The system is illustrated in Figure 11.4. We can check the system controllability and observability using the $\mathbf{P}_c$ and $\mathbf{P}_o$ matrices.

From the system definition, we obtain

$$\mathbf{B} = \begin{bmatrix} 1 \\ -1 \end{bmatrix} \quad \text{and} \quad \mathbf{AB} = \begin{bmatrix} 2 \\ -2 \end{bmatrix}.$$

Therefore, the controllability matrix is determined to be

$$\mathbf{P}_c = [\mathbf{B} \quad \mathbf{AB}] = \begin{bmatrix} 1 & 2 \\ -1 & -2 \end{bmatrix},$$

and $\det \mathbf{P}_c = 0$. Thus, the system is not controllable.

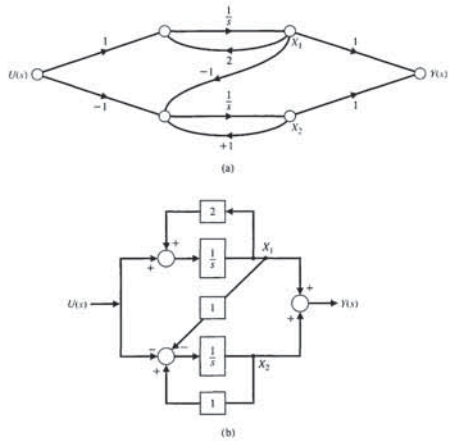

FIGURE 11.4
Two state system model for Example 11.4. (a) Signal-flow graph model. (b) Block diagram model.

Consider the single-input, single-output system

$$\dot{\mathbf{x}} = \mathbf{Ax} + \mathbf{B}u \quad \text{and} \quad y = \mathbf{Cx},$$

where $\mathbf{C}$ is a $1 \times n$ row vector, and $\mathbf{x}$ is an $n \times 1$ column vector. This system is completely observable when the determinant of the **observability matrix** $\mathbf{P}_o$ is nonzero, where

$$\mathbf{P}_o = \begin{bmatrix} \mathbf{C} \\ \mathbf{CA} \\ \vdots \\ \mathbf{CA}^{n-1} \end{bmatrix}. \tag{11.3}$$

which is an $n \times n$ matrix.

As discussed in this section, advanced state variable design techniques can handle situations wherein the system is not completely controllable, as long as the system is stabilizable. These same techniques can handle cases wherein the system is not completely observable, but where the states (or linear combinations thereof) that cannot be observed are inherently stable. These systems are classified as **detectable**. If a system is completely observable, it is also detectable. The Kalman state-space decomposition provides a mechanism for partitioning the state-space so that it becomes apparent which states (or state combinations) are observable and which are not [12, 18]. The unobservable subspace is thus exposed, and if the system is detectable, the control system design can, in theory, proceed. In this chapter, we consider only completely observable systems. The approach to state-variable design involves first verifying that the system under consideration is completely controllable and completely observable. If so, the pole placement design technique considered here can provide acceptable closed-loop system performance.

EXAMPLE 11.3 **Observability of a system**

Consider again the system of Example 11.1. The model is shown in Figure 11.2. To construct $\mathbf{P}_o$, we use

$$\mathbf{A} = \begin{bmatrix} 0 & 1 & 0 \\ 0 & 0 & 1 \\ -a_0 & -a_1 & -a_2 \end{bmatrix} \quad \text{and} \quad \mathbf{C} = [1 \quad 0 \quad 0].$$

Therefore,

$$\mathbf{CA} = [0 \quad 1 \quad 0] \quad \text{and} \quad \mathbf{CA}^2 = [0 \quad 0 \quad 1].$$

Thus, we obtain

$$\mathbf{P}_o = \begin{bmatrix} 1 & 0 & 0 \\ 0 & 1 & 0 \\ 0 & 0 & 1 \end{bmatrix}.$$

The $\det \mathbf{P}_o = 1$, and the system is completely observable. ■

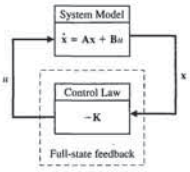

FIGURE 11.5
Full-state feedback block diagram (with no reference input).

we find the closed-loop system to be

$$\dot{\mathbf{x}} = \mathbf{Ax} + \mathbf{B}u = \mathbf{Ax} - \mathbf{BKx} = (\mathbf{A} - \mathbf{BK})\mathbf{x}. \tag{11.5}$$

As discussed in Section 6.4, the characteristic equation associated with Equation (11.5) is

$$\det(\lambda\mathbf{I} - (\mathbf{A} - \mathbf{BK})) = 0.$$

If all the roots of the characteristic equation lie in the left half-plane, then the closed-loop system is stable. In other words, for any initial condition $\mathbf{x}(t_0)$, it follows that

$$\mathbf{x}(t) = e^{(\mathbf{A}-\mathbf{BK})t}\mathbf{x}(t_0) \to 0 \qquad \text{as } t \to \infty.$$

Given the pair $(\mathbf{A}, \mathbf{B})$, we can always determine $\mathbf{K}$ to place *all* the system closed-loop poles in the left half-plane if and only if the system is completely controllable—that is, if and only if the controllability matrix $\mathbf{P}_c$ is full rank (for a single-input, single-output system, full rank implies that $\mathbf{P}_c$ is invertible).

The addition of a reference input can be written as

$$u(t) = -\mathbf{Kx}(t) + Nr(t),$$

where $r(t)$ is the reference input. The question of reference inputs is addressed in Section 11.6. When $r(t) = 0$ for all $t > t_0$, the control design problem is known as the regulator problem. That is, we want to compute $\mathbf{K}$ so that all initial conditions are driven to zero in a specified fashion (as determined by the design specifications).

When using this state variable feedback, the roots of the characteristic equation are placed where the transient performance meets the desired response.

EXAMPLE 11.5 **Design of a third-order system**

Let us consider the third-order system with the differential equation

$$\frac{d^3y}{dt^3} + 5\frac{d^2y}{dt^2} + 3\frac{dy}{dt} + 2y = u.$$

From the system definition, we have

$$\mathbf{C} = [1 \quad 1] \quad \text{and} \quad \mathbf{CA} = [1 \quad 1].$$

Therefore, computing the observability matrix yields

$$\mathbf{P}_o = \begin{bmatrix} \mathbf{C} \\ \mathbf{CA} \end{bmatrix} = \begin{bmatrix} 1 & 1 \\ 1 & 1 \end{bmatrix},$$

and $\det \mathbf{P}_o = 0$. Hence, the system is not observable.

If we look again at the state model, we note that

$$y = x_1 + x_2.$$

However,

$$\dot{x}_1 + \dot{x}_2 = 2x_1 + (x_2 - x_1) + u - u = x_1 + x_2.$$

Thus, the system state variables do not depend on u, and the system is not controllable. Similarly, the output $x_1 + x_2$ depends on $x_1(0)$ plus $x_2(0)$ and does not allow us to determine $x_1(0)$ and $x_2(0)$ independently. Consequently, the system is not observable. ■

11.3 FULL-STATE FEEDBACK CONTROL DESIGN

In this section, we consider full-state variable feedback to achieve the desired pole locations of the closed-loop system.

The first step in the state variable design process requires us to assume that all the states are available for feedback—that is, we have access to the complete state $\mathbf{x}(t)$ for all t. The system input $u(t)$ is given by

$$u = -\mathbf{Kx}. \tag{11.4}$$

Determining the gain matrix $\mathbf{K}$ is the objective of the full-state feedback design procedure. The beauty of the state variable design process is that the problem naturally separates into a full-state feedback component and an observer design component. These two design procedures can occur independently, and in fact, the **separation principle** provides the proof that this approach is optimal. We will show later that the stability of the closed-loop system is guaranteed if the full-state feedback control law stabilizes the system (under the assumption of access to the complete state) and the observer is stable (the tracking error is asymptotically stable). Observers are discussed in Section 11.4. The full-state feedback block diagram is illustrated in Figure 11.5. With the system defined by the state variable model

$$\dot{\mathbf{x}} = \mathbf{Ax} + \mathbf{B}u$$

and the control feedback given by

$$u = -\mathbf{Kx},$$

Comparing Equations (11.6) and (11.7) yields the three equations

$$5 + k_3 = 14.4$$
$$3 + k_2 = 82.1$$
$$2 + k_1 = 172.8.$$

Therefore, we require that $k_3 = 9.4$, $k_2 = 79.1$, and $k_1 = 170.8$. The step response has no overshoot and a settling time of 1 second, as desired. ■

EXAMPLE 11.6 **Inverted pendulum control**

Consider the control of the cart and the unstable inverted pendulum shown in Figure 3.22. We measure and utilize the state variables of the system in order to control the cart (see Example 3.4). Thus, if we want to measure the state variable $x_3 = \theta$, we could use a potentiometer connected to the shaft of the pendulum hinge. Similarly, we could measure the rate of change of the angle $x_4 = \dot{\theta}$ by using a tachometer generator. The state variables x_1 and x_2, which are the position and velocity of the cart, can also be measured by suitable sensors. If the state variables are all measured, then they can be used in a feedback controller so that $u = -\mathbf{Kx}$, where $\mathbf{K}$ is the feedback matrix. The state vector $\mathbf{x}$ represents the state of the system; therefore, knowledge of $\mathbf{x}(t)$ and the equations describing the system dynamics provide sufficient information for control and stabilization of a system [4, 5, 7].

To illustrate the use of state variable feedback, let us consider again the unstable portion of the inverted pendulum system and design a suitable state variable feedback control system. We begin by considering a reduced system. If we assume that the control signal is an acceleration signal and that the mass of the cart is negligible, we can focus on the unstable dynamics of the pendulum. When $u(t)$ is an acceleration signal, Equation (3.69) becomes

$$gx_3 - l\dot{x}_4 = \dot{x}_2 = \ddot{y} = u(t).$$

For the reduced system, where the control signal is an acceleration signal, the position and velocity of the cart are integral functions of $u(t)$. The portion of the state vector under consideration is $[x_3, x_4] = [\theta, \dot{\theta}]$. Thus, the state vector differential equation reduces to

$$\frac{d}{dt}\begin{bmatrix} x_3 \\ x_4 \end{bmatrix} = \begin{bmatrix} 0 & 1 \\ g/l & 0 \end{bmatrix}\begin{bmatrix} x_3 \\ x_4 \end{bmatrix} + \begin{bmatrix} 0 \\ -1/l \end{bmatrix}u(t). \tag{11.8}$$

The $\mathbf{A}$ matrix of Equation (11.8) is simply the lower right-hand portion of the $\mathbf{A}$ matrix of Equation (3.73), and the system has the characteristic equation $\lambda^2 - g/l = 0$ with one root in the right-hand s-plane. To stabilize the system, we generate a control signal that is a function of the two state variables, x_3 and x_4. Then we have

$$u(t) = -\mathbf{Kx} = -[k_1 \quad k_2]\begin{bmatrix} x_3 \\ x_4 \end{bmatrix} = -k_1x_3 - k_2x_4.$$

We can select the state variables as the phase variables (see Section 3.4) so that $x_1 = y$, $x_2 = dy/dt$, $x_3 = d^2y/dt^2$, and then

$$\dot{\mathbf{x}} = \begin{bmatrix} 0 & 1 & 0 \\ 0 & 0 & 1 \\ -2 & -3 & -5 \end{bmatrix}\mathbf{x} + \begin{bmatrix} 0 \\ 0 \\ 1 \end{bmatrix}u = \mathbf{Ax} + \mathbf{B}u$$

and

$$y = [1 \quad 0 \quad 0]\mathbf{x}.$$

If the state variable feedback matrix is

$$\mathbf{K} = [k_1 \quad k_2 \quad k_3]$$

and

$$u = -\mathbf{Kx},$$

then the closed-loop system is

$$\dot{\mathbf{x}} = \mathbf{Ax} - \mathbf{BKx} = (\mathbf{A} - \mathbf{BK})\mathbf{x}.$$

The state feedback matrix is

$$[\mathbf{A} - \mathbf{BK}] = \begin{bmatrix} 0 & 1 & 0 \\ 0 & 0 & 1 \\ -2 - k_1 & -3 - k_2 & -5 - k_3 \end{bmatrix},$$

and the characteristic equation is

$$\Delta(\lambda) = \det(\lambda\mathbf{I} - (\mathbf{A} - \mathbf{BK})) = \lambda^3 + (5 + k_3)\lambda^2 + (3 + k_2)\lambda + (2 + k_1) = 0. \tag{11.6}$$

If we seek a rapid response with a low overshoot, we choose a desired characteristic equation such as (see Equation 5.18 and Table 5.2)

$$\Delta(\lambda) = (\lambda^2 + 2\zeta\omega_n\lambda + \omega_n^2)(\lambda + \zeta\omega_n).$$

We choose $\zeta = 0.8$ for minimal overshoot and ω_n to meet the settling time requirement. If we want a settling time (with a 2% criterion) equal to 1 second, then

$$T_s = \frac{4}{\zeta\omega_n} = \frac{4}{(0.8)\omega_n} \approx 1.$$

If we choose $\omega_n = 6$, the desired characteristic equation is

$$(\lambda^2 + 9.6\lambda + 36)(\lambda + 4.8) = \lambda^3 + 14.4\lambda^2 + 82.1\lambda + 172.8. \tag{11.7}$$

where

$$q(\mathbf{A}) = \mathbf{A}^n + \alpha_{n-1}\mathbf{A}^{n-1} + \cdots\alpha_1\mathbf{A} + \alpha_0\mathbf{I},$$

and $\mathbf{P}_c$ is the controllability matrix of Equation (11.2).

EXAMPLE 11.7 **Second-order system**

Consider the system

$$\frac{Y(s)}{U(s)} = G(s) = \frac{1}{s^2}$$

and determine the feedback gain to place the closed-loop poles at $s = -1 \pm j$. Therefore, we require that

$$q(\lambda) = \lambda^2 + 2\lambda + 2,$$

and $\alpha_1 = \alpha_2 = 2$. With $x_1 = y$ and $x_2 = \dot{y}$, the matrix equation for the system $G(s)$ is

$$\dot{\mathbf{x}} = \begin{bmatrix} 0 & 1 \\ 0 & 0 \end{bmatrix}\mathbf{x} + \begin{bmatrix} 0 \\ 1 \end{bmatrix}u.$$

The controllability matrix is

$$\mathbf{P}_c = [\mathbf{B} \quad \mathbf{AB}] = \begin{bmatrix} 0 & 1 \\ 1 & 0 \end{bmatrix}.$$

Thus, we obtain

$$\mathbf{K} = [0 \quad 1]\mathbf{P}_c^{-1}q(\mathbf{A}),$$

where

$$\mathbf{P}_c^{-1} = \frac{1}{-1}\begin{bmatrix} 0 & -1 \\ -1 & 0 \end{bmatrix} = \begin{bmatrix} 0 & 1 \\ 1 & 0 \end{bmatrix}$$

and

$$q(\mathbf{A}) = \begin{bmatrix} 0 & 1 \\ 0 & 0 \end{bmatrix}^2 + 2\begin{bmatrix} 0 & 1 \\ 0 & 0 \end{bmatrix} + 2\begin{bmatrix} 1 & 0 \\ 0 & 1 \end{bmatrix} = \begin{bmatrix} 2 & 2 \\ 0 & 2 \end{bmatrix}.$$

Then we have

$$\mathbf{K} = [0 \quad 1]\begin{bmatrix} 0 & 1 \\ 1 & 0 \end{bmatrix}\begin{bmatrix} 2 & 2 \\ 0 & 2 \end{bmatrix} = [0 \quad 1]\begin{bmatrix} 0 & 2 \\ 2 & 2 \end{bmatrix} = [2 \quad 2]. \blacksquare$$

Note that computing the gain matrix $\mathbf{K}$ using Ackermann's formula requires the use of $\mathbf{P}_c^{-1}$. We see that complete controllability is essential because only then can we guarantee that the controllability matrix $\mathbf{P}_c$ has full rank and hence that $\mathbf{P}_c^{-1}$ exists.

Substituting this control signal relationship into Equation (11.8), we have

$$\begin{bmatrix} \dot{x}_3 \\ \dot{x}_4 \end{bmatrix} = \begin{bmatrix} 0 & 1 \\ g/l & 0 \end{bmatrix}\begin{bmatrix} x_3 \\ x_4 \end{bmatrix} + \begin{bmatrix} 0 \\ (1/l)(k_1x_3 + k_2x_4) \end{bmatrix}.$$

Combining the two additive terms on the right side of the equation, we find that

$$\begin{bmatrix} \dot{x}_3 \\ \dot{x}_4 \end{bmatrix} = \begin{bmatrix} 0 & 1 \\ (g + k_1)/l & k_2/l \end{bmatrix}\begin{bmatrix} x_3 \\ x_4 \end{bmatrix}.$$

Obtaining the characteristic equation, we have

$$\begin{bmatrix} \lambda & -1 \\ -(g + k_1)/l & \lambda - k_2/l \end{bmatrix} = \lambda\left(\lambda - \frac{k_2}{l}\right) - \frac{g + k_1}{l}$$
$$= \lambda^2 - \left(\frac{k_2}{l}\right)\lambda + \frac{g + k_1}{l}. \tag{11.9}$$

Thus, for the system to be stable, we require that $k_2/l < 0$ and $k_1 > -g$. Hence, we have stabilized an unstable system by measuring the state variables x_3 and x_4 and using the control function $u = -\mathbf{Kx}$ to obtain a stable system. If we wish to achieve a rapid response with modest overshoot, we select $\omega_n = 10$ and $\zeta = 0.8$. Then we require

$$\frac{k_2}{l} = -16 \quad \text{and} \quad \frac{k_1 + g}{l} = 100.$$

The step response would have an overshoot of 1.5% and a settling time of 0.5 second. ■

Thus far, we have established an approach for the design of a feedback control system by using the state variables as the feedback variables in order to increase the stability of the system and obtain the desired system response. Now we face the task of computing the gain matrix $\mathbf{K}$ to place the poles at desired locations. For a single-input, single-output system, Ackermann's formula is useful for determining the state variable feedback matrix

$$\mathbf{K} = [k_1 \quad k_2 \ldots k_n],$$

where

$$u = -\mathbf{Kx}.$$

Given the desired characteristic equation

$$q(\lambda) = \lambda^n + \alpha_{n-1}\lambda^{n-1} + \cdots + \alpha_0,$$

the state feedback gain matrix is

$$\boxed{\mathbf{K} = [0 \quad 0 \quad \ldots \quad 0 \quad 1]\mathbf{P}_c^{-1}q(\mathbf{A}),} \tag{11.10}$$

11.4 OBSERVER DESIGN

In the full-state feedback design procedure discussed in Section 11.3, it was assumed that all the states were available for feedback at all times. This is a good assumption for the control law design process. However, generally speaking, only a subset of the states are readily measurable and available for feedback. Having all the states available for feedback implies that these states are measured with a sensor or sensor combinations. The cost and complexity of the control system increase as the number of required sensors increases. So, even in situations where extra sensors are available, it may not be cost effective to employ these extra sensors, if indeed, the control system design goals can be accomplished without them. Fortunately, if the system is completely observable with a given set of outputs, then it is possible to determine (or to estimate) the states that are not directly measured (or observed).

According to Luenberger [26], the full-state observer for the system

$$\dot{\mathbf{x}} = \mathbf{A}\mathbf{x} + \mathbf{B}u$$
$$y = \mathbf{C}\mathbf{x}$$

is given by

$$\dot{\hat{\mathbf{x}}} = \mathbf{A}\hat{\mathbf{x}} + \mathbf{B}u + \mathbf{L}(y - \mathbf{C}\hat{\mathbf{x}}) \tag{11.11}$$

where $\hat{\mathbf{x}}$ denotes the estimate of the state $\mathbf{x}$. The matrix $\mathbf{L}$ is the observer gain matrix and is to be determined as part of the observer design procedure. The observer is depicted in Figure 11.6. The observer has two inputs, u and y, and one output, $\hat{\mathbf{x}}$.

The goal of the observer is to provide an estimate $\hat{\mathbf{x}}$ so that $\hat{\mathbf{x}} \to \mathbf{x}$ as $t \to \infty$. Remember that we do not know $\mathbf{x}(t_0)$ precisely; therefore we must provide an initial estimate $\hat{\mathbf{x}}(t_0)$ to the observer. Define the observer **estimation error** as

$$\mathbf{e}(t) = \mathbf{x}(t) - \hat{\mathbf{x}}(t). \tag{11.12}$$

The observer design should produce an observer with the property that $\mathbf{e}(t) \to 0$ as $t \to \infty$. One of the main results of systems theory is that if the system is completely observable, we can always find $\mathbf{L}$ so that the tracking error is asymptotically stable, as desired.

Taking the time-derivative of the estimation error in Equation (11.12) yields

$$\dot{\mathbf{e}} = \dot{\mathbf{x}} - \dot{\hat{\mathbf{x}}}$$

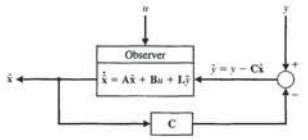

FIGURE 11.6
The full-state observer.

and using the system model and the observer in Equation (11.11), we obtain

$$\dot{\mathbf{e}} = \mathbf{A}\mathbf{x} + \mathbf{B}u - \mathbf{A}\hat{\mathbf{x}} - \mathbf{B}u - \mathbf{L}(y - \mathbf{C}\hat{\mathbf{x}})$$

or

$$\dot{\mathbf{e}}(t) = (\mathbf{A} - \mathbf{LC})\mathbf{e}(t). \tag{11.13}$$

We can guarantee that $\mathbf{e}(t) \to 0$ as $t \to \infty$ for any initial tracking error $\mathbf{e}(t_0)$ if the characteristic equation

$$\det(\lambda\mathbf{I} - (\mathbf{A} - \mathbf{LC})) = 0 \tag{11.14}$$

has all its roots in the left half-plane. Therefore, the observer design process reduces to finding the matrix $\mathbf{L}$ such that the roots of the characteristic equation in Equation (11.14) lie in the left half-plane. This can always be accomplished if the system is completely observable; that is, if the observability matrix $\mathbf{P}_o$ has full rank (for a single-input, single-output system, full rank implies that $\mathbf{P}_o$ is invertible).

EXAMPLE 11.8 **Second-order system observer design**

Consider the second-order system

$$\dot{\mathbf{x}} = \begin{bmatrix} 2 & 3 \\ -1 & 4 \end{bmatrix}\mathbf{x} + \begin{bmatrix} 0 \\ 1 \end{bmatrix}u$$
$$y = [1 \quad 0]\mathbf{x}.$$

In this example, we can only directly observe the state $y = x_1$. The observer will provide estimates of the second state x_2.

In this book, we only consider full-state observers, which implies that the observer will provide estimates of all the states. We might be inclined to suppose that since some states are directly measured, it may be possible to design an observer that provides just the estimates of the states not directly measured. This is, in fact, possible, and the resulting observers are known as reduced-order observers [12, 18]. However, since sensors are not noise free, even states that are directly measured are generally estimated in an effort to reduce the effect of sensor noise on the state estimate. The Kalman filter (which is a time-varying optimal observer) solves the observer problem in the presence of measurement noise (and process noise as well) [33, 34].

The observer design begins by checking the system observability to verify that an observer can be constructed to guarantee the stability of the estimation error. From the system model, we find that

$$\mathbf{A} = \begin{bmatrix} 2 & 3 \\ -1 & 4 \end{bmatrix} \quad \text{and} \quad \mathbf{C} = [1 \quad 0].$$

The corresponding observability matrix is

$$\mathbf{P}_o = \begin{bmatrix} \mathbf{C} \\ \mathbf{CA} \end{bmatrix} = \begin{bmatrix} 1 & 0 \\ 2 & 3 \end{bmatrix}.$$

Since $\det \mathbf{P}_o = 3 \neq 0$, the system is completely observable. Suppose that the desired characteristic equation is given by

$$\Delta_d(\lambda) = \lambda^2 + 2\zeta\omega_n\lambda + \omega_n^2. \tag{11.15}$$

We can select $\zeta = 0.8$ and $\omega_n = 10$, resulting in an expected settling time of less than 0.5 second. Computing the actual characteristic equation yields

$$\det(\lambda\mathbf{I} - (\mathbf{A} - \mathbf{LC})) = \lambda^2 + (L_1 - 6)\lambda - 4(L_1 - 2) + 3(L_2 + 1), \tag{11.16}$$

where $\mathbf{L} = [L_1 \quad L_2]^T$. Equating the coefficients in Equation (11.15) to those in Equation (11.16) yields the two equations

$$L_1 - 6 = 16$$
$$-4(L_1 - 2) + 3(L_2 + 1) = 100$$

which, when solved, produces

$$\mathbf{L} = \begin{bmatrix} L_1 \\ L_2 \end{bmatrix} = \begin{bmatrix} 22 \\ 59 \end{bmatrix}.$$

The observer is thus given by

$$\dot{\hat{\mathbf{x}}} = \begin{bmatrix} 2 & 3 \\ -1 & 4 \end{bmatrix}\hat{\mathbf{x}} + \begin{bmatrix} 0 \\ 1 \end{bmatrix}u + \begin{bmatrix} 22 \\ 59 \end{bmatrix}(y - \hat{x}_1).$$

The response of the estimation error to an initial error of

$$\mathbf{e} = \begin{bmatrix} 1 \\ -2 \end{bmatrix}$$

is shown in Figure 11.7. ■

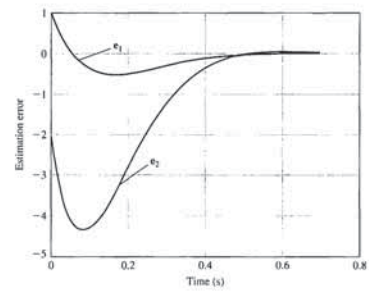

FIGURE 11.7
Second-order observer response to initial estimation errors.

Ackermann's formula can also be employed to place the roots of the observer characteristic equation at the desired locations. Consider the observer gain matrix

$$\mathbf{L} = [L_1 \quad L_2 \quad \cdots \quad L_n]^T$$

and the desired observer characteristic equation

$$p(\lambda) = \lambda^n + \beta_{n-1}\lambda^{n-1} + \cdots + \beta_1\lambda + \beta_0.$$

The β's are selected to meet given performance specifications for the observer. The observer gain matrix is then computed via

$$\boxed{\mathbf{L} = p(\mathbf{A})\mathbf{P}_o^{-1}[0 \cdots 0 \quad 1]^T.} \tag{11.17}$$

where $\mathbf{P}_o$ is the observability matrix given in Equation (11.3) and

$$p(\mathbf{A}) = \mathbf{A}^n + \beta_{n-1}\mathbf{A}^{n-1} + \cdots + \beta_1\mathbf{A} + \beta_0\mathbf{I}.$$

EXAMPLE 11.9 **Second-order system observer design using Ackermann's formula**

Consider the second-order system in Example 11.8. The desired characteristic equation was given as

$$p(\lambda) = \lambda^2 + 2\zeta\omega_n\lambda + \omega_n^2,$$

where $\zeta = 0.8$ and $\omega_n = 10$; hence, $\beta_1 = 16$ and $\beta_2 = 100$. Computing $p(\mathbf{A})$ yields

$$p(\mathbf{A}) = \begin{bmatrix} 2 & 3 \\ -1 & 4 \end{bmatrix}^2 + 16\begin{bmatrix} 2 & 3 \\ -1 & 4 \end{bmatrix} + 100\begin{bmatrix} 1 & 0 \\ 0 & 1 \end{bmatrix} = \begin{bmatrix} 133 & 66 \\ -22 & 177 \end{bmatrix},$$

and from Example 11.8, we have the observability matrix

$$\mathbf{P}_o = \begin{bmatrix} 1 & 0 \\ 2 & 3 \end{bmatrix},$$

which implies that

$$\mathbf{P}_o^{-1} = \begin{bmatrix} 1 & 0 \\ -2/3 & 1/3 \end{bmatrix}.$$

Using Ackermann's formula in Equation (11.17) yields the observer gain matrix

$$\mathbf{L} = p(\mathbf{A})\mathbf{P}_o^{-1}[0 \quad \cdots \quad 0 \quad 1]^T = \begin{bmatrix} 133 & 66 \\ -22 & 177 \end{bmatrix}\begin{bmatrix} 1 & 0 \\ -2/3 & 1/3 \end{bmatrix}\begin{bmatrix} 0 \\ 1 \end{bmatrix} = \begin{bmatrix} 22 \\ 59 \end{bmatrix}.$$

This is the identical result obtained in Example 11.8 using other methods. ■

Computing the estimation error using the compensator in Equation (11.19) yields

$$\dot{\mathbf{e}} = \dot{\mathbf{x}} - \dot{\hat{\mathbf{x}}} = \mathbf{A}\mathbf{x} + \mathbf{B}u - \mathbf{A}\hat{\mathbf{x}} - \mathbf{B}u - \mathbf{L}y + \mathbf{L}\mathbf{C}\hat{\mathbf{x}},$$

or

$$\dot{\mathbf{e}} = (\mathbf{A} - \mathbf{LC})\mathbf{e}. \tag{11.20}$$

This is the same result as we obtained for the estimation error in Section 11.4. The estimation error does not depend on the input as seen in Equation (11.20), where the input terms cancel. Recall that the underlying system model is given by

$$\begin{aligned}\dot{\mathbf{x}} &= \mathbf{A}\mathbf{x} + \mathbf{B}u\\ y &= \mathbf{C}\mathbf{x}.\end{aligned}$$

Substituting the feedback law $u(t) = -\mathbf{K}\hat{\mathbf{x}}(t)$ into the system model yields

$$\dot{\mathbf{x}} = \mathbf{A}\mathbf{x} + \mathbf{B}u = \mathbf{A}\mathbf{x} - \mathbf{B}\mathbf{K}\hat{\mathbf{x}},$$

and with $\hat{\mathbf{x}} = \mathbf{x} - \mathbf{e}$, we obtain

$$\dot{\mathbf{x}} = (\mathbf{A} - \mathbf{BK})\mathbf{x} + \mathbf{BK}\mathbf{e}. \tag{11.21}$$

Writing Equations (11.20) and (11.21) in matrix form, we have

$$\begin{pmatrix}\dot{\mathbf{x}}\\ \dot{\mathbf{e}}\end{pmatrix} = \begin{bmatrix}\mathbf{A} - \mathbf{BK} & \mathbf{BK}\\ \mathbf{0} & \mathbf{A} - \mathbf{LC}\end{bmatrix}\begin{pmatrix}\mathbf{x}\\ \mathbf{e}\end{pmatrix}. \tag{11.22}$$

Recall that our goal is to verify that, with $u(t) = -\mathbf{K}\hat{\mathbf{x}}(t)$, we retain stability of the closed-loop system and the observer. The characteristic equation associated with Equation (11.22) is

$$\Delta(\lambda) = \det(\lambda\mathbf{I} - (\mathbf{A} - \mathbf{BK}))\det(\lambda\mathbf{I} - (\mathbf{A} - \mathbf{LC})).$$

So if the roots of $\det(\lambda\mathbf{I} - (\mathbf{A} - \mathbf{BK})) = 0$ lie in the left half-plane (which they do by design of the full-state feedback law), and if the roots of $\det(\lambda\mathbf{I} - (\mathbf{A} - \mathbf{LC})) = 0$ lie in the left half-plane (which they do by design of the observer), then the overall system is stable. Therefore, employing the strategy of using the state estimates for the feedback is in fact a good strategy.

In other words, when we use $u(t) = -\mathbf{K}\hat{\mathbf{x}}(t)$ where $\mathbf{K}$ is designed using the methods proposed in Section 11.3 and $\hat{\mathbf{x}}$ is derived from the observer discussed in Section 11.4, then $\mathbf{x}(t) \to 0$ as $t \to \infty$ for any initial condition $\mathbf{x}(t_0)$ and $\mathbf{e}(t) \to 0$ as $t \to \infty$ for any initial estimation error $\mathbf{e}(t_0)$. The fact that the full-state feedback law and the observer can be designed independently is an illustration of the **separation principle**.

The design procedure is summarized as follows:

1. Determine $\mathbf{K}$ such that $\det(\lambda\mathbf{I} - (\mathbf{A} - \mathbf{BK})) = 0$ has roots in the left half-plane and place the poles appropriately to meet the control system design specifications. The ability to place the poles arbitrarily in the complex plane is guaranteed if the system is completely controllable.

11.5 INTEGRATED FULL-STATE FEEDBACK AND OBSERVER

The state variable compensator is constructed by appropriately connecting the full-state feedback control law (see Section 11.3) to the observer (see Section 11.4). The compensator is shown in Figure 11.1 (as discussed in Section 11.1). Our strategy was to design the state feedback control law as $u(t) = -\mathbf{K}\mathbf{x}(t)$, where we assumed that we had access to the complete state $\mathbf{x}(t)$. Then we designed an observer to provide an estimate of the state $\hat{\mathbf{x}}(t)$. It seems reasonable that we can employ the state estimate in the feedback control law in place of $\mathbf{x}(t)$. In other words, we can consider the feedback law

$$u(t) = -\mathbf{K}\hat{\mathbf{x}}(t). \tag{11.18}$$

But is this a good strategy? The feedback gain matrix $\mathbf{K}$ was designed to guarantee stability of the closed-loop system; that is, the roots of the characteristic equation

$$\det(\lambda\mathbf{I} - (\mathbf{A} - \mathbf{BK})) = 0$$

are in the left half-plane. Under the assumption that the complete state $\mathbf{x}(t)$ is available for feedback, the feedback control law (with properly designed gain matrix $\mathbf{K}$) leads to the desired result that $\mathbf{x}(t) \to 0$ as $t \to \infty$ for any initial condition $\mathbf{x}(t_0)$. We need to verify that, when using the feedback control law in Equation (11.18), we retain the stability of the closed-loop system.

Consider the observer (from Section 11.4)

$$\dot{\hat{\mathbf{x}}} = \mathbf{A}\hat{\mathbf{x}} + \mathbf{B}u + \mathbf{L}(y - \mathbf{C}\hat{\mathbf{x}}).$$

Substituting the feedback law in Equation (11.18) and rearranging terms in the observer yields the compensator system

$$\begin{aligned}\dot{\hat{\mathbf{x}}} &= (\mathbf{A} - \mathbf{BK} - \mathbf{LC})\hat{\mathbf{x}} + \mathbf{L}y\\ u &= -\mathbf{K}.\end{aligned} \tag{11.19}$$

Notice that the system in Equation (11.19) has the form of a state variable model with input y and output u, as illustrated in Figure 11.8.

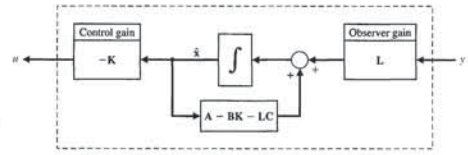

FIGURE 11.8
State variable compensator with integrated full-state feedback and observer.

Let the system parameters be

$$\begin{aligned}l &= 0.098\text{ m}\\ g &= 9.8\text{ m/s}^2\\ m &= 0.825\text{ kg}\\ M &= 8.085\text{ kg}.\end{aligned}$$

Therefore, using the parameter values, the system state and input matrices are

$$\mathbf{A} = \begin{bmatrix}0 & 1 & 0 & 0\\ 0 & 0 & -1 & 0\\ 0 & 0 & 0 & 1\\ 0 & 0 & 100 & 0\end{bmatrix} \quad\text{and}\quad \mathbf{B} = \begin{bmatrix}0\\ 0.1237\\ 0\\ -1.2621\end{bmatrix}.$$

Checking controllability yields the controllability matrix

$$\mathbf{P}_c = \begin{bmatrix}0 & 0.1237 & 0 & 1.2621\\ 0.1237 & 0 & 1.2621 & 0\\ 0 & -1.2621 & 0 & -126.21\\ -1.2621 & 0 & -126.21 & 0\end{bmatrix}.$$

Computing $\det \mathbf{P}_c = 196.49 \neq 0$; hence, the system is completely controllable. Likewise, computing the observability matrix

$$\mathbf{P}_o = \begin{bmatrix}1 & 0 & 0 & 0\\ 0 & 1 & 0 & 0\\ 0 & 0 & -1 & 0\\ 0 & 0 & 0 & -1\end{bmatrix}$$

and $\det \mathbf{P}_o = 1 \neq 0$; hence, the system is completely observable. We can now proceed with the three-step design procedure knowing that we can determine a control gain matrix $\mathbf{K}$ and observer gain matrix $\mathbf{L}$ to place all the closed-loop system poles at desired locations.

STEP 1: Design the Full-State Feedback Control Law.
The open-loop system poles are located at $\lambda = 0, 0, -10$, and 10. It is evident that the open-loop system is unstable (there is a pole in the right half-plane). Suppose that the desired closed-loop system characteristic equation is given by

$$q(\lambda) = (\lambda^2 + 2\zeta\omega_n\lambda + \omega_n^2)(\lambda^2 + a\lambda + b),$$

where we choose (1) the pair (ζ, ω_n) so that these poles are the dominant poles and (2) the pair (a, b) farther in the left half-plane so as not to dominate the response. To obtain a settling time less than 10 seconds with low overshoot, we can select $(\zeta, \omega_n) = (0.8, 0.5)$. Then, we choose a separation factor of 20 between the dominant poles and the remaining poles, from which it follows that $(a, b) = (16, 100)$. Figure 11.9 shows the pole zero map for the system design. The separation factor

2. Determine $\mathbf{L}$ such that $\det(\lambda\mathbf{I} - (\mathbf{A} - \mathbf{LC})) = 0$ has roots in the left half-plane and place the poles to achieve acceptable observer performance. The ability to place the observer poles arbitrarily in the complex plane is guaranteed if the system is completely observable.
3. Connect the observer to the full-state feedback law using

$$u(t) = -\mathbf{K}\hat{\mathbf{x}}(t).$$

Compensator Transfer Function. The compensator given in Equation (11.19) can be given equivalently in transfer function form with input $Y(s)$ and output $U(s)$. Taking the Laplace transform (with zero initial conditions) of the compensator yields

$$\begin{aligned}s\hat{\mathbf{X}}(s) &= (\mathbf{A} - \mathbf{BK} - \mathbf{LC})\hat{\mathbf{X}}(s) + \mathbf{L}Y(s)\\ U(s) &= -\mathbf{K}\hat{\mathbf{X}}(s),\end{aligned}$$

and rearranging and solving for $U(s)$, we obtain the transfer function

$$\boxed{U(s) = [-\mathbf{K}(s\mathbf{I} - (\mathbf{A} - \mathbf{BK} - \mathbf{LC}))^{-1}\mathbf{L}]Y(s).} \tag{11.23}$$

Note that the compensator transfer function itself (when viewed as a system) may or may not be stable. Even though $\mathbf{A} - \mathbf{BK}$ is stable and $\mathbf{A} - \mathbf{LC}$ is stable, it does not necessarily follow that $\mathbf{A} - \mathbf{BK} - \mathbf{LC}$ is stable. However, the overall closed-loop system is stable (as we proved in the previous discussions). The controller in Equation (11.23) is commonly referred to as a **stabilizing controller**.

EXAMPLE 11.10 **Compensator design for the inverted pendulum**

Consider the inverted pendulum of Example 3.4. The state variable model representing the inverted pendulum atop a moving cart is

$$\dot{\mathbf{x}} = \begin{bmatrix}0 & 1 & 0 & 0\\ 0 & 0 & \dfrac{-mg}{M} & 0\\ 0 & 0 & 0 & 1\\ 0 & 0 & \dfrac{g}{l} & 0\end{bmatrix}\mathbf{x} + \begin{bmatrix}0\\ \dfrac{1}{M}\\ 0\\ \dfrac{-1}{Ml}\end{bmatrix}u,$$

where $\mathbf{x} = (x_1, x_2, x_3, x_4)^T$, x_1 is the cart position, x_2 is the cart velocity, x_3 is the pendulum angular position (measured from the vertical), x_4 is the pendulum angular rate, and u is the input applied to the cart. As discussed in Example 11.6, we can measure the state variable $x_3 = \theta$ using a potentiometer attached to the shaft, or measure $x_4 = \dot{\theta}$ using a tachometer generator. However, suppose that we have a sensor available to measure the position of the cart. Is it possible to hold the angular position of the pendulum at the desired value ($\theta = 0°$) when only the output $y = x_1$ (the cart position) is available? In this case, we have the output equation

$$y = [1 \quad 0 \quad 0 \quad 0]\mathbf{x}.$$

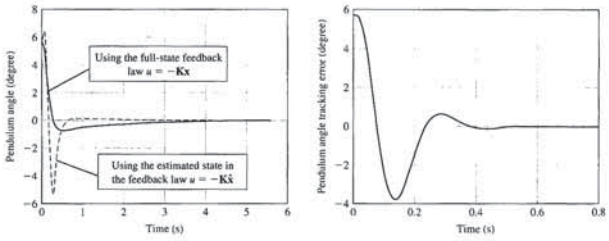

FIGURE 11.10 Pendulum performance under full-state feedback control with the observer in the loop.

where the constants c_1 and c_2 are appropriately chosen. As a first attempt, we select $c_1 = 32$ and $c_2 = 711.11$. These values should produce a response to an initial state estimation error that settles in less than 0.5 second with minimal overshoot. Using Ackermann's formula from Section 11.3, we determine that the observer gain that achieves the desired observer pole locations $\det(\lambda\mathbf{I} - (\mathbf{A} - \mathbf{LC})) = ((\lambda + 16 + j21.3)(\lambda + 16 - j21.3))^2$ is

$$\mathbf{L} = \begin{bmatrix} 64.0 \\ 2546.22 \\ -5.1911\text{E}04 \\ -7.6030\text{E}05 \end{bmatrix}.$$

STEP 3: Compensator Design

The final step in the design is to connect the observer to the full-state feedback control law via $u = -\mathbf{K}\hat{\mathbf{x}}$. As proved earlier, the closed-loop system will remain stable; however, we should not expect the closed-loop performance to be as good when using the state estimate from the observer. This makes sense, since it takes a finite amount of time for the observer to provide accurate state estimates. The response of the inverted pendulum design is shown in Figure 11.10. The pendulum is initially stationary at $\theta_0 = 5.72°$, and the cart is initially not moving. The initial state estimate in the observer is set to zero.

In Figure 11.10(a), we see that, indeed, the pendulum is balanced to the vertical in under 4 seconds. The response of the compensator (with the observer) is more oscillatory than without the observer in the loop—but this difference in performance is expected, since it takes about 0.4 second for the observer to converge to a minimal state tracking error, as seen in Figure 11.10(b). ■

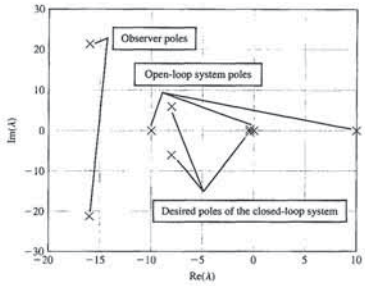

FIGURE 11.9 System pole map: open-loop poles, desired closed-loop poles, and observer poles.

between the dominant and nondominant poles is a parameter that can be varied as part of the design process. The larger the separation selected, the further left in the left half-plane the nondominant poles will be placed, and hence the larger the required control law gains. The desired roots are then specified to be

$$\det(\lambda\mathbf{I} - (\mathbf{A} - \mathbf{BK})) = (\lambda + 8 \pm j6)(\lambda + 0.4 \pm j0.3).$$

The poles at $\lambda = -0.4 \pm 0.3j$ are the dominant poles. Using Ackermann's formula yields the feedback gain matrix

$$\mathbf{K} = [-2.2509 \quad -7.5631 \quad -169.0265 \quad -14.0523].$$

STEP 2: Observer Design

The observer needs to provide an estimate of the states that cannot be directly observed. The goal is to achieve an accurate estimate as fast as possible without resulting in too large a gain matrix $\mathbf{L}$. How large is too large depends on the problem under consideration. In particular, if there are significant levels of measurement noise (this is sensor dependent), then the magnitude of the observer matrix should be kept correspondingly low to avoid amplifying the measurement noise. The trade-off between the time required to obtain accurate observer performance and the amount of noise amplification is a primary design issue. For design purposes, we will attempt to insure a separation of the desired closed-loop system poles and the observer poles on the order of 2 to 10 (as illustrated in Figure 11.9). The desired observer characteristic equation is selected to be of the form

$$p(\lambda) = (\lambda^2 + c_1\lambda + c_2)^2,$$

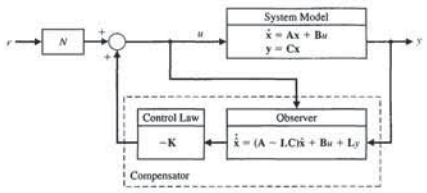

FIGURE 11.12 State variable compensator with reference input and $\mathbf{M} = \mathbf{B}N$.

or

$$\dot{\mathbf{e}} = (\mathbf{A} - \mathbf{LC})\mathbf{e} + (\mathbf{B}N - \mathbf{M})r.$$

Suppose that we select

$$\mathbf{M} = \mathbf{B}N. \tag{11.25}$$

Then the corresponding estimation error is given by

$$\dot{\mathbf{e}} = (\mathbf{A} - \mathbf{LC})\mathbf{e}.$$

In this case, the estimation error is independent of the reference input $r(t)$. This is the identical result found in Section 11.4, where we considered the observer design assuming no reference inputs. The remaining task is to determine a suitable value of N, since the value of $\mathbf{M}$ follows from Equation (11.25). For example, we might choose N to obtain a zero steady-state tracking error to a step input $r(t)$.

With $\mathbf{M} = \mathbf{B}N$, we find that the compensator is given by

$$\dot{\hat{\mathbf{x}}} = \mathbf{A}\hat{\mathbf{x}} + \mathbf{B}u + \mathbf{L}\tilde{y}$$
$$u = -\mathbf{K}\hat{\mathbf{x}} + Nr.$$

This implementation of the state variable compensator is illustrated in Figure 11.12.

As an alternative approach, suppose that we select $N = 0$ and $\mathbf{M} = -\mathbf{L}$. Then, the compensator in Equation (11.24) is given by

$$\dot{\hat{\mathbf{x}}} = \mathbf{A}\hat{\mathbf{x}} + \mathbf{B}u + \mathbf{L}\tilde{y} - \mathbf{L}r$$
$$u = -\mathbf{K}\hat{\mathbf{x}},$$

which can be rewritten as

$$\dot{\hat{\mathbf{x}}} = (\mathbf{A} - \mathbf{BK} - \mathbf{LC})\hat{\mathbf{x}} + \mathbf{L}(y - r)$$
$$u = -\mathbf{K}\hat{\mathbf{x}}.$$

In this formulation, the observer is driven by the tracking error $y - r$. The reference input tracking implementation is illustrated in Figure 11.13.

Notice that in the first implementation (with $\mathbf{M} = \mathbf{B}N$) the compensator is in the feedback loop, whereas in the second implementation ($N = 0$ and $\mathbf{M} = -\mathbf{L}$) the

11.6 REFERENCE INPUTS

The feedback strategies discussed in the previous sections (and illustrated in Figure 11.1) were constructed without consideration of reference inputs. We referred to the design of state variable feedback compensators without reference inputs (i.e., $r(t) = 0$) as regulators. Since **command following** is also an important aspect of feedback design, it is important to consider how we can introduce a reference signal into the state variable feedback compensator. There are, in fact, many different techniques that can be employed to permit the tracking of a reference input. Two of the more common methods are discussed in this section.

The general form of the state variable feedback compensator is

$$\dot{\hat{\mathbf{x}}} = \mathbf{A}\hat{\mathbf{x}} + \mathbf{B}\tilde{u} + \mathbf{L}\tilde{y} + \mathbf{M}r$$
$$u = \tilde{u} + Nr = -\mathbf{K}\hat{\mathbf{x}} + Nr, \tag{11.24}$$

where $\tilde{y} = y - \mathbf{C}\hat{\mathbf{x}}$ and $\tilde{u} = -\mathbf{K}\hat{\mathbf{x}}$. The state variable compensator with the reference input is illustrated in Figure 11.11. Notice that when $\mathbf{M} = \mathbf{0}$ and $N = 0$, the compensator in Equation (11.24) reduces to the regulator described in Section 11.5 and illustrated in Figure 11.1.

The compensator key design parameters required to implement the command tracking of the reference input are $\mathbf{M}$ and N. When the reference input is a scalar signal (i.e., a single input), the parameter $\mathbf{M}$ is a column vector of length n, where n is the length of the state vector $\mathbf{x}$, and N is a scalar. Here, we consider two possibilities for selecting $\mathbf{M}$ and N. In the first case, we select $\mathbf{M}$ and N so that the estimation error $\mathbf{e}(t)$ is independent of the reference input $r(t)$. In the second case, we select $\mathbf{M}$ and N so that the tracking error $y(t) - r(t)$ is used as an input to the compensator. These two cases will result in implementations wherein the compensator is in the feedback loop in the first case and in the forward loop in the second case.

Employing the generalized compensator in Equation (11.24), the estimation error is found to be described by the differential equation

$$\dot{\mathbf{e}} = \dot{\mathbf{x}} - \dot{\hat{\mathbf{x}}} = \mathbf{A}\mathbf{x} + \mathbf{B}u - \mathbf{A}\hat{\mathbf{x}} - \mathbf{B}\tilde{u} - \mathbf{L}\tilde{y} - \mathbf{M}r.$$

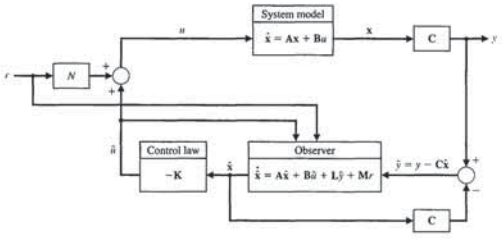

FIGURE 11.11 State variable compensator with a reference input.

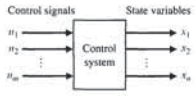

FIGURE 11.14
A control system in terms of x and u.

equilibrium, $\mathbf{x} = \mathbf{x}_d = \mathbf{0}$, and any deviation from equilibrium is considered an error. Therefore, in this section, we will consider the design of optimal control systems using state variable feedback and error-squared performance indices [1–3].

The control system we will consider is shown in Figure 11.14 and can be represented by the vector differential equation

$$\dot{\mathbf{x}} = \mathbf{A}\mathbf{x} + \mathbf{B}\mathbf{u}. \tag{11.27}$$

We will select a feedback controller so that $\mathbf{u}$ is some function of the measured state variables $\mathbf{x}$ and therefore

$$\mathbf{u} = -\mathbf{k}(\mathbf{x}).$$

For example, we might use

$$u_1 = -k_1 x_1, \quad u_2 = -k_2 x_2, \quad \ldots, \quad u_m = -k_m x_m. \tag{11.28}$$

Alternatively, we might choose the control vector as

$$u_1 = -k_1(x_1 + x_2), \quad u_2 = -k_2(x_2 + x_3), \quad \ldots. \tag{11.29}$$

The choice of the control signals is somewhat arbitrary and depends partially on the actual desired performance and the complexity of the feedback structure allowable. Often, we are limited in the number of state variables available for feedback, since we are only able to use measurable state variables.

In our case, we limit the feedback function to a linear function so that $\mathbf{u} = -\mathbf{K}\mathbf{x}$, where $\mathbf{K}$ is an $m \times n$ matrix, as in Section 11.3. Therefore, in expanded form, we have

$$\begin{bmatrix} u_1 \\ u_2 \\ \vdots \\ u_m \end{bmatrix} = -\begin{bmatrix} k_{11} & \cdots & k_{1n} \\ \vdots & & \vdots \\ k_{m1} & \cdots & k_{mn} \end{bmatrix} \begin{bmatrix} x_1 \\ x_2 \\ \vdots \\ x_n \end{bmatrix}. \tag{11.30}$$

Substituting Equation (11.30) into Equation (11.27), we obtain

$$\dot{\mathbf{x}} = \mathbf{A}\mathbf{x} - \mathbf{B}\mathbf{K}\mathbf{x} = \mathbf{H}\mathbf{x}, \tag{11.31}$$

where $\mathbf{H}$ is the $n \times n$ matrix resulting from the addition of the elements of $\mathbf{A}$ and $-\mathbf{B}\mathbf{K}$.

Now, returning to the error-squared performance index, we recall from Section 5.7 that the index for a single state variable, x_1, is written as

$$J = \int_0^{t_f} [x_1(t)]^2 \, dt. \tag{11.32}$$

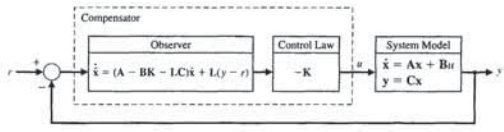

FIGURE 11.13
State variable compensator with reference input and $N = 0$ and $\mathbf{M} = -\mathbf{L}$.

compensator is in the forward path. These two implementations are representative of the possibilities open to control system designers when considering reference inputs.

Depending on the choice of N and $\mathbf{M}$, other implementations are possible. For example, Section 11.8 presents a method of tracking reference inputs with guaranteed steady-state tracking errors using **internal model design** techniques.

11.7 OPTIMAL CONTROL SYSTEMS

The design of optimal control systems is an important function of control engineering. The purpose of design is to realize a system with practical components that will provide the desired operating performance. The desired performance can be readily stated in terms of time-domain performance indices. For example, the maximum overshoot and rise time for a step input are valuable time-domain indices. In the case of steady-state and transient performance, the performance indices are normally specified in the time domain; therefore, it is natural that we wish to develop design procedures in the time domain.

The performance of a control system can be represented by integral performance measures, as we found in Section 5.7. Therefore, the design of a system must be based on minimizing a performance index, such as the integral of the squared error (ISE), as in Section 5.7. Systems that are adjusted to provide a minimum performance index are often called **optimal control systems**. In this section, we will consider the design of an optimal control system that is described by a state variable formulation. We will consider the measurement of the state variables and their use in developing a control signal $u(t)$ so that the performance of the system is optimized.

The performance of a control system, written in terms of the state variables of a system, can be expressed in general as

$$J = \int_0^{t_f} g(\mathbf{x}, \mathbf{u}, t) \, dt. \tag{11.26}$$

where $\mathbf{x}$ equals the state vector, $\mathbf{u}$ equals the control vector, and t_f equals the final time.[1]

We are interested in minimizing the error of the system; therefore, when the desired state vector is represented as $\mathbf{x}_d = \mathbf{0}$, we are able to consider the error as identically equal to the value of the state vector. That is, we intend the system to be at

[1]Note that to denote the performance index, J is used instead of I, as in Chapter 5. This will enable the reader to distinguish readily the performance index from the identity matrix, which is represented by the boldfaced capital $\mathbf{I}$.

which is the exact differential we are seeking. Substituting Equation (11.38) into Equation (11.35), we obtain

$$J = \int_0^{\infty} -\frac{d}{dt}(\mathbf{x}^T\mathbf{P}\mathbf{x}) \, dt = -\mathbf{x}^T\mathbf{P}\mathbf{x}\Big|_0^{\infty} = \mathbf{x}^T(0)\mathbf{P}\mathbf{x}(0). \tag{11.39}$$

In the evaluation of the limit at $t = \infty$, we have assumed that the system is stable, and hence $\mathbf{x}(\infty) = 0$, as desired. Therefore, to minimize the performance index J, we consider the two equations

$$\boxed{J = \int_0^{\infty} \mathbf{x}^T\mathbf{x} \, dt = \mathbf{x}^T(0)\mathbf{P}\mathbf{x}(0)} \tag{11.40}$$

and

$$\boxed{\mathbf{H}^T\mathbf{P} + \mathbf{P}\mathbf{H} = -\mathbf{I}} \tag{11.41}$$

The design steps are then as follows:

1. Determine the matrix $\mathbf{P}$ that satisfies Equation (11.41), where $\mathbf{H}$ is known.
2. Minimize J by determining the minimum of Equation (11.40) by adjusting one or more unspecified system parameters.

EXAMPLE 11.11 **State variable feedback**

Consider the open-loop control system shown in Figure 11.15. The state variables are identified as x_1 and x_2. The performance of this system is quite unsatisfactory because an undamped response results for a step input. The vector differential equation of this system is

$$\frac{d}{dt}\begin{bmatrix} x_1 \\ x_2 \end{bmatrix} = \begin{bmatrix} 0 & 1 \\ 0 & 0 \end{bmatrix}\begin{bmatrix} x_1 \\ x_2 \end{bmatrix} + \begin{bmatrix} 0 \\ 1 \end{bmatrix} u(t), \tag{11.42}$$

where

$$\mathbf{A} = \begin{bmatrix} 0 & 1 \\ 0 & 0 \end{bmatrix} \quad \text{and} \quad \mathbf{B} = \begin{bmatrix} 0 \\ 1 \end{bmatrix}.$$

We will choose a feedback control system so that

$$u(t) = -k_1 x_1 - k_2 x_2, \tag{11.43}$$

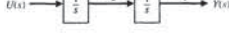

FIGURE 11.15
Open-loop control system of Example 11.11.

A performance index written in terms of two state variables would then be

$$J = \int_0^{t_f} (x_1^2 + x_2^2) \, dt. \tag{11.33}$$

Since we wish to define the performance index in terms of an integral of the sum of the state variables squared, we will use the matrix operation

$$\mathbf{x}^T\mathbf{x} = [x_1, x_2, x_3, \ldots, x_n]\begin{bmatrix} x_1 \\ x_2 \\ \vdots \\ x_n \end{bmatrix} = x_1^2 + x_2^2 + x_3^2 + \cdots + x_n^2, \tag{11.34}$$

where $\mathbf{x}^T$ indicates the transpose of the $\mathbf{x}$ matrix.[1] Then the specific form of the performance index, in terms of the state vector, is

$$J = \int_0^{t_f} \mathbf{x}^T\mathbf{x} \, dt. \tag{11.35}$$

The general form of the performance index (Equation 11.26) incorporates a term with $\mathbf{u}$ that we have not included at this point, but we will do so later in this section.

Again considering Equation (11.35), we will let the final time of interest be $t_f = \infty$. To obtain the minimum value of J, we postulate the existence of an exact differential so that

$$\frac{d}{dt}(\mathbf{x}^T\mathbf{P}\mathbf{x}) = -\mathbf{x}^T\mathbf{x}, \tag{11.36}$$

where $\mathbf{P}$ is to be determined. A symmetric $\mathbf{P}$ matrix will be used to simplify the algebra without any loss of generality. Then, for a symmetric $\mathbf{P}$ matrix, $p_{ij} = p_{ji}$. Completing the differentiation indicated on the left-hand side of Equation (11.36), we have

$$\frac{d}{dt}(\mathbf{x}^T\mathbf{P}\mathbf{x}) = \dot{\mathbf{x}}^T\mathbf{P}\mathbf{x} + \mathbf{x}^T\mathbf{P}\dot{\mathbf{x}}.$$

Substituting Equation (11.31), we obtain

$$\begin{aligned} \frac{d}{dt}(\mathbf{x}^T\mathbf{P}\mathbf{x}) &= (\mathbf{H}\mathbf{x})^T\mathbf{P}\mathbf{x} + \mathbf{x}^T\mathbf{P}(\mathbf{H}\mathbf{x}) \\ &= \mathbf{x}^T\mathbf{H}^T\mathbf{P}\mathbf{x} + \mathbf{x}^T\mathbf{P}\mathbf{H}\mathbf{x} \\ &= \mathbf{x}^T(\mathbf{H}^T\mathbf{P} + \mathbf{P}\mathbf{H})\mathbf{x}, \end{aligned} \tag{11.37}$$

where $(\mathbf{H}\mathbf{x})^T = \mathbf{x}^T\mathbf{H}^T$ by the definition of the transpose of a product. If we let $\mathbf{H}^T\mathbf{P} + \mathbf{P}\mathbf{H} = -\mathbf{I}$, then Equation (11.37) becomes

$$\frac{d}{dt}(\mathbf{x}^T\mathbf{P}\mathbf{x}) = -\mathbf{x}^T\mathbf{x}, \tag{11.38}$$

[1]The matrix operation $\mathbf{x}^T\mathbf{x}$ is discussed on the MCS website.

and therefore the control signal is a linear function of the two state variables. Then Equation (11.42) becomes

$$\begin{aligned} \dot{x}_1 &= x_2, \\ \dot{x}_2 &= -k_1 x_1 - k_2 x_2; \end{aligned} \tag{11.44}$$

in matrix form, we have

$$\begin{aligned} \dot{\mathbf{X}} &= \mathbf{H}\mathbf{x} \\ &= \begin{bmatrix} 0 & 1 \\ -k_1 & -k_2 \end{bmatrix} \mathbf{x}. \end{aligned} \tag{11.45}$$

We note that x_1 would represent the position of a position control system, and the transfer function of the system would be $G(s) = 1/(Ms^2)$, where $M = 1$ and the friction is negligible. We will let $k_1 = 1$ and determine a suitable value for k_2 so that the performance index is minimized. Writing Equation (11.41), we have

$$\mathbf{H}^T\mathbf{P} + \mathbf{P}\mathbf{H} = -\mathbf{I},$$

and in expanded form

$$\begin{bmatrix} 0 & -1 \\ 1 & -k_2 \end{bmatrix} \begin{bmatrix} p_{11} & p_{12} \\ p_{12} & p_{22} \end{bmatrix} + \begin{bmatrix} p_{11} & p_{12} \\ p_{12} & p_{22} \end{bmatrix} \begin{bmatrix} 0 & 1 \\ -1 & -k_2 \end{bmatrix} = \begin{bmatrix} -1 & 0 \\ 0 & -1 \end{bmatrix}. \tag{11.46}$$

Completing the matrix multiplication and addition, we have

$$\begin{aligned} -p_{12} - p_{12} &= -1, \\ p_{11} - k_2 p_{12} - p_{22} &= 0, \\ p_{12} - k_2 p_{22} + p_{12} - k_2 p_{22} &= -1. \end{aligned} \tag{11.47}$$

Solving these simultaneous equations, we obtain

$$p_{12} = \frac{1}{2}, \qquad p_{22} = \frac{1}{k_2}, \qquad p_{11} = \frac{k_2^2 + 2}{2k_2}.$$

The integral performance index is then

$$J = \mathbf{x}^T(0)\mathbf{P}\mathbf{x}(0), \tag{11.48}$$

and we will consider the case where each state is initially displaced one unit from equilibrium so that $\mathbf{x}^T(0) = [1, 1]$. Therefore Equation (11.48) becomes

$$\begin{aligned} J &= \begin{bmatrix} 1 & 1 \end{bmatrix} \begin{bmatrix} p_{11} & p_{12} \\ p_{12} & p_{22} \end{bmatrix} \begin{bmatrix} 1 \\ 1 \end{bmatrix} \\ &= \begin{bmatrix} 1 & 1 \end{bmatrix} \begin{bmatrix} p_{11} + p_{12} \\ p_{12} + p_{22} \end{bmatrix} \\ &= (p_{11} + p_{12}) + (p_{12} + p_{22}) = p_{11} + 2p_{12} + p_{22}. \end{aligned} \tag{11.49}$$

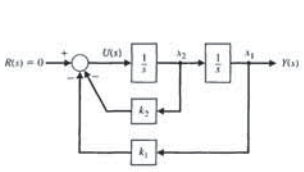

FIGURE 11.16 Compensated control system of Example 11.11.

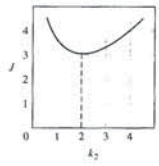

FIGURE 11.17 Performance index versus the parameter k_2.

EXAMPLE 11.12 **Determination of an optimal system**

Now let us consider again the system of Example 11.11, where both the feedback gains, k_1 and k_2, are unspecified. To simplify the algebra without any loss in insight into the problem, let us set $k_1 = k_2 = k$. We can prove that if k_1 and k_2 are unspecified, then $k_1 = k_2$ when the minimum of the performance index (Equation 11.40) is obtained. Then, for the system of Example 11.11, Equation (11.45) becomes

$$\dot{\mathbf{x}} = \mathbf{H}\mathbf{x} = \begin{bmatrix} 0 & 1 \\ -k & -k \end{bmatrix} \mathbf{x}. \tag{11.56}$$

To determine the $\mathbf{P}$ matrix, we use Equation (11.41), which is

$$\mathbf{H}^T\mathbf{P} + \mathbf{P}\mathbf{H} = -\mathbf{I}. \tag{11.57}$$

Solving the set of simultaneous equations resulting from Equation (11.57), we find that

$$p_{12} = \frac{1}{2k}, \qquad p_{22} = \frac{k+1}{2k^2}, \quad \text{and} \quad p_{11} = \frac{1+2k}{2k}.$$

Let us consider the case where the system is initially displaced one unit from equilibrium so that $\mathbf{x}^T(0) = [1 \;\; 0]$. Then the performance index (Equation 11.40) becomes

$$J = \int_0^\infty \mathbf{x}^T\mathbf{x}\, dt = \mathbf{x}^T(0)\mathbf{P}\mathbf{x}(0) = p_{11}. \tag{11.58}$$

Thus, the performance index to be minimized is

$$J = p_{11} = \frac{1+2k}{2k} = 1 + \frac{1}{2k}. \tag{11.59}$$

The minimum value of J is obtained when k approaches infinity; the result is $J_{\min} = 1$. A plot of J versus k, shown in Figure 11.18, illustrates that the performance index approaches a minimum asymptotically as k approaches an infinite

Substituting the values of the elements of $\mathbf{P}$, we have

$$J = \frac{k_2^2 + 2}{2k_2} + 1 + \frac{1}{k_2} = \frac{k_2^2 + 2k_2 + 4}{2k_2}. \tag{11.50}$$

To minimize as a function of k_2, we take the derivative with respect to k_2 and set it equal to zero:

$$\frac{dJ}{dk_2} = \frac{2k_2(2k_2 + 2) - 2(k_2^2 + 2k_2 + 4)}{(2k_2)^2} = 0. \tag{11.51}$$

Therefore, $k_2^2 = 4$, and $k_2 = 2$ when J is a minimum. The minimum value of J is obtained by substituting $k_2 = 2$ into Equation (11.50). Thus, we obtain

$$J_{\min} = 3.$$

The system matrix $\mathbf{H}$, obtained for the compensated system, is then

$$\mathbf{H} = \begin{bmatrix} 0 & 1 \\ -1 & -2 \end{bmatrix}. \tag{11.52}$$

The characteristic equation of the compensated system is therefore

$$\det[\lambda\mathbf{I} - \mathbf{H}] = \det\begin{bmatrix} \lambda & -1 \\ 1 & \lambda + 2 \end{bmatrix} = \lambda^2 + 2\lambda + 1. \tag{11.53}$$

Because this is a second-order system, we note that the characteristic equation is of the form $s^2 + 2\zeta\omega_n s + \omega_n^2 = 0$, and therefore the damping ratio of the compensated system is $\zeta = 1.0$. This compensated system is considered to be an optimal system in that the compensated system results in a minimum value for the performance index when $k_1 = 1$ is fixed. Of course, we recognize that this system is optimal only for the specific set of initial conditions that were assumed. The compensated system is shown in Figure 11.16. A curve of the performance index as a function of k_2 is shown in Figure 11.17. It is clear that this system is not very sensitive to changes in k_2 and will maintain a near-minimum performance index if the k_2 is altered by some percentage. We define the sensitivity of an optimal system as

$$S_k^{\text{opt}} = \frac{\Delta J/J}{\Delta k/k}, \tag{11.54}$$

where k is the design parameter. Then, for this example, we have $k = k_2$, and considering $k_2 = 2.5$, for which $J = 3.05$, we obtain

$$S_{k_2}^{\text{opt}} \approx \frac{0.05/3}{0.5/2} = 0.07. \tag{11.55}$$ ■

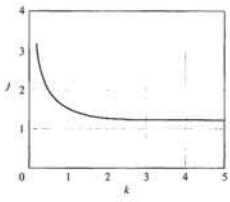

FIGURE 11.18 Performance index versus the feedback gain k for Example 11.12.

value. Now, we recognize that, in providing a very large gain k, we can cause the feedback signal

$$u(t) = -k[x_1(t) + x_2(t)]$$

to be very large. However, we are restricted to realizable magnitudes of the control signal $u(t)$. Therefore, we must introduce a constraint on $u(t)$ so that the gain k is not made too large. Then, for example, if we establish a constraint on $u(t)$ so that

$$|u(t)| \leq 50, \tag{11.60}$$

we require that the maximum acceptable value of k in this case be

$$k_{\max} = \frac{|u|_{\max}}{x_1(0)} = 50. \tag{11.61}$$

Then the minimum value of J is

$$J_{\min} = 1 + \frac{1}{2k_{\max}} = 1.01, \tag{11.62}$$

which is sufficiently close to the absolute minimum of J to satisfy our requirements.

Upon examining the performance index (Equation 11.35), we recognize that the reason the magnitude of the control signal is not accounted for in the original calculations is that $u(t)$ is not included within the expression for the performance index. However, in many cases, we are concerned with the expenditure of the control signal energy. For example, in an electric vehicle control system, $[u(t)]^2$ represents the expenditure of battery energy and must be restricted to conserve the energy for long periods of travel. To account for the expenditure of the energy of the control signal, we will use the performance index

$$\boxed{J = \int_0^\infty (\mathbf{x}^T\mathbf{I}\mathbf{x} + \lambda\mathbf{u}^T\mathbf{u})\, dt,} \tag{11.63}$$

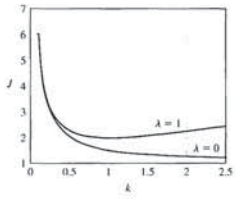

FIGURE 11.19
Performance index versus the feedback gain k for Example 11.13.

As in Example 11.12, we will let $\mathbf{x}^T(0) = [1, \quad 0]$ so that $J = p_{11}$. We evaluate p_{11} from Equation (11.68), namely,

$$\mathbf{H}^T\mathbf{P} + \mathbf{P}\mathbf{H} = -\mathbf{Q}. \tag{11.72}$$

Thus, we find that

$$J = p_{11} = (1 + \lambda k^2)\left(1 + \frac{1}{2k}\right) - \lambda k^2, \tag{11.73}$$

and we note that the right-hand side of Equation (11.73) reduces to Equation (11.59) when $\lambda = 0$. Now, the minimum of J is found by taking the derivative of J, which is

$$\frac{dJ}{dk} = \frac{1}{2}\left(\lambda - \frac{1}{k^2}\right) = 0. \tag{11.74}$$

Therefore, the minimum of the performance index occurs when $k = k_{\min} = \dfrac{1}{\sqrt{\lambda}}$, where $k_{\min}$ is the solution of Equation (11.74).

Let us complete this example for the case where the control energy and the state variables squared are equally important, so that $\lambda = 1$. Then Equation (11.74) is satisfied when $k^2 - 1 = 0$, and we find that $k_{\min} = 1.0$. The value of the performance index J obtained with $k_{\min}$ is greater than that of the previous example because the expenditure of energy is equally weighted as a cost. The plot of J versus k for this case is shown in Figure 11.19. The plot of J versus k for Example 11.12 is also shown for comparison in Figure 11.19. ■

It has become clear from the examples in this chapter that the actual minimum obtained depends on the initial conditions, the definition of the performance index, and the value of the scalar factor λ.

The design of several parameters can be accomplished in a manner similar to that illustrated in the examples. Also, the design procedure can be carried out for higher-order systems. However, we must then consider the use of a digital computer to determine the solution of Equation (11.41) in order to obtain the $\mathbf{P}$ matrix. The

where λ is a scalar weighting factor and $\mathbf{I}$ = identity matrix. The weighting factor λ will be chosen so that the relative importance of the state variable performance is contrasted with the importance of the expenditure of the system energy resource that is represented by $\mathbf{u}^T\mathbf{u}$. As in the previous paragraphs, we will represent the state variable feedback by the matrix equation

$$\mathbf{u} = -\mathbf{K}\mathbf{x}, \tag{11.64}$$

and the system with this state variable feedback as

$$\dot{\mathbf{x}} = \mathbf{A}\mathbf{x} + \mathbf{B}\mathbf{u} = \mathbf{H}\mathbf{x}. \tag{11.65}$$

Now, substituting Equation (11.64) into Equation (11.63), we have

$$\begin{aligned} J &= \int_0^\infty (\mathbf{x}^T\mathbf{I}\mathbf{x} + \lambda(\mathbf{K}\mathbf{x})^T(\mathbf{K}\mathbf{x}))\, dt \\ &= \int_0^\infty \mathbf{x}^T(\mathbf{I} + \lambda\mathbf{K}^T\mathbf{K})\mathbf{x}\, dt = \int_0^\infty \mathbf{x}^T\mathbf{Q}\mathbf{x}\, dt, \end{aligned} \tag{11.66}$$

where $\mathbf{Q} = \mathbf{I} + \lambda\mathbf{K}^T\mathbf{K}$ is an $n \times n$ matrix. Following the development of Equations (11.35) through (11.39), we postulate the existence of an exact differential so that

$$\frac{d}{dt}(\mathbf{x}^T\mathbf{P}\mathbf{x}) = -\mathbf{x}^T\mathbf{Q}\mathbf{x}. \tag{11.67}$$

Then, in this case, we require that

$$\mathbf{H}^T\mathbf{P} + \mathbf{P}\mathbf{H} = -\mathbf{Q}, \tag{11.68}$$

and thus we have, as before, (Equation 11.39):

$$J = \mathbf{x}^T(0)\mathbf{P}\mathbf{x}(0). \tag{11.69}$$

Now, the design steps are exactly as for Equations (11.40) and (11.41), with the exception that the left side of Equation (11.68) equals $-\mathbf{Q}$ instead of $-\mathbf{I}$. Of course, if $\lambda = 0$, Equation (11.68) reduces to Equation (11.41). Now, let us consider again Example 11.11 when λ is other than zero and account for the expenditure of control signal energy. ■

EXAMPLE 11.13 **Optimal system with control energy considerations**

Let us consider again the system of Example 11.11, which is shown in Figure 11.15. For this system, we use a state variable feedback so that

$$\mathbf{u} = -\mathbf{K}\mathbf{x} = [-k \quad -k]\begin{bmatrix} x_1 \\ x_2 \end{bmatrix}. \tag{11.70}$$

Therefore, the matrix

$$\mathbf{Q} = \mathbf{I} + \lambda\mathbf{K}^T\mathbf{K} = \begin{bmatrix} 1 + \lambda k^2 & \lambda k^2 \\ \lambda k^2 & 1 + \lambda k^2 \end{bmatrix}, \tag{11.71}$$

We begin by considering a familiar design problem, namely, the design of a controller to enable the tracking of a step reference input with zero steady-state error. In this case, the reference input is generated by

$$\dot{x}_r = 0, \qquad r = x_r, \tag{11.79}$$

or equivalently

$$\dot{r} = 0, \tag{11.80}$$

and the tracking error e is defined as

$$e = y - r.$$

Taking the time derivative yields

$$\dot{e} = \dot{y} = \mathbf{C}\dot{\mathbf{x}},$$

where we have used the reference input model of Equation (11.80) and the process model of Equation (11.76). If we define the two intermediate variables

$$\mathbf{z} = \dot{\mathbf{x}} \quad \text{and} \quad w = \dot{u},$$

we have

$$\begin{pmatrix} \dot{e} \\ \dot{\mathbf{z}} \end{pmatrix} = \begin{bmatrix} 0 & \mathbf{C} \\ 0 & \mathbf{A} \end{bmatrix}\begin{pmatrix} e \\ \mathbf{z} \end{pmatrix} + \begin{bmatrix} 0 \\ \mathbf{B} \end{bmatrix} w. \tag{11.81}$$

If the system in Equation (11.81) is controllable, we can find a feedback of the form

$$w = -K_1 e - \mathbf{K}_2\mathbf{z} \tag{11.82}$$

such that Equation (11.81) is stable. This implies that the tracking error e is stable; thus, we will have achieved the objective of asymptotic tracking with zero steady-state error. The control input, found by integrating Equation (11.82), is

$$u(t) = -K_1\int_0^t e(\tau)\, d\tau - \mathbf{K}_2\mathbf{x}(t).$$

The corresponding block diagram is shown in Figure 11.20. We see that the compensator includes an **internal model** (that is, an integrator) of the reference step input.

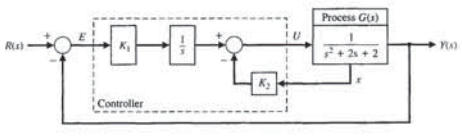

FIGURE 11.20
Internal model design for a step input.

computer may also provide a suitable approach for evaluating the minimum value of J for one or more parameters. However, the solution of Equation (11.68) may be difficult, especially when the system order is quite high ($n > 3$). An alternative method suitable for computer calculation is stated without proof in the following paragraph.

Consider the uncompensated single-input, single-output system with

$$\dot{\mathbf{x}} = \mathbf{A}\mathbf{x} + \mathbf{B}u$$

and feedback

$$u = -\mathbf{K}\mathbf{x} = -[k_1 \quad k_2 \ldots k_n]\mathbf{x}.$$

The performance index is

$$\boxed{J = \int_0^\infty (\mathbf{x}^T\mathbf{Q}\mathbf{x} + Ru^2)\, dt,}$$

where R is the scalar weighting factor. This index is minimized when

$$\mathbf{K} = R^{-1}\mathbf{B}^T\mathbf{P}.$$

The $n \times n$ matrix $\mathbf{P}$ is determined from the solution of the equation

$$\mathbf{A}^T\mathbf{P} + \mathbf{P}\mathbf{A} - \mathbf{P}\mathbf{B}R^{-1}\mathbf{B}^T\mathbf{P} + \mathbf{Q} = \mathbf{0}. \tag{11.75}$$

Equation (11.75) can be easily programmed and solved using numerical methods. Equation (11.75) is often called the Riccati equation. This optimal control is called the **linear quadratic regulator** (LQR) [12, 19].

11.8 INTERNAL MODEL DESIGN

In this section, we consider the problem of designing a compensator that provides asymptotic tracking of a reference input with zero steady-state error. The reference inputs considered can include steps, ramps, and other persistent signals, such as sinusoids. For a step input, we know that zero steady-state tracking errors can be achieved with a type-one system. This idea is formalized here by introducing an **internal model** of the reference input in the compensator [5, 18].

Let us consider a state variable model of the plant given by

$$\dot{\mathbf{x}} = \mathbf{A}\mathbf{x} + \mathbf{B}u, \qquad y = \mathbf{C}\mathbf{x}, \tag{11.76}$$

where $\mathbf{x}$ is the state vector, u is the input, and y is the output. We will consider a reference input to be generated by a linear system of the form

$$\dot{\mathbf{x}}_r = \mathbf{A}_r\mathbf{x}_r, \qquad r = \mathbf{d}_r\mathbf{x}_r, \tag{11.77}$$

with unknown initial conditions. An equivalent model of the reference input $r(t)$ is

$$r^{(n)} = \alpha_{n-1}r^{(n-1)} + \alpha_{n-2}r^{(n-2)} + \cdots + \alpha_1\dot{r} + \alpha_0 r, \tag{11.78}$$

where $r^{(n)}$ is the nth derivative of $r(t)$.

In input–output form, the reference model in Equation (11.86) is given by

$$\dddot{r} = 0.$$

Proceeding as before, we define the tracking error as

$$e = y - r,$$

and taking the time-derivative twice yields

$$\dddot{e} = \dddot{y} = \mathbf{C}\dddot{\mathbf{x}}.$$

With the definitions

$$\mathbf{z} = \ddot{\mathbf{x}}, \qquad w = \dddot{u},$$

we have

$$\begin{pmatrix} \dot{e} \\ \ddot{e} \\ \dot{\mathbf{z}} \end{pmatrix} = \begin{bmatrix} 0 & 1 & 0 \\ 0 & 0 & \mathbf{C} \\ 0 & 0 & \mathbf{A} \end{bmatrix} \begin{pmatrix} e \\ \dot{e} \\ \mathbf{z} \end{pmatrix} + \begin{bmatrix} 0 \\ 0 \\ \mathbf{B} \end{bmatrix} w. \tag{11.87}$$

So if the system of Equation (11.87) is controllable, then we can compute K_i, $i = 1, 2, 3$, such that with

$$w = -[K_1 \quad K_2 \quad \mathbf{K}_3] \begin{bmatrix} e \\ \dot{e} \\ \mathbf{z} \end{bmatrix}, \tag{11.88}$$

the system represented by Equation (11.87) is asymptotically stable; hence, the tracking error $e(t) \to 0$ as $t \to \infty$, as desired. The control, u, is found by integrating Equation (11.88) twice. In Figure 11.22, we see that the resulting controller has a double integrator, which is the internal model of the reference ramp input.

The internal model approach can be extended to other reference inputs by following the same general procedure outlined for the step and ramp inputs. In addition, the internal model design can be used to reject persistent disturbances by including models of the disturbances in the compensator.

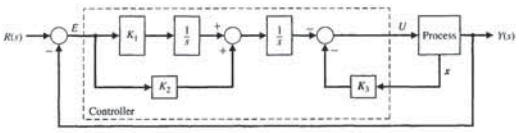

FIGURE 11.22
Internal model design for a ramp input. Note that $G(s)G_c(s)$ contains $1/s^2$, the reference input $R(s)$.

EXAMPLE 11.14 **Internal model design for a unit step input**

Let us consider a process given by

$$\dot{\mathbf{x}} = \begin{bmatrix} 0 & 1 \\ -2 & -2 \end{bmatrix} \mathbf{x} + \begin{bmatrix} 0 \\ 1 \end{bmatrix} u, \qquad y = [1 \quad 0]\mathbf{x}. \tag{11.83}$$

We want to design a controller for this system to track a reference step input with zero steady-state error. From Equation (11.81), we have

$$\begin{pmatrix} \dot{e} \\ \dot{\mathbf{z}} \end{pmatrix} = \begin{bmatrix} 0 & 1 & 0 \\ 0 & 0 & 1 \\ 0 & -2 & -2 \end{bmatrix} \begin{pmatrix} e \\ \mathbf{z} \end{pmatrix} + \begin{bmatrix} 0 \\ 0 \\ 1 \end{bmatrix} w. \tag{11.85}$$

A check of controllability shows that the system described by Equation (11.85) is completely controllable. We use

$$K_1 = 20, \qquad \mathbf{K}_2 = [20 \quad 10],$$

in order to locate the roots of the characteristic equation of Equation (11.85) at $s = -1 \pm j, -10$. With w given in Equation (11.82), we have the system of Equation (11.85) as asymptotically stable. So for any initial tracking error $e(0)$ we are guaranteed that $e(t) \to 0$ as $t \to \infty$. The asymptotic stability of the tracking error is illustrated in Figure 11.21 for a step input. ■

Consider the block diagram model of Figure 11.20 where the process is represented by $G(s)$ and the cascade controller is $G_c(s) = K_1/s$. The internal model principle states that if $G(s)G_c(s)$ contains $R(s)$, then $y(t)$ will track $r(t)$ asymptotically. In this case $R(s) = 1/s$, which is contained in $G(s)G_c(s)$, as we expect.

Consider the problem of designing a controller to provide asymptotic tracking of a ramp input with zero steady-state error $r(t) = Mt, t \geq 0$, where M is the ramp magnitude. In this case, the reference input model is

$$\dot{\mathbf{x}}_r = \mathbf{A}_r\mathbf{x}_r = \begin{bmatrix} 0 & 1 \\ 0 & 0 \end{bmatrix} \mathbf{x}_r$$
$$r = \mathbf{d}_r\mathbf{x}_r = [1 \quad 0]\mathbf{x}_r. \tag{11.86}$$

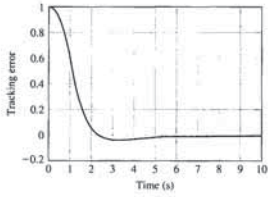

FIGURE 11.21
Internal model design response to an initial tracking error for a unit step input.

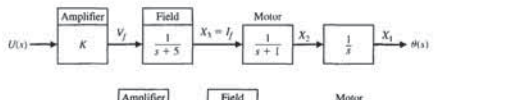

FIGURE 11.25
Open-loop block diagram of the DC motor with mounted encoder wheel.

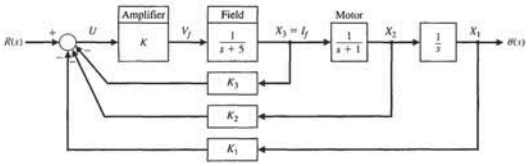

FIGURE 11.26
Closed-loop block diagram of the DC motor.

as shown in Figure 11.26. The goal is to select the gains so that the response to a step command has a settling time (with a 2% criterion) of less than 2 seconds and an overshoot of less than 4.0%.

To achieve an accurate output position, we let $K_1 = 1$ and determine K, K_2, and K_3. The characteristic equation of the system may be obtained in several ways.

The state variable model associated with Figure 11.25 is given by

$$\dot{\mathbf{x}} = \mathbf{A}\mathbf{x} + \mathbf{B}u = \begin{bmatrix} 0 & 1 & 0 \\ 0 & -1 & 1 \\ 0 & 0 & -5 \end{bmatrix} \mathbf{x} + \begin{bmatrix} 0 \\ 0 \\ K \end{bmatrix} u.$$
$$y = [1 \quad 0 \quad 0]\mathbf{x}. \tag{11.90}$$

Substituting for u, as defined by Equation (11.89), we have

$$\dot{\mathbf{x}} = \begin{bmatrix} 0 & 1 & 0 \\ 0 & -1 & 1 \\ -K & -KK_2 & -(5 + K_3K) \end{bmatrix} \mathbf{x} + \begin{bmatrix} 0 \\ 0 \\ K \end{bmatrix} r \tag{11.91}$$

when $K_1 = 1$. The characteristic equation can be obtained from Equation (11.91) as

$$\det \begin{bmatrix} s & -1 & 0 \\ 0 & s + 1 & -1 \\ K & KK_2 & s + (5 + K_3K) \end{bmatrix} = 0$$

yielding

$$s^3 + 6s^2 + 5s + K_3Ks^2 + K_3Ks + KK_2s + K = 0.$$

As will be shown in Section 11.10, we can plot a root locus for K_3K as

$$1 + \frac{KK_3(s^2 + as + b)}{s(s + 1)(s + 5)} = 0, \tag{11.92}$$

11.9 DESIGN EXAMPLES

In this section we present two illustrative examples. In the first example, a fourth-order state variable model of an automatic test system controller is used to illustrate the full-state feedback controller design to meet time-domain performance specifications. In the second example, a control system is designed to manage the speed of the electric motor shaft of a diesel electric locomotive. The design process focuses on the design of a full-state feedback control system using pole-placement methods.

EXAMPLE 11.15 **Automatic test system**

An automatic test and inspection system uses a DC motor to move a set of test probes, as shown in Figure 11.23. Low throughput and a high degree of error can occur from manually testing various panels of switches, relay, and indicator lights. Automating the test from a controller requires placing a plug across the leads of a part and testing for continuity, resistance, or functionality [17]. The system uses a DC motor with an encoded disk to measure position and velocity, as shown in Figure 11.24. The parameters of the system are shown in Figure 11.25 with K representing the required power amplifier.

We select the state variables as $x_1 = \theta$, $x_2 = d\theta/dt$, and $x_3 = i_f$, as shown in Figure 11.25. State variable feedback is available, and we let

$$u = [-K_1 \quad -K_2 \quad -K_3]\mathbf{x} + r,$$

or

$$u = -K_1x_1 - K_2x_2 - K_3x_3 + r. \tag{11.89}$$

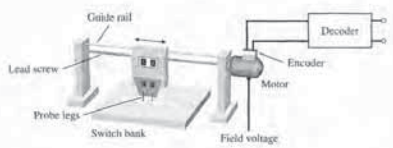

FIGURE 11.23
Automatic test system.

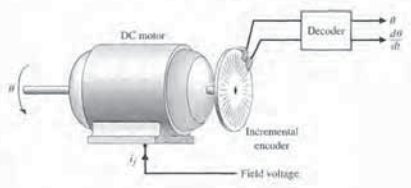

FIGURE 11.24
A DC motor with mounted encoder wheel.

EXAMPLE 11.16 **Diesel electric locomotive control**

The diesel electric locomotive is depicted in Figure 11.29. The efficiency of the diesel engine is very sensitive to the speed of rotation of the motors. We want to design a control system that drives the electric motors of a diesel electric locomotive for use on railroad trains. The locomotive is driven by DC motors located on each of the axles. The throttle position (see Figure 11.29) is set by moving the input potentiometers. The elements of the design process emphasized in this example are highlighted in Figure 11.30.

The control objective is to regulate the shaft rotation speed ω_o to the desired value ω_r.

Control Goal

Regulate the shaft rotation speed to the desired value in the presence of external load torque disturbances.

The corresponding variable to be controlled is the shaft rotation speed ω_o.

Variable to Be Controlled

Shaft rotation speed ω_o.

The controlled speed ω_o is sensed by a tachometer, which supplies a feedback voltage v_o. The electronic amplifier amplifies the error signal, $v_e = v_{in}$ between the reference and feedback voltage signals and provides a voltage v_f that is supplied to the field winding of a DC generator.

The generator is run at a constant speed ω_d by the diesel engine and generates a voltage v_g that is supplied to the armature of a DC motor. The motor is armature

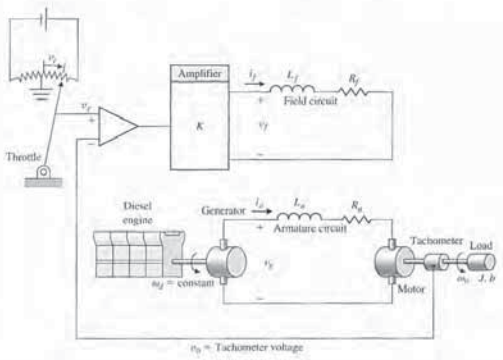

FIGURE 11.29 Diesel electric locomotive system.

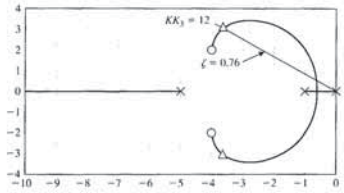

FIGURE 11.27 Root locus for the automatic test system.

where a and b are

$$a = (K_2 + K_3)/K_3$$

and

$$b = 1/K_3.$$

Setting $a = 8$ and $b = 20$, we place the zeros at $s = -4 \pm j2$ in order to pull the locus to the left in the s-plane. Then

$$\frac{K_2 + K_3}{K_3} = 8 \quad \text{and} \quad \frac{1}{K_3} = 20.$$

Therefore, $K_1 = 1$, $K_2 = 0.35$, and $K_3 = 0.05$. A plot of the root locus is shown in Figure 11.27. When $KK_3 = 12$, the roots lie on the $\zeta = 0.76$ line, as shown in Figure 11.27. Since $K_3 = 0.05$, we have $K = 240$. The roots at $K = 240$ are

$$s = -10.62, \quad \text{and} \quad s = -3.69 \pm j3.00.$$

The step response of this system is shown in Figure 11.28. The overshoot is 3%, and the settling time is 1.8 seconds. Thus the design is quite acceptable. ■

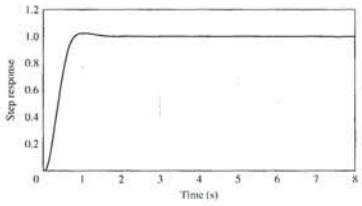

FIGURE 11.28 Step response of the automatic test system.

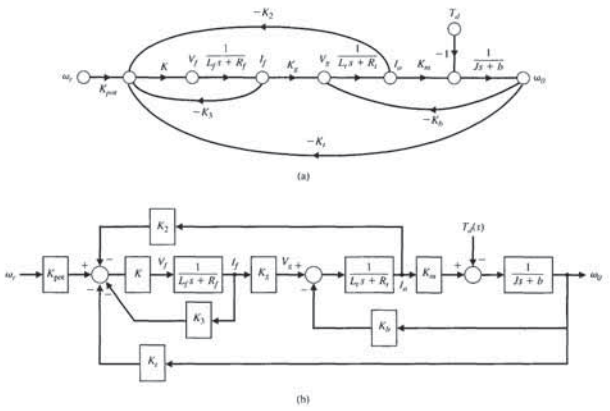

FIGURE 11.31 Signal flow graph of the diesel electric locomotive. (a) Signal flow graph. (b) Block diagram controller feedback loops are shown in light.

Table 11.1 Parameter Values for the Diesel Electric Locomotive

K_m	K_g	K_b	J	b	L_a	R_a	R_f	L_f	K_t	K_{pot}	L_g	R_g
10	100	0.62	1	1	0.2	1	1	0.1	1	1	0.1	1

The key tuning parameters are given by

Select Key Tuning Parameters

K and $\mathbf{K}$

The matrix $\mathbf{K}$ is the state feedback gain matrix. The design specifications are

Design Specifications

DS1 Steady-state tracking error less than 2% to a unit step input.

DS2 Percent overshoot of $\omega_o(t)$ less than 10% to a unit step input $\omega_r(s) = 1/s$.

DS3 Settling time less than 1 second to a unit step input.

The first step in the development of the vector differential equation that accurately describes the system is to choose a set of state variables. In practice the selection of

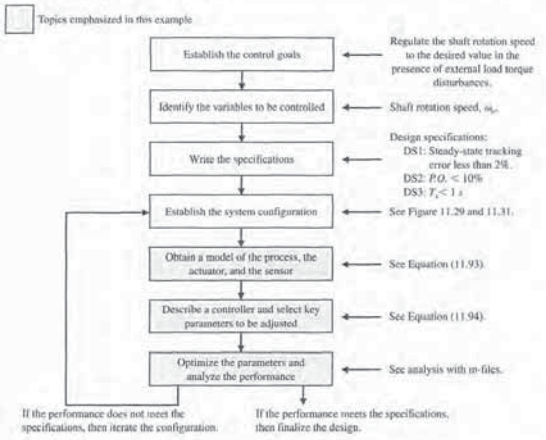

FIGURE 11.30 Elements of the control system design process emphasized in this diesel electric locomotive example.

controlled, with a fixed current supplied to its field. As a result, the motor produces a torque T and drives the load connected to its shaft so that the controlled speed ω_o tends to equal the command speed ω_r.

A block diagram and signal flow graph of the system are shown in Figure 11.31. In Figure 11.31 we use L_t and R_t, which are defined as

$$L_t = L_a + L_g,$$

$$R_t = R_a + R_g.$$

Values for the parameters of the diesel electric locomotive are given in Table 11.1.

Notice that the system has a feedback loop; we use the tachometer voltage v_o as a feedback signal to form an error signal $v_e = v_{in}$. Without additional state feedback, the only tuning parameter is the amplifier gain K. As a first step, we can investigate the system performance with tachometer voltage feedback only.

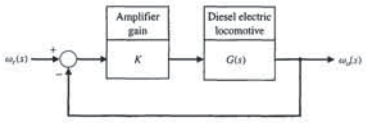

FIGURE 11.32
Block diagram representation of the diesel electric locomotive.

then (from an input–output perspective) the system has the simple feedback configuration shown in Figure 11.32.

Using the parameter values given in Table 11.1 and computing the steady-state tracking error for a unit step input yields

$$e_{ss} = \frac{1}{1 + KG(0)} = \frac{1}{1 + 121.95K}.$$

Using the Routh–Hurwitz method, we also find that the closed-loop system is stable for

$$-0.008 < K < 0.0468.$$

The smallest steady-state tracking error is achieved for the largest value of K. At best we can obtain a 15% tracking error, which does not meet the design specification DS1. Also, as K gets larger, the response becomes unacceptably oscillatory.

We now consider a full state feedback controller design. The feedback loops are shown in Figure 11.31, which shows that ω_o, i_a, and i_f are available for feedback. Without any loss of generality, we set $K = 1$. Any value of $K > 0$ would work as well.

The control input is

$$u = K_{pot}\omega_r - K_1x_1 - K_2x_2 - K_3x_3.$$

The feedback gains to be determined are K_1, K_2, and K_3. The tachometer gain, K_t, is now a key parameter of the design process. Also K_{pot} is a key variable for tuning. By adjusting the parameter K_{pot}, we have the freedom to scale the input ω_r. When we define

$$\mathbf{K} = [K_1 \quad K_2 \quad K_3],$$

then

$$u = -\mathbf{Kx} + K_{pot}\omega_r. \tag{11.94}$$

The closed-loop system with state feedback is

$$\dot{\mathbf{x}} = (\mathbf{A} - \mathbf{BK})\mathbf{x} + \mathbf{B}v,$$
$$y = \mathbf{Cx},$$

where

$$v = K_{pot}\omega_r.$$

state variables can be a difficult process, especially for complex systems. The state variables must be sufficient in number to determine the future behavior of the system when the present state and all future inputs are known. The selection of state variables is intimately related to the issue of complexity.

The diesel electric locomotive system has three major components: two electrical circuits and one mechanical system. It seems logical that the state vector will include state variables from both electrical circuits and from the mechanical system. One reasonable choice of state variables is $x_1 = \omega_o$, $x_2 = i_a$, and $x_3 = i_f$. This state variable selection is not unique. With the state variables defined above, the state variable model is

$$\dot{x}_1 = -\frac{b}{J}x_1 + \frac{K_m}{J}x_2 - \frac{1}{J}T_d,$$
$$\dot{x}_2 = -\frac{K_b}{L_t}x_1 - \frac{R_t}{L_t}x_2 + \frac{K_g}{L_t}x_3,$$
$$\dot{x}_3 = -\frac{R_f}{L_f}x_3 + \frac{1}{L_f}u,$$

where

$$u = KK_{pot}\omega_r.$$

In matrix form (with $T_d(s) = 0$), we have

$$\dot{\mathbf{x}} = \mathbf{Ax} + \mathbf{B}u,$$
$$y = \mathbf{Cx} + \mathbf{D}u, \tag{11.93}$$

where

$$\mathbf{A} = \begin{bmatrix} -\frac{b}{J} & \frac{K_m}{J} & 0 \\ -\frac{K_b}{L_t} & -\frac{R_t}{L_t} & \frac{K_g}{L_t} \\ 0 & 0 & -\frac{R_f}{L_f} \end{bmatrix}, \quad \mathbf{B} = \begin{bmatrix} 0 \\ 0 \\ \frac{1}{L_f} \end{bmatrix}, \text{ and}$$

$$\mathbf{C} = [1 \quad 0 \quad 0], \quad \mathbf{D} = [0].$$

The corresponding transfer function is

$$G(s) = \mathbf{C}(s\mathbf{I} - \mathbf{A})^{-1}\mathbf{B} = \frac{K_gK_m}{(R_f + L_fs)[(R_t + L_ts)(Js + b) + K_mK_b]}.$$

Begin by assuming the tachometer feedback is available, that is, that K_t is in the loop. If we take advantage of the fact that

$$K_{pot} = K_t = 1,$$

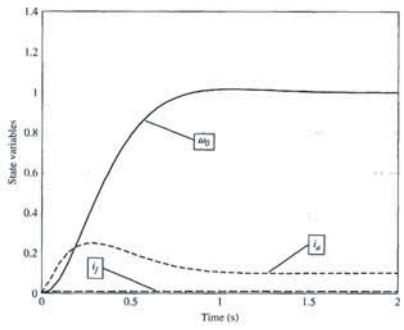

FIGURE 11.34
Closed-loop step response of the diesel electric locomotive.

To select the gain K_{pot}, we first compute the DC gain of the closed-loop transfer function. With the state feedback in place, the closed-loop transfer function is

$$T(s) = \mathbf{C}(s\mathbf{I} - \mathbf{A} + \mathbf{BK})^{-1}\mathbf{B}.$$

Then

$$K_{pot} = \frac{1}{T(0)}.$$

Using the gain K_{pot} in this manner effectively scales the closed-loop transfer function so that the DC gain is equal to 1. We then expect that a unit step input representing a 1°/s step command results in a 1°/s steady-state output at ω_o.

The step response of the system is shown in Figure 11.34. We can see that all the design specifications are satisfied. ■

11.10 STATE VARIABLE DESIGN USING CONTROL DESIGN SOFTWARE

Controllability and observability of a system in state variable feedback form can be checked using the functions ctrb and obsv, respectively. The inputs to the ctrb function, shown in Figure 11.35, are the system matrix **A** and the input matrix **B**; the output of ctrb is the controllability matrix $\mathbf{P}_c$. Similarly, the input to the obsv function, shown in Figure 11.35, is the system matrix **A** and the output matrix **C**; the output of obsv is the observability matrix $\mathbf{P}_o$.

We will use pole-placement methods to determine **K** such that the eigenvalues of $\mathbf{A} - \mathbf{BK}$ are in the desired locations. First we make sure the system is controllable. When $n = 3$ the controllability matrix is

$$\mathbf{P}_c = [\mathbf{B} \quad \mathbf{AB} \quad \mathbf{A}^2\mathbf{B}].$$

Computing the determinant of $\mathbf{P}_c$ yields

$$\det \mathbf{P}_c = -\frac{K_g^2K_m}{JL_f^3L_t^2}.$$

Since $K_g \neq 0$ and $K_m \neq 0$ and $JL_f^3L_t^2$ is nonzero, we determine that

$$\det \mathbf{P}_c \neq 0.$$

Thus the system is controllable. We can place all the poles of the system appropriately to satisfy DS2 and DS3.

The desired region to place the eigenvalues of $\mathbf{A} - \mathbf{BK}$ is illustrated in Figure 11.33. The specific pole locations are selected to be

$$p_1 = -50,$$
$$p_2 = -4 + 3j,$$
$$p_3 = -4 - 3j.$$

Selecting $p_1 = -50$ allows for a good second-order response that is governed by p_2 and p_3.

The gain matrix **K** that achieves the desired closed-loop poles is

$$\mathbf{K} = [-0.0041 \quad 0.0035 \quad 4.0333].$$

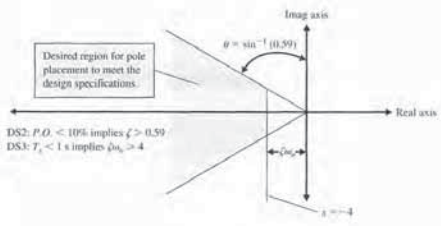

FIGURE 11.33
Desired location of the closed-loop poles (that is, the eigenvalues of $\mathbf{A} - \mathbf{BK}$).

radial.m

```
% This script computes the satellite controllability
% with a radial thruster only (i.e. tailed tangential thruster)
%
w=0.0011;
A=[0 1 0 0;3*w^2 0 0 2*w;0 0 0 1;0 -2*w 0 0];
b1=[0;1;0;0];
Pc=ctrb(A,b1);
n=det(Pc);
if abs(n) < eps
 disp('Satellite is uncontrollable with radial thruster only!')
else
 disp('Satellite is controllable with radial thruster only!')
end
```

Input matrix associated with radial thruster

Compute controllability matrix

n = determinant of controllability matrix

(a)

```
>>radial
Satellite is uncontrollable with radial thruster only!
```

Execute m-file script radial.m

radial.m output

(b)

FIGURE 11.37 Controllability with radial thrusters only: (a) m-file script, (b) output.

Suppose the tangential thruster fails (i.e., $u_t = 0$), and only the radial thruster is operational. Is the satellite controllable from u_r only? We answer this question by using an m-file script to determine the controllability. Using the script shown in Figure 11.37, we find that the determinant $\mathbf{P}_c$ is zero; thus, the satellite is not completely controllable when the tangential thruster fails.

Suppose now that the radial thruster fails (i.e., $u_r = 0$) and that the tangential thruster is functioning properly. Is the satellite controllable from u_t only? Using the script in Figure 11.38, we find that the satellite is completely controllable using the tangential thruster only. ■

We conclude this section with a controller design for an automatic test system using state variable models. The design approach utilizes root locus methods and incorporates m-file scripts to assist in the procedure.

EXAMPLE 11.18 **Automatic test system**

The state-space representation for the automatic test system of Example 11.15 is

$$\dot{\mathbf{x}} = \mathbf{A}\mathbf{x} + \mathbf{B}u, \tag{11.96}$$

where

$$\mathbf{A} = \begin{bmatrix} 0 & 1 & 0 \\ 0 & -1 & 1 \\ 0 & 0 & -5 \end{bmatrix} \quad \text{and} \quad \mathbf{B} = \begin{bmatrix} 0 \\ 0 \\ K \end{bmatrix}.$$

Our design specifications are a step response with (1) a settling time (with a 2% criterion) less than 2 seconds and (2) an overshoot less than 4%. We assume that the

Notice that the controllability matrix $\mathbf{P}_c$ is a function only of $\mathbf{A}$ and $\mathbf{B}$, while the observability matrix $\mathbf{P}_o$ is a function only of $\mathbf{A}$ and $\mathbf{C}$.

EXAMPLE 11.17 **Satellite trajectory control**

Let us consider a satellite in a circular, equatorial orbit at an altitude of 250 nautical miles above the Earth, as illustrated in Figure 11.36 [14, 24]. The satellite motion (in the orbit plane) is described by the normalized state variable model

$$\dot{\mathbf{x}} = \begin{bmatrix} 0 & 1 & 0 & 0 \\ 3\omega^2 & 0 & 0 & 2\omega \\ 0 & 0 & 0 & 1 \\ 0 & -2\omega & 0 & 0 \end{bmatrix} \mathbf{x} + \begin{bmatrix} 0 \\ 1 \\ 0 \\ 0 \end{bmatrix} u_r + \begin{bmatrix} 0 \\ 0 \\ 0 \\ 1 \end{bmatrix} u_t, \tag{11.95}$$

where the state vector $\mathbf{x}$ represents normalized perturbations from the circular, equatorial orbit; u_r is the input from a radial thruster; u_t is the input from a tangential thruster; and $\omega = 0.0011$ rad/s (approximately one orbit of 90 minutes) is the orbital rate for the satellite at the specific altitude. In the absence of perturbations, the satellite will remain in the nominal circular equatorial orbit. However, disturbances such as aerodynamic drag can cause the satellite to deviate from its nominal path. The problem is to design a controller that commands the satellite thrusters in such a manner that the actual orbit remains near the desired circular orbit. Before commencing with the design, we check controllability. In this case, we investigate controllability using the radial and tangential thrusters independently.

Controllability matrix $\dot{\mathbf{x}} = \mathbf{A}\mathbf{x} + \mathbf{B}u$, $y = \mathbf{C}\mathbf{x} + \mathbf{D}u$

Pc=ctrb(A,B)

Po=obsv(A,C)

Observability matrix $\dot{\mathbf{x}} = \mathbf{A}\mathbf{x} + \mathbf{B}u$, $y = \mathbf{C}\mathbf{x} + \mathbf{D}u$

FIGURE 11.35 The ctrb and obsv functions.

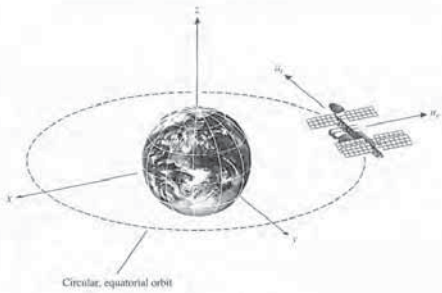

FIGURE 11.36 The satellite in an equatorial circular orbit.

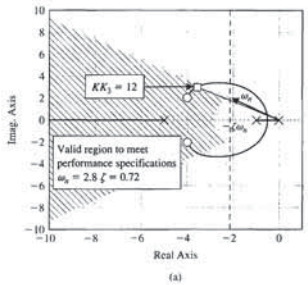

(a)

```
% Root locus script for the Automatic Test System
% including performance specs regions
num=[1 8 20]; den=[1 6 5 0]; sys=tf(num,den);
clf; rlocus(sys); hold on
%
zeta=0.72; wn=2.8;
x=[-10:0.1:-zeta*wn]; y=-(sqrt(1-zeta^2)/zeta)*x;
xc=[-10:0.1:-zeta*wn];c=sqrt(wn^2-xc.^2);
plot(x,y,'-',x,-y,'-',xc,c,'-',xc,-c,'-')
```

Hold plot to add stability regions

(b)

FIGURE 11.39 (a) Root locus for the automatic test system, (b) m-file script.

If we view KK_3 as a parameter and let $K_1 = 1$, then we can write Equation (11.99) as

$$1 + KK_3 \frac{s^2 + \dfrac{K_3 + K_2}{K_3} s + \dfrac{1}{K_3}}{s(s+1)(s+5)} = 0.$$

We place the zeros at $s = -4 \pm 2j$ in order to pull the locus to the left in the s-plane. Thus, our desired numerator polynomial is $s^2 + 8s + 20$. Comparing corresponding coefficients leads to

$$\frac{K_3 + K_2}{K_3} = 8 \quad \text{and} \quad \frac{1}{K_3} = 20.$$

Therefore, $K_2 = 0.35$ and $K_3 = 0.05$. We can now plot a root locus with KK_3 as the parameter, as shown in Figure 11.39.

tangent.m

```
% This script computes the satellite controllability
% with a tangential thruster only (i.e. failed radial thruster)
%
w=0.0011;
A=[0 1 0 0;3*w^2 0 0 2*w;0 0 0 1;0 -2*w 0 0];
b2=[0;0;0;1];
Pc=ctrb(A,b2);
n=det(Pc);
if abs(n) < eps
 disp('Satellite is uncontrollable with tangential thruster only!')
else
 disp('Satellite is controllable with tangential thruster only!')
end
```

Input matrix associated with tangential thruster

Compute controllability matrix

n = determinant of controllability matrix

(a)

```
>>tangent
Satellite is controllable with tangential thruster only!
```

Execute MATLAB script tangent.m

Tangent.m output

(b)

FIGURE 11.38 Controllability with tangential thrusters only: (a) m-file script, (b) output.

state variables are available for feedback, so that the control is given by

$$u = -[K_1 \quad K_2 \quad K_3]\mathbf{x} + r = -\mathbf{K}\mathbf{x} + r. \tag{11.97}$$

We must select the gains K, K_1, K_2, and K_3 to meet the performance specifications. Using the design approximations

$$T_s = \frac{4}{\zeta\omega_n} < 2 \quad \text{and} \quad P.O. = 100e^{-\zeta\pi/\sqrt{1-\zeta^2}} < 4,$$

we find that

$$\zeta > 0.72 \quad \text{and} \quad \omega_n > 2.8.$$

This defines a region in the complex plane in which our dominant roots must lie, so that we expect to meet the design specifications, as shown in Figure 11.39. Substituting Equation (11.97) into Equation (11.96) yields

$$\dot{\mathbf{x}} = \begin{bmatrix} 0 & 1 & 0 \\ 0 & -1 & 1 \\ -KK_1 & -KK_2 & -(5 + KK_3) \end{bmatrix} \mathbf{x} + \begin{bmatrix} 0 \\ 0 \\ K \end{bmatrix} r = \mathbf{H}\mathbf{x} + \mathbf{B}r, \tag{11.98}$$

where $\mathbf{H} = \mathbf{A} - \mathbf{B}\mathbf{K}$. The characteristic equation associated with Equation (11.98) can be obtained by evaluating $\det(s\mathbf{I} - \mathbf{H}) = 0$, resulting in

$$s(s+1)(s+5) + KK_3\left(s^2 + \frac{K_3 + K_2}{K_3} s + \frac{K_1}{K_3}\right) = 0. \tag{11.99}$$

```
A=[0 1;0 0];
B=[0;1];
P=[-1+j; -1-j];
K=acker(A,B,P)
```

```
K =
    2    2
```

The feedback gain matrix.

FIGURE 11.42
Using **acker** to compute **K** to place the poles at $\mathbf{P} = [-1 + j \quad -1 - j]^T$.

EXAMPLE 11.19 **Second-order system design using the acker function**

Consider again the second-order system in Example 11.7. The system model is

$$\dot{\mathbf{x}} = \begin{bmatrix} 0 & 1 \\ 0 & 0 \end{bmatrix}\mathbf{x} + \begin{bmatrix} 0 \\ 1 \end{bmatrix}u.$$

The desired closed-loop pole locations are $s_{1,2} = -1 \pm j$. To apply Ackermann's formula using the acker function, form the vector

$$\mathbf{P} = \begin{bmatrix} -1 + j \\ -1 - j \end{bmatrix}.$$

Then, with

$$\mathbf{A} = \begin{bmatrix} 0 & 1 \\ 0 & 0 \end{bmatrix} \quad \text{and} \quad \mathbf{B} = \begin{bmatrix} 0 \\ 1 \end{bmatrix},$$

the acker formula, illustrated in Figure 11.42, determines that the gain matrix that achieves the desired pole locations is

$$\mathbf{K} = [2 \quad 2].$$

This confirms the result in Example 11.7. ■

11.11 SEQUENTIAL DESIGN EXAMPLE: DISK DRIVE READ SYSTEM

In this chapter, we will design a state variable feedback system that will achieve the desired system response. The specifications for the system are given in Table 11.2. The second-order open-loop model is shown in Figure 11.43. We will design the system for this second-order model and then test the system response for both the second-order and third-order models.

First, we select the two state variables as $x_1(t) = y(t)$ and $x_2(t) = dy/dt = dx_1/dt$, as shown in Figure 11.44. It is practical to measure these variables as the position and velocity of the reader head. We then add the state variable feedback, as shown in Figure 11.44. We choose $K_1 = 1$, since our goal is for $y(t)$ to closely and accurately follow the command $r(t)$. The state variable differential equation for the open-loop system is

$$\dot{\mathbf{x}} = \begin{bmatrix} 0 & 1 \\ 0 & -20 \end{bmatrix}\mathbf{x} + \begin{bmatrix} 0 \\ 5K_a \end{bmatrix}r(t).$$

Therefore, we require that $5K_a = 19290$ or $K_a = 3858$. Furthermore, we require that

$$20 + 5K_2K_a = 250,$$

or $K_2 = 0.012$.

The system with the second-order model has the desired response and meets all the specifications, as shown in Table 11.2. If we add the field inductance $L = 1$ mH, we have a third-order model with

$$G_1(s) = \frac{5000}{s + 1000}.$$

Using this model, which incorporates the field inductance, we test the response of the system with the feedback gains selected for the second-order model. The results are provided in Table 11.2, illustrating that the second-order model is a very good model of the system. The actual results of the third-order system meet the specifications.

11.12 SUMMARY

In this chapter, the design of control systems in the time domain was examined. The three-step design procedure for constructing state variable compensators was presented. The optimal design of a system using state variable feedback and an integral performance index was considered. Also, the s-plane design of systems utilizing state variable feedback was examined. Finally, internal model design was discussed.

SKILLS CHECK

In this section, we provide three sets of problems to test your knowledge: True or False, Multiple Choice, and Word Match. To obtain direct feedback, check your answers with the answer key provided at the conclusion of the end-of-chapter problems. Use the block diagram in Figure 11.45 as specified in the various problem statements.

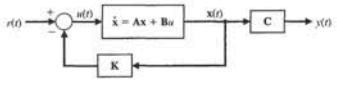

FIGURE 11.45 Block diagram for the Skills Check.

In the following **True or False** and **Multiple Choice** problems, circle the correct answer.

1. A system is said to be controllable on the interval $[t_0, t_f]$ if there exists a continuous input $u(t)$ such that any initial state $x(t_0)$ can be transformed to any arbitrary state $x(t_f)$ in a finite interval $t_f - t_0 > 0$. *True or False*
2. The poles of a system can be arbitrarily assigned through full-state feedback if and only if the system is completely controllable and observable. *True or False*

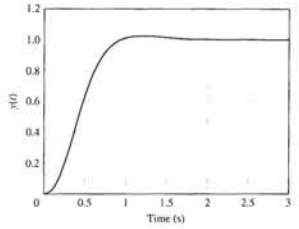

FIGURE 11.40
Step response for the automatic test system.

The characteristic equation, Equation (11.99), is

$$1 + KK_3\frac{s^2 + 8s + 20}{s(s + 1)(s + 5)} = 0.$$

The roots for the selected gain, $KK_3 = 12$, lie in the performance region, as shown in Figure 11.39. The rlocfind function is used to determine the value of KK_3 at the selected point. The final gains are as follows:

$$K = 240.00,$$
$$K_1 = 1.00,$$
$$K_2 = 0.35,$$
$$K_3 = 0.05.$$

The controller design results in a settling time of about 1.8 seconds and an overshoot of 3%, as shown in Figure 11.40. ■

In Section 11.4, we discussed Ackermann's formula to place the poles of the system at desired locations. The function acker calculates the gain matrix **K** to place the closed-loop poles at the desired locations. The acker function is illustrated in Figure 11.41.

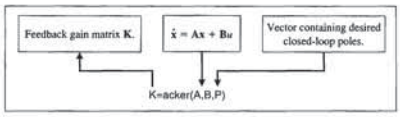

FIGURE 11.41
The **acker** function.

Table 11.2 Disk Drive Control System Specifications and Actual Performance

Performance Measure	Desired Value	Response for Second-Order Model	Response for Third-Order Model
Percent overshoot	<5%	<1%	0%
Settling time	<50 ms	34.3 ms	34.2 ms
Maximum response for a unit step disturbance	$<5 \times 10^{-3}$	5.2×10^{-5}	5.2×10^{-5}

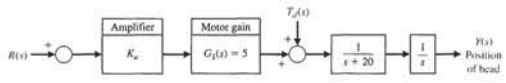

FIGURE 11.43
Open-loop model of head control system.

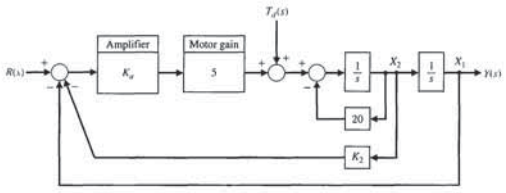

FIGURE 11.44
Closed-loop system with feedback of the two state variables.

The closed-loop state variable differential equation obtained from Figure 11.44 is

$$\dot{\mathbf{x}} = \begin{bmatrix} 0 & 1 \\ -5K_1K_a & -(20 + 5K_2K_a) \end{bmatrix}\mathbf{x} + \begin{bmatrix} 0 \\ 5K_a \end{bmatrix}r(t).$$

The characteristic equation of the closed-loop system is

$$s^2 + (20 + 5K_2K_a)s + 5K_a = 0,$$

since $K_1 = 1$. In order to achieve the specifications, we select $\zeta = 0.90$ and $\zeta\omega_n = 125$. Then the desired closed-loop characteristic equation is

$$s^2 + 2\zeta\omega_n s + \omega_n^2 = s^2 + 250s + 19290 = 0.$$

Determine the state-variable feedback control gain matrix **K** so that the closed-loop system poles are $s = -3, -4$, and -6.

a. $\mathbf{K} = [1 \quad 44 \quad 67]$
b. $\mathbf{K} = [10 \quad 44 \quad 67]$
c. $\mathbf{K} = [44 \quad 1 \quad 1]$
d. $\mathbf{K} = [1 \quad 67 \quad 44]$

10. Consider the system depicted in the block diagram in Figure 11.46.

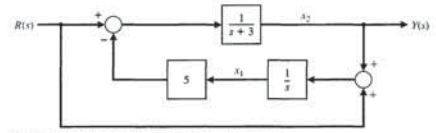

FIGURE 11.46 Two-loop feedback control system.

This system is:

a. Controllable, observable
b. Not controllable, not observable
c. Controllable, not observable
d. Not controllable, observable

11. A system has the transfer function

$$T(s) = \frac{s + a}{s^4 + 6s^3 + 12s^2 + 12s + 6}.$$

Determine the values of a that render the system unobservable.

a. $a = 1.30$ or $a = -1.43$
b. $a = 3.30$ or $a = 1.43$
c. $a = -3.30$ or $a = -1.43$
d. $a = -5.7$ or $a = -2.04$

12. Consider the closed-loop system in Figure 11.45, where

$$\mathbf{A} = \begin{bmatrix} -7 & -10 \\ 1 & 0 \end{bmatrix} \quad \mathbf{B} = \begin{bmatrix} 1 \\ 0 \end{bmatrix} \quad \mathbf{C} = [0 \quad 1].$$

Determine the state variable feedback control gain matrix **K** for a zero steady-state tracking error to a step input.

a. $\mathbf{K} = [3 \quad -9]$
b. $\mathbf{K} = [3 \quad -6]$
c. $\mathbf{K} = [-3 \quad 2]$
d. $\mathbf{K} = [-1 \quad 4]$

13. Consider the system where

$$\mathbf{A} = \begin{bmatrix} -3 & 0 \\ 1 & 0 \end{bmatrix} \quad \mathbf{B} = \begin{bmatrix} 1 \\ 0 \end{bmatrix} \quad \mathbf{C} = [0 \quad 1].$$

It is desired to place the observer poles at $s_{1,2} = -3 \pm j3$. Determine the appropriate state-variable feedback control gain matrix **L**.

3. The problem of designing a compensator that provides asymptotic tracking of a reference input with zero steady-state error is called state-variable feedback. *True or False*

4. Optimal control systems are systems whose parameters are adjusted so that the performance index reaches an extremum value. *True or False*

5. Ackerman's formula is used to check observability of a system. *True or False*

6. Consider the system

$$\dot{\mathbf{x}} = \begin{bmatrix} 0 & 1 \\ 0 & -4 \end{bmatrix}\mathbf{x} + \begin{bmatrix} 0 \\ 2 \end{bmatrix}u$$
$$y = [0 \quad 2]\mathbf{x}$$

The system is:

a. Controllable, observable
b. Not controllable, not observable
c. Controllable, not observable
d. Not controllable, observable

7. Consider the system

$$G(s) = \frac{10}{s^2(s + 2)(s^2 + 2s + 5)}.$$

This system is:

a. Controllable, observable
b. Not controllable, not observable
c. Controllable, not observable
d. Not controllable, observable

8. A system has the state variable representation

$$\dot{\mathbf{x}} = \begin{bmatrix} -1 & 0 & 0 \\ 0 & -3 & 0 \\ 0 & 0 & -5 \end{bmatrix}\mathbf{x} + \begin{bmatrix} 1 \\ 1 \\ 1 \end{bmatrix}u$$
$$y = [1 \quad 2 \quad -1]\mathbf{x}$$

Determine the associated transfer function model $G(s) = \dfrac{Y(s)}{U(s)}$.

a. $G(s) = \dfrac{5s^2 + 32s + 35}{s^3 + 9s^2 + 23s + 15}$
b. $G(s) = \dfrac{5s^2 + 32s + 35}{s^4 + 9s^3 + 23s + 15}$
c. $G(s) = \dfrac{2s^2 + 16s + 22}{s^3 + 9s^2 + 23s + 15}$
d. $G(s) = \dfrac{5s + 32}{s^2 + 32s + 9}$

9. Consider the closed-loop system in Figure 11.45, where

$$\mathbf{A} = \begin{bmatrix} -12 & -10 & -5 \\ 1 & 0 & 0 \\ 0 & 1 & 0 \end{bmatrix} \quad \mathbf{B} = \begin{bmatrix} 1 \\ 0 \\ 0 \end{bmatrix} \quad \mathbf{C} = [3 \quad 5 \quad -5].$$

h. Linear quadratic regulator	The difference between the actual state and the estimated state.	
i. Optimal control system	A control law of the form $u(t) = -\mathbf{K}\mathbf{x}(t)$ where $\mathbf{x}(t)$ is the state of the system assumed known at all times.	
j. Detectable	A partition of the state space that illuminates the states that are controllable and unobservable, uncontrollable and unobservable, controllable and observable, and uncontrollable and observable.	
k. Controllable system	An optimal controller designed to minimize a quadratic performance index.	
l. Pole placement	A linear system is (completely) observable if and only if this matrix has full rank.	
m. Estimation error	A dynamic system used to estimate the state of another dynamic system given knowledge of the system inputs and measurements of the system outputs.	
n. Kalman state-space decomposition	A design methodology wherein the objective is to place the eigenvalues of the closed-loop system in desired regions of the complex plane.	
o. Observable system	The principle that states that the full-state feedback law and the observer can be designed independently and when connected will function as an integrated control system in the desired manner (that is, stable).	
p. Separation principle	A system in which the states that are not controllable are naturally stable.	
q. Observability matrix	A controller that stabilizes the closed-loop system.	

EXERCISES

E11.1 The ability to balance actively is a key ingredient in the mobility of a device that hops and runs on one springy leg, as shown in Figure E11.1 [8]. The control of the attitude of the device uses a gyroscope and a feedback such that $u = \mathbf{K}\mathbf{x}$, where

$$\mathbf{K} = \begin{bmatrix} -k & 0 \\ 0 & -2k \end{bmatrix},$$

and

$$\dot{\mathbf{x}}(t) = \mathbf{A}\mathbf{x}(t) + \mathbf{B}u(t)$$

where

$$\mathbf{A} = \begin{bmatrix} 0 & 1 \\ -1 & 0 \end{bmatrix}, \text{ and } \mathbf{B} = \mathbf{I}.$$

Determine a value for k so that the response of each hop is critically damped.

E11.2 A magnetically suspended steel ball can be described by the linear equation

$$\dot{\mathbf{x}} = \begin{bmatrix} 0 & 1 \\ 9 & 0 \end{bmatrix}\mathbf{x} + \begin{bmatrix} 0 \\ 1 \end{bmatrix}u.$$

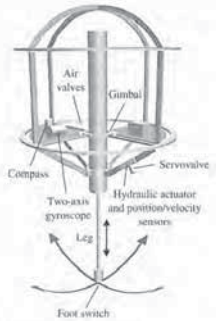

FIGURE E11.1 Single-leg control.

a. $\mathbf{L} = \begin{bmatrix} -9 \\ 3 \end{bmatrix}$
b. $\mathbf{L} = \begin{bmatrix} 9 \\ 3 \end{bmatrix}$
c. $\mathbf{L} = \begin{bmatrix} 3 \\ 9 \end{bmatrix}$
d. None of the above

14. A feedback system has a state-space representation

$$\dot{\mathbf{x}} = \begin{bmatrix} -75 & 0 \\ 1 & 0 \end{bmatrix}\mathbf{x} + \begin{bmatrix} 1 \\ 0 \end{bmatrix}u$$
$$y = [0 \quad 3600]\mathbf{x},$$

where the feedback is $u(t) = -\mathbf{K}\mathbf{x} + r(t)$. The control system design specifications are: (i) the overshoot to a step input approximately $P.O. \approx 6\%$, and (ii) the settling time $T_s \approx 0.1$ second. A state variable feedback gain matrix which satisfies the specifications is:

a. $\mathbf{K} = [10 \quad 200]$
b. $\mathbf{K} = [6 \quad 3600]$
c. $\mathbf{K} = [3600 \quad 10]$
d. $\mathbf{K} = [100 \quad 40]$

15. Consider the system

$$Y(s) = G(s)U(s) = \left[\frac{1}{s^2}\right]U(s).$$

Determine the eigenvalues of the closed-loop system when utilizing state variable feedback, where $u(t) = -2x_2 - 2x_1 + r(t)$. We define $x_1 = y(t)$ and $r(t)$ is a reference input.

a. $s_1 = -1 + j1 \quad s_2 = -1 - j1$
b. $s_1 = -2 + j2 \quad s_2 = -2 - j2$
c. $s_1 = -1 + j2 \quad s_2 = -1 - j2$
d. $s_1 = -1 \quad s_2 = -1$

In the following **Word Match** problems, match the term with the definition by writing the correct letter in the space provided.

a. Stabilizing controller	Occurs when the control signal for the process is a direct function of all the state variables.	
b. Controllability matrix	A system in which any initial state $\mathbf{x}(t_o)$ is uniquely determined by observing the output $y(t)$ on the interval $[t_o, t_f]$.	
c. Stabilizable	A system in which there exists a continuous input $u(t)$ such that any initial state $\mathbf{x}(t_o)$ can be driven to any arbitrary trial state $\mathbf{x}(t_f)$ in a finite time interval $t_f - t_o > 0$.	
d. Command following	A system whose parameters are adjusted so that the performance index reaches an extremum value.	
e. State variable feedback	An important aspect of control system design wherein a nonzero reference input is tracked.	
f. Full-state feedback control law	A linear system is (completely) controllable if and only if this matrix has full rank.	
g. Observer	A system in which the states that are unobservable are naturally stable.	

The state variables are x_1 = position and x_2 = velocity, and both are measurable. Select a feedback so that the system is critically damped and the settling time (with a 2% criterion) is 4 seconds. Choose the feedback in the form

$$u = -k_1x_1 - k_2x_2 + r$$

where r is the reference input and the gains k_1 and k_2 are to be determined.

E11.3 A system is described by the matrix equations

$$\dot{\mathbf{x}} = \begin{bmatrix} 0 & 1 \\ 0 & -3 \end{bmatrix}\mathbf{x} + \begin{bmatrix} 0 \\ 1 \end{bmatrix}u$$
$$y = [0 \quad 2]\mathbf{x}.$$

Determine whether the system is controllable and observable.

Answer: controllable, not observable

E11.4 A system is described by the matrix equations

$$\dot{\mathbf{x}} = \begin{bmatrix} -10 & 0 \\ 0 & -2 \end{bmatrix}\mathbf{x} + \begin{bmatrix} 0 \\ 2 \end{bmatrix}u$$
$$y = [1 \quad 0]\mathbf{x}.$$

Determine whether the system is controllable and observable.

E11.5 A system is described by the matrix equations

$$\dot{\mathbf{x}} = \begin{bmatrix} 0 & 1 \\ -1 & -2 \end{bmatrix}\mathbf{x} + \begin{bmatrix} 1 \\ -2 \end{bmatrix}u$$
$$y = [1 \quad 0]\mathbf{x}.$$

Determine whether the system is controllable and observable.

E11.6 A system is described by the matrix equations

$$\dot{\mathbf{x}} = \begin{bmatrix} 0 & 1 \\ -1 & -2 \end{bmatrix}\mathbf{x} + \begin{bmatrix} 0 \\ 1 \end{bmatrix}u$$
$$y = [1 \quad 0]\mathbf{x}.$$

Determine whether the system is controllable and observable.

Answer: controllable and observable

E11.7 Consider the system represented in state variable form

$$\dot{\mathbf{x}} = \mathbf{A}\mathbf{x} + \mathbf{B}u$$
$$y = \mathbf{C}\mathbf{x} + \mathbf{D}u.$$

where

$$\mathbf{A} = \begin{bmatrix} 0 & 1 \\ -3 & -5 \end{bmatrix}, \quad \mathbf{B} = \begin{bmatrix} 0 \\ 12 \end{bmatrix},$$
$$\mathbf{C} = [2 \quad -2], \text{ and } \mathbf{D} = [0].$$

Sketch a block diagram model of the system.

E11.8 Consider the third-order system

$$\dot{\mathbf{x}} = \begin{bmatrix} 0 & 1 & 0 \\ 0 & 0 & 1 \\ -9 & -3 & -1 \end{bmatrix}\mathbf{x} + \begin{bmatrix} 0 \\ -1 \\ 4 \end{bmatrix}u$$
$$y = [2 \quad 8 \quad 10]\mathbf{x} + [1]u.$$

Sketch a block diagram model of the system.

E11.9 Consider the second-order system

$$\dot{\mathbf{x}} = \begin{bmatrix} 1 & -1 \\ -1 & 1 \end{bmatrix}\mathbf{x} + \begin{bmatrix} k_1 \\ k_2 \end{bmatrix}u$$
$$y = [1 \quad 0]\mathbf{x} + [0]u.$$

For what values of k_1 and k_2 is the system completely controllable?

E11.10 Consider the block diagram model in Figure E11.10. Write the corresponding state variable model in the form

$$\dot{\mathbf{x}} = \mathbf{A}\mathbf{x} + \mathbf{B}u$$
$$y = \mathbf{C}\mathbf{x} + \mathbf{D}u.$$

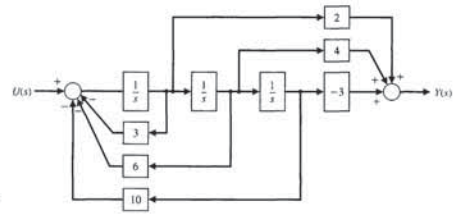

FIGURE E11.10
State variable block diagram.

E11.11 Consider the system shown in block diagram form in Figure E11.11. Obtain a state variable representation of the system. Determine if the system is controllable and observable.

E11.12 Consider the single-input, single-output system is described by

$$\dot{\mathbf{x}}(t) = \mathbf{A}\mathbf{x}(t) + \mathbf{B}u(t)$$
$$y(t) = \mathbf{C}\mathbf{x}(t)$$

where

$$\mathbf{A} = \begin{bmatrix} 0 & 1 \\ -6 & -5 \end{bmatrix}, \mathbf{B} = \begin{bmatrix} 0 \\ 6 \end{bmatrix}, \mathbf{C} = [1 \quad 0].$$

Compute the corresponding transfer function representation of the system. If the initial conditions are zero (i.e., $x_1(0) = 0$ and $x_2(0) = 0$), determine the response when $u(t)$ is a unit step input for $t \geq 0$.

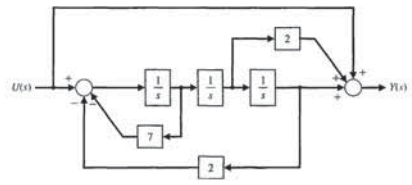

FIGURE E11.11
State variable block diagram with a feedforward term.

PROBLEMS

P11.1 A first-order system is represented by the time-domain differential equation

$$\dot{x} = x + u.$$

A feedback controller is to be designed such that

$$u(t) = -kx,$$

and the desired equilibrium condition is $x(t) = 0$ as $t \to \infty$. The performance integral is defined as

$$J = \int_0^\infty x^2\,dt,$$

and the initial value of the state variable is $x(0) = \sqrt{2}$. Obtain the value of k in order to make J a minimum. Is this k physically realizable? Select a practical value for the gain k and evaluate the performance index with that gain. Is the system stable without the feedback due to $u(t)$?

P11.2 To account for the expenditure of energy and resources, the control signal is often included in the performance integral. Then the operation will not involve an unlimited control signal $u(t)$. One suitable performance index, which includes the effect of the magnitude of the control signal, is

$$J = \int_0^\infty (x^2(t) + \lambda u^2(t))\,dt.$$

(a) Repeat Problem P11.1 for the performance index.
(b) If $\lambda = 2$, obtain the value of k that minimizes the performance index. Calculate the resulting minimum value of J.

P11.3 An unstable robot system is described by the vector differential equation [9]

$$\frac{d}{dt}\begin{bmatrix} x_1 \\ x_2 \end{bmatrix} = \begin{bmatrix} 1 & 0 \\ -1 & 2 \end{bmatrix}\begin{bmatrix} x_1 \\ x_2 \end{bmatrix} + \begin{bmatrix} 1 \\ 1 \end{bmatrix}u(t).$$

Both state variables are measurable, and so the control signal is set as $u(t) = -k(x_1 + x_2)$. Following the method of Section 11.7, design gain k so that the performance index is minimized. Evaluate the minimum value of the performance index. Determine the sensitivity of the performance to a change in k. Assume that the initial conditions are

$$\mathbf{x}(0) = \begin{bmatrix} 1 \\ 1 \end{bmatrix}.$$

Is the system stable without the feedback signals due to $u(t)$?

P11.4 Determine the feedback gain k of Example 11.12 that minimizes the performance index

$$J = \int_0^\infty \mathbf{x}^T\mathbf{x}\,dt$$

when $\mathbf{x}^T(0) = [1 \quad -1]$. Plot the performance index J versus the gain k.

P11.5 Determine the feedback gain k of Example 11.13 that minimizes the performance index

$$J = \int_0^\infty (\mathbf{x}^T\mathbf{x} + u^T\mathbf{u})\,dt$$

when $\mathbf{x}^T(0) = [1 \quad 1]$. Plot the performance index J versus the gain k.

P11.6 For the solutions of Problems P11.3, P11.4, and P11.5, determine the roots of the closed-loop optimal control system. Note that the resulting closed-loop roots depend on the performance index selected.

P11.7 A system has the vector differential equation as given in Equation (11.42). We want both state variables to be used in the feedback so that $u(t) = -k_1x_1 - k_2x_2$. Also, we desire to have a natural frequency ω_n for this system equal to 2. Find a set of gains k_1 and k_2 in order to achieve an optimal system when J is given by Equation (11.63). Assume $\mathbf{x}^T(0) = [1 \quad 0]$.

P11.8 For the system of Example 11.11 determine the optimum value for k_2 when $k_1 = 1$ and $\mathbf{x}^T(0) = [1 \quad 0]$.

P11.9 An interesting mechanical system with a challenging control problem is the ball and beam, shown in Figure P11.9(a) [10]. It consists of a rigid beam that is free to rotate in the plane of the paper around a center pivot, with a solid ball rolling along a groove in the top of the beam. The control problem is to position the ball at a desired point on the beam using a torque applied to the beam as a control input at the pivot.

A linear model of the system with a measured value of the angle ϕ and its angular velocity $d\phi/dt = \omega$ is available. Select a feedback scheme so that the response of the closed-loop system has an overshoot of 4% and a settling time (with a 2% criterion) of 1 second for a step input.

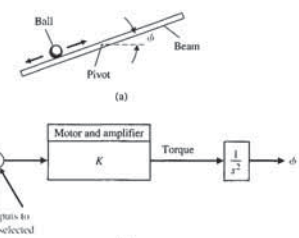

FIGURE P11.9
(a) Ball and beam.
(b) Model of the ball and beam.

P11.10 The dynamics of a rocket are represented by

$$\dot{\mathbf{x}} = \begin{bmatrix} 0 & 0 \\ 1 & 0 \end{bmatrix}\mathbf{x} + \begin{bmatrix} 1 \\ 0 \end{bmatrix}u$$
$$y = [0 \quad 1]\mathbf{x}$$

and state variable feedback is used, where $u = -10x_1 - 25x_2 + r$. Determine the roots of the characteristic equation of this system and the response of the system when the initial conditions are $x_1(0) = 1$ and $x_2(0) = -1$. Assume the reference input $r(t) = 0$.

P11.11 The state variable model of a plant to be controlled is

$$\dot{\mathbf{x}} = \begin{bmatrix} -5 & -2 \\ 2 & 0 \end{bmatrix}\mathbf{x} + \begin{bmatrix} 0.5 \\ 0 \end{bmatrix}u$$
$$y = [0 \quad 1]\mathbf{x} + [0]u.$$

Use state variable feedback and incorporate a command input $u = -\mathbf{K}\mathbf{x} + \alpha r$. Select the gains $\mathbf{K}$ and α so that the system has a rapid response with an overshoot of approximately 1%, a settling time (with a 2%

criterion) less than 1 second, and a zero steady-state error to a unit step input.

P11.12 A DC motor has the state variable model

$$\dot{\mathbf{x}} = \begin{bmatrix} -3 & -2 & -0.75 & 0 & 0 \\ -3 & 0 & 0 & 0 & 0 \\ 0 & 2 & 0 & 0 & 0 \\ 0 & 0 & 1 & 0 & 0 \\ 0 & 0 & 0 & 2 & 0 \end{bmatrix}\mathbf{x} + \begin{bmatrix} 1 \\ 0 \\ 0 \\ 0 \\ 0 \end{bmatrix}u$$
$$y = [0 \quad 0 \quad 0 \quad 0 \quad 2.75]\mathbf{x}.$$

Determine whether this system is controllable and observable.

P11.13 A feedback system has a plant transfer function

$$\frac{Y(s)}{R(s)} = G(s) = \frac{K}{s(s + 70)}.$$

We want the velocity error constant K_v to be 35 and the overshoot to a step to be approximately 4% so that ζ is $1/\sqrt{2}$. The settling time (with a 2% criterion) desired is 0.11 second. Design an appropriate state variable feedback system for $r(t) = -k_1x_1 - k_2x_2$.

P11.14 A process has the transfer function

$$\dot{\mathbf{x}} = \begin{bmatrix} -10 & 0 \\ 1 & 0 \end{bmatrix}\mathbf{x} + \begin{bmatrix} 1 \\ 0 \end{bmatrix}u$$
$$y = [0 \quad 1]\mathbf{x} + [0]u.$$

Determine the state variable feedback gains to achieve a settling time (with a 2% criterion) of 1 second and an overshoot of about 10%. Also sketch the block diagram of the resulting system. Assume the complete state vector is available for feedback.

P11.15 A telerobot system has the matrix equations [16]

$$\dot{\mathbf{x}} = \begin{bmatrix} -1 & 0 & 0 \\ 0 & -2 & 0 \\ 0 & 0 & -3 \end{bmatrix}\mathbf{x} + \begin{bmatrix} 1 \\ 1 \\ 0 \end{bmatrix}u$$

and

$$y = [1 \quad 0 \quad 2]\mathbf{x}.$$

(a) Determine the transfer function, $G(s) = Y(s)/U(s)$. (b) Draw the block diagram indicating the state variables. (c) Determine whether the system is controllable. (d) Determine whether the system is observable.

P11.16 Hydraulic power actuators were used to drive the dinosaurs of the movie *Jurassic Park* [20]. The motions of the large monsters required high-power actuators requiring 1200 watts.

One specific limb motion has dynamics represented by

$$\dot{\mathbf{x}} = \begin{bmatrix} -4 & 0 \\ 1 & -1 \end{bmatrix}\mathbf{x} + \begin{bmatrix} 1 \\ 0 \end{bmatrix}u$$
$$y = [0 \quad 1]\mathbf{x} + [0]u.$$

We want to place the closed-loop poles at $s = -1 \pm 3j$. Determine the required state variable feedback using Ackermann's formula. Assume that the complete state vector is available for feedback.

P11.17 A system has a transfer function

$$\frac{Y(s)}{R(s)} = \frac{s + a}{s^4 + 15s^3 + 68s^2 + 106s + 80}.$$

Determine a real value of a so that the system is either uncontrollable or unobservable.

P11.18 A system has a plant

$$\frac{Y(s)}{U(s)} = G(s) = \frac{1}{(s + 1)^2}.$$

(a) Find the matrix differential equation to represent this system. Identify the state variables on a block diagram model. (b) Select a state variable feedback structure using $u(t)$, and select the feedback gains so that the response $y(t)$ of the unforced system is critically damped when the initial condition is $x_1(0) = 1$ and $x_2(0) = 0$, where $x_1 = y(t)$. The repeated roots are at $s = -\sqrt{2}$.

P11.19 The block diagram of a system is shown in Figure P11.19. Determine whether the system is controllable and observable.

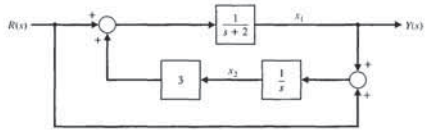

FIGURE P11.19
Multiloop feedback control system.

(a) Determine the value of K resulting in a zero steady-state tracking error when $u(t)$ is a unit step input for $t \geq 0$. The tracking error is defined here as $e(t) = u(t) - y(t)$.
(b) Plot the response to a unit step input and verify that the tracking error is zero for the gain K determined in part (a).

P11.29 The block diagram shown in Figure P11.29 is an example of an interacting system. Determine a state variable representation of the system in the form

$$\dot{\mathbf{x}}(t) = \mathbf{A}\mathbf{x}(t) + \mathbf{B}u(t)$$
$$y(t) = \mathbf{C}\mathbf{x}(t) + \mathbf{D}u(t)$$

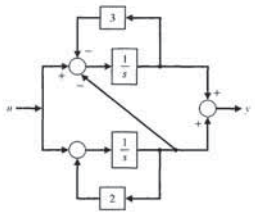

FIGURE P11.29 Interacting feedback system.

ADVANCED PROBLEMS

AP11.1 A DC motor control system has the form shown in Figure AP11.1 [6]. The three state variables are available for measurement; the output position is $x_1(t)$. Select the feedback gains so that the system has a steady-state error equal to zero for a step input and a response with a percent overshoot less than 3%.

AP11.2 A system has the model

$$\dot{\mathbf{x}} = \begin{bmatrix} -3 & -1 & -1 \\ 4 & 0 & 0 \\ 0 & 1 & 0 \end{bmatrix}\mathbf{x} + \begin{bmatrix} 3 \\ 0 \\ 0 \end{bmatrix}u.$$

Add state variable feedback so that the closed-loop poles are $s = -4$, -5, and -6.

AP11.3 A system has a matrix differential equation

$$\dot{\mathbf{x}} = \begin{bmatrix} 0 & 1 \\ -1 & -2 \end{bmatrix}\mathbf{x} + \begin{bmatrix} b_1 \\ b_2 \end{bmatrix}u.$$

What values for b_1 and b_2 are required so that the system is controllable?

AP11.4 The vector differential equation describing the inverted pendulum of Example 3.3 is

$$\frac{d\mathbf{x}}{dt} = \begin{bmatrix} 0 & 1 & 0 & 0 \\ 0 & 0 & -1 & 0 \\ 0 & 0 & 0 & 1 \\ 0 & 0 & 9.8 & 0 \end{bmatrix}\mathbf{x} + \begin{bmatrix} 0 \\ 1 \\ 0 \\ -1 \end{bmatrix}u.$$

Assume that all state variables are available for measurement and use state variable feedback. Place the system characteristic roots at $s = -2 \pm j$, -5, and -5.

AP11.5 An automobile suspension system has three physical state variables, as shown in Figure AP11.5 [13]. The state variable feedback structure is shown in the figure, with $K_1 = 1$. Select K_2 and K_3 so that the roots of the characteristic equation are three real roots lying between $s = -3$ and $s = -6$. Also, select K_p so that the steady-state error for a step input is equal to zero.

AP11.6 A system is represented by the differential equation

$$\frac{d^2y}{dt^2} + 2\frac{dy}{dt} + y = \frac{du}{dt} + u,$$

where y = output and u = input.

(a) Develop a state variable representation and show that it is a controllable system. (b) Define the state variables as $x_1 = y$ and $x_2 = dy/dt - u$, and determine whether the system is controllable. Note that the controllability of a system depends on the definition of the state variables.

AP11.7 The *Radisson Diamond* uses pontoons and stabilizers to damp out the effect of waves hitting the ship.

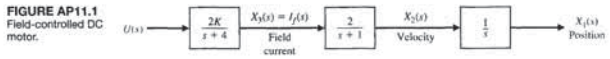

FIGURE AP11.1 Field-controlled DC motor.

P11.20 Consider the automatic ship-steering system discussed in Problems P8.11 and P9.15. The state variable form of the system differential equation is

$$\dot{\mathbf{x}}(t) = \begin{bmatrix} -0.05 & -6 & 0 & 0 \\ -10^{-3} & -0.15 & 0 & 0 \\ 1 & 0 & 0 & 13 \\ 0 & 1 & 0 & 0 \end{bmatrix}\mathbf{x}(t) + \begin{bmatrix} -0.2 \\ 0.03 \\ 0 \\ 0 \end{bmatrix}\delta(t),$$

where $\mathbf{x}^T(t) = [v \quad \omega_z \quad y \quad \theta]$. The state variables are $x_1 = v$ = the transverse velocity; $x_2 = \omega_z$ = angular rate of ship's coordinate frame relative to response frame; $x_3 = y$ = deviation distance on an axis perpendicular to the track; $x_4 = \theta$ = deviation angle. (a) Determine whether the system is stable. (b) Feedback can be added so that

$$\delta(t) = -k_1x_1 - k_3x_3.$$

Determine whether this system is stable for suitable values of k_1 and k_3.

P11.21 An RL circuit is shown in Figure P11.21. (a) Select the two stable variables and obtain the vector differential equation where the output is $v_0(t)$. (b) Determine whether the state variables are observable when $R_3/L_1 = R_2/L_2$. (c) Find the conditions when the system has two equal roots.

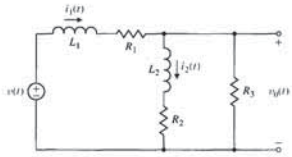

FIGURE P11.21 RL circuit.

P11.22 A manipulator control system has a loop transfer function of

$$G(s) = \frac{1}{s(s + 0.4)}$$

and negative unity feedback [15]. Represent this system by a state variable signal-flow graph or block diagram and a vector differential equation. (a) Plot the response of the closed-loop system to a step input. (b) Use state variable feedback so that the overshoot is 5% and the settling time (with a 2% criterion) is 1.35 seconds. (c) Plot the response of the state variable feedback system to a step input.

P11.23 Consider again the system of Example 11.7 when we desire that the steady-state error for a step input be zero and the desired roots of the characteristic equation be $s = -2 \pm j1$ and $s = -10$.

P11.24 Consider again the system of Example 11.7 when we desire that the steady-state error for a ramp input be zero and the roots of the characteristic equation be $s = -2 \pm j2$ and $s = -20$.

P11.25 Consider the system represented in state variable form

$$\dot{\mathbf{x}} = \mathbf{A}\mathbf{x} + \mathbf{B}u$$
$$y = \mathbf{C}\mathbf{x} + \mathbf{D}u,$$

where

$$\mathbf{A} = \begin{bmatrix} 1 & 4 \\ -5 & 10 \end{bmatrix}, \quad \mathbf{B} = \begin{bmatrix} 0 \\ 1 \end{bmatrix},$$
$$\mathbf{C} = [1 \quad -4], \quad \text{and} \quad \mathbf{D} = [0].$$

Verify that the system is observable. Then design a full-state observer by placing the observer poles at $s_{1,2} = -1$. Plot the response of the estimation error $\mathbf{e} = \mathbf{x} - \hat{\mathbf{x}}$ with an initial estimation error of $\mathbf{e}(0) = [1 \quad 1]^T$.

P11.26 Consider the third-order system

$$\dot{\mathbf{x}} = \begin{bmatrix} 0 & 1 & 0 \\ 0 & 0 & 1 \\ -8 & -5 & -3 \end{bmatrix}\mathbf{x} + \begin{bmatrix} 0 \\ 0 \\ 4 \end{bmatrix}u$$
$$y = [2 \quad -4 \quad 0]\mathbf{x} + [0]u.$$

Verify that the system is observable. If so, determine the observer gain matrix required to place the observer poles at $s_{1,2} = -1 \pm j$ and $s_3 = -5$.

P11.27 Consider the second-order system

$$\dot{\mathbf{x}} = \begin{bmatrix} 1 & 0 \\ -3 & -2 \end{bmatrix}\mathbf{x} + \begin{bmatrix} 10 \\ 0 \end{bmatrix}u$$
$$y = [1 \quad 0]\mathbf{x} + [0]u.$$

Determine the observer gain matrix required to place the observer poles at $s_{1,2} = -1 \pm j$.

P11.28 Consider the single-input, single-output system is described by

$$\dot{\mathbf{x}}(t) = \mathbf{A}\mathbf{x}(t) + \mathbf{B}u(t)$$
$$y(t) = \mathbf{C}\mathbf{x}(t)$$

where

$$\mathbf{A} = \begin{bmatrix} 0 & 1 \\ -16 & -8 \end{bmatrix}, \mathbf{B} = \begin{bmatrix} 0 \\ K \end{bmatrix}, \mathbf{C} = [1 \quad 0].$$

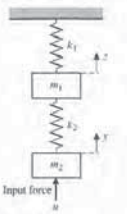

FIGURE AP11.9 Model of hospital vehicle.

AP11.10 Consider the inverted pendulum mounted to a motor, as shown in Figure AP11.10. The motor and load are assumed to have no friction damping. The pendulum to be balanced is attached to the horizontal shaft of a servomotor. The servomotor carries a tachogenerator, so that a velocity signal is available, but there is no position signal. When the motor is unpowered, the pendulum will hang vertically downward and, if slightly disturbed, will perform oscillations. If lifted to the top of its arc, the pendulum is unstable in that position. Devise a feedback compensator $G_c(s)$ using only the velocity signal from the tachometer.

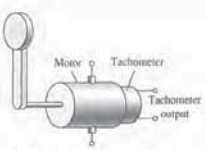

FIGURE AP11.10 Motor and inverted pendulum.

AP11.11 Determine an internal model controller $G_c(s)$ for the system shown in Figure AP11.11. We want the steady-state error to a step input to be zero. We also want the settling time (with a 2% criterion) to be less than 5 seconds.

AP11.12 Repeat Advanced Problem AP11.11 when we want the steady-state error to a ramp input to be zero and the settling time (with a 2% criterion) of the ramp response to be less than 6 seconds.

AP11.13 Consider the system represented in state variable form

$$\dot{\mathbf{x}} = \mathbf{A}\mathbf{x} + \mathbf{B}u$$
$$y = \mathbf{C}\mathbf{x} + \mathbf{D}u,$$

where

$$\mathbf{A} = \begin{bmatrix} 1 & 2 \\ -6 & -12 \end{bmatrix}, \quad \mathbf{B} = \begin{bmatrix} -5 \\ 1 \end{bmatrix},$$
$$\mathbf{C} = [4 \quad -3], \quad \text{and} \quad \mathbf{D} = [0].$$

Verify that the system is observable and controllable. If so, design a full-state feedback law and an observer by placing the closed-loop system poles at $s_{1,2} = -1 \pm j$ and the observer poles at $s_{1,2} = -12$.

AP11.14 Consider the third-order system

$$\dot{\mathbf{x}} = \begin{bmatrix} 0 & 1 & 0 \\ 0 & 0 & 1 \\ -8 & -3 & -3 \end{bmatrix}\mathbf{x} + \begin{bmatrix} 0 \\ 0 \\ 4 \end{bmatrix}u$$
$$y = [2 \quad -9 \quad 2]\mathbf{x} + [0]u.$$

Verify that the system is observable and controllable. Then, design a full-state feedback law and an

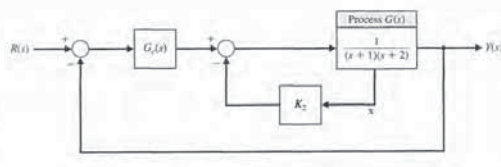

FIGURE AP11.11 Internal model control.

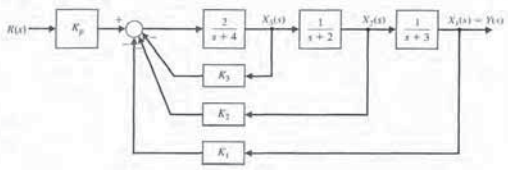

FIGURE AP11.5 Automobile suspension system.

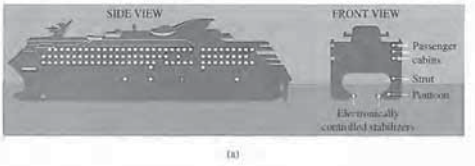

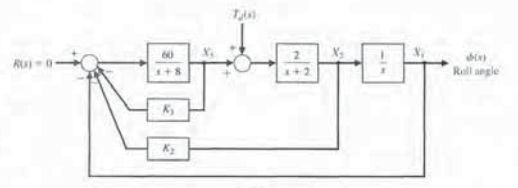

FIGURE AP11.7 (a) *Radisson Diamond* (courtesy of *Conde-Nast Traveler*, July 1993, 23). (b) Control system to reduce the effect of the disturbance.

as shown in Figure AP11.7(a). The block diagram of the ship's roll control system is shown in Figure AP11.7(b). Determine the feedback gains K_2 and K_3 so that the characteristic roots are $s = -15$ and $s = -2 \pm j2$. Plot the roll output $\phi(t)$ for a unit step disturbance.

AP11.8 Consider again the liquid-level control system described in Problem P3.36.

(a) Design a state variable controller using only $h(t)$ as the feedback variable, so that the step response has an overshoot less than 10% and a settling time (with a 2% criterion) less than or equal to 5 seconds. (b) Design a state variable controller feedback using two state variables, level $h(t)$ and shaft position $\theta(t)$, to satisfy the specifications of part (a). (c) Compare the results of parts (a) and (b).

AP11.9 The motion control of a lightweight hospital transport vehicle can be represented by a system of two masses, as shown in Figure AP11.9, where $m_1 = m_2 = 1$ and $k_1 = k_2 = 1$ [21]. (a) Determine the state vector differential equation. (b) Find the roots of the characteristic equation. (c) We wish to stabilize the system by letting $u = -kx_c$, where u is the force on the lower mass, and x_c is one of the state variables. Select an appropriate state variable x_c. (d) Choose a value for the gain k and sketch the root locus as k varies.

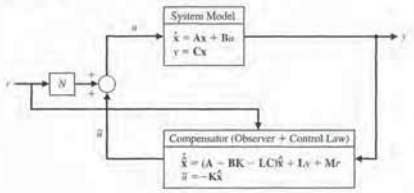

FIGURE DP11.3 Feedback system constructed to track a desired input $r(t)$.

DP11.4 A high-performance helicopter has a model shown in Figure DP11.4. The goal is to control the pitch angle θ of the helicopter by adjusting the rotor thrust angle δ.

The equations of motion of the helicopter are

$$\frac{d^2\theta}{dt^2} = -\sigma_1\frac{d\theta}{dt} - \alpha_1\frac{dx}{dt} + n\delta$$

$$\frac{d^2x}{dt^2} = g\theta - \alpha_2\frac{d\theta}{dt} - \sigma_2\frac{dx}{dt} + g\delta,$$

where x is the translation in the horizontal direction. For a military high-performance helicopter, we find that

$$\sigma_1 = 0.415 \qquad \alpha_2 = 1.43$$
$$\sigma_2 = 0.0198 \qquad n = 6.27$$
$$\alpha_1 = 0.0111 \qquad g = 9.8$$

all in appropriate SI units.

Find (a) a state variable representation of this system and (b) the transfer function representation for $\theta(s)/\delta(s)$. (c) Use state variable feedback to achieve adequate performances for the controlled system.

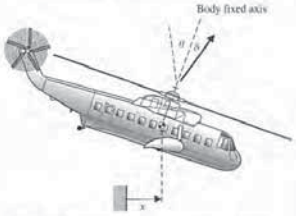

FIGURE DP11.4 Helicopter pitch angle, θ, control.

Desired specifications include (1) a steady-state for an input step command for $\theta_d(s)$, the desired pitch angle, less than 20% of the input step magnitude; (2) an overshoot for a step input command less than 20%; and (3) a settling (with a 2% criterion) time for a step command of less than 1.5 seconds.

DP11.5 The headbox process is used in the manufacture of paper to transform the pulp slurry flow into a jet of 2 cm and then spread it onto a mesh belt [22]. To achieve desirable paper quality, the pulp slurry must be distributed as evenly as possible on the belt, and the relationship between the velocity of the jet and that of the belt, called the jet/belt ratio, must be maintained. One of the main control variables is the pressure in the headbox, which in turn controls the velocity of the slurry at the jet. The total pressure in the headbox is the sum of the liquid-level pressure and the air pressure that is pumped into the headbox. Because the pressurized headbox is a highly dynamic and coupled system, manual control would be difficult to maintain and could result in degradation in the sheet properties.

The state-space model of a typical headbox, linearized about a particular stationary point, is given by

$$\dot{\mathbf{x}} = \begin{bmatrix} -0.8 & +0.02 \\ -0.02 & 0 \end{bmatrix}\mathbf{x} + \begin{bmatrix} 0.05 \\ 0.001 \end{bmatrix}u$$

and $y = [1 \quad 0]\mathbf{x}$.

The state variables are x_1 = liquid level and x_2 = pressure. The control variable is u_1 = pump current. (a) Design a state variable feedback system that has a characteristic equation with real roots with a magnitude greater than five. (b) Design an observer with observer poles located at least ten times farther in the left half-plane than the state variable feedback system. (c) Connect the observer and full-state feedback system and sketch the block diagram of the integrated system.

observer by placing the closed-loop system poles at $s_{1,2} = -1 \pm j$, $s_3 = -3$ and the observer poles at $s_{1,2} = -12 \pm j2$, $s_3 = -30$.

AP11.15 Consider the system depicted in Figure AP11.15. Design a full-staie observer for the system. Determine the observer gain matrix $\mathbf{L}$ to place the observer poles at $s_{1,2} = -10 \pm j10$.

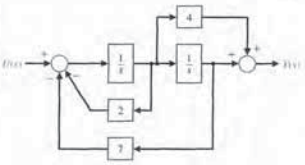

FIGURE AP11.15 A second-order system block diagram.

DESIGN PROBLEMS

CDP11.1 We wish to obtain a state variable feedback system for the capstan-slide the state variable model developed in CDP3.1 and determine the feedback system. The step response should have an overshoot less than 2% and a settling time less than 250 ms.

DP11.1 Consider the device for the magnetic levitation of a steel ball, as shown in Figures DP11.1(a) and (b). Obtain a design that will provide a stable response where the ball will remain within 10% of its desired position. Assume that y and dy/dt are measurable.

DP11.2 The control of the fuel-to-air ratio in an automobile carburetor became of prime importance in the 1980s as automakers worked to reduce exhaust-pollution emissions. Thus, auto engine designers turned to the feedback control of the fuel-to-air ratio. A sensor was placed in the exhaust stream and used as an input to a controller. The controller actually adjusts the orifice that controls the flow of fuel into the engine [3].

Select the devices and develop a linear model for the entire system. Assume that the sensor measures the actual fuel-to-air ratio with a negligible delay. With this model, determine the optimum controller when we desire a system with a zero steady-state error to a step input and an overshoot for a step command of less than 10%.

DP11.3 Consider the feedback system depicted in Figure DP11.3. The system model is given by

$$\dot{\mathbf{x}}(t) = \mathbf{A}\mathbf{x}(t) + \mathbf{B}u(t)$$
$$y(t) = \mathbf{C}\mathbf{x}(t)$$

where

$$\mathbf{A} = \begin{bmatrix} 0 & 1 \\ -10.5 & -11.3 \end{bmatrix}, \mathbf{B} = \begin{bmatrix} 0 \\ 0.55 \end{bmatrix}, \mathbf{C} = [1 \quad 0].$$

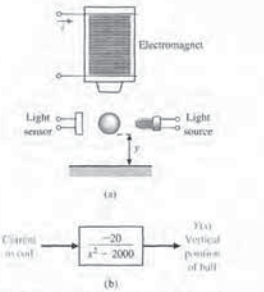

FIGURE DP11.1 (a) The levitation of a ball using an electromagnet. (b) The model of the electromagnet and the ball.

Design the compensator to meet the following specifications:

1. The steady-state error to a unit step input is zero.
2. The settling time $T_s < 1$ s and the percent overshoot is $P.O. < 5\%$.
3. Select initial conditions for $\mathbf{x}$ and different initial conditions for $\hat{\mathbf{x}}$ and simulate the response of the closed-loop system to a unit step input.

COMPUTER PROBLEMS

CP11.1 Consider the system

$$\dot{\mathbf{x}} = \begin{bmatrix} -6 & 2 & 0 \\ 4 & 0 & 7 \\ -10 & 1 & 11 \end{bmatrix}\mathbf{x} + \begin{bmatrix} 5 \\ 0 \\ 1 \end{bmatrix}u,$$
$$y = [1 \quad 2 \quad 1]\mathbf{x}.$$

Using the ctrb and obsv functions, show that the system is controllable and observable.

CP11.2 Consider the system

$$\dot{\mathbf{x}} = \begin{bmatrix} 0 & 1 \\ -6 & -5 \end{bmatrix}\mathbf{x} + \begin{bmatrix} 0 \\ 6 \end{bmatrix}u,$$
$$y = [1 \quad 0]\mathbf{x}.$$

Determine if the system is controllable and observable. Compute the transfer function from u to y.

CP11.3 Find a gain matrix $\mathbf{K}$ so that the closed-loop poles of the system

$$\dot{\mathbf{x}} = \begin{bmatrix} 0 & 1 \\ -1 & 2 \end{bmatrix}\mathbf{x} + \begin{bmatrix} 1 \\ 1 \end{bmatrix}u,$$
$$y = [1 \quad -1]\mathbf{x}$$

are $s_1 = -1$ and $s_2 = -2$. Use state feedback $u = -\mathbf{K}\mathbf{x}$.

CP11.4 The following model has been proposed to describe the motion of a constant-velocity guided missile:

$$\dot{\mathbf{x}} = \begin{bmatrix} 0 & 1 & 0 & 0 & 0 \\ -0.1 & -0.5 & 0 & 0 & 0 \\ 0.5 & 0 & 0 & 0 & 0 \\ 0 & 0 & 10 & 0 & 0 \\ 0.5 & 1 & 0 & 0 & 0 \end{bmatrix}\mathbf{x} + \begin{bmatrix} 0 \\ 1 \\ 0 \\ 0 \\ 0 \end{bmatrix}u,$$
$$y = [0 \quad 0 \quad 0 \quad 1 \quad 0]\mathbf{x}.$$

(a) Verify that the system is not controllable by analyzing the controllability matrix using the ctrb function.
(b) Develop a controllable state variable model by first computing the transfer function from u to y, then cancel any common factors in the numerator and denominator polynomials of the transfer function. With the modified transfer function just obtained, use the ss function to determine a modified state variable model for the system.
(c) Verify that the modified state variable model in part (b) is controllable.
(d) Is the constant velocity guided missile stable?
(e) Comment on the relationship between the controllability and the complexity of the state variable model (where complexity is measured by the number of state variables).

CP11.5 A linearized model of a vertical takeoff and landing (VTOL) aircraft is [24]

$$\dot{\mathbf{x}} = \mathbf{A}\mathbf{x} + \mathbf{B}_1u_1 + \mathbf{B}_2u_2,$$

where

$$\mathbf{A} = \begin{bmatrix} -0.0389 & 0.0271 & 0.0188 & -0.4555 \\ 0.0482 & -1.0100 & 0.0019 & -4.0208 \\ 0.1024 & 0.3681 & -0.7070 & 1.4200 \\ 0 & 0 & 1 & 0 \end{bmatrix}$$

and

$$\mathbf{B}_1 = \begin{bmatrix} 0.4422 \\ 3.5446 \\ -6.0214 \\ 0 \end{bmatrix}, \quad \mathbf{B}_2 = \begin{bmatrix} 0.1291 \\ -7.5922 \\ 4.4900 \\ 0 \end{bmatrix}.$$

The state vector components are (i) x_1 is the horizontal velocity (knots), (ii) x_2 is the vertical velocity (knots), (iii) x_3 is the pitch rate (degrees/second), and (iv) x_4 is the pitch angle (degrees). The input u_1 is used mainly to control the vertical motion, and u_2 is used for the horizontal motion.

(a) Compute the eigenvalues of the system matrix $\mathbf{A}$. Is the system stable? (b) Determine the characteristic polynomial associated with $\mathbf{A}$ using the poly function. Compute the roots of the characteristic equation, and compare them with the eigenvalues in part (a). (c) Is the system controllable from u_1 alone? What about from u_2 alone? Comment on the results.

CP11.6 In an effort to open up the far side of the Moon to exploration, studies have been conducted to determine the feasibility of operating a communication satellite around the translunar equilibrium point in the Earth–Sun–Moon system. The desired satellite orbit, known as a halo orbit, is shown in Figure CP11.6. The objective of the controller is to keep the satellite on a halo orbit trajectory that can be seen from the Earth so that the lines of communication are accessible at all times. The communication link is from the Earth to the satellite and then to the far side of the Moon.

The linearized (and normalized) equations of motion of the satellite around the translunar equilibrium point are [25]

$$\dot{\mathbf{x}} = \begin{bmatrix} 0 & 0 & 0 & 1 & 0 & 0 \\ 0 & 0 & 0 & 0 & 1 & 0 \\ 0 & 0 & 0 & 0 & 0 & 1 \\ 7.3809 & 0 & 0 & 0 & 2 & 0 \\ 0 & -2.1904 & 0 & -2 & 0 & 0 \\ 0 & 0 & -3.1904 & 0 & 0 & 0 \end{bmatrix}\mathbf{x}$$

DP11.6 A coupled-drive apparatus is shown in Figure DP11.6. The coupled drives consist of two pulleys connected via an elastic belt, which is tensioned by a third pulley mounted on springs providing an underdamped dynamic mode. One of the main pulleys, pulley A, is driven by an electric DC motor. Both pulleys A and B are fitted with tachometers that generate measurable voltages proportional to the rate of rotation of the pulley. When a voltage is applied to the DC motor, pulley A will accelerate at a rate governed by the total inertia experienced by the system. Pulley B, at the other end of the elastic belt, will also accelerate owing to the applied voltage or torque, but with a lagging effect caused by the elasticity of the belt. Integration of the velocity signals measured at each pulley will provide an angular position estimate for the pulley [23].

The second-order model of a coupled-drive is

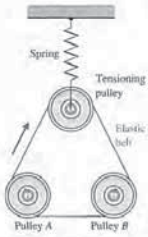

FIGURE DP11.6

$$\dot{\mathbf{x}} = \begin{bmatrix} 0 & 1 \\ -36 & -12 \end{bmatrix}\mathbf{x} + \begin{bmatrix} 0 \\ 1 \end{bmatrix}u$$

and $y = x_1$.

(a) Design a state variable feedback controller that will yield a step response with deadbeat response and a settling time (with a 2% criterion) less than 0.5 second. (b) Design an observer for the system by placing the observer poles appropriately in the left half-plane. (c) Draw the block diagram of the system including the compensator with the observer and state feedback. (d) Simulate the response to an initial state of $\mathbf{x}(0) = [1 \quad 0]^T$ and $\hat{\mathbf{x}}(0) = [0 \quad 0]^T$.

DP11.7 A closed-loop feedback system is to be designed to track a reference input. The desired feedback block diagram is shown in Figure DP11.3. The system model is given by

$$\dot{\mathbf{x}}(t) = \mathbf{A}\mathbf{x}(t) + \mathbf{B}u(t)$$
$$y(t) = \mathbf{C}\mathbf{x}(t)$$

where

$$\mathbf{A} = \begin{bmatrix} 0 & 1 & 0 \\ 0 & 0 & 1 \\ -2 & -5 & -10 \end{bmatrix}, \mathbf{B} = \begin{bmatrix} 0 \\ 0 \\ 1 \end{bmatrix}, \mathbf{C} = [1 \quad 0 \quad 0].$$

Design the observer and the control law to meet the following specifications:

1. The steady-state error of the closed-loop system to a unit step input is zero.
2. The gain margin $G.M. \geq 6$ dB.
3. The bandwidth of the closed-loop system $\omega_B \geq 10$ rad/s.
4. Select initial conditions for $\mathbf{x}$ and different initial conditions for $\hat{\mathbf{x}}$ and simulate the response of the closed-loop system to a unit step input. Verify that the tracking error is zero in the steady-state.

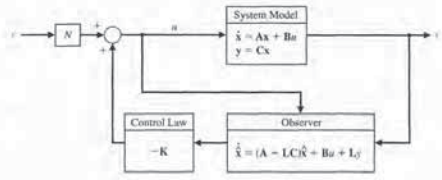

FIGURE DP11.7 Feedback system constructed to track a desired input $r(t)$.

where

$$\mathbf{A} = \begin{bmatrix} 0 & 1 \\ -18.7 & -10.4 \end{bmatrix}, \quad \mathbf{B} = \begin{bmatrix} 10.1 \\ 24.6 \end{bmatrix},$$

$$\mathbf{C} = [1 \quad 0] \quad \text{and} \quad \mathbf{D} = [0].$$

Using the acker function, determine a full-state feedback gain matrix and an observer gain matrix to place the closed-loop system poles at $s_{1,2} = -2$ and the observer poles at $s_{1,2} = -20 \pm j4$.

CP11.11 Consider the third-order system

$$\dot{\mathbf{x}} = \begin{bmatrix} 0 & 1 & 0 \\ 0 & 0 & 1 \\ -4.3 & -1.7 & -6.7 \end{bmatrix}\mathbf{x} + \begin{bmatrix} 0 \\ 0 \\ 0.35 \end{bmatrix}u$$

$$y = [0 \quad 1 \quad 0]\mathbf{x} + [0]u.$$

(a) Using the acker function, determine a full-state feedback gain matrix and an observer gain matrix to place the closed-loop system poles at $s_{1,2} = -1.4 \pm j1.4$, $s_3 = -2$ and the observer poles at $s_{1,2} = -18 \pm j5$, $s_3 = -20$. (b) Construct the state variable compensator using Figure 11.1 as a guide. (c) Simulate the closed-loop system with the state initial conditions $\mathbf{x}(0) = (1 \quad 0 \quad 0)^T$ and initial state estimate of $\hat{\mathbf{x}}(0) = (0.5 \quad 0.1 \quad 0.1)^T$.

CP11.12 Implement the system shown in Figure CP11.12 in an m-file. Obtain the step response of the system.

CP11.13 Consider the system in state variable form

$$\dot{\mathbf{x}} = \begin{bmatrix} 0 & 1 & 0 & 0 \\ 0 & 0 & 1 & 0 \\ 0 & 0 & 0 & 1 \\ -2 & -5 & -1 & -13 \end{bmatrix}\mathbf{x} + \begin{bmatrix} 0 \\ 0 \\ 0 \\ 1 \end{bmatrix}u$$

$$y = [1 \quad 0 \quad 0 \quad 0]\mathbf{x} + [0]u.$$

Design a full-state feedback gain matrix and an observer gain matrix to place the closed-loop system poles at $s_{1,2} = -1.4 \pm j1.4$, $s_{3,4} = -2 \pm j$ and the observer poles $s_{1,2} = -18 \pm j5$, $s_{3,4} = -20$. Construct the state variable compensator using Figure 11.1 as a guide and simulate the closed-loop system using Simulink. Select several values of initial states and initial state estimates in the observer and display the tracking results on an x-y-graph.

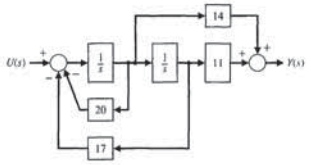

FIGURE CP11.12 Control system for Simulink implementation.

ANSWERS TO SKILLS CHECK

True or False: (1) True; (2) True; (3) False; (4) True; (5) False

Multiple Choice: (6) c; (7) a; (8) c; (9) a; (10) a; (11) b; (12) a; (13) b; (14) b; (15) a

Word Match (in order, top to bottom): e, o, k, i, d, b, j, m, f, n, h, q, g, l, p, c, a

TERMS AND CONCEPTS

Command following An important aspect of control system design wherein a nonzero reference input is tracked.

Controllability matrix A linear system is (completely) controllable if and only if the controllability matrix $\mathbf{P}_c = [\mathbf{B} \quad \mathbf{AB} \quad \mathbf{A}^2\mathbf{B} \ldots \mathbf{A}^{n-1}\mathbf{B}]$ has full rank, where $\mathbf{A}$ is an $n \times n$ matrix. For single-input, single-output linear systems, the system is controllable if and only if the determinant of the $n \times n$ controllability matrix $\mathbf{P}_c$ is nonzero.

Controllable system A system is controllable on the interval $[t_0, t_f]$ if there exists a continuous input $u(t)$ such that any initial state $\mathbf{x}(t_0)$ can be driven to any arbitrary trial state $\mathbf{x}(t_f)$ in a finite time interval $t_f - t_0 > 0$.

Detectable A system in which the states that are unobservable are naturally stable.

Estimation error The difference between the actual state and the estimated state $\mathbf{e}(t) = \mathbf{x}(t) - \hat{\mathbf{x}}(t)$.

$$+ \begin{bmatrix} 0 \\ 0 \\ 0 \\ 1 \\ 0 \\ 0 \end{bmatrix}u_1 + \begin{bmatrix} 0 \\ 0 \\ 0 \\ 0 \\ 1 \\ 0 \end{bmatrix}u_2 + \begin{bmatrix} 0 \\ 0 \\ 0 \\ 0 \\ 0 \\ 1 \end{bmatrix}u_3.$$

The state vector $\mathbf{x}$ is the satellite position and velocity, and the inputs u_i, $i = 1, 2, 3$, are the engine thrust accelerations in the ξ, η, and ζ directions, respectively.

(a) Is the translunar equilibrium point a stable location? (b) Is the system controllable from u_1 alone? (c) Repeat part (b) for u_2. (d) Repeat part (b) for u_3. (e) Suppose that we can observe the position in the η direction. Determine the transfer function from u_2 to η. (*Hint:* Let $y = [0 \quad 1 \quad 0 \quad 0 \quad 0 \quad 0]\mathbf{x}$.) (f) Compute a state-space representation of the transfer function in part (e) using the ss function. Verify that the system is controllable. (g) Using state feedback

$$u_2 = -\mathbf{K}x,$$

design a controller (i.e., find $\mathbf{K}$) for the system in part (f) such that the closed-loop system poles are at $s_{1,2} = -1 \pm j$ and $s_{3,4} = -10$.

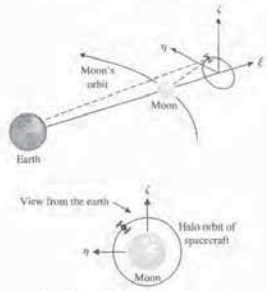

FIGURE CP11.6 The translunar satellite halo orbit.

CP11.7 Consider the system

$$\dot{\mathbf{x}}(t) = \begin{bmatrix} 0 & 1 & 0 \\ 0 & 0 & 1 \\ -2 & -4 & -6 \end{bmatrix}\mathbf{x}(t),$$

$$y(t) = [1 \quad 0 \quad 0]\mathbf{x}(t). \qquad \text{(CP11.1)}$$

Suppose that we are given three observations $y(t_i)$, $i = 1, 2, 3$, as follows:

$$y(t_1) = 1 \quad \text{at} \quad t_1 = 0$$
$$y(t_2) = -0.0256 \quad \text{at} \quad t_2 = 2$$
$$y(t_3) = -0.2522 \quad \text{at} \quad t_3 = 4.$$

(a) Using the three observations, develop a method to determine the initial value of the state vector $\mathbf{x}(t_0)$ for the system in Equation CP11.1 that will reproduce the three observations when simulated using the lsim function. (b) With the observations given, compute $\mathbf{x}(t_0)$ and discuss the condition under which this problem can be solved in general. (c) Verify the result by simulating the system response to the computed initial condition. (*Hint:* Recall that $\mathbf{x}(t) = e^{\mathbf{A}(t-t_0)}\mathbf{x}(t_0)$ for the system in Equation CP11.1.)

CP11.8 A system is described by a single-input state equation with

$$\mathbf{A} = \begin{bmatrix} 0 & 0 \\ -1 & 0 \end{bmatrix} \quad \text{and} \quad \mathbf{B} = \begin{bmatrix} 0 \\ 1 \end{bmatrix}.$$

Using the method of Section 11.7 (Equation 11.40) and a negative unity feedback, determine the optimal system when $\mathbf{x}^T(0) = [1 \quad 0]$.

CP11.9 A first-order system is given by

$$\dot{x} = -x + u$$

with the initial condition $x(0) = x_0$. We want to design a feedback controller

$$u = -kx$$

such that the performance index

$$J = \int_0^\infty (x^2(t) + \lambda u^2(t))\, dt$$

is minimized.

(a) Let $\lambda = 1$. Develop a formula for J in terms of k, valid for any x_0, and use an m-file to plot J/x_0^2 versus k. From the plot, determine the approximate value of $k = k_{min}$ that minimizes J/x_0^2. (b) Verify the result in part (a) analytically. (c) Using the procedure developed in part (a), obtain a plot of k_{min} versus λ, where k_{min} is the gain that minimizes the performance index.

CP11.10 Consider the system represented in state variable form

$$\dot{\mathbf{x}} = \mathbf{A}\mathbf{x} + \mathbf{B}u$$
$$y = \mathbf{C}\mathbf{x} + \mathbf{D}u,$$

CHAPTER

12 Robust Control Systems

PREVIEW

Physical systems and the external environment in which they operate cannot be modeled precisely, may change in an unpredictable manner, and may be subject to significant disturbances. The design of control systems in the presence of significant uncertainty requires the designer to seek a robust system. Recent advances in robust control design methodologies can address stability robustness and performance robustness in the presence of uncertainty. In this chapter, we describe five methods for robust design, including root locus, frequency response, ITAE methods for a robust PID systems, internal model control, and pseudo-quantitative feedback methods. However, we should also realize that classical design techniques may also produce robust control systems. Control engineers who are aware of these issues can design robust PID controllers, robust lead-lag controllers, and so forth. The chapter concludes with a PID controller design for the Sequential Design Example: Disk Drive Read System.

DESIRED OUTCOMES

Upon completion of Chapter 12, students should:

- ❑ Appreciate the role of robustness in control system design.
- ❑ Be familiar with uncertainty models, including additive uncertainty, multiplicative uncertainty, and parameter uncertainty.
- ❑ Understand the various methods of tackling the robust control design problem using root locus, frequency response, ITAE methods for PID control, internal model, and pseudo-quantitative feedback methods.

Full-state feedback control law A control law of the form $\mathbf{u} = -\mathbf{K}\mathbf{x}$ where $\mathbf{x}$ is the state of the system assumed known at all times.

Internal model design A method of tracking reference inputs with guaranteed steady-state tracking errors.

Kalman state-space decomposition A partition of the state space that illuminates the states that are controllable and unobservable, uncontrollable and unobservable, controllable and observable, and uncontrollable and observable.

Linear quadratic regulator An optimal controller designed to minimize the quadratic performance index $J = \int_0^\infty (\mathbf{x}^T\mathbf{Q}\mathbf{x} + \mathbf{u}^T\mathbf{R}\mathbf{u})\, dt$, where $\mathbf{Q}$ and $\mathbf{R}$ are design parameters.

Observability matrix A linear system is (completely) observable if and only if the observability matrix $\mathbf{P}_o = [\mathbf{C}^T \quad (\mathbf{CA})^T \quad (\mathbf{CA}^2)^T \ldots (\mathbf{CA}^{n-1})^T]^T$ has full rank, where $\mathbf{A}$ is an $n \times n$ matrix. For single-input, single-output linear systems, the system is observable if and only if the determinant of the $n \times n$ observability matrix $\mathbf{P}_o$ is nonzero.

Observable system A system is observable on the interval $[t_0, t_f]$ if any initial state $\mathbf{x}(t_0)$ is uniquely determined by observing the output $y(t)$ on the interval $[t_0, t_f]$.

Observer A dynamic system used to estimate the state of another dynamic system given knowledge of the system inputs and measurements of the system outputs.

Optimal control system A system whose parameters are adjusted so that the performance index reaches an extremum value.

Pole placement A design methodology wherein the objective is to place the eigenvalues of the closed-loop system in desired regions of the complex plane.

Separation principle The principle that states that the full-state feedback law and the observer can be designed independently and when connected will function as an integrated control system in the desired manner (i.e., stable).

Stabilizable A system in which the states that are not controllable are naturally stable.

Stabilizing controller A controller that stabilizes the closed-loop system.

State variable feedback Occurs when the control signal u for the process is a direct function of all the state variables.

12.1 INTRODUCTION

A control system designed using the methods and concepts of the preceding chapters assumes knowledge of the model of the process and controller and constant parameters. The process model will always be an inaccurate representation of the actual physical system because of

- parameter changes
- unmodeled dynamics
- unmodeled time delays
- changes in equilibrium point (operating point)
- sensor noise
- unpredicted disturbance inputs.

The goal of robust systems design is to retain assurance of system performance in spite of model inaccuracies and changes. A system is robust when the system has acceptable changes in performance due to model changes or inaccuracies.

A robust control system exhibits the desired performance despite the presence of significant process uncertainty.

A system structure that incorporates potential system uncertainties is shown in Figure 12.1. This model includes the sensor noise $N(s)$, the unpredicted disturbance

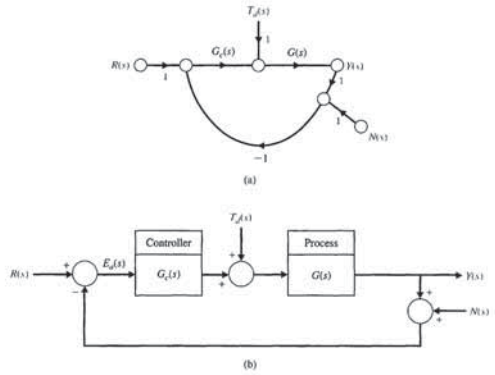

FIGURE 12.1
Closed-loop control system. (a) Signal flow graph; (b) Block diagram.

input $T_d(s)$, and a process $G(s)$ with potentially unmodeled dynamics or parameter changes. The unmodeled dynamics and parameter changes may be significant or very large, and for these systems the challenge is to create a design that retains the desired performance.

12.2 ROBUST CONTROL SYSTEMS AND SYSTEM SENSITIVITY

Designing highly accurate systems in the presence of significant plant uncertainty is a classical feedback design problem. The theoretical bases for the solution of this problem date back to the works of H. S. Black and H. W. Bode in the early 1930s, when this problem was referred to as the sensitivities design problem. A significant amount of literature has been published since then regarding the design of systems subject to large process uncertainty. The designer seeks to obtain a system that performs adequately over a large range of uncertain parameters. A system is said to be robust when it is durable, hardy, and resilient.

A control system is robust when (1) it has low sensitivities, (2) it is stable over the range of parameter variations, and (3) the performance continues to meet the specifications in the presence of a set of changes in the system parameters [3, 4]. Robustness is the low sensitivity to effects that are not considered in the analysis and design phase—for example, disturbances, measurement noise, and unmodeled dynamics. The system should be able to withstand these neglected effects when performing the tasks for which it was designed.

For small-parameter perturbations, we may use, as a measure of robustness, the differential sensitivities discussed in Sections 4.3 (system sensitivity) and Section 7.5 (root sensitivity) [6]. The **system sensitivity** is defined as

$$S_\alpha^T = \frac{\partial T/T}{\partial \alpha/\alpha}, \tag{12.1}$$

where α is the parameter and T the transfer function of the system. The **root sensitivity** is defined as

$$S_\alpha^{r_i} = \frac{\partial r_i}{\partial \alpha/\alpha}, \tag{12.2}$$

When the zeros of $T(s)$ are independent of the parameter α, we showed that

$$S_\alpha^T = -\sum_{i=1}^{n} S_\alpha^{r_i} \cdot \frac{1}{s + r_i}, \tag{12.3}$$

for an nth-order system. For example, if we have a closed-loop system, as shown in Figure 12.2, where the variable parameter is α, then $T(s) = 1/[s + (\alpha + 1)]$, and

$$S_\alpha^T = \frac{-\alpha}{s + \alpha + 1}. \tag{12.4}$$

This follows because $r_1 = +(\alpha + 1)$, and

$$-S_\alpha^{r_1} = -\alpha. \tag{12.5}$$

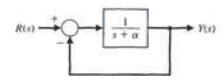

FIGURE 12.2
A first-order system.

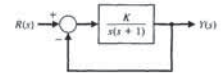

FIGURE 12.3
A second-order system.

Therefore,

$$S_\alpha^T = -S_\alpha^{r_1} \frac{1}{s + \alpha + 1} = \frac{-\alpha}{s + \alpha + 1}. \tag{12.6}$$

Let us examine the sensitivity of the second-order system shown in Figure 12.3. The transfer function of the closed-loop system is

$$T(s) = \frac{K}{s^2 + s + K}. \tag{12.7}$$

The system sensitivity for K is

$$S(s) = S_K^T = \frac{s(s + 1)}{s^2 + s + K}. \tag{12.8}$$

A Bode plot of the asymptotes of $20 \log|T(j\omega)|$ and $20 \log|S(j\omega)|$ is shown in Figure 12.4 for $K = 1/4$ (critical damping). Note that the sensitivity is small for lower frequencies, while the transfer function primarily passes low frequencies.

Of course, the sensitivity $S(s)$ only represents robustness for small changes in gain. If K changes from 1/4 within the range $K = 1/16$ to $K = 1$, the resulting range of step response is shown in Figure 12.5. This system, with an expected wide range of

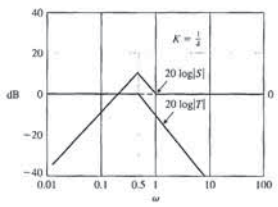

FIGURE 12.4 Sensitivity and $20 \log |T(j\omega)|$ for the second-order system in Figure 12.3. The asymptotic approximations are shown for $K = \frac{1}{4}$.

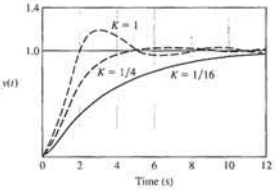

FIGURE 12.5 The step response for selected gain K.

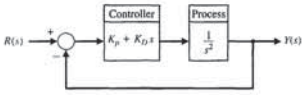

FIGURE 12.6
A system with a PD controller.

K, may not be considered adequately robust. A robust system would be expected to yield essentially the same (within an agreed-upon variation) response to a selected input.

EXAMPLE 12.1 **Sensitivity of a controlled system**

Consider the system shown in Figure 12.6, where $G(s) = 1/s^2$ and a PD controller $G_c(s) = K_p + K_D s$. Then the sensitivity with respect to changes in $G(s)$ is

$$S_G^T = \frac{1}{1 + G_c(s)G(s)} = \frac{s^2}{s^2 + K_D s + K_p}, \tag{12.9}$$

and

$$T(s) = \frac{K_D s + K_p}{s^2 + K_D s + K_p}. \tag{12.10}$$

Consider the normal condition $\zeta = 1$ and $\omega_n = \sqrt{K_p}$. Then, $K_D = 2\omega_n$ to achieve $\zeta = 1$. Therefore, we may plot $20 \log|S|$ and $20 \log|T|$ on a Bode diagram, as shown in Figure 12.7. Note that the frequency ω_n is an indicator on the boundary between the frequency region in which the sensitivity is the important design criterion and the region in which the stability margin is important. Thus, if we specify ω_n properly to take into consideration the extent of modeling error and the frequency of external disturbance, we can expect the system to have an acceptable amount of robustness. ■

EXAMPLE 12.2 **System with a right-hand-plane zero**

Consider the system shown in Figure 12.8, where the plant has a zero in the right-hand plane. The closed-loop transfer function is

$$T(s) = \frac{K(s - 1)}{s^2 + (2 + K)s + (1 - K)}. \tag{12.11}$$

The system is stable for a gain $-2 < K < 1$. The steady-state error due to a negative unit step input $R(s) = -1/s$ is

$$e_{ss} = \frac{1 - 2K}{1 - K}, \tag{12.12}$$

12.3 ANALYSIS OF ROBUSTNESS

Consider the closed-loop system shown in Figure 12.1. System goals include maintaining a small tracking error $[E(s) = R(s) - Y(s)]$ for an input $R(s)$ and keeping the output $Y(s)$ small for a disturbance $T_d(s)$.

Following the discussion in Section 4.1, the **sensitivity function** is

$$\boxed{S(s) = [1 + G_c(s)G(s)]^{-1},}$$

and the **complementary sensitivity function** is

$$\boxed{C(s) = \frac{G_c(s)G(s)}{1 + G_c(s)G(s)}.}$$

We also have the relationship

$$\boxed{S(s) + C(s) = 1.} \tag{12.13}$$

For physically realizable systems, the loop gain $L(s) = G_c(s)G(s)$ must be small for high frequencies. This means that $S(j\omega)$ approaches 1 at high frequencies.

An **additive perturbation** characterizes the set of possible processes as follows (here we assume that $G_c(s) = 1$):

$$G_a(s) = G(s) + A(s),$$

where $G(s)$ is the nominal process, and $A(s)$ is the perturbation that is bounded in magnitude. We assume that $G_a(s)$ and $G(s)$ have the same number of poles in the right-hand s-plane (if any) [32]. Then the system stability will not change if

$$|A(j\omega)| < |1 + G(j\omega)| \qquad \text{for all } \omega. \tag{12.14}$$

This assures stability but not dynamic performance.

A **multiplicative perturbation** is modeled as

$$G_m(s) = G(s)[1 + M(s)].$$

The perturbation is bounded in magnitude, and it is again assumed that $G_m(s)$ and $G(s)$ have the same number of poles in the right-hand s-plane. Then the system stability will not change if

$$\boxed{|M(j\omega)| < \left|1 + \frac{1}{G(j\omega)}\right| \qquad \text{for all } \omega.} \tag{12.15}$$

Equation (12.15) is called the **robust stability criterion**. This is a test for robustness with respect to a multiplicative perturbation. This form of perturbation is often used

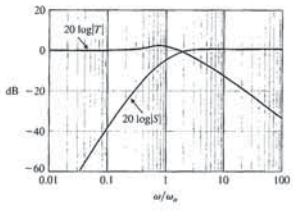

FIGURE 12.7 Sensitivity and $T(s)$ for the second-order system in Figure 12.6.

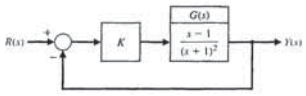

FIGURE 12.8 A second-order system.

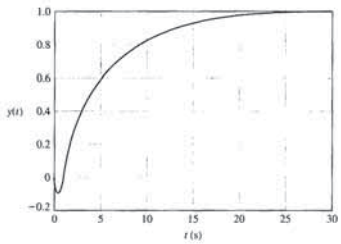

FIGURE 12.9 Step response of the system in Figure 12.8 with $K = \frac{1}{2}$.

and $e_{ss} = 0$ when $K = 1/2$. The response is shown in Figure 12.9. Note the initial undershoot at $t = 1$ s. This system is sensitive to changes in K, as recorded in Table 12.1. The performance of this system might be considered barely acceptable for a change of gain of only ±10%. Thus, this system would not be considered robust. The steady-state error of this system changes greatly as K changes. ■

Table 12.1 Results for Example 12.2

K	0.25	0.45	0.50	0.55	0.75
$\lvert e_{ss}\rvert$	0.67	0.18	0	0.22	1.0
Undershoot	5%	9%	10%	11%	15%
Settling time (seconds)	15	24	27	30	45

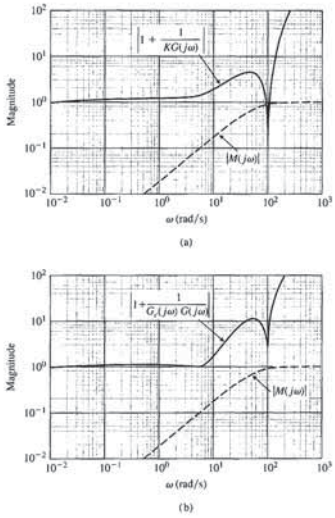

FIGURE 12.10 The robust stability criterion for Example 12.3.

12.4 SYSTEMS WITH UNCERTAIN PARAMETERS

Many systems have several parameters that are constants but uncertain within a range. For example, consider a system with a characteristic equation

$$s^n + a_{n-1}s^{n-1} + a_{n-2}s^{n-2} + \cdots + a_0 = 0 \tag{12.16}$$

with known coefficients within bounds

$$\alpha_i \le a_i \le \beta_i \text{ and } i = 0, \ldots, n,$$

where $a_n = 1$.

To ascertain the stability of the system, we might have to investigate all possible combinations of parameters. Fortunately, it is possible to investigate a limited number of worst-case polynomials [20]. The analysis of only four polynomials is sufficient,

because it satisfies the intuitive properties of (1) being small at low frequencies, where the nominal process model is usually well known, and (2) being large at high frequencies, where the nominal model is always inexact.

EXAMPLE 12.3 **System with multiplicative perturbation**

Consider the system of Figure 12.1 with $G_c = K$, and

$$G(s) = \frac{170{,}000\,(s + 0.1)}{s(s + 3)(s^2 + 10s + 10{,}000)}.$$

The system is unstable with $K = 1$, but a reduction in gain to $K = 0.5$ will stabilize it. Now, consider the effect of an unmodeled pole at 50 rad/s. In this case, the multiplicative perturbation is determined from

$$1 + M(s) = \frac{50}{s + 50},$$

or $M(s) = -s/(s + 50)$. The magnitude bound is then

$$|M(j\omega)| = \left|\frac{-j\omega}{j\omega + 50}\right|.$$

$|M(j\omega)|$ and $|1 + 1/(KG(j\omega))|$ are plotted in Figure 12.10(a), where it is seen that the criterion of Equation (12.15) is not satisfied. Thus, the system may not be stable.

If we use a lag compensator

$$G_c(s) = \frac{0.15(s + 25)}{s + 2.5},$$

the loop transfer function is $1 + G_c(s)G(s)$, and we reshape the function $G_c(j\omega)G(j\omega)$ in the frequency range $2 < \omega < 25$. Then we have the altered magnitude

$$\left|1 + \frac{1}{G_c(j\omega)G(j\omega)}\right|,$$

as plotted in Figure 12.10(b). Here the robustness inequality is satisfied, and the system remains stable. ■

The control objective is to design a compensator $G_c(s)$ so that the transient, steady-state, and frequency-domain specifications are achieved and the cost of feedback measured by the bandwidth of the compensator $G_c(j\omega)$ is sufficiently small. This bandwidth constraint is needed mainly because of noise that is inevitable in measuring the system output. A large noise amplification can saturate either the latter stages of $G_c(s)$ or the early process stages. In subsequent sections, we can add a pre-filter in a two-degree-of-freedom configuration to help achieve the design goals.

then we must examine the four polynomials:

$$q_1(s) = s^3 + 2s^2 + 3s + 5,$$
$$q_2(s) = s^3 + 4s^2 + 1s + 4,$$
$$q_3(s) = s^3 + 4s^2 + 3s + 4,$$
$$q_4(s) = s^3 + 2s^2 + 1s + 5.$$

Using the Routh–Hurwitz criterion, $q_1(s)$ and $q_3(s)$ are stable and $q_2(s)$ is marginally stable. For $q_4(s)$, we have

$$\begin{array}{c|cc} s^3 & 1 & 1 \\ s^2 & 2 & 5 \\ s^1 & -3/2 & \\ s^0 & 5 & \end{array}.$$

Therefore, the system is unstable for the worst case, where α_2 = minimum, α_1 = minimum, and β_0 = maximum. This occurs when the process has changed to

$$G(s) = \frac{5}{s(s+1)(s+1)}.$$

Note that the third pole has moved toward the $j\omega$-axis to its limit at $s = -1$ and that the gain has increased to its limit at $K = 5$. Often, we are able to examine the transfer function $G(s)$ and predict the worst-case conditions. ■

12.5 THE DESIGN OF ROBUST CONTROL SYSTEMS

The design of robust control systems is based on two tasks: determining the structure of the controller and adjusting the controller's parameters to give an "optimal" system performance. This design process is normally done with "assumed complete knowledge" of the process. Furthermore, the process is normally described by a linear time-invariant continuous model. The structure of the controller is chosen such that the system's response can meet certain performance criteria.

One possible objective in the design of a control system is that the controlled system's output should exactly and instantaneously reproduce its input. That is, the system transfer function should be unity:

$$T(s) = \frac{Y(s)}{R(s)} = 1. \tag{12.18}$$

In other words, the system should be presentable on a Bode gain versus frequency diagram with a 0-dB gain of infinite bandwidth and zero phase shift. In practice, this is not possible, since every system will contain inductive- and capacitive-type components that store energy in some form. These elements and their interconnections with energy-dissipative components produce the system's dynamic response characteristics. Such systems reproduce some inputs almost exactly, while other inputs are not reproduced at all, signifying that the system bandwidth is less than infinite.

and they are readily defined for a third-order system with a characteristic equation

$$s^3 + a_2s^2 + a_1s + a_0 = 0. \tag{12.17}$$

Then the four polynomials are

$$q_1(s) = s^3 + \alpha_2s^2 + \beta_1s + \beta_0,$$
$$q_2(s) = s^3 + \beta_2s^2 + \alpha_1s + \alpha_0,$$
$$q_3(s) = s^3 + \beta_2s^2 + \beta_1s + \alpha_0,$$
$$q_4(s) = s^3 + \alpha_2s^2 + \alpha_1s + \beta_0.$$

One of the four polynomials represents the worst case and may indicate either unstable performance or at least the worst performance for the system in that case.

EXAMPLE 12.4 **Third-order system with uncertain coefficients**

Consider a third-order system with uncertain coefficients such that

$$8 \le a_0 \le 60 \Rightarrow \alpha_0 = 8, \beta_0 = 60;$$
$$12 \le a_1 \le 100 \Rightarrow \alpha_1 = 12, \beta_1 = 100;$$
$$7 \le a_2 \le 25 \Rightarrow \alpha_2 = 7, \beta_2 = 25.$$

The four polynomials are

$$q_1(s) = s^3 + 7s^2 + 100s + 60,$$
$$q_2(s) = s^3 + 25s^2 + 12s + 8,$$
$$q_3(s) = s^3 + 25s^2 + 100s + 8,$$
$$q_4(s) = s^3 + 7s^2 + 12s + 60.$$

We then proceed to check these four polynomials by means of the Routh–Hurwitz criterion, and hence we determine that the system is stable for all the range of uncertain parameters. ■

EXAMPLE 12.5 **Stability of uncertain system**

Consider a unity feedback system with a process transfer function (under nominal conditions)

$$G(s) = \frac{4.5}{s(s+1)(s+2)}.$$

The nominal characteristic equation is then

$$q(s) = s^3 + 3s^2 + 2s + 4.5 = 0.$$

Using the Routh–Hurwitz criterion, we find that this system is nominally stable. However, if the system has uncertain coefficients such that

$$4 \le a_0 \le 5 \Rightarrow \alpha_0 = 4, \beta_0 = 5;$$
$$1 \le a_1 \le 3 \Rightarrow \alpha_1 = 1, \beta_1 = 3; \text{ and}$$
$$2 \le a_2 \le 4 \Rightarrow \alpha_2 = 2, \beta_2 = 4,$$

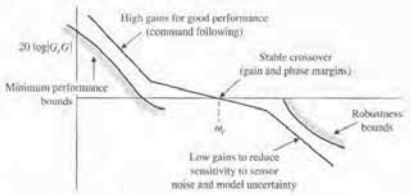

FIGURE 12.12
Bode diagram for $20 \log |G_c(j\omega)G(j\omega)|$.

sensitivity. Similarly, the gain margin problem is to find a proper compensator to achieve some prescribed gain margin. But gain margin maximization involves finding a proper compensator to achieve the maximal attainable gain margin. For the frequency-domain specifications, we require the following conditions for the Bode diagram of $G_c(j\omega)G(j\omega)$, shown in Figure 12.12:

1. For relative stability, $G_c(j\omega)G(j\omega)$ must have, for an adequate range of ω, not more than a −20-dB/decade slope at or near the crossover frequency ω_c.
2. Steady-state accuracy achieved by the low frequency gain.
3. Accuracy over a bandwidth ω_B, by maintaining $|G_c(j\omega)G(j\omega)|$ above a prescribed level.
4. Disturbance rejection by a high gain for $G_c(j\omega)$ over the system bandwidth.

Using the root sensitivity concept, we can state that S_K^r must be minimized while attaining $T(s)$ with dominant roots that will provide the appropriate response and minimize the effect of $T_d(s)$. Again, we see that the goal is to have the gain of the loop primarily attained by $G_c(s)$. As an example, let $G_c(s) = K$, $G_1(s) = 1$, and $G_2(s) = 1/(s(s+1))$ for the system in Figure 12.11. This system has two roots, and we select a gain K so that $Y(s)/T_d(s)$ is minimized, S_K^r is minimized, and $T(s)$ has desirable dominant roots. The sensitivity is

$$S_K^r = \frac{dr}{dK} \cdot \frac{K}{r} = \left.\frac{ds}{dK}\right|_{s=r} \cdot \frac{K}{r}, \tag{12.23}$$

and the characteristic equation is

$$s(s+1) + K = 0. \tag{12.24}$$

Therefore, $dK/ds = -(2s+1)$, since $K = -s(s+1)$. We then obtain

$$S_K^r = \frac{-1}{2s+1} \left.\frac{-s(s+1)}{s}\right|_{s=r}. \tag{12.25}$$

When $\zeta < 1$, the roots are complex and $r = -0.5 + j\omega$. Then,

$$|S_K^r| = \left(\frac{0.25 + \omega^2}{4\omega^2}\right)^{1/2}. \tag{12.26}$$

Once we recognize that the system dynamics cannot be ignored, we need a new design objective. One possible design objective is to maintain the magnitude response curve as flat and as close to unity for as large a bandwidth as possible for a given plant and controller combination [20].

Another important goal of a control system design is that the effect on the output of the system due to disturbances is minimized. Thus, we wish to minimize $Y(s)/T_d(s)$ over a range of frequency.

Consider the control system shown in Figure 12.11, where $G(s) = G_1(s)G_2(s)$ is the plant and $T_d(s)$ is the disturbance. We then have

$$T(s) = \frac{Y(s)}{R(s)} = \frac{G_c(s)G_1(s)G_2(s)}{1 + G_c(s)G_1(s)G_2(s)}, \tag{12.19}$$

and

$$\frac{Y(s)}{T_d(s)} = \frac{G_2(s)}{1 + G_c(s)G_1(s)G_2(s)}. \tag{12.20}$$

Note that both the reference and disturbance transfer functions have the same denominator; in other words, they have the same characteristic equation—namely,

$$1 + G_c(s)G_1(s)G_2(s) = 1 + L(s) = 0. \tag{12.21}$$

Recall that the sensitivity of $T(s)$ with respect to $G(s)$ is

$$S_G^T = \frac{1}{1 + G_c(s)G_1(s)G_2(s)}, \tag{12.22}$$

and the characteristic equation is the influencing factor on the sensitivity. Equation (12.22) shows that for low sensitivity S, we require a high value of loop gain $L(j\omega)$, but it is known that a high gain could cause instability or poor responsiveness of $T(s)$. Thus, we seek the following:

1. $T(s)$ with wide bandwidth and faithful reproduction of $R(s)$.
2. Large loop gain $L(s)$ in order to minimize sensitivity S.
3. Large loop gain $L(s)$ attained primarily by $G_c(s)G_1(s)$, since $Y(s)/T_d(s) \simeq 1/G_c(s)G_1(s)$.

Setting the design of robust systems in frequency-domain terms, we must find a proper compensator $G_c(s)$ such that the closed-loop sensitivity is less than some tolerance value. But sensitivity minimization involves finding a proper compensator such that the closed-loop sensitivity equals or is arbitrarily close to the minimal attainable

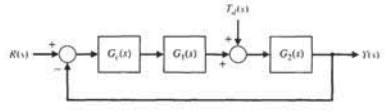

FIGURE 12.11
A system with a disturbance.

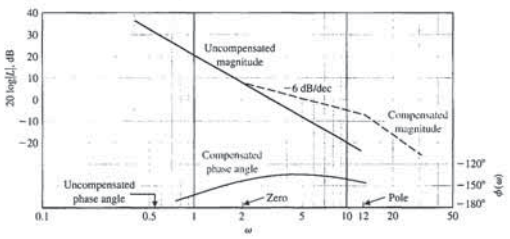

FIGURE 12.14
Bode diagram for Example 12.6.

To estimate $|S_G^T|$, we recall that the Nichols chart enables us to obtain

$$|T(j\omega)| = \left| \frac{G_c(j\omega)G(j\omega)}{1 + G_c(j\omega)G(j\omega)} \right|. \tag{12.29}$$

Thus, we can plot a few points of $G_c(j\omega)G(j\omega)$ on the Nichols chart and then read $T(\omega)$ from the chart. Then

$$|S_G^T(j\omega_1)| = \frac{|T(j\omega_1)|}{|G_c(j\omega_1)G(j\omega_1)|}, \tag{12.30}$$

where ω_1 is chosen arbitrarily as $\omega_c/2.5$. In general, we choose a frequency below ω_c to determine the value of $|S(\omega_1)|$. Of course, we desire a low value of sensitivity. The Nichols chart for the compensated system is shown in Figure 12.15. For $\omega_1 = \omega_c/2.5 = 2$, we have $20 \log|T(\omega_1)| = 2.5$ dB and $20 \log |G_c(j\omega_1)G(j\omega_1)| = 9$ dB. Therefore,

$$|S(j\omega_1)| = \frac{|T(j\omega_1)|}{|G_c(j\omega_1)G(j\omega_1)|} = \frac{1.33}{2.8} = 0.47. \blacksquare$$

EXAMPLE 12.7 **Sensitivity with a lead compensator**

Let us again consider the system in Example 12.6, using the root locus design obtained in Example 10.3. The compensator was chosen as

$$G_c(s) = \frac{8.1(s + 1)}{s + 3.6}, \tag{12.31}$$

for the system of Figure 12.16. The dominant roots are thus $s = -1 \pm j2$. Because the gain is 8.1, the effect of the disturbance is reduced, and the time response meets the specifications. The sensitivity at a root r may be obtained by assuming that the

system, with dominant roots, may be approximated by the second-order system

$$T(s) = \frac{K}{s^2 + 2\zeta\omega_n s + K} = \frac{K}{s^2 + 2s + K},$$

since $\zeta\omega_n = 1$. The characteristic equation is thus

$$s^2 + 2s + K = 0.$$

Then $dK/ds = -(2s + 2)$, since $K = -(s^2 + 2s)$. Therefore,

$$S_K^T = \frac{-1}{2s + 2} \cdot \frac{-(s^2 + 2s)}{1}\bigg|_{s=r} = \frac{s(s + 2)}{(2s + 2)}\bigg|_{s=r}, \tag{12.32}$$

where $r = -1 + j2$. Then, substituting $s = r$, we obtain

$$|S_K^T| = 1.25.$$

If we raise the gain to in Equation (12.31) from 8.1 to 10, we expect $r \simeq -1.1 \pm j2.4$. Then the sensitivity is

$$|S_K^T| = 1.4. \blacksquare$$

12.6 THE DESIGN OF ROBUST PID-CONTROLLED SYSTEMS

The **PID controller** has the transfer function

$$G_c(s) = K_P + \frac{K_I}{s} + K_D s.$$

The popularity of PID controllers can be attributed partly to their robust performance in a wide range of operating conditions and partly to their functional simplicity, which allows engineers to operate them in a simple straightforward manner. To implement such a controller, three parameters must be determined for the given process: proportional gain, integral gain, and derivative gain [31].

Consider the PID controller

$$G_c(s) = K_P + \frac{K_I}{s} + K_D s = \frac{K_D s^2 + K_P s + K_I}{s}$$
$$= \frac{K_D(s^2 + as + b)}{s} = \frac{K_D(s + z_1)(s + z_2)}{s}, \tag{12.33}$$

where $a = K_P/K_D$ and $b = K_I/K_D$. Therefore, a PID controller introduces a transfer function with one pole at the origin and two zeros that can be located anywhere in the left-hand s-plane.

Recall that a root locus begins at the poles and ends at the zeros. If we have a system as shown in Figure 12.16 with

$$G(s) = \frac{1}{(s + 2)(s + 5)},$$

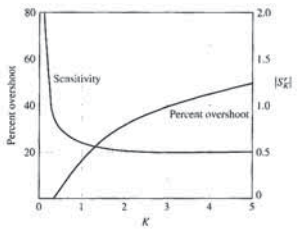

FIGURE 12.13
Sensitivity and percent overshoot for a second-order system.

The magnitude of the sensitivity is plotted in Figure 12.13 for $K = 0.2$ to $K = 5$. The percent overshoot to a step is also shown. It is best to reduce the sensitivity while limiting K to 1.5 or less. We then attain the majority of the attainable reduction in sensitivity while maintaining good performance for the step response. In general, we can use the design procedure as follows:

1. Sketch the root locus of the compensated system with $G_c(s)$ chosen to attain the desired location for the dominant roots.
2. Maximize the gain of $G_c(s)$ to reduce the effect of the disturbance.
3. Determine S_K^T and attain the minimum value of the sensitivity consistent with the transient response required, as described in Step 1.

EXAMPLE 12.6 **Sensitivity and compensation**

Let us consider again the system in Example 10.1 when $G(s) = 1/s^2$, $H(s) = 1$, and $G_c(s)$ is to be selected by frequency response methods. Therefore, the compensator is to be selected to achieve an appropriate gain and phase margin while minimizing sensitivity and the effect of the disturbance. Thus, we choose

$$G_c(s) = \frac{K(s/z + 1)}{s/p + 1}. \tag{12.27}$$

As in Example 10.1, we choose $K = 10$ to reduce the effect of the disturbance. To attain a phase margin of 45°, we select $z = 2.0$ and $p = 12.0$. We then attain the compensated diagram shown in Figure 10.9 and repeated in Figure 12.14. Recall that the closed-loop bandwidth is $\omega_B = 1.6\omega_c$. Thus, we will increase the bandwidth by using the compensator and improve the fidelity of reproduction of the input signals.

The sensitivity at ω_c may be ascertained as

$$|S_G^T(j\omega_c)| = \left| \frac{1}{1 + G_c(j\omega)G(j\omega)} \right|_{\omega_c}. \tag{12.28}$$

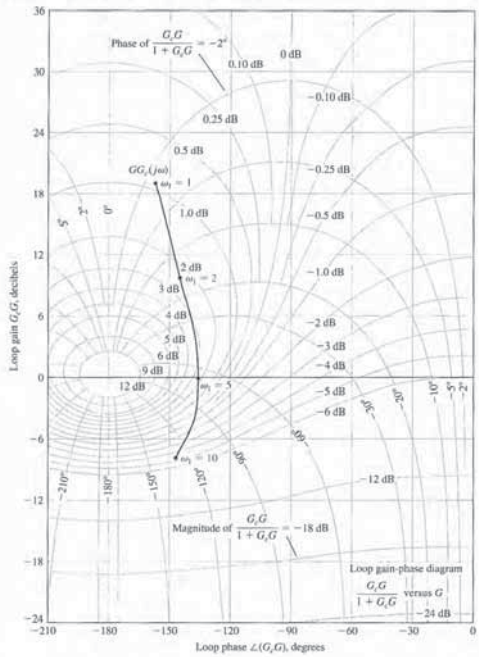

FIGURE 12.15
Nichols chart for Example 12.7.

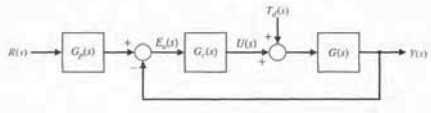

FIGURE 12.16
Feedback control system with a desired input $R(s)$ and an undesired input $T_d(s)$.

have been proposed to solve this problem. In this section, we consider several design methods using root locus and performance indices.

The first design method uses the ITAE performance index of Section 5.7 and the optimum coefficients of Table 5.6 for a step input or Table 5.7 for a ramp input. Hence, we select the three PID coefficients to minimize the ITAE performance index, which produces an excellent transient response to a step (Figure 5.30c) or a ramp. The design procedure consists of three steps:

1. Select the ω_n of the closed-loop system by specifying the settling time.
2. Determine the three coefficients using the appropriate optimum equation (Table 5.6) and the ω_n of step 1 to obtain $G_c(s)$.
3. Determine a **prefilter** $G_p(s)$ so that the closed-loop system transfer function, $T(s)$, does not have any zeros, as required by Equation (5.47).

EXAMPLE 12.8 **Robust control of temperature**

Consider a temperature controller with a control system as shown in Figure 12.16 and a process

$$G(s) = \frac{1}{(s+1)^2}. \tag{12.36}$$

If $G_c(s) = 1$, the steady-state error is 50%, and the settling time (with a 2% criterion) is 3.2 seconds for a step input. We want to obtain an optimum ITAE performance for a step input and a settling time of less than 0.5 second. Using a PID controller, we have

$$G_c(s) = \frac{K_D s^2 + K_P s + K_I}{s}. \tag{12.37}$$

Therefore, the closed-loop transfer function without prefiltering $[G_p(s) = 1]$ is

$$T_1(s) = \frac{Y(s)}{R(s)} = \frac{G_c(s)G(s)}{1 + G_c(s)G(s)} = \frac{K_D s^2 + K_P s + K_I}{s^3 + (2 + K_D)s^2 + (1 + K_P)s + K_I}. \tag{12.38}$$

The optimum coefficients of the characteristic equation for ITAE are obtained from Table 5.6 as

$$s^3 + 1.75\omega_n s^2 + 2.15\omega_n^2 s + \omega_n^3. \tag{12.39}$$

We need to select ω_n in order to meet the settling time requirement. Since $T_s = 4/(\zeta\omega_n)$ and ζ is unknown but near 0.8, we set $\omega_n = 10$. Then, equating the denominator of Equation (12.38) to Equation (12.39), we obtain the three coefficients as $K_P = 214$, $K_D = 15.5$, and $K_I = 1000$.

Then Equation (12.38) becomes

$$T_1(s) = \frac{15.5s^2 + 214s + 1000}{s^3 + 17.5s^2 + 215s + 1000} = \frac{15.5(s + 6.9 + j4.1)(s + 6.9 - j4.1)}{s^3 + 17.5s^2 + 215s + 1000}. \tag{12.40}$$

and we use a PID controller with complex zeros, we can plot the root locus as shown in Figure 12.17. As the gain K_D of the controller is increased, the complex roots approach the zeros. The closed-loop transfer function is

$$T(s) = \frac{G(s)G_c(s)G_p(s)}{1 + G(s)G_c(s)} = \frac{K_D(s + z_1)(s + \hat{z}_1)}{(s + r_2)(s + r_1)(s + \hat{r}_1)}G_p(s) \simeq \frac{K_D G_p(s)}{s + r_2}, \tag{12.34}$$

because the zeros and the complex roots are approximately equal ($r_1 \approx z_1$). Setting $G_p(s) = 1$, we have

$$T(s) = \frac{K_D}{s + r_2} \approx \frac{K_D}{s + K_D} \tag{12.35}$$

when $K_D \gg 1$. The only limiting factor is the allowable magnitude of $U(s)$ (Figure 12.16) when K_D is large. If K_D is 100, the system has a fast response and zero steady-state error. Furthermore, the effect of the disturbance is reduced significantly.

In general, we note that PID controllers are particularly useful for reducing steady-state error and improving the transient response when $G(s)$ has one or two poles (or may be approximated by a second-order process).

The selection of the three coefficients of PID controllers is basically a search problem in a three-dimensional space. Points in the search space correspond to different selections of a PID controller parameters. By choosing different points of the parameter space, we can produce, for example, different step responses for a step input. A PID controller can be determined by moving in this search space on a trial-and-error basis.

The main problem in the selection of the three coefficients is that these coefficients do not readily translate into the desired performance and robustness characteristics that the control system designer has in mind. Several rules and methods

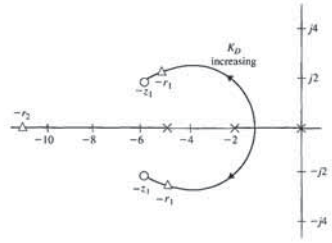

FIGURE 12.17 Root locus with $-z_1 = -6 + j2$.

and

$$G_c(s) = \frac{12(s^2 + 11.38s + 42.67)}{s}. \tag{12.45}$$

We select a prefilter

$$G_p(s) = \frac{42.67}{s^2 + 11.38s + 42.67} \tag{12.46}$$

to obtain the optimum ITAE transfer function

$$T(s) = \frac{512}{s^3 + 14s^2 + 137.6s + 512}. \tag{12.47}$$

We then obtain the step response for the four conditions: $\tau = 1$, $K = 1$; $\tau = 0.5$, $K = 1$; $\tau = 1$, $K = 2$; and $\tau = 0.5$, $K = 2$. The results are summarized in Table 12.3. This is a very robust system. ■

The value of ω_n that can be chosen will be limited by considering the maximum allowable $u(t)$, where $u(t)$ is the output of the controller, as shown in Figure 12.16. If the maximum value of $e_a(t)$ is 1, then $u(t)$ would normally be limited to 100 or less. As an example, consider the system in Figure 12.16 with a PID controller, $G(s) = 1/(s(s + 1))$, and the necessary prefilter $G_p(s)$ to achieve ITAE performance. If we select $\omega_n = 10$, 20, and 40, the maximum value of $u(t)$ is as recorded in Table 12.4. If we wish to limit $u(t)$ to a maximum equal to 100, we need to limit ω_n to 16. Thus, we are limited in the settling time we can achieve.

Let us consider the design of a PID compensator using frequency response techniques for a system with a time delay so that

$$G(s) = \frac{Ke^{-Ts}}{\tau s + 1}. \tag{12.48}$$

This type of system represents many industrial processes that incorporate a time delay. We use a PID compensator to introduce two equal zeros so that

$$G_c(s) = \frac{K_I(\tau_1 s + 1)^2}{s}. \tag{12.49}$$

Table 12.3 Results for Example 12.9 with $\omega_n = 8$

Plant Conditions	$\tau = 1$, $K = 1$	$\tau = 0.5$, $K = 1$	$\tau = 1$, $K = 2$	$\tau = 0.5$, $K = 2$
Percent overshoot	2%	0%	0%	1%
Settling time (seconds)	1.25	0.8	0.8	0.9

Table 12.4 Maximum Value of Plant Input

ω_n	10	20	40
$u(t)$ maximum for $R(s) = 1/s$	35	135	550
Settling time (seconds)	0.9	0.5	0.3

The response of this system to a step input has an overshoot of 32%, as recorded in Table 12.2.

We select a prefilter $G_p(s)$ so that we achieve the desired ITAE response with

$$T(s) = \frac{G_c(s)G(s)G_p(s)}{1 + G_c(s)G(s)} = \frac{1000}{s^3 + 17.5s^2 + 215s + 1000}. \tag{12.41}$$

Therefore, we require that

$$G_p(s) = \frac{64.5}{s^2 + 13.8s + 64.5} \tag{12.42}$$

in order to eliminate the zeros in Equation (12.40) and bring the overall numerator to 1000. The response of the system $T(s)$ to a step input is indicated in Table 12.2. The system has a small overshoot, a settling time of less than $\frac{1}{2}$ second, and zero steady-state error. Furthermore, for a disturbance $T_d(s) = 1/s$, the maximum value of $y(t)$ due to the disturbance is 0.4% of the magnitude of the disturbance. This is a very favorable design. ■

EXAMPLE 12.9 **Robust system design**

Let us consider again the system in Example 12.8 when the plant varies significantly, so that

$$G(s) = \frac{K}{(\tau s + 1)^2}, \tag{12.43}$$

where $0.5 \le \tau \le 1$ and $1 \le K \le 2$. We want to achieve robust behavior using an ITAE optimum system with a prefilter while attaining an overshoot of less than 4% and a settling time (with a 2% criterion) of less than 2 seconds, while $G(s)$ can attain any value in the range indicated. We select $\omega_n = 8$ in order to attain the settling time and determine the ITAE coefficients for $K = 1$ and $\tau = 1$. Completing the calculation, we obtain the system without a prefilter $[G_p(s) = 1]$ as

$$T_1(s) = \frac{12(s^2 + 11.38s + 42.67)}{s^3 + 14s^2 + 137.6s + 512}, \tag{12.44}$$

Table 12.2 Results for Example 12.8

Controller	$G_c(s) = 1$	PID and $G_p(s) = 1$	PID with $G_p(s)$ Prefilter
Percent overshoot	0	31.7%	1.9%
Settling time (seconds)	3.2	0.20	0.45
Steady-state error	50.1%	0.0%	0.0%
Disturbance error	52%	0.4%	0.4%

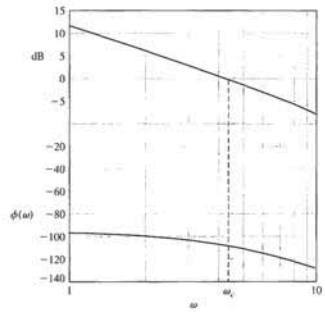

FIGURE 12.19
Bode diagram for $G_c(s)G(s)$ for Example 12.10.

place the two zeros at or near the crossover $\omega_c = 11$. We choose to set $\tau_1 = 0.06$ so that the two zeros are set at $\omega = 16.7$. Also, we reduce the gain to $K_I K = 4.5$. Then we obtain the frequency response shown in Figure 12.19, where

$$G_c(s)G(s) = \frac{4.5(0.06s + 1)^2 e^{-0.1s}}{s(0.1s + 1)}. \tag{12.52}$$

The new crossover frequency is $\omega_c = 4.5$, and the phase margin is 70°. The step response of this system has no overshoot and has a settling time (with a 2% criterion) of 0.80 second. This response satisfies the requirements. However, if we wanted to adjust the system further, we could raise $K_I K$ to 10 and achieve a somewhat faster response with an overshoot of less than 5%. ■

As a final consideration of the design of robust control systems using a PID controller, we turn to an s-plane root locus method. This design approach may be simply stated as follows:

1. Place the poles and zeros of $G(s)/s$ on the s-plane.
2. Select a location for the zeros of $G_c(s)$ that will result in an acceptable root locus and suitable dominant roots.
3. Test the transient response of the compensated system and iterate Step 2, if necessary.

12.7 THE ROBUST INTERNAL MODEL CONTROL SYSTEM

The internal model control system is shown in Figure 12.20 and was previously considered in Section 11.8. We now consider again the use of the internal model design with special attention to robust system performance. The **internal model principle**

The design method is as follows:

1. Plot the uncompensated Bode diagram for $K_I G(s)/s$ with a gain K_I that satisfies the steady-state error requirement.
2. Place the two equal zeros at or near the crossover frequency ω_c.
3. Test the results and adjust K_I or the zero locations, if necessary.

EXAMPLE 12.10 **PID control of a system with a delay**

Consider the system of Figure 12.16 when

$$G(s) = \frac{Ke^{-0.1s}}{0.1s + 1}, \tag{12.50}$$

where $K = 20$ is selected to achieve a small steady-state error for a step input, and where $G_p(s) = 1$. We want an overshoot to a step input of less than 5%.

Plotting the Bode diagram for $G(j\omega)$, we find that the uncompensated system has a negative phase margin and that the system is unstable.

We will use a PID controller of the form of Equation (12.49) to attain a desirable phase margin of 70°. Then the loop transfer function is

$$G_c(s)G(s) = \frac{20e^{-0.1s}(\tau_1 s + 1)^2}{s(0.1s + 1)}, \tag{12.51}$$

where $K_I K = 20$. We plot the Bode diagram without the two zeros, as shown in Figure 12.18. The phase margin is −32°, and the system is unstable prior to the introduction of the zeros.

Because we have introduced a pole at the origin due to the integration term in the PID compensator, we may reduce the gain $K_I K$ because e_{ss} is now zero. We

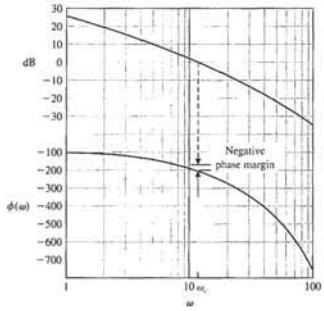

FIGURE 12.18
Bode diagram for $G(s)/s$ for Example 12.10.

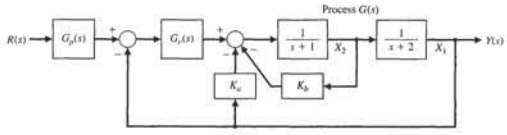

FIGURE 12.21
An internal model control with state variable feedback and $G_c(s)$.

and $G(s)G_c(s)$ will contain $R(s) = 1/s$, the input command. Note that we feed back both state variables and add these additional signals after $G_c(s)$ in order to retain the integrator in $G_c(s)$.

The goal is to achieve a settling time (to within 2% of the final value) in less than 1 second and a deadbeat response (see Section 10.11) while retaining a robust response. Here, we assume that the two poles of $G(s)$ can change by ±50%. Then the worst-case condition is

$$\hat{G}(s) = \frac{1}{(s + 0.5)(s + 1)}.$$

One design approach is to design the control for this worst-case condition. Another approach, which we use here, is to design for the nominal $G(s)$ and one-half the desired settling time. Then we expect to meet the settling time requirement and attain a very fast, highly robust system. Note that the prefilter $G_P(s)$ is used to attain the desired form for $T(s)$.

The response desired is deadbeat (see Table 10.2), so we use a third-order transfer function as

$$T(s) = \frac{\omega_n^3}{s^3 + 1.9\omega_n s^2 + 2.20\omega_n^2 s + \omega_n^3}, \tag{12.56}$$

and the settling time (with a 2% criterion) is $T_s = 4.04/\omega_n$. For a settling time of $\frac{1}{2}$ second, we use $\omega_n = 8.08$.

The closed-loop transfer function of the system of Figure 12.21 with the appropriate $G_P(s)$ is

$$T(s) = \frac{K_I}{s^3 + (3 + K_D + K_b)s^2 + (2 + K_P + K_a + 2K_b)s + K_I}. \tag{12.57}$$

We let $K_a = 10$, $K_b = 2$, $K_P = 127.6$, $K_I = 527.5$, and $K_D = 10.35$. Note that $T(s)$ could be achieved with other gains, including $K_b = 0$.

The step response of this system has a deadbeat response with an overshoot of 1.65% and a settling time of 0.5 second. When the poles of $G(s)$ change by ±50%, the overshoot changes to 1.86%, and the settling time becomes 0.95 second. This is an outstanding design of a very robust, deadbeat response system. ■

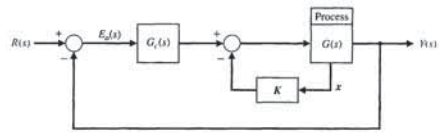

FIGURE 12.20
The internal model control system.

states that if $G_c(s)G(s)$ contains $R(s)$ then $y(t)$ will track $r(t)$ asymptotically (in the steady state), and the tracking is robust.

Examining the system of Figure 12.20, we note that for lower-order processes, state variable feedback will not be required, and a suitable $G_c(s)$ can be obtained. However, with higher-order systems, the feedback of all state variables may be required.

Consider a simple system with $G(s) = 1/s$, for which we seek a ramp response with a steady-state error of zero. A PI controller is sufficient, and we let $\mathbf{K} = \mathbf{0}$ (no state variable feedback). Then we have

$$G_c(s)G(s) = \left(K_p + \frac{K_I}{s}\right)\frac{1}{s} = \frac{K_p s + K_I}{s^2}. \tag{12.53}$$

Note that for a ramp, $R(s) = 1/s^2$, which is contained as a factor of Equation (12.53), and the closed-loop transfer function is

$$T(s) = \frac{K_p s + K_I}{s^2 + K_p s + K_I}. \tag{12.54}$$

Using the ITAE specifications for a ramp response (Table 5.7), we require that

$$T(s) = \frac{3.2\omega_n s + \omega_n^2}{s^2 + 3.2\omega_n s + \omega_n^2}. \tag{12.55}$$

We select ω_n to satisfy a specification for the settling time. For a settling time (with a 2% criterion) of 1 second, we select $\omega_n = 5$. Then we require $K_p = 16$ and $K_I = 25$. The response of this system settles in 1 second and then tracks the ramp with zero steady-state error. If this system (designed for a ramp input) receives a step input, the response has an overshoot of 5% and a settling time of 1.5 seconds. This system is very robust to changes in the plant. For example, if $G(s) = K/s$ changes gain so that K shifts from $K = 1$ by ±50%, the change in the ramp response is insignificant.

EXAMPLE 12.11 **Design of an internal model control system**

Consider the system of Figure 12.21 with state variable feedback and a compensator $G_c(s)$. We wish to track a step input with zero steady-state error. Here, we select a PID controller for $G_c(s)$. We then have

$$G_c(s) = \frac{K_D s^2 + K_P s + K_I}{s},$$

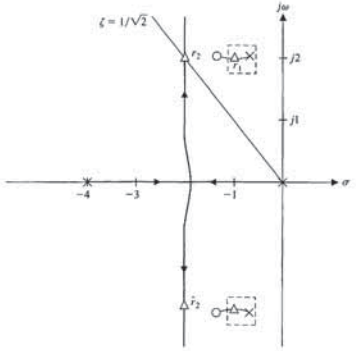

FIGURE 12.22
Root locus for aircraft autopilot. The complex poles can vary within the dashed-line box.

to use it only when the shuttle is attached [16, 19]. The ISF will be the first permanent, human-operated commercial space facility designed for R&D, testing, and, eventually, processing in the space environment.

We will consider an experiment operated in space but controlled from Earth. The goal is to manipulate and position a small telescope to accurately point at a planet. We want to have a steady-state error equal to zero, while maintaining a fast response to a step with an overshoot of less than 5%. The actuator chosen is a low-power actuator, and the model of the combined actuator and telescope is shown in Figure 12.23. The command signal is received from an Earth station with a delay of $\pi/16$ seconds. A sensor will measure the pointing direction of the telescope accurately. However, this measurement is relayed back to Earth with a delay of $\pi/16$ seconds. Thus, the total transfer function of the telescope, actuator, sensor, and round-trip delay (Figure 12.24) is

$$G(s) = \frac{e^{-s\pi/8}}{(s+1)^2}. \tag{12.60}$$

We propose a PID controller where

$$G_c(s) = K_P + \frac{K_I}{s} + K_D s = \frac{K_P s + K_I + K_D s^2}{s}. \tag{12.61}$$

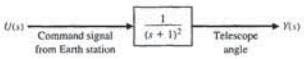

FIGURE 12.23
Model of a low-power actuator and telescope.

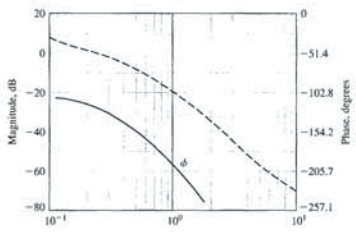

FIGURE 12.25
Bode diagram for the system with the PI controller.

Table 12.5 Step Response of the Space Telescope for Two Controllers

	Steady-State Error	Percent Overshoot	Settling Time (seconds)
PI controller	0	4.7	16.0
PID controller	0	3.7	5.8

EXAMPLE 12.14 **Robust bobbin drive**

Monofilament nylon is produced by an extrusion process that outputs filament at a constant rate. The product is wound onto a bobbin that rotates at a maximum speed of 2000 rpm. The tension in the filament must be held between 0.2 and 0.6 pound to ensure that it is not stretched. The winding diameter varies between 2 to 4 inches.

The filament is laid onto the bobbin by a ballscrew-driven arm that oscillates back and forth at constant speed, as shown in Figure 12.26(a). The arm must reverse rapidly at the end of the move. The required ballscrew speed is 60 rpm. The prime requirement of the bobbin drive is to provide a controlled tension. Since the winding diameter varies by 2 to 1, the tension will fall by 50% from start to finish.

The control system will have a system structure as shown in Figure 12.26(b), for which we select a PID controller. The parameter variations are $1.5 \le K_m \le 2.5$ and $3 \le p \le 5$ with the nominal conditions $K_m = 2$ and $p = 4$. Furthermore, a third pole at $s = -50$ has been omitted from the model. The requirements are an overshoot less than 2.5% and a settling time (with a 2% criterion) less than 0.4 second. The magnitude of $u(t)$ must be less than 100.

Using a PID controller, the ITAE design, and the nominal parameters, we determine ω_n from the settling time requirement. Since we expect that $\zeta \approx 0.8$, we use

$$T_s = \frac{4}{0.8\omega_n} < 0.4.$$

We select $\omega_n = 23$ as the maximum allowable for $|u| < 100$. Then, for

$$G_c(s) = K_P + \frac{K_I}{s} + K_D s,$$

12.8 DESIGN EXAMPLES

In this section we present five illustrative examples. In the first example, an aircraft autopilot is analyzed using root locus methods. In the second example, a PI controller and a PID controller are designed for a space telescope control system in the presence of time delays. The third example is the design of a robust bobbin drive using robust PID controller design approach with ITAE optimal performance objectives. The fourth example illustrates the design of two degree-of-freedom controllers (that is, two separate controllers) for an ultra-precision diamond turning machine. In the fifth and final design example, we consider the practical problem of designing a controller in the presence of an uncertain time delay. The specific problem under investigation is a PID controller for a digital audio tape drive. The design process is highlighted with an emphasis on robustness.

EXAMPLE 12.12 **Aircraft autopilot**

A typical aircraft autopilot control system consists of electrical, mechanical, and hydraulic devices that move the flaps, elevators, fuel-flow controllers, and other components that cause the aircraft to vary its flight. Sensors provide information on velocity, heading, rate of rotation, and other flight data. This information is combined with the desired flight characteristics (commands) available electronically to the autopilot. The autopilot should be able to fly the aircraft on a heading and under conditions set by the pilot. The command often consists of a predetermined heading. Design often focuses on a forward-moving aircraft that moves somewhat up or down without moving right or left and without rolling (tipping the wings). Such a study is called pitch axis design. The aircraft is represented by a process [23]

$$G(s) = \frac{K}{s(s + 1/\tau)(s^2 + 2\zeta_1\omega_1 s + \omega_1^2)}, \tag{12.58}$$

where τ is the time constant of the actuator. Let $\tau = \frac{1}{4}$, $\omega_1 = 2$, and $\zeta = \frac{1}{2}$. Then the s-plane plot has two complex poles, a pole at the origin, and a pole at $s = -4$, as shown in Figure 12.22. The complex poles, representing the aircraft dynamics, can vary within the dashed-line box shown in the figure. We then choose the zeros of the controller as $s = -1.3 \pm j2$, as shown. We select the gain K so that the roots r_2 and $\hat{r}_2$ are complex with a ζ of $1/\sqrt{2}$. The other roots, r_1 and $\hat{r}_1$, lie very near the zeros. Therefore, the closed-loop transfer function is approximately

$$T(s) \approx \frac{\omega_n^2}{s^2 + 2\zeta\omega_n s + \omega_n^2} = \frac{5}{s^2 + 3.16s + 5}, \tag{12.59}$$

with $\omega_n = \sqrt{5}$ and $\zeta = 1/\sqrt{2}$. The resulting response to a step input has an overshoot of 4.5% and a settling time (with a 2% criterion) of 2.5 seconds, as expected. ■

EXAMPLE 12.13 **Space telescope control system**

Scientists have proposed the operation of a space vehicle as a space-based research laboratory and test bed for equipment to be used on a manned space station. The industrial space facility (ISF) would remain in space, and the astronauts would be able

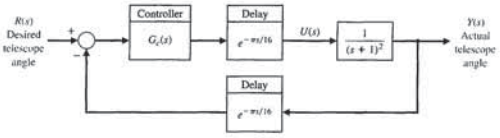

FIGURE 12.24
Feedback control system for the telescope experiment.

The use of only the proportional term will not be acceptable since we require a steady-state error of zero for a step input. Thus, we must use a nonzero value of K_I, and hence we may elect to use either a proportional plus integral control (PI) or a proportional plus integral plus derivative control (PID).

We will first try PI control, so that

$$G_c(s) = K_P + \frac{K_I}{s} = \frac{K_P s + K_I}{s}. \tag{12.62}$$

Since we have a pure delay e^{-sT}, we use the frequency response methods for the design process. Thus, we will translate the overshoot specification to the frequency domain. If we have two dominant characteristic roots, the overshoot to a step is 5% when $\zeta = 0.7$, or the phase margin requirement is about 70°.

If we choose $K_P = 0.022$ and $K_I = 0.22$, we have

$$G_c(s)G(s) = \frac{0.22(0.1s + 1)e^{-s\pi/8}}{s(s+1)^2}, \tag{12.63}$$

and the Bode diagram is shown in Figure 12.25. The location of the zero at $s = -10$ was chosen to add a phase lead angle in order to attain the desired phase margin. An iterative procedure yields a series of trials for K_1 and K_2 until the desired phase margin is achieved. Note that we have achieved a phase margin of about 63°. The actual step response was plotted, and we determine that the overshoot was 4.7% with a settling time (with a 2% criterion) of 16 seconds, as recorded in Table 12.5.

The proportional plus integral plus derivative controller is

$$G_c(s) = \frac{K_P s + K_I + K_D s^2}{s}. \tag{12.64}$$

We now have three parameters to vary to achieve the desired phase margin. If we select, after some iteration, $K_P = 0.8$, $K_I = 0.5$, and $K_D = 10^{-3}$, we obtain a phase margin of 64°. The percentage overshoot is 3.7%, and the settling time (with a 2% criterion) is 5.8 seconds. Perhaps the easiest way to select the gain constants is to let K_D be a small, but nonzero, number initially and $K_P = K_I = 0$, then plot the frequency response. In this case, we choose $K_D = 10^{-3}$ and obtain a Bode plot. We then use $K_P \approx K_I$ and iterate to obtain the appropriate values of these unspecified gains.

The performance of the PI- and the PID-compensated systems is recorded in Table 12.5. The PID controller is the most desirable, since it provides a shorter settling time. ■

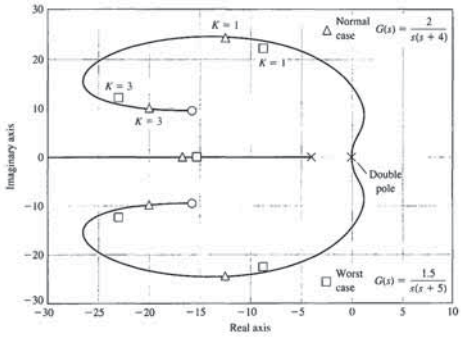

FIGURE 12.27
Root locus for the normal case and the worst case for $K = 1$ and $K = 3$.

(Note that the DC gain, $\lim_{s\to 0} sG(s)$, remains 0.5.) The response of the PID controller with the added pole is recorded in Table 12.6. Again, the system fails the requirement of robust performance.

We need to adjust the system so that the performance with the worst-case parameters is acceptable. Examine the root locus for the nominal parameters shown in Figure 12.27. Insert a cascade gain K prior to $G_c(s)$ so that we have $KG_c(s)G(s)$. Then the roots for $K = 1$ and $K = 3$ are shown on the locus. Since the worst-case response occurs when the motor constant K_m drops to 1.5, we use the cascade gain $K = 3$ to move the roots to the left on the s-plane. Then, when the gain K_m drops to 1.5, the roots still are in the desired region. The response of the system with $K = 3$ is recorded in Table 12.7 for the nominal and worst-case conditions, as well as with the added pole. This system meets all the specifications. This approach uses a cascade gain that, when adjusted correctly, will drive the dominant roots near the complex zeros of the PID controller. Then, when the worst parameter change occurs, the system will still maintain the required performance. ■

EXAMPLE 12.15 **Ultra-precision diamond turning machine**

The design of an ultra-precision diamond turning machine has been studied at Lawrence Livermore National Laboratory. This machine shapes optical devices such as mirrors with ultra-high precision using a diamond tool as the cutting device. In this discussion, we will consider only the z-axis control. Using frequency response identification with sinusoidal input to the actuator we determined that

$$G(s) = \frac{4500}{s + 60}. \tag{12.66}$$

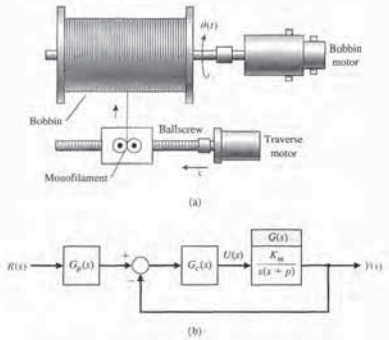

FIGURE 12.26
A monofilament bobbin winder.

we obtain $K_P = 568.68$, $K_I = 6083.5$, and $K_D = 18.13$. Using the appropriate prefilter, we obtain the response recorded in Table 12.6. The system does not offer robust performance since the overshoot requirement is not satisfied when the worst-case parameters are considered.

We also examine the performance of the system with the nominal parameters but with the unmodeled pole added, so that the actual process is

$$G(s) = \frac{2(50)}{s(s + 4)(s + 50)}. \tag{12.65}$$

Table 12.6 Response of the Bobbin Drive System for a Unit Step Input (original design)

	Parameters	Percent Overshoot	Settling Time	$\left\|\frac{u(t)}{r(t)}\right\|_{\text{maximum}}$
Nominal parameters	$K_m = 2$, $p = 4$	1.96%	0.318	98
Worst-case parameters	$K_m = 1.5$, $p = 3$	7.48%	0.375	95
Nominal parameters and added third pole at $s = -50$		9.82%	0.732	90

Table 12.8 Specifications for Turning Machine Control System

	Transfer Function	
Specification	Velocity, $V(s)/U(s)$	Position $Y(s)/R(s)$
Minimum bandwidth	950 rad/s	95 rad/s
Steady-state error to a step	0	0
Minimum damping ratio ζ	0.8	0.9
Maximum root sensitivity $\lvert S_K^r \rvert$	1.0	1.5
Minimum phase margin	90°	75°
Minimum gain margin	40 dB	60 dB

The root locus for $G_2(s)G(s)$ is shown in Figure 12.29. When $K_P = 2$, we have, for the velocity closed-loop transfer function,

$$T_2(s) = \frac{V(s)}{U(s)} = \frac{9000(s + 188)(s + 368)}{(s + 205)(s + 305)(s + 10^4)} \approx \frac{10^4}{(s + 10^4)}, \tag{12.67}$$

which is a large-bandwidth system. The actual bandwidth and root sensitivity are summarized in Table 12.9. Note that we have exceeded the specifications for the velocity transfer function.

We will use a lead network for the position loop of the form

$$G_1(s) = K_1 \frac{1 + K_5 s}{\alpha\left(1 + \frac{K_5}{\alpha} s\right)}.$$

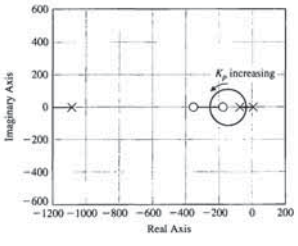

FIGURE 12.29
Root locus for velocity loop as K_p varies.

Table 12.7 Response of the Bobbin Drive System for a Unit Step with Additional Cascade Gain $K = 3$

	Percent Overshoot	Settling Time (seconds)
Nominal parameters	0.12%	0.218
Worst-case parameters	0.47%	0.214
Nominal parameters and third pole	0.50%	0.242

The system can accommodate high gains, such as 4500, since the input command, $r(t)$, is a series of step commands of very small magnitude (a fraction of a micron). The system has an outer loop for position feedback using a laser interferometer with an accuracy of 0.1 micron (10^{-7} m). An inner feedback loop is also used for velocity feedback, as shown in Figure 12.28.

We want to select the controllers, $G_1(s)$ and $G_2(s)$, to obtain an overdamped, highly robust, high-bandwidth system. The robust system must accommodate changes in $G(s)$ due to varying loads, materials, and cutting requirements. Thus, we seek a large phase margin and gain margin for the inner and outer loops, and low root sensitivity. The specifications are summarized in Table 12.8.

Since we want zero steady-state error for the velocity loop, we use a velocity loop controller $G_2(s) = G_3(s)G_4(s)$, where $G_3(s)$ is a PI controller and $G_4(s)$ is a lead controller. We use

$$G_2(s) = G_3(s)G_4(s) = \left(K_p + \frac{K_I}{s}\right) \cdot \frac{1 + K_4 s}{\alpha\left(1 + \frac{K_4}{\alpha} s\right)}$$

and choose $K_P/K_I = 0.00532$, $K_4 = 0.00272$, and $\alpha = 2.95$. We now have

$$G_2(s) = K_P \frac{s + 188}{s} \cdot \frac{s + 368}{s + 1085}.$$

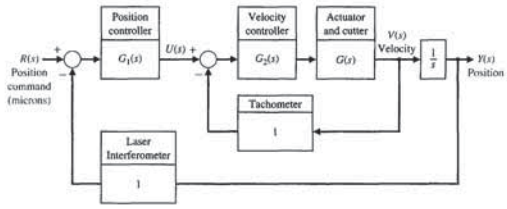

FIGURE 12.28
Turning machine control system.

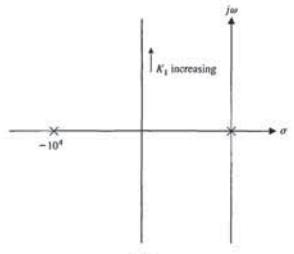

(a)

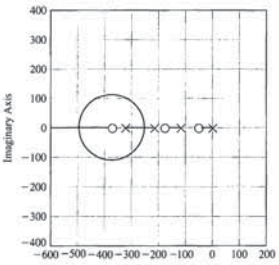

(b)

FIGURE 12.30
The root locus for $K_1 > 0$ for (a) overview and (b) close-up near origin of the s-plane.

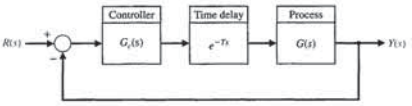

FIGURE 12.31
A feedback system with a time delay in the loop.

Then

$$G_m(s) - G(s) = e^{-Ts}G(s) - G(s) = (e^{-Ts} - 1)G(s),$$

or

$$\frac{G_m(s)}{G(s)} - 1 = e^{-Ts} - 1.$$

Table 12.9 Design Results for Turning Machine Control System

Achieved Result	Velocity Transfer Function	Position Transfer Function Y(s)/R(s)
Closed-loop bandwidth	4000 rad/s	1000 rad/s
Steady-state error	0	0
Damping ratio, ζ	1.0	1.0
Root sensitivity, $\lvert S_K^r \rvert$	0.92	1.2
Phase margin	93°	85°
Gain margin	Infinite	76 dB

and we choose $\alpha = 2.0$ and $K_5 = 0.0185$ so that

$$G_1(s) = \frac{K_1(s + 54)}{s + 108}.$$

We then plot the root locus for

$$G_1(s) \cdot T_2(s) \cdot \frac{1}{s}.$$

If we use the approximate $T_2(s)$ of Equation (12.67), we have the root locus of Figure 12.30(a). Using the actual $T_2(s)$, we get the close-up of the root locus shown in Figure 12.30(b). We select $K_P = 1000$ and achieve the actual results for the total system transfer function as recorded in Table 12.9. The total system has a high phase margin, has a low sensitivity, and is overdamped with a large bandwidth. This system is very robust. ■

EXAMPLE 12.16 **Digital audio tape controller**

Consider the feedback control system shown in Figure 12.31, where

$$G_d(s) = e^{-Ts}.$$

The exact value of the time delay is uncertain, but it is known to lie in the interval $T_1 \le T \le T_2$. For example, if a robot on Mars is being remotely controlled from Earth, the time it takes the signals to reach the planetary robot is not precisely known since transient time depends on the distance between the transmitter and the planetary robot, the atmospheric medium through which the signals travel, interplanetary space effects, and so forth—all of which are time varying and cannot be precisely modeled.

Define

$$G_m(s) = e^{-Ts}G(s).$$

Therefore, the robust stability condition can be satisfied by

$$|W(j\omega)| < \left| 1 + \frac{1}{G_c(j\omega)G(j\omega)} \right| \quad \text{for all } \omega. \tag{12.69}$$

This is a conservative bound. If the condition in Equation (12.69) is satisfied, then stability is guaranteed in the presence of any time delay in the range $T_1 \le T \le T_2$ [5, 32]. If the condition is not satisfied, the system may or may not be stable.

Suppose we have an uncertain time delay that is known to lie in the range $0.1 \le T \le 1$. We can determine a suitable weighting function $W(s)$ by plotting the magnitude of $e^{-j\omega T} - 1$, as shown in Figure 12.34 for various values of T in the range $T_1 \le T \le T_2$. A reasonable weighting function obtained by trial and error is

$$W(s) = \frac{2.5s}{1.2s + 1}.$$

This function satisfies the condition

$$|e^{-j\omega T} - 1| < |W(j\omega)|.$$

Keep in mind that the selection of the weighting function is not unique.

A digital audio tape (DAT) stores 1.3 gigabytes of data in a package the size of a credit card—roughly nine times more than a half-inch-wide reel-to-reel tape or quarter-inch-wide cartridge tape. A DAT sells for about the same amount as a floppy disk, even though it can store 1000 times more data. A DAT can record for two

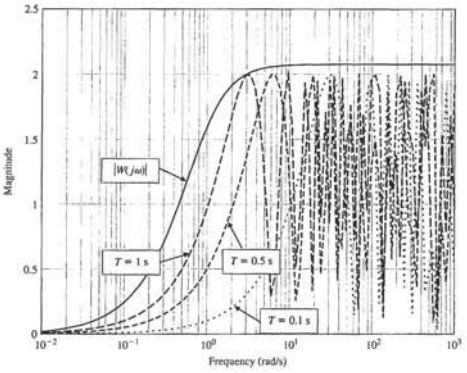

FIGURE 12.34
Magnitude plot of $|e^{-j\omega T} - 1|$ for $T = 0.1$, 0.5, and 1.

If we define

$$M(s) = e^{-Ts} - 1,$$

then we have

$$G_m(s) = (1 + M(s))G(s). \tag{12.68}$$

In the development of a robust stability controller, we would like to represent the time-delay uncertainty in the form shown in Figure 12.32 where we need to determine a function $M(s)$ that approximately models the time delay. This will lead to the establishment of a straightforward method of testing the system for stability robustness in the presence of the uncertain time-delay. The uncertainty model is known as a multiplicative uncertainty representation, as discussed in Section 12.3.

Since we are concerned with stability, we can consider $R(s) = 0$. Then we can manipulate the block diagram in Figure 12.32 to obtain the form shown in Figure 12.33. Using the so-called small gain theorem, we have the condition that the closed-loop system is stable if

$$|M(j\omega)| \left| \frac{G_c(j\omega)G(j\omega)}{1 + G_c(j\omega)G(j\omega)} \right| < 1,$$

or equivalently (see Equation (12.15))

$$|M(j\omega)| < \left| 1 + \frac{1}{G_c(j\omega)G(j\omega)} \right| \quad \text{for all } \omega.$$

The problem is that the time delay T is not known exactly. One approach to solving the problem is to find a weighting function, denoted by $W(s)$, such that

$$|e^{-j\omega T} - 1| < |W(j\omega)| \quad \text{for all } \omega \text{ and } T_1 \le T \le T_2.$$

If $W(s)$ satisfies the above inequality, it follows that

$$|M(j\omega)| < |W(j\omega)|.$$

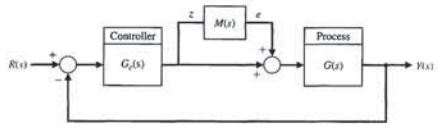

FIGURE 12.32
Multiplicative uncertainty representation.

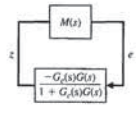

FIGURE 12.33
Equivalent block diagram depiction of the multiplicative uncertainty.

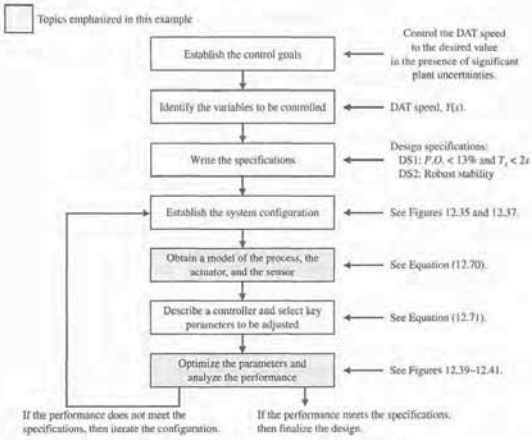

FIGURE 12.36 Elements of the control system design process emphasized in this digital audio tape speed control design.

DS2 Robust stability in the presence of a time delay at the plant input. The time delay value is uncertain but known to be in the range $0 \le T \le 0.1$.

Design specification DS1 must be satisfied for all process in the family. Design specification DS2 must be satisfied by the nominal process ($K_m = 4$, $p_1 = 1$, $p_2 = 4$).

The following constraints on the design are given:

- Fast peak time requires that an overdamped condition is not acceptable.
- Use a PID controller:

$$G_c(s) = K_P + \frac{K_I}{s} + K_D s. \tag{12.71}$$

- $K_m K_D \le 20$ when $K_m = 4$.

The key tuning parameters are the PID gains:

Select Key Tuning Parameters
K_P, K_I, and K_D.

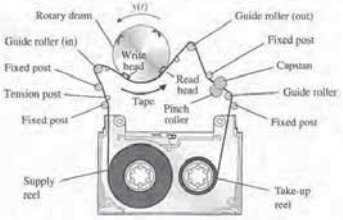

FIGURE 12.35 Digital audio tape driver mechanism.

hours (longer than either reel-to-reel or cartridge tape), which means that it can run longer unattended and requires fewer changes and hence fewer interruptions of data transfer. DAT gives access to a given data file within 20 seconds, on the average, compared with several minutes for either cartridge or reel-to-reel tape [2].

The tape drive electronically controls the relative speeds of the drum and tape so that the heads follow the tracks on the tape, as shown in Figure 12.35. The control system is much more complex than that for a CD-ROM because more motors have to be accurately controlled: capstan, take-up and supply reels, drum, and tension control. The elements of the design process emphasized in this example are highlighted in Figure 12.36.

Consider the speed control system shown in Figure 12.37. The motor and load transfer function varies because the tape moves from one reel to the other. The transfer function is

$$G(s) = \frac{K_m}{(s + p_1)(s + p_2)}, \tag{12.70}$$

where nominal values are $K_m = 4$, $p_1 = 1$, and $p_2 = 4$.

However, the range of variation is $3 \le K_m \le 5$, $0.5 \le p_1 \le 1.5$, and $3.5 \le p_2 \le 4.5$. Thus, the process belongs to a family of processes, where each member corresponds to different values of K_m, p_1, and p_2. The design goal is

Design Goal
Control the DAT speed to the desired value in the presence of significant process uncertainties.

Associated with the design goal we have the variable to be controlled defined as the tape speed:

Variable to Be Controlled
DAT speed $Y(s)$.

The design specifications are

Design Specifications

DS1 Percent overshoot less than 13% and settling time less than 2 seconds for a unit step input.

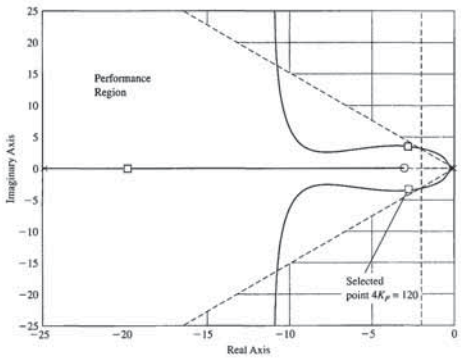

FIGURE 12.38 Root locus for the DAT system with $K_D = 5$ and $\tau = K_I/K_P = 3$.

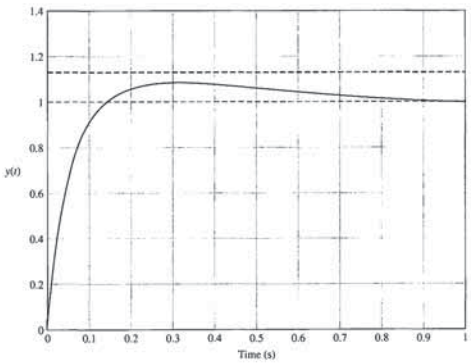

FIGURE 12.39 Unit step response for the DAT system with $K_P = 30$, $K_D = 5$, and $K_I = 90$.

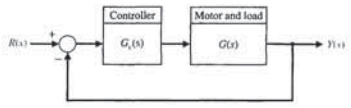

FIGURE 12.37 Block diagram of the digital audio tape speed control system.

Since we are constrained to have $K_m K_D \le 20$ when $K_m = 4$, we must select $K_D \le 5$. We will design the PID controller using nominal values for K_m, p_1, and p_2. We will analyze the performance of the controlled system for the various values of the process parameters, using a simulation to check that DS1 is satisfied. The nominal process is given by

$$G(s) = \frac{4}{(s + 1)(s + 4)}.$$

The closed-loop transfer function is

$$T(s) = \frac{4K_D s^2 + 4K_P s + 4K_I}{s^3 + (5 + 4K_D)s^2 + (4 + 4K_P)s + 4K_I}.$$

If we choose $K_D = 5$, then we write the characteristic equation as

$$s^3 + 25s^2 + 4s + 4(K_P s + K_I) = 0,$$

or

$$1 + \frac{4K_P(s + K_I/K_P)}{s(s^2 + 25s + 4)} = 0.$$

Per specifications, we try to place the dominant poles in the region defined by $\zeta\omega_n > 2$ and $\zeta > 0.55$. We need to select a value of $\tau = K_I/K_P$, and then we can plot the root locus with the gain $4K_P$ as the varying parameter. After several iterations, we choose a reasonable value of $\tau = 3$. The root locus is shown in Figure 12.38. We determine that $4K_P \approx 120$ represents a valid selection since the roots lie inside the desired performance region. This value of $4K_P$ has been rounded off from the exact value on the root locus plot of $4K_P = 121.7683$. We obtain $K_P = 30$, and $K_I = \tau K_P = 90$. The PID controller is then given by

$$G_c(s) = 30 + \frac{90}{s} + 5s. \tag{12.72}$$

The step response (for the process with nominal parameter values) is shown in Figure 12.39. A family of responses is shown in Figure 12.40 for various values of

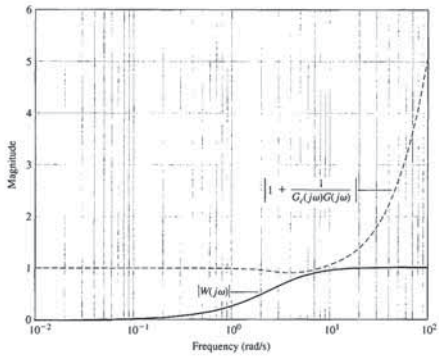

FIGURE 12.41
Stability robustness to a time delay of uncertain magnitude.

12.9 THE PSEUDO-QUANTITATIVE FEEDBACK SYSTEM

Quantitative feedback theory (QFT) uses a controller, as shown in Figure 12.42, to achieve robust performance. The goal is to achieve a wide bandwidth for the closed-loop transfer function with a high loop gain K. Typical QFT design methods use graphical and numerical methods in conjunction with the Nichols chart. Generally, QFT design seeks a high loop gain and large phase margin so that robust performance is achieved [24–26, 28].

In this section, we pursue a simple method of achieving the goals of QFT with an s-plane, root locus approach to the selection of the gain K and the compensator $G_c(s)$. This approach, dubbed pseudo-QFT, follows these steps:

1. Place the n poles and m zeros of $G(s)$ on the s-plane for the nth order $G(s)$. Also, add any poles of $G_c(s)$.
2. Starting near the origin, place the zeros of $G_c(s)$ immediately to the left of each of the $(n - 1)$ poles on the left-hand s-plane. This leaves one pole far to the left of the left-hand side of the s-plane.
3. Increase the gain K so that the roots of the characteristic equation (poles of the closed-loop transfer function) are close to the zeros of $G_c(s)G(s)$.

This method introduces zeros so that all but one of the root loci end on finite zeros. If the gain K is sufficiently large, then the poles of $T(s)$ are almost equal to the zeros of $G_c(s)G(s)$. This leaves one pole of $T(s)$ with a significant partial fraction residue and the system with a phase margin of approximately 90° (actually about 85°).

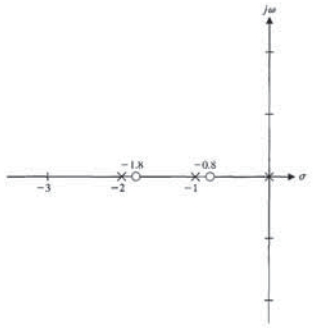

FIGURE 12.43
Root locus for $KG_c(s)G(s)$.

Table 12.10 Performance of Pseudo-QFT Design

	Percent Overshoot	Settling Time
Nominal $G(s)$	0.01%	40 ms
Worst-case $G(s)$	0.97%	40 ms

The PID controller has the form

$$G_c(s) = \frac{K_D s^2 + K_P s + K_I}{s}.$$

Note that the PID controller is not a proper rational function (i.e., the degree of the numerator polynomial is greater than the degree of the denominator polynomial). The objective is to choose the parameters K_P, K_I, and K_D to meet the performance specifications and have desirable robustness properties. Unfortunately, it is not immediately clear how to choose the parameters in the PID controller to obtain certain robustness characteristics. An illustrative example will show that it is possible to choose the parameters iteratively and verify the robustness by simulation. Using the computer helps in this process, because the entire design and simulation can be automated using scripts and can easily be executed repeatedly.

EXAMPLE 12.18 **Robust control of temperature**

Consider the feedback control system in Figure 12.16, where

$$G(s) = \frac{1}{(s + c_0)^2},$$

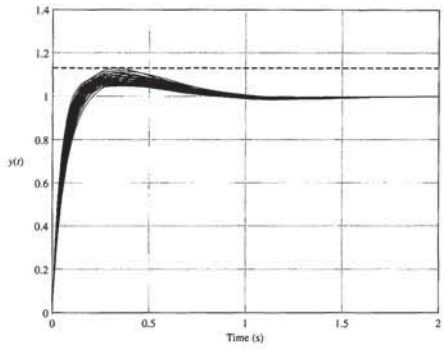

FIGURE 12.40
A family of step responses for the DAT system for various values of the process parameters K_m, p_1, and p_2.

K_m, p_1, and p_2. None of the responses suggests a percent overshoot over the specified value of 13%, and the settling times are all under the 2 second specification as well. As we can see in Figure 12.40, all of the tested processes in the family are adequately controlled by the single PID controller in Equation (12.72). Therefore DS1 is satisfied for all processes in the family.

Suppose the system has a time delay at the input to the process. The actual time delay is uncertain but known to be in the range $0 \le T \le 0.1$ s. Following the method discussed previously, we determine that a reasonable function $W(s)$ which bounds the plots of $|e^{-j\omega T} - 1|$ for various values of T is

$$W(s) = \frac{0.29s}{0.28s + 1}.$$

To check the stability robustness property, we need to verify that

$$|W(j\omega)| < \left|1 + \frac{1}{G_c(j\omega)G(j\omega)}\right| \quad \text{for all } \omega. \tag{12.73}$$

The plot of both $|W(j\omega)|$ and $\left|1 + \frac{1}{G_c(j\omega)G(j\omega)}\right|$ is shown in Figure 12.41. It can be seen that the condition in Equation (12.73) is indeed satisfied. Therefore, we expect that the nominal system will remain stable in the presence of time-delays up to 0.1 seconds. ■

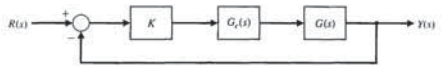

FIGURE 12.42
Feedback system.

EXAMPLE 12.17 **Design using the pseudo-QFT method**

Consider the system of Figure 12.42 with

$$G(s) = \frac{1}{(s + p_1)(s + p_2)},$$

where the nominal case is $p_1 = 1$ and $p_2 = 2$, with ±50% variation. The worst case is with $p_1 = 0.5$ and $p_2 = 1$. We wish to design the system for zero steady-state error for a step input, so we use the PID controller

$$G_c(s) = \frac{(s + z_1)(s + z_2)}{s}.$$

We then invoke the internal model principle, with $R(s) = 1/s$ incorporated within $G_c(s)G(s)$. Using Step 1, we place the poles of $G_c(s)G(s)$ on the s-plane, as shown in Figure 12.43. There are three poles (at $s = 0, -1$, and -2), as shown. Step 2 calls for placing a zero to the left of the pole at the origin and at the pole at $s = -1$, as shown in Figure 12.43.

The compensator is thus

$$G_c(s) = \frac{(s + 0.8)(s + 1.8)}{s}. \tag{12.74}$$

We select $K = 100$, so that the roots of the characteristic equation are close to the zeros. The closed-loop transfer function is

$$T(s) = \frac{100(s + 0.80)(s + 1.80)}{(s + 0.798)(s + 1.797)(s + 100.4)} \approx \frac{100}{s + 100}. \tag{12.75}$$

This closed-loop system provides a fast response and possesses a phase margin of approximately 85°. The performance is summarized in Table 12.10.

When the worst-case conditions are realized ($p_1 = 0.5$ and $p_2 = 1$), the performance remains essentially unchanged, as shown in Table 12.10. Pseudo-QFT design results in very robust systems. ■

12.10 ROBUST CONTROL SYSTEMS USING CONTROL DESIGN SOFTWARE

In this section, we will investigate robust control systems using control design software. In particular, we will consider the commonly used PID controller in the feedback control system shown in Figure 12.16. Note that the system has a prefilter $G_p(s)$. The contribution of the prefilter to optimum performance is discussed in Section 10.10.

our chosen point, we find that

$$\hat{K} = 118.$$

Then, with $\hat{K}$, a, and b, we can solve for the PID coefficients as follows:

$$K_D = \hat{K} - 2 = 116,$$
$$K_P = a(2 + K_D) - 1 = 1887,$$
$$K_I = b(2 + K_D) = 8260.$$

To meet the overshoot performance requirements for a step input, we will use a cascade gain K that will be chosen by iterative methods using the step function, as illustrated in Figure 12.45. The step response corresponding to $K = 5$ has an acceptable overshoot of 2%. With the addition of the gain $K = 5$, the final PID controller is

$$G_c(s) = K\frac{K_D s^2 + K_P s + K_I}{s} = 5\frac{116s^2 + 1887s + 8260}{s}. \qquad (12.77)$$

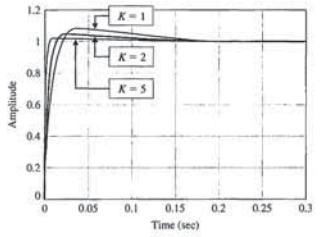


```
Ks=118;          Gain from uncompensated root locus.
a=16; b=70;      Increase system gain to reduce overshoot.
K=5;
KD=Ks-2, KP=a*(2+KD)-1, KI=b*(2+KD)
numgc=K*[KD KP KI]; dengc=[1 0]; sysgc=tf(numgc,dengc);
numg=[1]; deng=[1 2 1]; sysg=tf(numg,deng);
%
syso=series(sysgc,sysg);          PID gains.
%
sys=feedback(syso,[1]);
step(sys)
```

FIGURE 12.45 Step response of the PID temperature controller.

and the nominal value is $c_0 = 1$, and $G_p(s) = 1$. We will design a compensator based on $c_0 = 1$ and check robustness by simulation. Our design specifications include

1. A settling time (with a 2% criterion) $T_s \leq 0.5$ s, and
2. An optimum ITAE performance for a step input.

For this design, we will not use a prefilter to meet specification (2), but will instead show that acceptable performance (i.e., low overshoot) can be obtained by increasing a cascade gain.

The closed-loop transfer function is

$$T(s) = \frac{K_D s^2 + K_P s + K_I}{s^3 + (2 + K_D)s^2 + (1 + K_P)s + K_I}. \qquad (12.76)$$

The associated root locus equation is

$$1 + \hat{K}\left(\frac{s^2 + as + b}{s^3}\right) = 0,$$

where

$$\hat{K} = K_D + 2, \quad a = \frac{1 + K_P}{2 + K_D}, \quad \text{and} \quad b = \frac{K_I}{2 + K_D}.$$

The settling time requirement $T_s < 0.5$ s leads us to choose the roots of $s^2 + as + b$ to the left of the $s = -\zeta\omega_n = -8$ line in the s-plane, as shown in Figure 12.44, to ensure that the locus travels into the required s-plane region. We have chosen $a = 16$ and $b = 70$ to ensure the locus travels past the $s = -8$ line. We select a point on the root locus in the performance region, and using the rlocfind function, we find the associated gain $\hat{K}$ and the associated value of ω_n. For

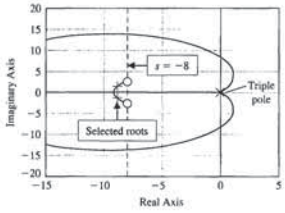

FIGURE 12.44 Root locus for the PID-compensated temperature controller as $\hat{K}$ varies.

```
>>a=16; b=70; num=[1 a b]; den=[1 0 0 0]; sys=tf(num,den);
>>rlocus(sys)
>>rlocfind(sys)
```


12.11 SEQUENTIAL DESIGN EXAMPLE: DISK DRIVE READ SYSTEM

In this section, we will design a PID controller to achieve the desired system response. Many actual disk drive head control systems use a PID controller and use a command signal $r(t)$ that utilizes an ideal velocity profile at the maximum allowable velocity until the head arrives near the desired track, when $r(t)$ is switched to a step-type input. Thus, we want zero steady-state error for a ramp (velocity) signal and a step signal. Examining the system shown in Figure 12.47, we note that the forward path possesses two pure integrations, and we expect zero steady-state error for a velocity input $r(t) = At$, $t > 0$.

The PID controller is

$$G_c(s) = K_P + \frac{K_I}{s} + K_D s = \frac{K_D(s + z_1)(s + \hat{z}_1)}{s}.$$

The motor field transfer function is

$$G_1(s) = \frac{5000}{(s + 1000)} \approx 5.$$

The second-order model uses $G_1(s) = 5$, and the design is determined for this model.

We use the second-order model and the PID controller for the s-plane design technique illustrated in Section 12.6. The poles and zeros of the system are shown in the s-plane in Figure 12.48 for the second-order model and $G_1(s) = 5$. Then we have

$$G_c(s)G_1(s)G_2(s) = \frac{5K_D(s + z_1)(s + \hat{z}_1)}{s^2(s + 20)}.$$

We select $-z_1 = -120 + j40$ and determine $5K_D$ so that the roots are to the left of the line $s = -100$. If we achieve that requirement, then

$$T_s < \frac{4}{100},$$

and the overshoot to a step input is (ideally) less than 2% since ζ of the complex roots is approximately 0.8. Of course, this sketch is only a first step. As a second step,

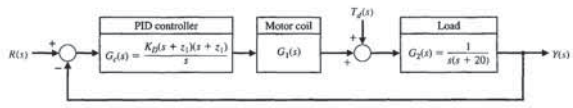

FIGURE 12.47 Disk drive feedback system with a PID controller.

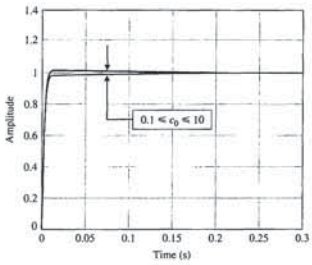


```
c0=10 ←          Specify process parameter.
numg=[1]; deng=[1 2*c0 c0^2];
numgc=5*[116 1887 8260]; dengc=[1 0];
sysg=tf(numg,deng);
sysgc=tf(numgc,dengc);
%
syso=series(sysgc,sysg);
%
sys=feedback(syso,[1]);
%
step(sys)
```

FIGURE 12.46 Robust PID controller analysis with variations in c_0.

We do not use the prefilter, as in Example 12.8. Instead, we increase the cascade gain K to obtain satisfactory transient response. Now we can consider the question of robustness to changes in the plant parameter c_0.

The investigation into the robustness of the design consists of a step response analysis using the PID controller given in Equation (12.77) for a range of plant parameter variations of $0.1 \leq c_0 \leq 10$. The results are displayed in Figure 12.46. The script is written to compute the step response for a given c_0. It can be convenient to place the input of c_0 at the command prompt level to make the script more interactive.

The simulation results indicate that the PID design is robust with respect to changes in c_0. The differences in the step responses for $0.1 \leq c_0 \leq 10$ are barely discernible on the plot. If the results showed otherwise, it would be possible to iterate on the design until an acceptable performance was achieved. The interactive capability of the m-file allows us to check the robustness by simulation. ■

Table 12.11 Disk Drive Control System Specifications and Actual Performance

Performance Measure	Desired Value	Response for Second-Order Model
Percent overshoot	<5%	4.5%
Settling time for step input	<50 ms	6 ms
Maximum response for a unit step disturbance	$<5 \times 10^{-3}$	7.7×10^{-7}

12.12 SUMMARY

The design of highly accurate control systems in the presence of significant plant uncertainty requires the designer to seek a robust control system. A robust control system exhibits low sensitivities to parameter change and is stable over a wide range of parameter variations.

The PID controller was considered as a compensator to aid in the design of robust control systems. The design issue for a PID controller is the selection of the gain and two zeros of the controller transfer function. We used three design methods for the selection of the controller: the root locus method, the frequency response method, and the ITAE performance index method. An operational amplifier circuit used for a PID controller is shown in Figure 12.50. In general, the use of a PID controller will enable the designer to attain a robust control system.

The internal model control system with state variable feedback and a controller $G_c(s)$ was used to obtain a robust control system. Finally, the robust nature of a pseudo-QFT control system was demonstrated.

$$G_c(s) = \frac{V_0(s)}{V_1(s)} = \frac{R_4R_2(R_1C_1s + 1)(R_2C_2s + 1)}{R_3R_1(R_2C_2s)}$$

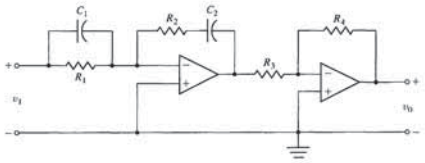

FIGURE 12.50 Operational amplifier circuit used for PID controller.

3. The PID controller consists of three terms in which the output is the sum of a proportional term, an integrating term, and a differentiating term, with an adjustable gain for each term. *True or False*
4. A plant model will always be an inaccurate representation of the actual physical system. *True or False*
5. Control system designers seek small loop gain $L(s)$ in order to minimize the sensitivity $S(s)$. *True or False*
6. A closed-loop feedback system has the third-order characteristic equation

$$q(s) = s^3 + a_2s^2 + a_1s + a_0 = 0,$$

where the nominal values of the coefficients are $a_2 = 3$, $a_1 = 6$, and $a_0 = 11$. The uncertainty in the coefficients is such that the actual values of the coefficients can lie in the intervals

$$2 \le a_2 \le 4, \quad 4 \le a_1 \le 9, \quad 6 \le a_0 \le 17.$$

Considering all possible combinations of coefficients in the given intervals, the system is:

a. Stable for all combinations of coefficients.
b. Unstable for some combinations of coefficients.
c. Marginally stable for some combinations of coefficients.
d. Unstable for all combinations of coefficients.

In Problems 7 and 8, consider the unity feedback system in Figure 12.52, where

$$G(s) = \frac{2}{(s + 3)}.$$

7. Assume that the prefilter is $G_p(s) = 1$. The proportional-plus-integral (PI) controller, $G_c(s)$, that provides optimum coefficients of the characteristic equation for ITAE (assuming $\omega_n = 12$ and a step input) is which of the following:

a. $G_c = 72 + \frac{6.9}{s}$
b. $G_c = 6.9 + \frac{72}{s}$
c. $G_c = 1 + \frac{1}{s}$
d. $G_c = 14 + 10s$

8. Considering the same PI controller as in Problem 7, a suitable prefilter, $G_p(s)$, which provides optimum ITAE response to a step input is:

a. $G_p(s) = \frac{10.44}{s + 12.5}$
b. $G_p(s) = \frac{12.5}{s + 12.5}$
c. $G_p(s) = \frac{10.44}{s + 10.44}$
d. $G_p(s) = \frac{144}{s + 144}$

9. Consider the closed-loop system block-diagram in Figure 12.52, where

$$G(s) = \frac{1}{s(s^2 + 8s)} \quad \text{and} \quad G_p(s) = 1.$$

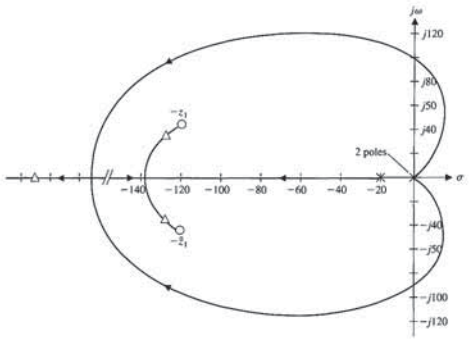

FIGURE 12.48 A sketch of a root locus at K_D increases for estimated root locations with a desirable system response.

we determine K_D. We then obtain the actual root locus as shown in Figure 12.49 with $K_D = 800$. The system response is recorded in Table 12.11. The system meets all the specifications.

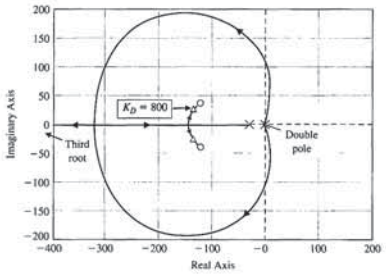

FIGURE 12.49 Actual root locus for the second-order model.

A robust control system provides stable, consistent performance as specified by the designer in spite of the wide variation of plant parameters and disturbances. It also provides a highly robust response to command inputs and a steady-state tracking error equal to zero.

For systems with uncertain parameters, the need for robust systems will require the incorporation of advanced machine intelligence, as shown in Figure 12.51.

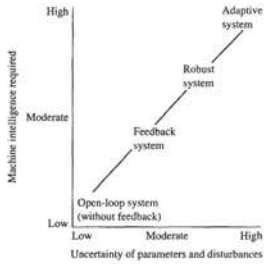

FIGURE 12.51 Intelligence required versus uncertainty for modern control systems.

SKILLS CHECK

In this section, we provide three sets of problems to test your knowledge: True or False, Multiple Choice, and Word Match. To obtain direct feedback, check your answers with the answer key provided at the conclusion of the end-of-chapter problems. Use the block diagram in Figure 12.52 as specified in the various problem statements.

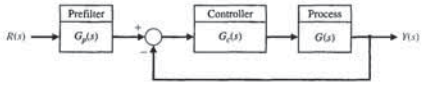

FIGURE 12.52 Block diagram for the Skills Check.

In the following **True or False** and **Multiple Choice** problems, circle the correct answer.

1. A robust control system exhibits the desired performance in the presence of significant plant uncertainty. *True or False*
2. For physically realizable systems, the loop gain $L(s) = G_c(s)G(s)$ must be large for high frequencies. *True or False*

c. $G_c(s) = 1 + \frac{5}{s}$ and $G_p(s) = \frac{5}{s+5}$

d. $G_c(s) = 12.5 + \frac{500}{s}$ and $G_p(s) = \frac{500}{12.5s + 500}$

13. Consider a unity negative feedback system with a loop transfer function (with nominal values)

$$L(s) = G_c(s)G(s) = \frac{K}{s(s+a)(s+b)} = \frac{4.5}{s(s+1)(s+2)}.$$

Using the Routh-Hurwitz stability analysis, it can be shown that the closed-loop system is nominally stable. However, if the system has uncertain coefficients such that

$$0.25 \le a \le 3, \quad 2 \le b \le 4, \quad \text{and} \quad 4 \le K \le 5,$$

the closed-loop system may exhibit instability. Which of the following situations is true:

a. Unstable for $a = 1, b = 2$, and $K = 4$.

b. Unstable for $a = 2, b = 4$, and $K = 4.5$.

c. Unstable for $a = 0.25, b = 3$, and $K = 5$.

d. Stable for all a, b, and K in the given intervals.

14. Consider the feedback control system in Figure 12.52 with $G_p(s) = 1$ and $G(s) = \frac{1}{Js^2}$. The nominal value of $J = 5$, but it is known to change with time. It is thus necessary to design controller with sufficient phase margin to retain stability as J changes. A suitable PID controller such that the phase margin is greater than $P.M. > 40°$ and bandwidth $\omega_b < 20$ rad/s is which of the following:

a. $G_c(s) = \frac{50(s^2 + 10s + 26)}{s}$

b. $G_c(s) = \frac{5(s^2 + 2s + 2)}{s}$

c. $G_c(s) = \frac{60(s^2 + 20s + 200)}{s}$

d. None of the above

15. A feedback control system has the nominal characteristic equation

$$q(s) = s^3 + a_2s^2 + a_1s + a_0 = s^3 + 3s^2 + 2s + 3 = 0.$$

The process varies such that

$$2 \le a_2 \le 4, \quad 1 \le a_1 \le 3, \quad 1 \le a_0 \le 5.$$

Considering all possible combinations of coefficients a_2, a_1, and a_0 in the given intervals, the system is:

a. Stable for all combinations of coefficients.

b. Unstable for some combinations of coefficients.

c. Marginally stable for some combinations of coefficients.

d. Unstable for all combinations of coefficients.

In the following **Word Match** problems, match the term with the definition by writing the correct letter in the space provided.

a. Root sensitivity	A system that exhibits the desired performance in the presence of significant plant uncertainty.	_____
b. Additive perturbation	A controller with three terms in which the output is the sum of a proportional term, an integrating term, and a differentiating term, with an adjustable gain for each term.	_____

Determine which of the following PID controllers results in a closed-loop system possessing two pairs of equal roots.

a. $G_c(s) = \frac{22.5(s + 1.11)^2}{s}$

b. $G_c(s) = \frac{10.5(s + 1.11)^2}{s}$

c. $G_c(s) = \frac{2.5(s + 2.3)^2}{s}$

d. None of the above

10. Consider the system in Figure 12.52 with $G_p(s) = 1$,

$$G(s) = \frac{b}{s^2 + as + b},$$

and $1 \le a \le 3$ and $7 \le b \le 11$. Which of the following PID controllers yields a robustly stable system?

a. $G_c(s) = \frac{13.5(s + 1.2)^2}{s}$

b. $G_c(s) = \frac{10(s + 100)^2}{s}$

c. $G_c(s) = \frac{0.1(s + 10)^2}{s}$

d. None of the above

11. Consider the system in Figure 12.52 with $G_p(s) = 1$ and loop transfer function

$$L(s) = G_c(s)G(s) = \frac{K}{s(s+5)}.$$

The sensitivity of the closed-loop system with respect to variations in the parameter K is

a. $S_K^T = \frac{s(s+3)}{s^2 + 3s + K}$

b. $S_K^T = \frac{s+5}{s^2 + 5s + K}$

c. $S_K^T = \frac{s}{s^2 + 5s + K}$

d. $S_K^T = \frac{s(s+5)}{s^2 + 5s + K}$

12. Consider the feedback control system in Figure 12.52 with plant

$$G(s) = \frac{1}{s+2}.$$

A proportional-plus-integral (PI) controller and prefilter pair that results in a settling time $T_s < 1.8$ seconds and an ITAE step response are which of the following:

a. $G_c(s) = 3.2 + \frac{13.8}{s}$ and $G_p(s) = \frac{13.8}{3.2s + 13.8}$

b. $G_c(s) = 10 + \frac{10}{s}$ and $G_p(s) = \frac{1}{s+1}$

with $K = 10$ and negative unity feedback with a PD compensator

$$G_c(s) = K_P + K_D s.$$

The objective is to design $G_c(s)$ so that the overshoot to a step is less than 5% and the settling time (with a 2% criterion) is less than 3 sec. Find a suitable $G_c(s)$. What is the effect of varying the process gain $5 \le K \le 20$ on the percent overshoot and settling time?

E12.6 Consider the control system shown in Figure E12.6 when $G(s) = 1/(s+5)^2$, and select a PID controller so that the settling time (with a 2% criterion) is less than 1.5 second for an ITAE step response. Plot $y(t)$ for a step input $r(t)$ with and without a prefilter. Determine and plot $y(t)$ for a step disturbance. Discuss the effectiveness of the system.

Answer: One possible controller is

$$G_c(s) = \frac{0.5s^2 + 52.4s + 216}{s}.$$

E12.7 For the control system of Figure E12.6 with $G(s) = 1/(s+4)^2$, select a PID controller to achieve a settling time (with a 2% criterion) of less than 1.0 second for an ITAE step response. Plot $y(t)$ for a step input $r(t)$ with and without a prefilter. Determine and plot $y(t)$ for a step disturbance. Discuss the effectiveness of the system.

E12.8 Repeat Exercise 12.6, striving to achieve a minimum settling time while adding the constraint that $|u(t)| \le 80$ for $t > 0$ for a unit step input, $r(t) = 1, t \ge 0$.

Answer: $G_c(s) = \frac{3600 + 80s}{s}$.

E12.9 A system has the form shown in Figure E12.6 with

$$G(s) = \frac{K}{s(s+7)(s+9)},$$

where $K = 1$. Design a PD controller such that the dominant closed-loop poles possess a damping ratio of $\zeta = 0.6$. Determine the step response of the system. Predict the effect of a change in K of ±50% on the percent overshoot. Estimate the step response of the worst-case system.

E12.10 A system has the form shown in Figure E12.6 with

$$G(s) = \frac{K}{s(s+3)(s+6)},$$

where $K = 1$. Design a PI controller so that the dominant roots have a damping ratio $\zeta = 0.70$. Determine the step response of the system. Predict the effect of a change in K of ±50% on the percent overshoot. Estimate the step response of the worst-case system.

E12.11 Consider the closed-loop system represented in state variable form

$$\dot{\mathbf{x}} = \mathbf{A}\mathbf{x} + \mathbf{B}r$$
$$y = \mathbf{C}\mathbf{x} + \mathbf{D}r,$$

where

$$\mathbf{A} = \begin{bmatrix} 0 & 1 \\ -4 & -k \end{bmatrix},$$

$$\mathbf{B} = \begin{bmatrix} 0 \\ 1 \end{bmatrix}, \mathbf{C} = [5 \quad 0], \text{ and } \mathbf{D} = [0].$$

The nominal value of $k = 2$. However, the value of k can vary in the range $0.1 \le k \le 4$. Plot the percent overshoot to a unit step input as k varies from 0.1 to 4.

E12.12 Consider the second-order system

$$\dot{\mathbf{x}} = \begin{bmatrix} 0 & 1 \\ -a & -b \end{bmatrix}\mathbf{x} + \begin{bmatrix} c_1 \\ c_2 \end{bmatrix}u$$
$$y = [1 \quad 0]\mathbf{x} + [0]u.$$

The parameters a, b, c_1, and c_2 are unknown *a priori*. Under what conditions is the system completely controllable? Select valid values of a, b, c_1, and c_2 to ensure controllability and plot the step response.

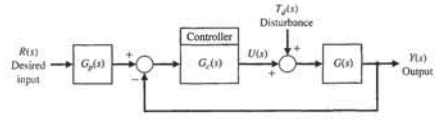

FIGURE E12.6
System with controller.

c. Complementary sensitivity function	A transfer function that filters the input signal $R(s)$ prior to the calculation of the error signal.	_____
d. Robust control system	A system perturbation model expressed in the additive form $G_a(s) = G(s) + A(s)$ where $G(s)$ is the nominal plant, $A(s)$ is the perturbation that is bounded in magnitude, and $G_a(s)$ is the family of perturbed plants.	_____
e. System sensitivity	The function $C(s) = G_c(s)G(s)[1 + G_c(s)G(s)]^{-1}$ that satisfies the relationship $C(s) + S(s) = 1$, where $S(s)$ is the sensitivity function.	_____
f. Multiplicative perturbation	The principle that states that if $G_c(s)G(s)$ contains the input $R(s)$, then the output $y(t)$ will track the input asymptotically (in the steady state) and the tracking is robust.	_____
g. PID controller	A system perturbation model expressed in the multiplicative form $G_m(s) = G(s)[1 + M(s)]$ where $G(s)$ is the nominal plant, $M(s)$ is the perturbation that is bounded in magnitude, and $G_m(s)$ is the family of perturbed plants.	_____
h. Robust stability criterion	A test for robustness with respect to multiplicative perturbations.	_____
i. Prefilter	A measure of the sensitivity of the roots (that is, the poles and zeros) of the system to changes in a parameter.	_____
j. Sensitivity function	The function $S(s) = [1 + G_c(s)G(s)]^{-1}$ that satisfies the relationship $C(s) + S(s) = 1$, where $C(s)$ is the complementary sensitivity function.	_____
k. Internal model principle	A measure of the system sensitivity to changes in a parameter.	_____

EXERCISES

E12.1 Consider a system of the form shown in Figure 12.1, where

$$G(s) = \frac{3}{(s+3)}.$$

Using the ITAE performance method for a step input, determine the required $G_c(s)$. Assume $\omega_n = 30$ for Table 5.6. Determine the step response with and without a prefilter $G_p(s)$.

E12.2 For the ITAE design obtained in Exercise E12.1, determine the response due to a disturbance $T_d(s) = 1/s$.

E12.3 A closed-loop unity feedback system has the loop transfer function

$$L(s) = G_c(s)G(s) = \frac{25}{s(s+b)},$$

where b is normally equal to 8. Determine S_b^T and plot $|T(j\omega)|$ and $|S(j\omega)|$ on a Bode plot.

Answer: $S_b^T = \frac{-bs}{s^2 + bs + 25}$

E12.4 A PID controller is used in the system in Figure 12.1, where

$$G(s) = \frac{1}{(s+20)(s+36)}.$$

The gain K_D of the controller (Equation (12.33)) is limited to 200. Select a set of compensator zeros so that the pair of closed-loop roots is approximately equal to the zeros. Find the step response for the approximation in Equation (12.35) and the actual response, and compare them.

E12.5 A system has a process function

$$G(s) = \frac{K}{s(s+3)(s+10)}$$

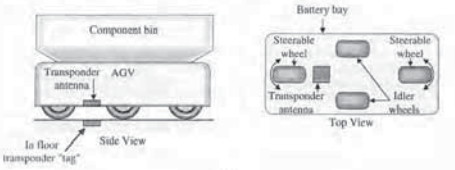

(a)

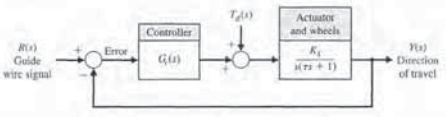

(b)

FIGURE P12.4
Automatically guided vehicle.

(d) Determine the effect of $T_d(s) = 1/s$ by plotting $y(t)$ when $R(s) = 0$.

P12.5 A roll-wrapping machine (RWM) receives, wraps, and labels large paper rolls produced in a paper mill [9, 16]. The RWM consists of several major stations: positioning station, waiting station, wrapping station, and so forth. We will focus on the positioning station shown in Figure P12.5(a). The positioning station is the first station that sees a paper roll. This station is responsible for receiving and weighing the roll, measuring its diameter and width, determining the desired

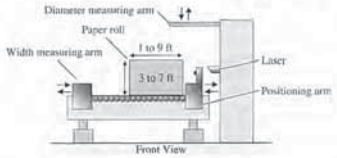

(a)

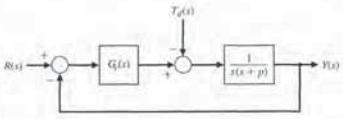

(b)

FIGURE P12.5
Roll-wrapping machine control.

PROBLEMS

P12.1 Consider the unmanned underwater vehicle (UUV) problem presented in DP4.7. The control system is shown in Figure P12.1, where $R(s) = 0$, the desired roll angle, and $T_d(s) = 1/s$. We select $G_c(s) = K(s + 2)$, where $K = 4$. (a) Plot 20 $\log|T|$ and 20 $\log|S_K'|$ on a Bode diagram. (b) Evaluate $|S_K'|$ at ω_B, $\omega_{B/2}$, and $\omega_{B/4}$ ($T(s) = Y(s)/R(s)$).

P12.2 Consider the mobile, remote-controlled video camera system presented in DP4.8. The control system is shown in Figure P12.2, where $\tau_1 = 20$ ms and $\tau_2 = 2$ ms.

(a) Select K so that $M_{pw} = 1.84$. (b) Plot 20 $\log|T|$ and 20 $\log|S_K'|$ on one Bode diagram. (c) Evaluate $|S_K'|$ at ω_B, $\omega_{B/2}$, and $\omega_{B/4}$. (d) Let $R(s) = 0$ and determine the effect of $T_d(s) = 1/s$ for the gain K of part (a) by plotting $y(t)$.

P12.3 Magnetic levitation (maglev) trains may replace airplanes on routes shorter than 200 miles. The maglev train developed by a German firm uses electromagnetic attraction to propel and levitate heavy vehicles, carrying up to 400 passengers at 300-mph speeds. But the $\frac{1}{4}$-inch gap between car and track is difficult to maintain [7, 12, 17].

The block diagram of the air-gap control system is shown in Figure P12.3. The compensator is

$$G_c(s) = \frac{K(s-1)}{(s+0.02)}.$$

(a) Find the range of K for a stable system. (b) Select a gain so that the steady-state error of the system is less than 0.1 for a step input command. (c) Find $y(t)$ for the gain of part (b). (d) Find $y(t)$ when K varies ±15% from the gain of part (b).

P12.4 An automatically guided vehicle is shown in Figure P12.4(a) and its control system is shown in Figure P12.4(b). The goal is to track the guide wire accurately, to be insensitive to changes in the gain K_1, and to reduce the effect of the disturbance [15, 22]. The gain K_1 is normally equal to 1 and $\tau_1 = 1/25$ second.

(a) Select a compensator $G_c(s)$ so that the percent overshoot to a step input is less than or equal to 10%, the settling time (with a 2% criterion) is less than 100 ms, and the velocity constant K_v for a ramp input is 100.

(b) For the compensator selected in part (a), determine the sensitivity of the system to small changes in K_1 by determining S_{K_1}' or $S_{K_1}^T$.

(c) If K_1 changes to 2 while $G_c(s)$ of part (a) remains unchanged, find the step response of the system and compare selected performance figures with those obtained in part (a).

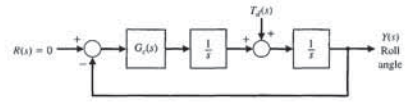

FIGURE P12.1
Control of an underwater vehicle [13].

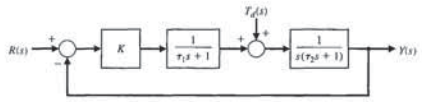

FIGURE P12.2
Remote-controlled TV camera.

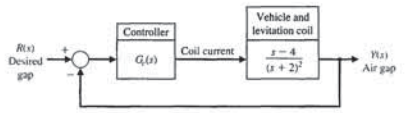

FIGURE P12.3
Maglev train control.

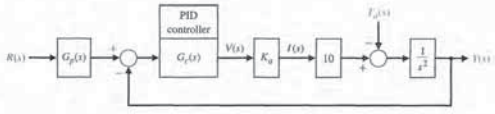

FIGURE P12.7
PID controller for the motor and load system.

The coefficients vary as follows:

$$2 \le a_2 \le 4, \quad 1 \le a_1 \le 4,$$
$$4 \le a_0 \le 5.$$

Determine whether the system is stable for these uncertain coefficients.

P12.9 Future astronauts may drive on the Moon in a pressurized vehicle, shown in Figure P12.9(a), that would have a range of 620 miles and could be used for missions of up to six months. Boeing Company engineers first analyzed the Apollo-era Lunar Roving Vehicle, then designed the new vehicle, incorporating improvements in radiation and thermal protection, shock and vibration control, and lubrication and sealants.

The steering control of the moon buggy is shown in Figure P12.9(b). The objective of the control design is to achieve a step response to a steering command with

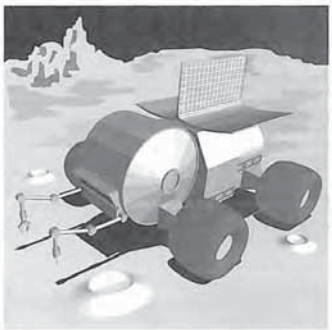

(a)

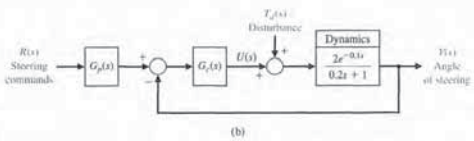

(b)

FIGURE P12.9
(a) A moon vehicle. (b) Steering control for the moon vehicle.

wrap for the roll, positioning it for downstream processing, and finally ejecting it from the station.

Functionally, the RWM can be categorized as a complex operation because each functional step (e.g., measuring the width) involves a large number of field device actions and relies upon a number of accompanying sensors.

The control system for accurately positioning the width-measuring arm is shown in Figure P12.5(b). The negative pole p of the positioning arm is normally equal to 2, but it is subject to change because of loading and misalignment of the machine. (a) For $p = 2$, design a compensator so that the complex roots are $s = -2 \pm j2\sqrt{3}$. (b) Plot $y(t)$ for a step input $R(s) = 1/s$. (c) Plot $y(t)$ for a disturbance $T_d(s) = 1/s$, with $R(s) = 0$. (d) Repeat parts (b) and (c) when p changes to 1 and $G_c(s)$ remains as designed in part (a). Compare the results for the two values of the negative pole p.

P12.6 The function of a steel plate mill is to roll reheated slabs into plates of scheduled thickness and dimension [5, 10]. The final products are of rectangular plane view shapes having a width of up to 3300 mm and a thickness of 180 mm.

A schematic layout of the mill is shown in Figure P12.6(a). The mill has two major rolling stands, denoted No. 1 and No. 2. These are equipped with large rolls (up to 508 mm in diameter), which are driven by high-power electric motors (up to 4470 kW). Roll gaps and forces are maintained by large hydraulic cylinders.

Typical operation of the mill can be described as follows. Slabs coming from the reheating furnace initially go through the No. 1 stand, whose function is to reduce the slabs to the required width. The slabs proceed through the No. 2 stand, where finishing passes are carried out to produce the required slab thickness. Finally, they go through the hot plate leveller, which gives each plate a smooth finish.

One of the key systems controls the thickness of the plates by adjusting the rolls. The block diagram of this control system is shown in Figure P12.6(b). The plant is represented by

$$G(s) = \frac{1}{s(s^2 + 4s + 5)}.$$

The controller is a PID with two equal real zeros. (a) Select the PID zeros and the gains so that the closed-loop system has two pairs of equal roots. (b) For the design of part (a), obtain the step response without a prefilter ($G_p(s) = 1$). (c) Repeat part (b) for an appropriate prefilter. (d) For the system, determine the effect of a unit step disturbance by evaluating $y(t)$ with $r(t) = 0$.

P12.7 A motor and load with negligible friction and a voltage-to-current amplifier K_a is used in the feedback control system, shown in Figure P12.7. A designer selects a PID controller

$$G_c(s) = K_P + \frac{K_I}{s} + K_D s,$$

where $K_P = 5$, $K_I = 500$, and $K_D = 0.0475$.

(a) Determine the appropriate value of K_a so that the phase margin of the system is 30°. (b) For the gain K_a, plot the root locus of the system and determine the roots of the system for the K_a of part (a). (c) Determine the maximum value of $y(t)$ when $T_d(s) = 1/s$ and $R(s) = 0$ for the K_a of part (a). (d) Determine the response to a step input $r(t)$, with and without a prefilter.

P12.8 A unity feedback system has a nominal characteristic equation

$$q(s) = s^3 + 3s^2 + 3s + 6 = 0.$$

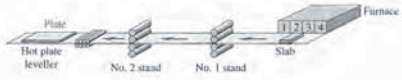

(a)

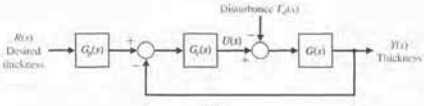

(b)

FIGURE P12.6
Steel-rolling mill control.

zero steady-state error, an overshoot less than 20%, and a peak time less than 0.3 second with a $|u(t)| \leq 50$. It is also necessary to determine the effect of a step disturbance $T_d(s) = 1/s$ when $R(s) = 0$, in order to ensure the reduction of moon surface effects. Using (a) a PI controller and (b) a PID controller, design an acceptable controller. Record the results for each design in a table. Compare the performance of each design. Use a prefilter $G_p(s)$ if necessary.

P12.10 A plant has a transfer function

$$G(s) = \frac{25}{s^2}.$$

We want to use a negative unity feedback with a PID controller and a prefilter. The goal is to achieve a peak time of 1 second with ITAE-type performance. Predict the system overshoot and settling time (with a 2% criterion) for a step input.

P12.11 Consider the three dimensional cam shown in Figure P12.11 [18]. This problem was first introduced in DP5.7. The control of x may be achieved with a DC motor and position feedback of the form shown in Figure P12.11, with the DC motor and load represented by

$$G(s) = \frac{K}{s(s + p)(s + 4)},$$

where $1 \leq K \leq 3$ and $1 \leq p \leq 3$. Normally $K = 2.5$ and $p = 2$. Design an ITAE system with a PID controller so that the peak time response to a step input is less than 3 seconds for the worst-case performance.

P12.12 Consider the closed-loop second-order system

$$\dot{\mathbf{x}} = \begin{bmatrix} 0 & 3 \\ -5 & -K \end{bmatrix}\mathbf{x} + \begin{bmatrix} 0 \\ 1 \end{bmatrix}r,$$

$$y = [2 \quad 0]\mathbf{x} + [0]u.$$

Compute the sensitivity of the closed-loop system to variations in the parameter K.

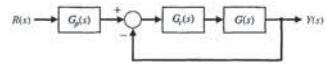

FIGURE P12.11
An x-axis control system.

ADVANCED PROBLEMS

AP12.1 To minimize vibrational effects, a telescope is magnetically levitated. This method also eliminates friction in the azimuth magnetic drive system. The photodetectors for the sensing system require electrical connections. The system block diagram is shown in Figure AP12.1. Design a PID controller so that the velocity error constant is $K_v = 100$ and the maximum overshoot for a step input is less than 10%.

AP12.2 One promising solution to traffic gridlock is a magnetic levitation (maglev) system. Vehicles are suspended on a guideway above the highway and guided by magnetic forces instead of relying on wheels or aerodynamic forces. Magnets provide the propulsion for the vehicles [7, 12, 17]. Ideally, maglev can offer the environmental and safety advantages of a high-speed train, the speed and low friction of an airplane, and the convenience of an automobile. All these shared attributes notwithstanding, the maglev system is truly a new mode of travel and will enhance the other modes of travel by relieving congestion and providing connections among them. Maglev travel would be fast, operating at 150 to 300 miles per hour.

The tilt control of a maglev vehicle is illustrated in Figures AP12.2(a) and (b). The dynamics of the plant $G(s)$ are subject to variation so that the poles will lie within the boxes shown in Figure AP12.2(c), and $1 \leq K \leq 2$.

The objective is to achieve a robust system with a step response possessing an overshoot less than 10%, as well as a settling time (with a 2% criterion) less

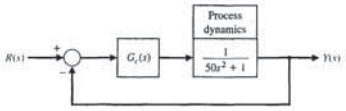

FIGURE AP12.1
Magnetically levitated telescope position control system.

than 2 seconds when $|u(t)| \leq 100$. Obtain a design with a PI, PD, and PID controller and compare the results. Use a prefilter $G_p(s)$ if necessary.

AP12.3 Antiskid braking systems present a challenging control problem, since brake/automotive system parameter variations can vary significantly (e.g., due to the brake-pad coefficient of friction changes or road slope variations) and environmental influences (e.g., due to adverse road conditions). The objective of the antiskid system is to regulate wheel slip to maximize the coefficient of friction between the tire and road for any given road surface [8]. As we expect, the braking coefficient of friction is greatest for dry asphalt, slightly reduced for wet asphalt, and greatly reduced for ice.

One simplified model of the braking system is represented by a plant transfer function $G(s)$ with a system as shown in Figure 12.16 with

$$G(s) = \frac{Y(s)}{U(s)} = \frac{1}{(s + a)(s + b)},$$

where normally $a = 1$ and $b = 4$.

(a) Using a PID controller, design a very robust system where, for a step input, the overshoot is less than 4% and the settling time (with a 2% criterion) is 1 second or less. The steady-state error must be less than 1% for a step. We expect a and b to vary by ±50%.

(b) Design a system to yield the specifications of part (a) using an ITAE performance index. Predict the overshoot and settling time for this design.

AP12.4 A robot has been designed to aid in hip-replacement surgery. The device, called RoBoDoc, is used to precisely orient and mill the femoral cavity for acceptance of the prosthetic hip implant. Clearly, we want a very robust surgical tool control, because there is no opportunity to redrill a bone [21, 27]. The control system will be as shown in Figure 12.1 with

$$G(s) = \frac{b}{s^2 + as + b},$$

where $1 \leq a \leq 2$, and $4 \leq b \leq 12$.

Select a PID controller so that the system is very robust. Use the s-plane root locus method. Select the appropriate $G_p(s)$ and plot the response to a step input.

AP12.5 Consider the system of Figure 12.1 with

$$G(s) = \frac{K_1}{s(s + 10)},$$

where $K_1 = 1$ under normal conditions. Design a PID controller to achieve a phase margin of 50°. The controller is

$$G_c(s) = \frac{K(s^2 + 20s + b)}{s}$$

with complex zeros. Determine the effect of a change of ±25% in K_1 by developing a tabular record of the phase margin as K_1 varies.

AP12.6 Consider the system of Figure 12.1 with

$$G(s) = \frac{K_1}{s(\tau s + 1)},$$

where $K_1 = 1.5$ and $\tau = 0.001$ second, which may be neglected. (Check this later in the design process.) Select a PID controller so that the settling time (with a 2% criterion) for a step input is less than 1 second and the overshoot is less than 10%. Also, the effect of a disturbance at the output must be reduced to less than 5% of the magnitude of the disturbance. Select ω_n, and use the ITAE design method.

AP12.7 Consider the system of Figure 12.1 with

$$G(s) = \frac{1}{s}.$$

The goal is to select a PI controller using the ITAE design criterion while constraining the control signal as $|u(t)| \leq 1$ for a unit step input. Determine the appropriate PI controller and the settling time (with a 2% criterion) for a step input. Use a prefilter.

AP12.8 A machine tool control system is shown in Figure AP12.8. The transfer function of the power amplifier, prime mover, moving carriage, and tool bit is

$$G(s) = \frac{50}{s(s + 1)(s + 4)(s + 5)}.$$

The goal is to have an overshoot less than 25% for a step input while achieving a peak time less than 3 seconds. Determine a suitable controller using (a) PD control, (b) PI control, and (c) PID control. (d) Then select the best controller.

AP12.9 Consider a system with the structure shown in Figure 12.1 with

$$G(s) = \frac{K}{s^2 + 2as + a^2},$$

where $1 \leq a \leq 3$ and $2 \leq K \leq 4$.

Use a PID controller and design the controller for the worst-case condition. We desire that the settling time (with a 2% criterion) be less than 0.8 second with an ITAE performance.

AP12.10 A system of the form shown in Figure 12.1 has

$$G(s) = \frac{s + r}{(s + p)(s + q)},$$

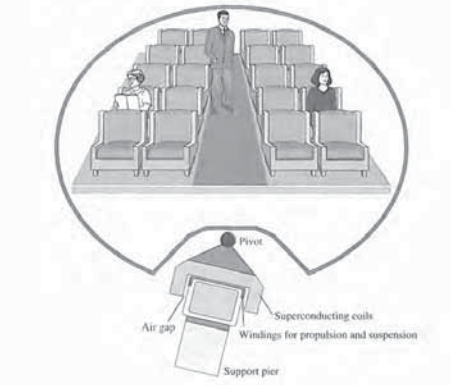

(a)

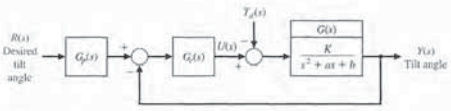

(b)

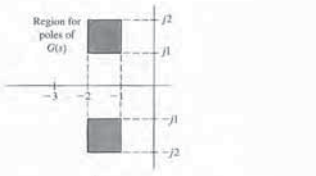

(c)

FIGURE AP12.2 (a) and (b) Tilt control for a maglev vehicle. (c) Plant dynamics.

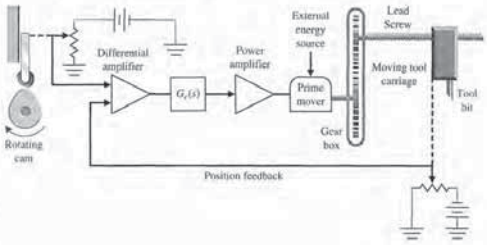

FIGURE AP12.8
A machine tool control system.

where $3 \leq p \leq 5$, $0 \leq q \leq 1$, and $1 \leq r \leq 2$. We will use a compensator

$$G_c(s) = \frac{K(s + z_1)(s + z_2)}{(s + p_1)(s + p_2)},$$

with all real poles and zeros. Select an appropriate compensator to achieve robust performance.

AP12.11 A system of the form shown in Figure 12.44 has a plant

$$G(s) = \frac{1}{(s + 2)(s + 4)(s + 6)}.$$

We want to attain a steady-state error for a step input. Select a compensator $G_c(s)$ and gain K, using the pseudo-QFT method, and determine the performance of the system when all the poles of $G(s)$ change by −50%. Describe the robust nature of the system.

DESIGN PROBLEMS

CDP12.1 Design a PID controller for the capstan-slide system of Figure CDP4.1. The percent overshoot should be less than 3% and the settling time should be (with a 2% criterion) less than 250 ms for a step input $r(t)$. Determine the response to a disturbance for the designed system.

DP12.1 A position control system for a large turntable is shown in Figure DP12.1(a), and the block diagram of the system is shown in Figure DP12.1(b) [11, 14]. This system uses a large torque motor with $K_m = 15$. The objective is to reduce the steady-state effect of a step change in the load disturbance to 5% of the magnitude of the step disturbance while maintaining a fast response to a step input command $R(s)$, with less than 5% overshoot. Select K_1 and the compensator when (a) $G_c(s) = K$ and (b) $G_c(s) = K_p + K_D s$ (a PD compensator). Plot the step response for the disturbance and the input for both compensators. Determine whether a prefilter is required to meet the overshoot requirement.

DP12.2 Consider the closed-loop system depicted in Figure DP12.2. The process has a parameter K that is nominally $K = 1$. Design a controller that results in a percent overshoot $P.O. \leq 10\%$ for a unit step input for all K in the range $0.1 \leq K \leq 2$.

DP12.3 Many university and government laboratories have constructed robot hands capable of grasping and manipulating objects. But teaching the artificial devices to perform even simple tasks required formidable computer programming. Now, however, the Dexterous Hand Master (DHM) can be worn over a human hand to record the side-to-side and bending motions of finger joints. Each joint is fitted with a sensor that changes its signal depending on position. The signals from all the sensors are translated into computer data and used to operate robot hands [1].

The DHM is shown in parts (a) and (b) of Figure DP12.3. The joint angle control system is shown in part (c). The normal value of K_m is 1.0. The goal is to design a PID controller so that the steady-state error

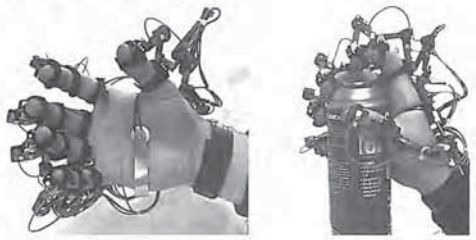

(a) (b)

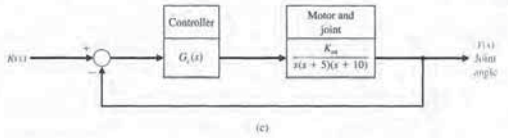

(c)

FIGURE DP12.3
Dexterous Hand Master.

microscope's tip and the surface. The control system is shown in Figure DP12.4(a), and the block diagram is shown in Figure DP12.4(b). The process is

$$G(s) = \frac{17{,}640}{s(s^2 + 59.4s + 1764)}.$$

and the controller is chosen to have two real, unequal zeros so that we have

$$G_c(s) = \frac{K_I(\tau_1 s + 1)(\tau_2 s + 1)}{s}.$$

(a) Use the ITAE design method to determine $G_c(s)$. (b) Determine the step response of the system with and without a prefilter $G_p(s)$. (c) Determine the response of the system to a disturbance when $T_d(s) = 1/s$. (d) Using the prefilter and $G_c(s)$ of parts (a) and (b), determine the actual response when the process changes to

$$G(s) = \frac{16{,}000}{s(s^2 + 40s + 1600)}.$$

DP12.5 The system described in DP12.4 is to be designed using the frequency response techniques described in Section 12.6 with

$$G_c(s) = \frac{K_I(\tau_1 s + 1)(\tau_2 s + 1)}{s}.$$

Select the coefficients of $G_c(s)$ so that the phase margin is approximately 45°. Obtain the step response of the system with and without a prefilter $G_p(s)$.

DP12.6 The use of control theory to provide insight into neurophysiology has a long history. As early as the beginning of the last century, many investigators described a muscle control phenomenon caused by the feedback action of muscle spindles and by sensors based on a combination of muscle length and rate of change of muscle length.

This analysis of muscle regulation has been based on the theory of single-input, single-output control systems. An example is a proposal that the stretch reflex is an experimental observation of a motor control strategy, namely, control of individual muscle length by the spindles. Others later proposed the regulation of individual muscle stiffness (by sensors of both length and force) as the motor control strategy [30].

One model of the human standing-balance mechanism is shown in Figure DP12.6. Consider the case of a paraplegic who has lost control of his standing mechanism. We propose to add an artificial

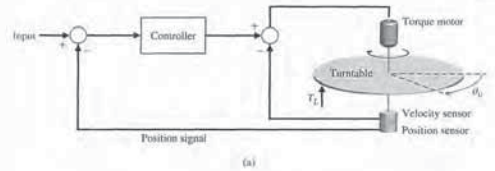

(a)

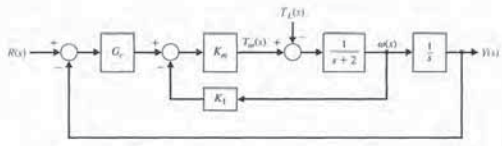

(b)

FIGURE DP12.1
Turntable control.

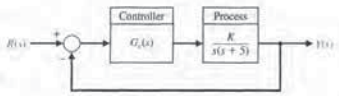

FIGURE DP12.2
A unity feedback system with a process with varying parameter K.

for a ramp input is zero. Also, the settling time (with a 2% criterion) must be less than 3 seconds for the ramp input. We want the controller to be

$$G_c(s) = \frac{K_D(s^2 + 6s + 18)}{s}.$$

(a) Select K_D and obtain the ramp response. Plot the root locus as K_D varies. (b) If K_m changes to one-half of its normal value and $G_c(s)$ remains as designed in part (a), obtain the ramp response of the system. Compare the results of parts (a) and (b) and discuss the robustness of the system.

DP12.4 Objects smaller than the wavelengths of visible light are a staple of contemporary science and technology. Biologists study single molecules of protein or DNA; materials scientists examine atomic-scale flaws in crystals; microelectronics engineers lay out circuit patterns only a few tenths of atoms thick. Until recently, this minute world could be seen only by cumbersome, often destructive methods, such as electron microscopy and X-ray diffraction. It lay beyond the reach of any instrument as simple and direct as the familiar light microscope. New microscopes, typified by the scanning tunneling microscope (STM), are now available [3].

The precision of position control required is in the order of nanometers. The STM relies on piezoelectric sensors that change size when an electric voltage across the material is changed. The "aperture" in the STM is a tiny tungsten probe, its tip ground so fine that it may consist of only a single atom and measure just 0.2 nanometer in width. Piezoelectric controls maneuver the tip to within a nanometer or two of the surface of a conducting specimen—so close that the electron clouds of the atom at the probe tip and of the nearest atom of the specimen overlap. A feedback mechanism senses the variations in tunneling current and varies the voltage applied to a third, z-axis, control. The z-axis piezoelectric moves the probe vertically to stabilize the current and to maintain a constant gap between the

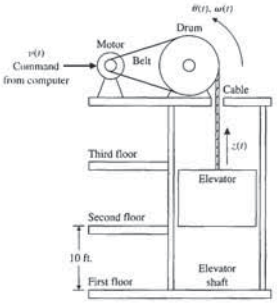

FIGURE DP12.7
Elevator position control.

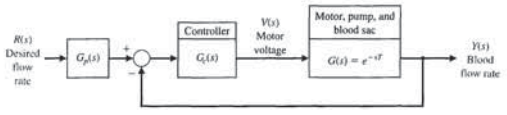

FIGURE DP12.8
Feedback control system for an electric ventricular assist device.

DP12.8 A model of the feedback control system is shown in Figure DP12.8 for an electric ventricular assist device. This problem was introduced in AP9.11. The motor, pump, and blood sac can be modeled by a time delay with $T = 1$ s. The goal is to achieve a step response with less than 5% steady-state error and less than 10% overshoot. Furthermore, to prolong the batteries, the voltage is limited to 30 V [26]. Design a controller using (a) $G_c(s) = K/s$, (b) a PI controller, and (c) a PID controller. In each case, also design the pre-filter $G_p(s)$. Compare the results for the three controllers by recording in a table the percent overshoot, peak time, settling time (with 2% criterion) and the maximum value of $v(t)$.

DP12.9 One arm of a space robot is shown in Figure DP12.9(a). The block diagram for the control of the arm is shown in Figure DP12.9(b). The transfer function of the motor and arm is

$$G(s) = \frac{1}{s(s + 10)}.$$

(a) If $G_c(s) = K$, determine the gain necessary for an overshoot of 4.5%, and plot the step response. (b) Design a proportional plus derivative (PD) controller using the ITAE method and $\omega_n = 10$. Determine the required prefilter $G_p(s)$. (c) Design a PI controller and a prefilter using the ITAE method. (d) Design a PID controller and a prefilter using the ITAE method with $\omega_n = 10$. (e) Determine the effect of a unit step disturbance for each design. Record the maximum value of $y(t)$ and the final value of $y(t)$ for the disturbance input. (f) Determine the overshoot, peak time, and settling time (with a 2% criterion) step $R(s)$ for each design above. (g) The process is subject to variation due to load changes. Find the magnitude of the sensitivity at $\omega = 5$, $|S_G^T(j5)|$, where

$$T = \frac{G_c(s)G(s)}{1 + G_c(s)G(s)}.$$

(h) Based on the results of parts (e), (f), and (g), select the best controller.

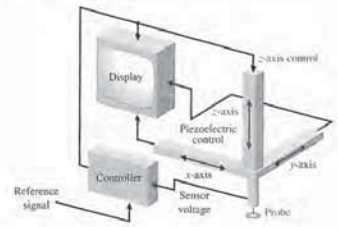

(a)

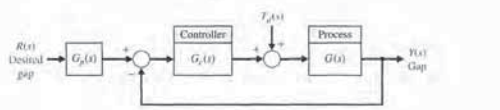

(b)

FIGURE DP12.4
Microscope control.

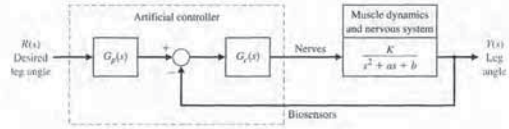

FIGURE DP12.6
Artificial control of standing and leg articulation.

controller to enable the person to stand and move his legs. (a) Design a controller when the normal values of the parameters are $K = 10$, $a = 12$, and $b = 100$, in order to achieve a step response with percent overshoot less than 10%, steady-state error less than 5%, and a settling time (with a 2% criterion) less than 2 seconds. Try a controller with proportional gain, PI, PD, and PID. (b) When the person is fatigued, the parameters may change to $K = 15$, $a = 8$, and $b = 144$. Examine the performance of this system with the controllers of part (a). Prepare a table contrasting the results of parts (a) and (b).

DP12.7 The goal is to design an elevator control system so that the elevator will move from floor to floor rapidly and stop accurately at the selected floor (Figure DP12.7). The elevator will contain from one to three occupants. However, the weight of the elevator should be greater than the weight of the occupants; you may assume that the elevator weighs 1000 pounds and each occupant weighs 150 pounds. Design a system to accurately control the elevator to within one centimeter. Assume that the large DC motor is field-controlled. Also, assume that the time constant of the motor and load is one second, the time constant of the power amplifier driving the motor is one-half second, and the time constant of the field is negligible. We seek an overshoot less than 6% and a settling time (with a 2% criterion) less than 4 seconds.

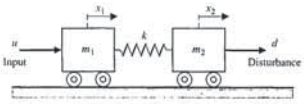

FIGURE DP12.13 Two-mass cart system.

COMPUTER PROBLEMS

CP12.1 A closed-loop feedback system is shown in Figure CP12.1. Use an m-file to obtain a plot of $|S_K^T|$ versus ω. Plot $|T(s)|$ versus ω, where $T(s)$ is the closed-loop transfer function.

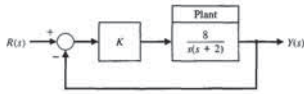

FIGURE CP12.1 Closed-loop feedback system with gain K.

CP12.2 An aircraft aileron can be modeled as a first-order system

$$G(s) = \frac{p}{s + p},$$

where p depends on the aircraft. Obtain a family of step responses for the aileron system in the feedback configuration shown in Figure CP12.2.

The nominal value of $p = 10$. Compute a reasonable value of K so that the step response (with $p = 10$) has $T_s < 0.1$s. Then, use an m-file to obtain the step responses for $0.5 < p < 20$, with the gain K as determined above. Plot the settling time as a function of p.

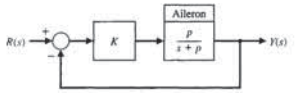

FIGURE CP12.2 Closed-loop control system for the aircraft aileron.

CP12.3 Consider the control system in Figure CP12.3, where

$$G(s) = \frac{1}{Js^2}.$$

The value of J is known to change slowly with time, although, for design purposes, the nominal value is chosen to be $J = 25$.

(a) Design a PID compensator (denoted by $G_c(s)$) to achieve a phase margin greater than 45° and a bandwidth less than 4 rad/s. (b) Using the PID controller designed in part (a), develop an m-file script to generate a plot of the phase margin as J varies from 10 to 40. At what J is the closed-loop system unstable.

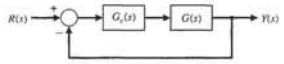

FIGURE CP12.3 A feedback control system with compensation.

CP12.4 Consider the feedback control system in Figure CP12.4. The exact value of parameter b is unknown; however, for design purposes, the nominal value is taken to be $b = 4$. The value of $a = 8$ is known very precisely.

(a) Design the proportional controller K so that the closed-loop system response to a unit step input has a settling time (with a 2% criterion) less than 5 seconds and an overshoot of less than 10%. Use the nominal value of b in the design.
(b) Investigate the effects of variations in the parameter b on the closed-loop system unit step response.

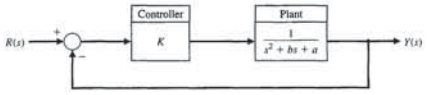

FIGURE CP12.4 A feedback control system with uncertain parameter b.

(a)

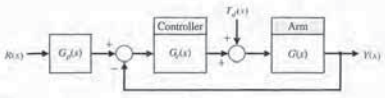

(b)

FIGURE DP12.9 Space robot control.

DP12.10 A photovoltaic system is mounted on a space station in order to develop the power for the station. The photovoltaic panels should follow the Sun with good accuracy in order to maximize the energy from the panels. The system uses a DC motor, so that the transfer function of the panel mount and the motor is

$$G(s) = \frac{1}{s(s + 19)}.$$

We will select a controller $G_c(s)$ assuming that an optical sensor is available to accurately track the sun's position, and thus $H(s) = 1$.

The goal is to design $G_c(s)$ so that (1) the percent overshoot to a step is less than 7% and (2) the steady-state error to a ramp input is less than or equal to 1%. Determine the best phase-lead controller. Examine the robustness of the system to a 10% variation in the motor time constant.

DP12.11 Electromagnetic suspension systems for air-cushioned trains are known as magnetic levitation (maglev) trains. One maglev train uses a superconducting magnet system [17]. It uses superconducting coils, and the levitation distance $x(t)$ is inherently unstable. The model of the levitation is

$$G(s) = \frac{X(s)}{V(s)} = \frac{K}{(s\tau_1 + 1)(s^2 - \omega_1^2)},$$

where $V(s)$ is the coil voltage; τ_1 is the magnet time constant; and ω_1 is the natural frequency. The system uses a position sensor with a negligible time constant. A train traveling at 250 km/hr would have $\tau_1 = 0.75$ s and $\omega_1 = 75$ rad/s. Determine a controller that can maintain steady, accurate levitation when disturbances occur along the railway. Use the system model of Figure 12.1.

DP12.12 Consider again the Mars rover problem described in DP6.2. The system uses a PID controller, and a robust system is desired. The specifications are (1) maximum overshoot equal to 18%, (2) settling time (with a 2% criterion) less than 2 seconds, (3) rise time equal to or greater than 0.20 to limit the power requirements, (4) phase margin greater than 65°, (5) gain margin greater than 8 dB, (6) maximum root sensitivity (magnitude of real and imaginary parts) less than 1. Select the best value of the gain K.

DP12.13 A benchmark problem consists of the mass–spring system shown in Figure DP12.13, which represents a flexible structure. Let $m_1 = m_2 = 1$ and $0.5 \le k \le 2.0$ [29]. It is possible to measure x_1 and x_2 and use a controller prior to $u(t)$. Obtain the system description, choose a control structure, and design a robust system. Determine the response of the system to a unit step disturbance. Assume that the output $x_3(t)$ is the variable to be controlled.

(a)

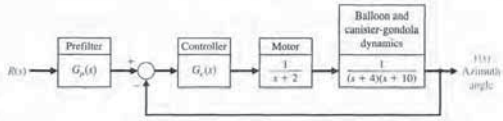

(b)

FIGURE CP12.8 The GRID device.

where a and b are to be selected. A prefilter is used as shown in Figure CP12.8(b). Determine the value of K_D, a, and b so that the dominant roots have a ζ of 0.8 and the overshoot to a step input is less than 3%. Develop a simulation to study the control system performance. Use a step response to confirm the percent overshoot meets the specification.

ANSWERS TO SKILLS CHECK

True or False: (1) True; (2) False; (3) True; (4) True; (5) False

Multiple Choice: (6) b; (7) b; (8) c; (9) d; (10) a; (11) d; (12) a; (13) c; (14) a; (15) b

Word Match (in order, top to bottom): d, g, i, b, c, k, f, h, a, j, e

TERMS AND CONCEPTS

Additive perturbation A system perturbation model expressed in the additive form $G_p(s) = G(s) + A(s)$, where $G(s)$ is the nominal process function, $A(s)$ is the perturbation that is bounded in magnitude, and $G_p(s)$ is the family of perturbed process functions.

Complementary sensitivity function The function $T(s) = \frac{G_c(s)G(s)}{1 + G_c(s)G(s)}$ that satisfies the relationship $S(s) + T(s) = 1$, where $S(s)$ is the sensitivity function. The function $T(s)$ is the closed-loop transfer function.

Internal model principle The principle that states that if $G_c(s)G(s)$ contains the input $R(s)$, then the output $y(t)$ will track $R(s)$ asymptotically (in the steady-state) and the tracking is robust.

Multiplicative perturbation A system perturbation model expressed in the multiplicative form $G_m(s) = G(s)(1 + M(s))$, where $G(s)$ is the nominal process function, $M(s)$ is the perturbation that is bounded in magnitude, and $G_m(s)$ is the family of perturbed process functions.

PID controller A controller with three terms in which the output is the sum of a proportional term, an integrating

Let $b = 0, 1, 4$, and 40, and co-plot the step response associated with each value of b. In all cases, use the proportional controller from part (a). Discuss the results.

CP12.5 A model of a flexible structure is given by

$$G(s) = \frac{(1 + k\omega_n^2)s^2 + 2\zeta\omega_n s + \omega_n^2}{s^2(s^2 + 2\zeta\omega_n s + \omega_n^2)},$$

where ω_n is the natural frequency of the flexible mode, and ζ is the corresponding damping ratio. In general, it is difficult to know the structural damping precisely, while the natural frequency can be predicted more accurately using well-established modeling techniques. Assume the nominal values of $\omega_n = 2$ rad/s, $\zeta = 0.005$, and $k = 0.1$.

(a) Design a lead compensator to meet the following specifications: (1) a closed-loop system response to a unit step input with a settling time (with a 2% criterion) less than 200 seconds and (2) an overshoot of less than 50%.
(b) With the controller from part (a), investigate the closed-loop system unit step response with $\zeta = 0, 0.005, 0.1$, and 1. Co-plot the various unit step responses and discuss the results.
(c) From a control system point of view, is it preferable to have the actual flexible structure damping less than or greater than the design value? Explain.

CP12.6 The industrial process shown in Figure CP12.6 is known to have a time delay in the loop. In practice, it is often the case that the magnitude of system time delays cannot be precisely determined. The magnitude of the time delay may change in an unpredictable manner depending on the process environment. A robust control system should be able to operate satisfactorily in the presence of the system time delays.

(a) Develop an m-file script to compute and plot the phase margin for the industrial process in Figure CP12.6 when the time delay, T, varies between 0 and 5 seconds. Use the pade function with a second-order approximation to approximate the time delay. Plot the phase margin as a function of the time delay.
(b) Determine the maximum time delay allowable for system stability. Use the plot generated in part (a) to compute the maximum time delay approximately.

CP12.7 A unity negative feedback loop has the loop transfer function

$$G_c(s)G(s) = \frac{a(s - 0.5)}{s^2 + 2s + 1}.$$

We know from the underlying physics of the problem that the parameter a can vary only between $0 < a < 1$. Develop an m-file script to generate the following plots:

(a) The steady-state tracking error due to a negative unit step input (i.e., $R(s) = -1/s$) versus the parameter a.
(b) The maximum percent initial undershoot (or overshoot) versus parameter a.
(c) The gain margin versus the parameter a.
(d) Based on the results in parts (a)–(c), comment on the robustness of the system to changes in parameter a in terms of steady-state errors, stability, and transient time response.

CP12.8 The Gamma-Ray Imaging Device (GRID) is a NASA experiment to be flown on a long-duration, high-altitude balloon during the coming solar maximum. The GRID on a balloon is an instrument that will qualitatively improve hard X-ray imaging and carry out the first gamma-ray imaging for the study of solar high-energy phenomena in the next phase of peak solar activity. From its long-duration balloon platform, GRID will observe numerous hard X-ray bursts, coronal hard X-ray sources, "superhot" thermal events, and microflares [2]. Figure CP12.8(a) depicts the GRID payload attached to the balloon. The major components of the GRID experiment consist of a 5.2-meter canister and mounting gondola, a high-altitude balloon, and a cable connecting the gondola and balloon. The instrument–sun pointing requirements of the experiment are 0.1 degree pointing accuracy and 0.2 arcsecond per 4 ms pointing stability.

An optical sun sensor provides a measure of the sun–instrument angle and is modeled as a first-order system with a DC gain and a pole at $s = -500$. A torque motor actuates the canister/gondola assembly. The azimuth angle control system is shown in Figure CP12.8(b). The PID controller is selected by the design team so that

$$G_c(s) = \frac{K_p(s^2 + as + b)}{s}.$$

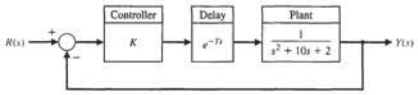

FIGURE CP12.6 An industrial controlled process with a time delay in the loop.

CHAPTER

13 Digital Control Systems

PREVIEW

A digital computer often hosts the controller algorithm in a feedback control system. Since the computer receives data only at specific intervals, it is necessary to develop a method for describing and analyzing the performance of computer control systems. In this chapter, we provide an introduction to the topic of digital control systems. The notion of a sampled-data system is presented followed by a discussion of the z-transform. We may use the z-transform of a transfer function to analyze the stability and transient response of a system. The basics of closed-loop stability with a digital controller in the loop are covered with a short presentation on the role of root locus in the design process. This chapter concludes with the design of a digital controller for the Sequential Design Example: Disk Drive Read System.

DESIRED OUTCOMES

Upon completion of Chapter 13, students should:

- ❑ Understand the role of digital computers in control system design and application.
- ❑ Be familiar with the z-transform and sampled-data systems.
- ❑ Be able to design digital controllers using root locus methods.
- ❑ Appreciate the issues associated with the implementation of digital controllers.

term, and a differentiating term, with an adjustable gain for each term.

Prefilter A transfer function $G_p(s)$ that filters the input signal $R(s)$ prior to the calculation of the error signal.

Process controller *See* PID controller.

Robust control system A system that exhibits the desired performance in the presence of significant plant uncertainty.

Robust stability criterion A test for robustness with respect to multiplicative perturbations in which stability is guaranteed if $|M(j\omega)| < \left|1 + \frac{1}{G(j\omega)}\right|$, for all ω, where $M(s)$ is the multiplicative perturbation.

Root sensitivity A measure of the sensitivity of the roots (i.e., the poles and zeros) of the system to changes in a parameter defined by $S_\alpha^{r_i} = \frac{\partial r_i}{\partial \alpha / \alpha}$, where α is the parameter and r_i is the root.

Sensitivity function The function $S(s) = [1 + G_c(s)G(s)]^{-1}$ that satisfies the relationship $S(s) + T(s) = 1$, where $T(s)$ is the complementary sensitivity function.

System sensitivity A measure of the system sensitivity to changes in a parameter defined by $S_\alpha^T \approx \frac{\partial T / T}{\partial \alpha / \alpha}$, where α is the parameter and T is the system transfer function.

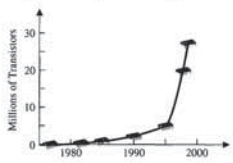

FIGURE 13.2
The development of INTEL microprocessors measured in millions of transistors. (*Source*: INTEL.)

The size of computers and the cost for the active logic devices used to construct them have both declined exponentially. The active components per cubic centimeter have increased so that the actual computer can be reduced in size to the point where relatively inexpensive, powerful laptop computers are providing mobile high-performance computational capability to students and professionals alike, and are, in many instances, replacing traditional desktop microcomputers. The speed of computers has also increased exponentially. The transistor density (a measure of computational performance) on INTEL microprocessor integrated circuits has increased exponentially over the last 30 years, as illustrated in Figure 13.2. In fact, according to "Moore's law," the transistor density doubles every year, and will probably continue to do so for the next twenty years. A simple calculation shows that by 2012, microprocessors will contain over a billion transistors with operating speeds approaching 10 GHz! In 1976, the popular 8086 central processing units containing only 29,000 transistors and operating at 10 MHz were introduced. Since then, significant progress in computation capability has been and will continue to be made. Clearly, improvements in computational capability have revolutionized the application of control theory and design in the modern era. With the availability of fast, low-priced, and small-sized microprocessors, much of the control of industrial and commercial processes is moving toward the use of computers within the control system.

Digital control systems are used in many applications: for machine tools, metal-working processes, chemical processes, aircraft control, and automobile traffic control, and others [4–8]. An example of a computer control system used in the aircraft industry is shown in Figure 13.3. Automatic computer-controlled systems are used for purposes as diverse as measuring the objective refraction of the human eye and controlling the engine spark timing or air–fuel ratio of automobile engines. The latter innovations are necessary to reduce automobile emissions and increase fuel economy.

The advantages of using digital control include: improved measurement sensitivity; the use of digitally coded signals, digital sensors and transducers, and microprocessors; reduced sensitivity to signal noise; and the capability to easily reconfigure the control algorithm in software. Improved sensitivity results from the low-energy signals required by digital sensors and devices. The use of digitally coded signals permits the wide application of digital devices and communications. Digital sensors and transducers can effectively measure, transmit, and couple signals and devices. In addition, many systems are inherently digital because they send out pulse signals. Examples of such a digital system are a radar tracking system and a space satellite.

13.1 INTRODUCTION

The use of **digital computer compensator** (controller) devices has grown during the past three decades as the price and reliability of digital computers have improved dramatically [1, 2]. A block diagram of a single-loop digital control system is shown in Figure 13.1. The digital computer in this system configuration receives the error in digital form and performs calculations in order to provide an output in digital form. The computer may be programmed to provide an output so that the performance of the process is near or equal to the desired performance. Many computers are able to receive and manipulate several inputs, so a digital computer control system can often be a multivariable system.

A digital computer receives and operates on signals in digital (numerical) form, as contrasted to continuous signals [3]. A **digital control system** uses digital signals and a digital computer to control a process. The measurement data are converted from analog form to digital form by means of the analog-to-digital converter shown in Figure 13.1. After processing the inputs, the digital computer provides an output in digital form. This output is then converted to analog form by the digital-to-analog converter shown in Figure 13.1.

13.2 DIGITAL COMPUTER CONTROL SYSTEM APPLICATIONS

The total number of computer control systems installed in industry has grown over the past three decades [2]. Currently, there are approximately 100 million control systems using computers, although the computer size and power may vary significantly. If we consider only computer control systems of a relatively complex nature, such as chemical process control or aircraft control, the number of computer control systems is approximately 20 million.

A digital computer consists of a central processing unit (CPU), input–output units, and a memory unit. The size and power of a computer will vary according to the size, speed, and power of the CPU, as well as the size, speed, and organization of the memory unit. Small computers, called **minicomputers**, have become increasingly common since 1980. Powerful but inexpensive computers, called **microcomputers**, which use a 16-bit word or 32-bit word, have become readily available. These systems use a microprocessor as a CPU. Therefore, the nature of the control task, the extent of the data required in memory, and the speed of calculation required will dictate the selection of the computer within the range of available computers.

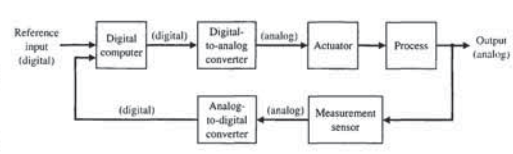

FIGURE 13.1
A block diagram of a computer control system, including the signal converters. The signal is indicated as digital or analog.

FIGURE 13.3 The flight deck of the Boeing 757 and 767 features digital control electronics, including an engine indicating system and a crew alerting system. All systems controls are within reach of either pilot. The system includes an inertial reference system making use of laser gyroscopes and an electronic attitude director indicator. A flight-management computer system integrates navigation, guidance, and performance data functions. When coupled with the automatic flight control system, the flight-management system provides accurate engine thrust settings and flight-path guidance during all phases of flight from immediately after takeoff to final approach and landing. (Courtesy of Boeing Airplane Co.)

13.3 SAMPLED-DATA SYSTEMS

Computers used in control systems are interconnected to the actuator and the process by means of signal converters. The output of the computer is processed by a digital-to-analog converter. We will assume that all the numbers that enter or leave the computer do so at the same fixed period T, called the **sampling period**. Thus, for example, the reference input shown in Figure 13.4 is a sequence of sample values $r(kT)$. The variables $r(kT)$, $m(kT)$, and $u(kT)$ are discrete signals in contrast to $m(t)$ and $y(t)$, which are continuous functions of time.

Sampled data (or a discrete signal) are data obtained for the system variables only at discrete intervals and are denoted as $x(kT)$.

A system where part of the system acts on sampled data is called a **sampled-data system**. A sampler is basically a switch that closes every T seconds for one instant of time. Consider an ideal sampler, as shown in Figure 13.5. The input is $r(t)$, and the

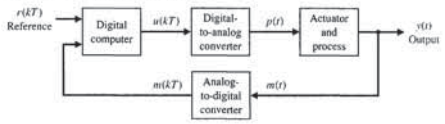

FIGURE 13.4
A digital control system.

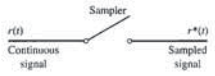

FIGURE 13.5
An ideal sampler with an input $r(t)$.

output is $r^*(t)$, where nT is the current sample time, and the current value of $r^*(t)$ is $r(nT)$. We then have $r^*(t) = r(nT)\delta(t - nT)$, where δ is the impulse function.

Let us assume that we sample a signal $r(t)$, as shown in Figure 13.5, and obtain $r^*(t)$. Then, we portray the series for $r^*(t)$ as a string of impulses starting at $t = 0$, spaced at T seconds, and of amplitude $r(kT)$. For example, consider the input signal $r(t)$ shown in Figure 13.6(a). The sampled signal is shown in Figure 13.6(b) with an impulse represented by a vertical arrow of magnitude $r(kT)$.

A digital-to-analog converter serves as a device that converts the sampled signal $r^*(t)$ to a continuous signal $p(t)$. The digital-to-analog converter can usually be represented by a zero-order hold circuit, as shown in Figure 13.7. The zero-order hold takes the value $r(kT)$ and holds it constant for $kT \leq t < (k + 1)T$, as shown in Figure 13.8 for $k = 0$. Thus, we use $r(kT)$ during the sampling period.

A sampler and zero-order hold can accurately follow the input signal if T is small compared to the transient changes in the signal. The response of a sampler

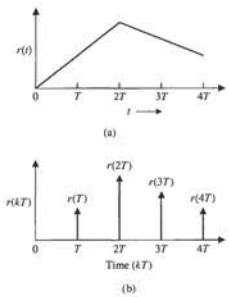

FIGURE 13.6
(a) An input signal $r(t)$. (b) The sampled signal $r^*(t) = \sum_{k=0}^{4} r(kT)\delta(t - kT)$. The vertical arrow represents an impulse.

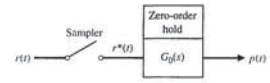

FIGURE 13.7
A sampler and zero-order hold circuit.

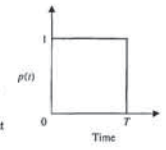

FIGURE 13.8
The response of a zero-order hold to an impulse input $r(kT)$, which equals unity when $k = 0$ and equals zero when $k \neq 0$, so that $r^*(t) = r(0)\delta(t)$.

and zero-order hold for a ramp input is shown in Figure 13.9. Finally, the response of a sampler and zero-order hold for an exponentially decaying signal is shown in Figure 13.10 for two values of the sampling period. Clearly, the output $p(t)$ will approach the input $r(t)$ as T approaches zero, meaning that we sample frequently.

The impulse response of a zero-order hold is shown in Figure 13.8. The transfer function of the **zero-order hold** is

$$G_0(s) = \frac{1}{s} - \frac{1}{s}e^{-sT} = \frac{1 - e^{-sT}}{s}. \tag{13.1}$$

The precision of the digital computer and the associated signal converters is limited (see Figure 13.4). **Precision** is the degree of exactness or discrimination with which a quantity is stated. The precision of the computer is limited by a finite word length. The precision of the analog-to-digital converter is limited by an ability to store its output only in digital logic composed of a finite number of binary digits. The converted signal $m(kT)$ is then said to include an **amplitude quantization error**. When the quantization error and the error due to a computer's finite word size are

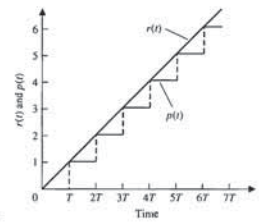

FIGURE 13.9
The response of a sampler and zero-order hold for a ramp input $r(t) = t$.

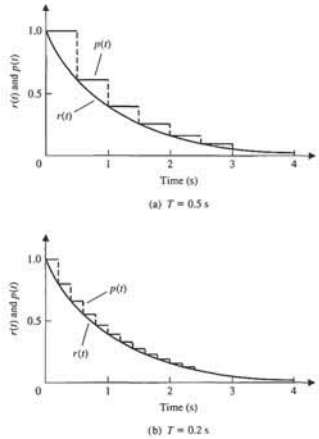

FIGURE 13.10
The response of a sampler and zero-order hold to an input $r(t) = e^{-t}$ for two values of sampling period T.

small relative to the amplitude of the signal [13, 16], the system is sufficiently precise, and the precision limitations can be neglected.

13.4 THE z-TRANSFORM

Because the output of the ideal sampler, $r^*(t)$, is a series of impulses with values $r(kT)$, we have

$$r^*(t) = \sum_{k=0}^{\infty} r(kT)\delta(t - kT), \tag{13.2}$$

for a signal for $t > 0$. Using the Laplace transform, we have

$$\mathcal{L}\{r^*(t)\} = \sum_{k=0}^{\infty} r(kT)e^{-ksT}. \tag{13.3}$$

We now have an infinite series that involves multiples of e^{sT} and its powers. We define

$$\boxed{z = e^{sT},} \tag{13.4}$$

Table 13.1 z-Transforms

$x(t)$	$X(s)$	$X(z)$
$\delta(t) = \begin{cases} \frac{1}{\epsilon}, & t < \epsilon, \epsilon \to 0 \\ 0 & \text{otherwise} \end{cases}$	1	—
$\delta(t-a) = \begin{cases} \frac{1}{\epsilon}, & a < t < a+\epsilon, \epsilon \to 0 \\ 0 & \text{otherwise} \end{cases}$	e^{-as}	—
$\delta_0(t) = \begin{cases} 1 & t = 0, \\ 0 & t = kT, k \neq 0 \end{cases}$	—	1
$\delta_0(t-kT) = \begin{cases} 1 & t = kT, \\ 0 & t \neq kT \end{cases}$	—	z^{-k}
$u(t)$, unit step	$1/s$	$\frac{z}{z-1}$
t	$1/s^2$	$\frac{Tz}{(z-1)^2}$
e^{-at}	$\frac{1}{s+a}$	$\frac{z}{z-e^{-aT}}$
$1-e^{-at}$	$\frac{1}{s(s+a)}$	$\frac{(1-e^{-aT})z}{(z-1)(z-e^{-aT})}$
$\sin(\omega t)$	$\frac{\omega}{s^2+\omega^2}$	$\frac{z\sin(\omega T)}{z^2-2z\cos(\omega T)+1}$
$\cos(\omega t)$	$\frac{s}{s^2+\omega^2}$	$\frac{z(z-\cos(\omega T))}{z^2-2z\cos(\omega T)+1}$
$e^{-at}\sin(\omega t)$	$\frac{\omega}{(s+a)^2+\omega^2}$	$\frac{(ze^{-aT}\sin(\omega T))}{z^2-2ze^{-aT}\cos(\omega T)+e^{-2aT}}$
$e^{-at}\cos(\omega t)$	$\frac{s+a}{(s+a)^2+\omega^2}$	$\frac{z^2-ze^{-aT}\cos(\omega T)}{z^2-2ze^{-aT}\cos(\omega T)+e^{-2aT}}$

Then

$$F(z) = \frac{1}{2j}\left(\frac{z}{z-e^{j\omega T}} - \frac{z}{z-e^{-j\omega T}}\right)$$
$$= \frac{1}{2j}\left(\frac{z(e^{j\omega T}-e^{-j\omega T})}{z^2 - z(e^{j\omega T}+e^{-j\omega T})+1}\right) \tag{13.12}$$
$$= \frac{z\sin(\omega T)}{z^2 - 2z\cos(\omega T)+1}. \blacksquare$$

A table of z-transforms is given in Table 13.1 and at the MCS website. Note that we use the same letter to denote both the Laplace and z-transforms, distinguishing

where this relationship involves a conformal mapping from the s-plane to the z-plane. We then define a new transform, called the z-transform, so that

$$Z\{r(t)\} = Z\{r^*(t)\} = \sum_{k=0}^{\infty} r(kT)z^{-k}. \tag{13.5}$$

As an example, let us determine the z-transform of the unit step function $u(t)$ (not to be confused with the control signal $u(t)$). We obtain

$$Z\{u(t)\} = \sum_{k=0}^{\infty} u(kT)z^{-k} = \sum_{k=0}^{\infty} z^{-k}, \tag{13.6}$$

since $u(kT) = 1$ for $k \geq 0$. This series can be written in closed form as[1]

$$U(z) = \frac{1}{1-z^{-1}} = \frac{z}{z-1}. \tag{13.7}$$

In general, we will define the **z-transform** of a function $f(t)$ as

$$\boxed{Z\{f(t)\} = F(z) = \sum_{k=0}^{\infty} f(kT)z^{-k}.} \tag{13.8}$$

EXAMPLE 13.1 **Transform of an exponential**

Let us determine the z-transform of $f(t) = e^{-at}$ for $t \geq 0$. Then

$$Z\{e^{-at}\} = F(z) = \sum_{k=0}^{\infty} e^{-akT}z^{-k} = \sum_{k=0}^{\infty} (ze^{+aT})^{-k}. \tag{13.9}$$

Again, this series can be written in closed form as

$$F(z) = \frac{1}{1-(ze^{aT})^{-1}} = \frac{z}{z-e^{-aT}}. \tag{13.10}$$

In general, we may show that

$$Z\{e^{-at}f(t)\} = F(e^{aT}z). \blacksquare$$

EXAMPLE 13.2 **Transform of a sinusoid**

Let us determine the z-transform of $f(t) = \sin(\omega t)$ for $t \geq 0$. We can write $\sin(\omega t)$ as

$$\sin(\omega t) = \frac{e^{j\omega T} - e^{-j\omega T}}{2j}.$$

Therefore,

$$\sin(\omega t) = \frac{e^{j\omega T}}{2j} - \frac{e^{-j\omega T}}{2j}. \tag{13.11}$$

[1]Recall that the infinite geometric series may be written $(1-bx)^{-1} = 1 + bx + (bx)^2 + (bx)^3 + \ldots$, if $|bx| < 1$.

Using the entries of Table 13.1 to convert from the Laplace transform to the corresponding z-transform of each term, we have

$$G(z) = (1-z^{-1})\left[\frac{Tz}{(z-1)^2} - \frac{z}{z-1} + \frac{z}{z-e^{-T}}\right]$$
$$= \frac{(ze^{-T} - z + Tz) + (1 - e^{-T} - Te^{-T})}{(z-1)(z-e^{-T})}.$$

When $T = 1$, we obtain

$$G(z) = \frac{ze^{-1} + 1 - 2e^{-1}}{(z-1)(z-e^{-1})}$$
$$= \frac{0.3678z + 0.2644}{(z-1)(z-0.3678)} = \frac{0.3678z + 0.2644}{z^2 - 1.3678z + 0.3678}. \tag{13.16}$$

The response of this system to a unit impulse is obtained for $R(z) = 1$ so that $Y(z) = G(z)\cdot 1$. We may obtain $Y(z)$ by dividing the denominator into the numerator:

$$\begin{array}{r} 0.3678z^{-1} + 0.7675z^{-2} + 0.9145z^{-3} + \ldots = Y(z) \\ z^2 - 1.3678z + 0.3678 \overline{)\,0.3678z + 0.2644} \\ \underline{0.3678z - 0.5031 + 0.1353z^{-1}} \\ + 0.7675 - 0.1353z^{-1} \\ \underline{+ 0.7675 - 1.0497z^{-1} + 0.2823z^{-2}} \\ 0.9145z^{-1} - 0.2823z^{-2} \end{array} \tag{13.17}$$

This calculation yields the response at the sampling instants and can be carried as far as is needed for $Y(z)$. From Equation (13.5), we have

$$Y(z) = \sum_{k=0}^{\infty} y(kT)z^{-k}.$$

In this case, we have obtained $y(kT)$ as follows: $y(0) = 0$, $y(T) = 0.3678$, $y(2T) = 0.7675$, and $y(3T) = 0.9145$. Note that $y(kT)$ provides the values of $y(t)$ at $t = kT$. $\blacksquare$

We have determined $Y(z)$, the z-transform of the output sampled signal. The z-transform of the input sampled signal is $R(z)$. The transfer function in the z-domain is

$$\frac{Y(z)}{R(z)} = G(z). \tag{13.18}$$

Since we determined the sampled output, we can use an output sampler to depict this condition, as shown in Figure 13.12; this represents the system of Figure 13.11

Table 13.2 Properties of the z-Transform

	$x(t)$	$X(z)$
1.	$kx(t)$	$kX(z)$
2.	$x_1(t) + x_2(t)$	$X_1(z) + X_2(z)$
3.	$x(t+T)$	$zX(z) - zx(0)$
4.	$tx(t)$	$-Tz\frac{dX(z)}{dz}$
5.	$e^{-at}x(t)$	$X(ze^{aT})$
6.	$x(0)$, initial value	$\lim_{z\to\infty} X(z)$ if the limit exists
7.	$x(\infty)$, final value	$\lim_{z\to 1}(z-1)X(z)$ if the limit exists and the system is stable; that is, if all poles of $(z-1)X(z)$ are inside the unit circle $\lvert z\rvert = 1$ on z-plane.

them by the argument s or z. A table of properties of the z-transform is given in Table 13.2. As in the case of Laplace transforms, we are ultimately interested in the output $y(t)$ of the system. Therefore, we must use an inverse transform to obtain $y(t)$ from $Y(z)$. We may obtain the output by (1) expanding $Y(z)$ in a power series, (2) expanding $Y(z)$ into partial fractions and using Table 13.1 to obtain the inverse of each term, or (3) obtaining the inverse z-transform by an inversion integral. We will limit our methods to (1) and (2) in this limited discussion.

EXAMPLE 13.3 **Transfer function of an open-loop system**

Let us consider the system shown in Figure 13.11 for $T = 1$. The transfer function of the zero-order hold (Equation 13.1) is

$$G_0(s) = \frac{1-e^{-sT}}{s}.$$

Therefore, the transfer function $Y(s)/R^*(s)$ is

$$\frac{Y(s)}{R^*(s)} = G_0(s)G_p(s) = G(s) = \frac{1-e^{-sT}}{s^2(s+1)}. \tag{13.13}$$

Expanding into partial fractions, we have

$$G(s) = (1-e^{-sT})\left(\frac{1}{s^2} - \frac{1}{s} + \frac{1}{s+1}\right) \tag{13.14}$$

$$G(z) = Z\{G(s)\} = (1-z^{-1})Z\left(\frac{1}{s^2} - \frac{1}{s} + \frac{1}{s+1}\right). \tag{13.15}$$

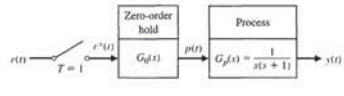

FIGURE 13.11 An open-loop, sampled-data system (without feedback).

(a)

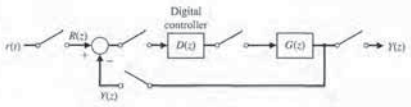

(b)

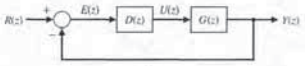

(c)

FIGURE 13.15
(a) Aibo is a sophisticated entertainment robot. Aibo looks like a Chihuahua and wags its tail, does tricks, and goes for walks. Aibo depends on a wide range of sensors, including touch, color CCD camera, range finder, and velocity sensors. A 64-bit RISC microprocessor and 16MB of memory are built in. It has 18 joints powered by 18 motors. Photo courtesy of Sony Electronics Inc. (b) Feedback control system with a digital controller. (c) Block diagram model. Note that $G(z) = Z\{G_0(s)G_p(s)\}$.

An example of a digital control system is the robotic dog Aibo, shown in Figure 13.15(a). The feedback control system of one joint with a digital controller is shown in Figure 13.15(b). The z-transform block diagram model is shown in Figure 13.15(c). The closed-loop transfer function is

$$\frac{Y(z)}{R(z)} = T(z) = \frac{G(z)D(z)}{1 + G(z)D(z)}. \tag{13.21}$$

EXAMPLE 13.4 **Response of a closed-loop system**

Now, let us consider the closed-loop system, as shown in Figure 13.16. We have obtained the z-transform model of this system, as shown in Figure 13.14. Therefore, we have

$$\frac{Y(z)}{R(z)} = \frac{G(z)}{1 + G(z)}, \tag{13.22}$$

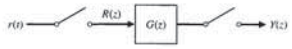

FIGURE 13.12
System with sampled output.

FIGURE 13.13
The z-transform transfer function in block diagram form.

with the sampled input passing to the process. We assume that both samplers have the same sampling period and operate synchronously. Then

$$Y(z) = G(z)R(z), \tag{13.19}$$

as required. We may represent Equation (13.19), which is a z-transform equation, by the block diagram of Figure 13.13.

13.5 CLOSED-LOOP FEEDBACK SAMPLED-DATA SYSTEMS

In this section, we consider closed-loop, sampled-data control systems. Consider the system shown in Figure 13.14(a). The sampled-data z-transform model of this figure with a sampled-output signal $Y(z)$ is shown in Figure 13.14(b). The closed-loop transfer function (using block diagram reduction) is

$$\frac{Y(z)}{R(z)} = T(z) = \frac{G(z)}{1 + G(z)}. \tag{13.20}$$

Here, we assume that the $G(z)$ is the z-transform of $G(s) = G_0(s)G_p(s)$, where $G_0(s)$ is the zero-order hold, and $G_p(s)$ is the process transfer function.

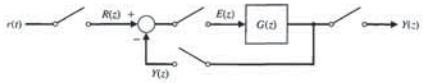

(a)

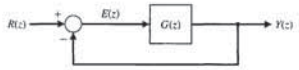

(b)

FIGURE 13.14
Feedback control system with unity feedback. $G(z)$ is the z-transform corresponding to $G(s)$, which represents the process and the zero-order hold.

A linear continuous feedback control system is stable if all poles of the closed-loop transfer function $T(s)$ lie in the left half of the s-plane. The z-plane is related to the s-plane by the transformation

$$z = e^{sT} = e^{(\sigma + j\omega)T}. \tag{13.26}$$

We may also write this relationship as

$$|z| = e^{\sigma T}$$

and

$$\angle z = \omega T. \tag{13.27}$$

In the left-hand s-plane, $\sigma < 0$; therefore, the related magnitude of z varies between 0 and 1. Thus, the imaginary axis of the s-plane corresponds to the unit circle in the z-plane, and the inside of the unit circle corresponds to the left half of the s-plane [14].

Therefore, we can state that the **stability of a sampled-data system** exists if all the poles of the closed-loop transfer function $T(z)$ lie within the unit circle of the z-plane.

EXAMPLE 13.5 **Stability of a closed-loop system**

Let us consider the system shown in Figure 13.18 when $T = 1$ and

$$G_p(s) = \frac{K}{s(s + 1)}. \tag{13.28}$$

Recalling Equation (13.16), we note that

$$G(z) = \frac{K(0.3678z + 0.2644)}{z^2 - 1.3678z + 0.3678} = \frac{K(az + b)}{z^2 - (1 + a)z + a}, \tag{13.29}$$

where $a = 0.3678$ and $b = 0.2644$.

The poles of the closed-loop transfer function $T(z)$ are the roots of the equation $1 + G(z) = 0$. We call $q(z) = 1 + G(z) = 0$ the characteristic equation. Therefore, we obtain

$$q(z) = 1 + G(z) = z^2 - (1 + a)z + a + Kaz + Kb = 0. \tag{13.30}$$

When $K = 1$, we have

$$\begin{aligned} q(z) &= z^2 - z + 0.6322 \\ &= (z - 0.50 + j0.6182)(z - 0.50 - j0.6182) = 0. \end{aligned} \tag{13.31}$$

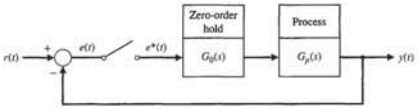

FIGURE 13.18
A closed-loop sampled system.

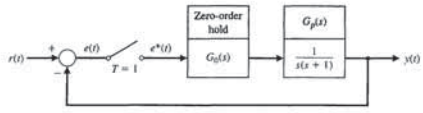

FIGURE 13.16
A closed-loop, sampled-data system.

In Example 13.3, we obtained $G(z)$ as Equation (13.16) when $T = 1$ s. Substituting $G(z)$ into Equation (13.22), we obtain

$$\frac{Y(z)}{R(z)} = \frac{0.3678z + 0.2644}{z^2 - z + 0.6322}. \tag{13.23}$$

Since the input is a unit step,

$$R(z) = \frac{z}{z - 1}, \tag{13.24}$$

it follows that

$$Y(z) = \frac{z(0.3678z + 0.2644)}{(z - 1)(z^2 - z + 0.6322)} = \frac{0.3678z^2 + 0.2644z}{z^3 - 2z^2 + 1.6322z - 0.6322}.$$

Completing the division, we have

$$Y(z) = 0.3678z^{-1} + z^{-2} + 1.4z^{-3} + 1.4z^{-4} + 1.147z^{-5} \ldots. \tag{13.25}$$

The values of $y(kT)$ are shown in Figure 13.17, using the symbol □. The complete response of the sampled-data, closed-loop system is shown and contrasted to the response of a continuous system (when $T = 0$). The overshoot of the sampled system is 45%, in contrast to 17% for the continuous system. Furthermore, the settling time of the sampled system is twice as long as that of the continuous system. ■

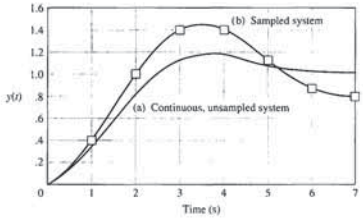

FIGURE 13.17
The response of a second-order system: (a) continuous ($T = 0$), not sampled; (b) sampled system, $T = 1$ s.

Table 13.3 Maximum Gain for a Second-Order Sampled System

	T/τ	0	0.1	0.5	1	2
Maximum	$K\tau$	∞	20.4	4.0	2.32	1.45

values of T/τ. If the computer system has sufficient speed of computation and data handling, it is possible to set $T/\tau = 0.1$ and obtain system characteristics approaching those of a continuous (nonsampled) system.

The maximum overshoot of the second-order system for a unit step input is shown in Figure 13.19.

The performance criterion, integral squared error, can be written as

$$I = \frac{1}{\tau}\int_0^\infty e^2(t)\,dt. \tag{13.38}$$

The loci of this criterion are given in Figure 13.20 for constant values of I. For a given value of T/τ, we can determine the minimum value of I and the required

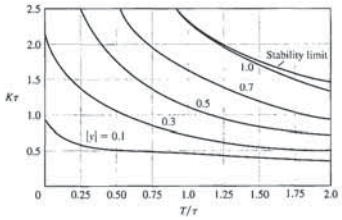

FIGURE 13.19
The maximum overshoot |z| for a second-order sampled system for a unit step input.

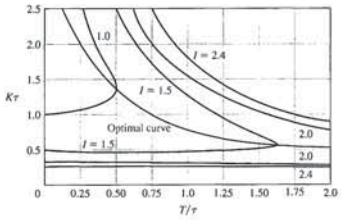

FIGURE 13.20
The loci of integral squared error for a second-order sampled system for constant values of I.

Therefore, the system is stable because the roots lie within the unit circle. When $K = 10$, we have

$$q(z) = z^2 + 2.310z + 3.012$$
$$= (z + 1.155 + j1.295)(z + 1.155 - j1.295), \tag{13.32}$$

and the system is unstable because both roots lie outside the unit circle. This system is stable for $0 < K < 2.39$. The locus of the roots as K varies is discussed in Section 13.8.

We notice that a second-order sampled system can be unstable with increasing gain where a second-order continuous system is stable for all values of gain (assuming both the poles of the open-loop system lie in the left half s-plane). ■

13.6 PERFORMANCE OF A SAMPLED-DATA, SECOND-ORDER SYSTEM

Let us consider the performance of a sampled second-order system with a zero-order hold, as shown in Figure 13.18, when the process is

$$G_p(s) = \frac{K}{s(\tau s + 1)}. \tag{13.33}$$

We then obtain $G(z)$ for the arbitrary sampling period T as

$$G(z) = \frac{K\{(z - E)[T - \tau(z - 1)] + \tau(z - 1)^2\}}{(z - 1)(z - E)}, \tag{13.34}$$

where $E = e^{-T/\tau}$. The stability of the system is analyzed by considering the characteristic equation

$$q(z) = z^2 + z\{K[T - \tau(1 - E)] - (1 + E)\} + K[\tau(1 - E) - TE] + E = 0. \tag{13.35}$$

Because the polynomial $q(z)$ is a quadratic and has real coefficients, the necessary and sufficient conditions for $q(z)$ to have all its roots within the unit circle are

$$|q(0)| < 1, \quad q(1) > 0, \quad \text{and} \quad q(-1) > 0.$$

These stability conditions for a second-order system can be established by mapping the z-plane characteristic equation into the s-plane and checking for positive coefficients of $q(s)$. Using these conditions, we establish the necessary conditions from Equation (13.35) as

$$K\tau < \frac{1 - E}{1 - E - (T/\tau)E}, \tag{13.36}$$

$$K\tau < \frac{2(1 + E)}{(T/\tau)(1 + E) - 2(1 - E)}, \tag{13.37}$$

and $K > 0, T > 0$. For this system, we can calculate the maximum gain permissible for a stable system. The maximum gain allowable is given in Table 13.3 for several

The transfer function of the computer is represented by

$$\frac{U(z)}{E(z)} = D(z). \tag{13.41}$$

In our prior calculations, $D(z)$ was represented simply by a gain K. As an illustration of the power of the computer as a compensator, we will consider again the second-order system with a zero-order hold and process

$$G_p(s) = \frac{1}{s(s + 1)} \text{ when } T = 1.$$

Then (see Equation 13.16)

$$G(z) = \frac{0.3678(z + 0.7189)}{(z - 1)(z - 0.3678)}. \tag{13.42}$$

If we select

$$D(z) = \frac{K(z - 0.3678)}{z + r}, \tag{13.43}$$

we cancel the pole of $G(z)$ at $z = 0.3678$ and have to set two parameters, r and K. If we select

$$D(z) = \frac{1.359(z - 0.3678)}{z + 0.240}, \tag{13.44}$$

we have

$$G(z)D(z) = \frac{0.50(z + 0.7189)}{(z - 1)(z + 0.240)}. \tag{13.45}$$

If we calculate the response of the system to a unit step, we find that the output is equal to the input at the fourth sampling instant and thereafter. The responses for both the uncompensated and the compensated system are shown in Figure 13.22.

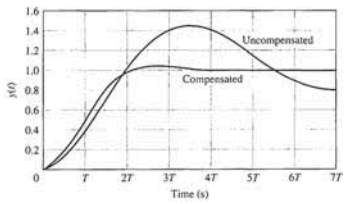

FIGURE 13.22
The response of a sampled-data second-order system to a unit step input.

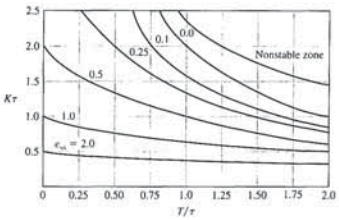

FIGURE 13.21
The steady-state error of a second-order sampled system for a unit ramp input $r(t) = t, t > 0$.

value of $K\tau$. The optimal curve shown in Figure 13.20 indicates the required $K\tau$ for a specified T/τ that minimizes I. For example, when $T/\tau = 0.75$, we require $K\tau = 1$ in order to minimize the performance criterion I.

The steady-state error for a unit ramp input $r(t) = t$ is shown in Figure 13.21. For a given T/τ, we can reduce the steady-state error, but then the system yields a greater overshoot and settling time for a step input.

EXAMPLE 13.6 **Design of a sampled system**

Let us consider a closed-loop sampled system as shown in Figure 13.18 when

$$G_p(s) = \frac{K}{s(0.1s + 1)(0.005s + 1)} \tag{13.39}$$

and we need to select T and K for suitable performance. As an approximation, we neglect the effects of the time constant $\tau_2 = 0.005$ s, because it is only 5% of the primary time constant $\tau_1 = 0.1$. Then we can use Figures 13.19, 13.20, and 13.21 to select K and T. Limiting the overshoot to 30% for the step input, we select $T/\tau = 0.25$, yielding $K\tau = 1.4$. For these values, the steady-state error for a unit ramp input is approximately 0.6 (see Figure 13.21).

Because $\tau = 0.1$, we then set $T = 0.025$ s and $K = 14$. The sampling rate is then required to be 40 samples per second.

The overshoot to the step input and the steady-state error for a ramp input may be reduced if we set T/τ to 0.1. The overshoot to a step input will be 25% for $K\tau = 1.6$. Using Figure 13.21, we estimate that the steady-state error for a unit ramp input is 0.55 for $K\tau = 1.6$. ■

13.7 CLOSED-LOOP SYSTEMS WITH DIGITAL COMPUTER COMPENSATION

A closed-loop, sampled system with a digital computer used to improve the performance is shown in Figure 13.15. The closed-loop transfer function is

$$\frac{Y(z)}{R(z)} = T(z) = \frac{G(z)D(z)}{1 + G(z)D(z)}. \tag{13.40}$$

the phase margin is 2°. Using the method of Section 10.4, we find that the required pole–zero ratio is $\alpha = 6.25$. It is specified that $\omega_c = 125$, so we note that $\omega_c = (ab)^{1/2}$. Therefore, $a = 50$ and $b = 312$. The lead compensator is then

$$G_c(s) = \frac{K(s + 50)}{s + 312}. \tag{13.51}$$

We select K in order to yield $|GG_c(j\omega)| = 1$ when $\omega = \omega_c = 125$ rad/s. Then we find that $K = 5.6$. The compensator $G_c(s)$ is to be realized by $D(z)$, so we solve the relationships with a selected sampling period. Setting $T = 0.001$ s, we have

$$A = e^{-0.05} = 0.95, \qquad B = e^{-0.312} = 0.73, \quad \text{and} \quad C = 4.85.$$

Then we have

$$D(z) = \frac{4.85(z - 0.95)}{z - 0.73}. \tag{13.52}$$

Of course, if we select another value for the sampling period, then the coefficients of $D(z)$ would differ. ■

In general, we select a small sampling period so that the design based on the continuous system will accurately carry over to the z-plane. However, we should not select too small a T, or the computation requirements may be more than necessary. In general, we use a sampling period $T \approx 1/(10f_B)$, where $f_B = \omega_B/(2\pi)$, and ω_B is the bandwidth of the closed-loop continuous system.

The bandwidth of the system designed in Example 13.7 is $\omega_B = 180$ rad/s or $f_B = 28.6$ Hz. Thus we select a period $T = 0.003$ s. Note that $T = 0.001$ s was used in Example 13.7.

13.8 THE ROOT LOCUS OF DIGITAL CONTROL SYSTEMS

Let us consider the transfer function of the system shown in Figure 13.24. Recall that $G(s) = G_0(s)G_p(s)$. The closed-loop transfer function is

$$\frac{Y(z)}{R(z)} = \frac{KG(z)D(z)}{1 + KG(z)D(z)}. \tag{13.53}$$

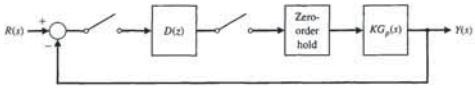

FIGURE 13.24
Closed-loop system with a digital controller.

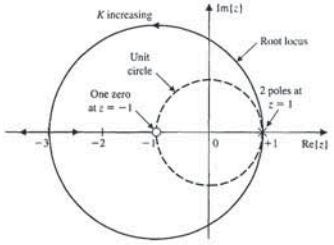

FIGURE 13.25
Root locus for Example 13.8.

Then obtain the derivative $dF(\sigma)/d\sigma = 0$ and calculate the roots as $\sigma_1 = -3$ and $\sigma_2 = 1$. The locus leaves the two poles at $\sigma_2 = 1$ and reenters at $\sigma_1 = -3$, as shown in Figure 13.25. The unit circle is also shown in Figure 13.25. The system always has two roots outside the unit circle and is always unstable for all $K > 0$. ■

We now turn to the design of a digital controller $D(z)$ to achieve a specified response utilizing a root locus method. We will select a controller

$$D(z) = \frac{z - a}{z - b}.$$

We then use $z - a$ to cancel one pole at $G(z)$ that lies on the positive real axis of the z-plane. Then we select $z - b$ so that the locus of the compensated system will give a set of complex roots at a desired point within the unit circle on the z-plane.

EXAMPLE 13.9 **Design of a digital compensator**

Let us design a compensator $D(z)$ that will result in a stable system when $G_p(s)$ is as described in Example 13.8. With $D(z) = 1$, we have an unstable system. Select

$$D(z) = \frac{z - a}{z - b}$$

so that

$$KG(z)D(z) = \frac{K(z + 1)(z - a)}{(z - 1)^2(z - b)}.$$

If we set $a = 1$ and $b = 0.2$, we have

$$KG(z)D(z) = \frac{K(z + 1)}{(z - 1)(z - 0.2)}.$$

Using the equation for $F(\sigma)$, we obtain the entry point as $z = -2.56$, as shown in Figure 13.26. The root locus is on the unit circle at $K = 0.8$. Thus, the system is stable

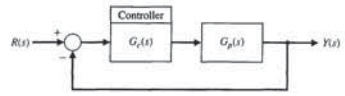

FIGURE 13.23
The continuous system model of a sampled system.

The overshoot of the compensated system is 4%, whereas the overshoot of the uncompensated system is 45%. It is beyond the objective of this book to discuss all the extensive methods for the analytical selection of the parameters of $D(z)$; other texts [2–4] can provide further information. However, we will consider two methods of compensator design: (1) the $G_c(s)$-to-$D(z)$ conversion method (in the following paragraphs) and (2) the root locus z-plane method (in Section 13.8).

One method for determining $D(z)$ first determines a controller $G_c(s)$ for a given process $G_p(s)$ for the system shown in Figure 13.23. Then, the controller is converted to $D(z)$ for the given sampling period T. The methods described in Chapter 10 are used to determine $G_c(s)$. This design method is called the $G_c(s)$-to-$D(z)$ conversion method. It converts the $G_c(s)$ of Figure 13.23 to $D(z)$ of Figure 13.15 [7].

We consider a first-order compensator

$$G_c(s) = K\frac{s + a}{s + b} \tag{13.46}$$

and a digital controller

$$\boxed{D(z) = C\frac{z - A}{z - B}.} \tag{13.47}$$

We determine the z-transform corresponding to $G_c(s)$ and set it equal to $D(z)$ as

$$Z\{G_c(s)\} = D(z). \tag{13.48}$$

Then the relationship between the two transfer functions is $A = e^{-aT}$, $B = e^{-bT}$, and when $s = 0$, we require that

$$C\frac{1 - A}{1 - B} = K\frac{a}{b}. \tag{13.49}$$

EXAMPLE 13.7 **Design to meet a phase margin specification**

Consider a system with a process

$$G_p(s) = \frac{1740}{s(0.25s + 1)}. \tag{13.50}$$

We will attempt to design $G_c(s)$ so that we achieve a phase margin of 45° with a crossover frequency $\omega_c = 125$ rad/s. Using the Bode diagram of $G_p(s)$, we find that

Table 13.4 Root Locus in the z-Plane

1. The root locus starts at the poles and progresses to the zeros.
2. The root locus lies on a section of the real axis to the left of an odd number of poles and zeros.
3. The root locus is symmetrical with respect to the horizontal real axis.
4. The root locus may break away from the real axis and may reenter the real axis. The breakaway and entry points are determined from the equation
$$K = -\frac{N(z)}{D(z)} = F(z).$$
with $z = \sigma$. Then obtain the solution of $\dfrac{dF(\sigma)}{d\sigma} = 0$.
5. Plot the locus of roots that satisfy
$$1 + KG(z)D(z) = 0,$$
or
$$|KG(z)D(z)| = 1$$
and
$$\angle G(z)D(z) = 180° \pm k360°, \qquad k = 0, 1, 2, \ldots$$

The characteristic equation is

$$\boxed{1 + KG(z)D(z) = 0,}$$

which is analogous to the characteristic equation for the s-plane analysis of $KG(s)$. Thus, we can plot the root locus for the characteristic equation of the sampled system as K varies. The rules for obtaining the root locus are summarized in Table 13.4.

EXAMPLE 13.8 **Root locus of a second-order system**

Consider the system shown in Figure 13.24 with $D(z) = 1$ and $G_p(s) = 1/s^2$. Then we obtain

$$KG(z) = \frac{T^2}{2}\frac{K(z + 1)}{(z - 1)^2}.$$

Let $T = \sqrt{2}$ and plot the root locus. We now have

$$KG(z) = \frac{K(z + 1)}{(z - 1)^2},$$

and the poles and zeros are shown on the z-plane in Figure 13.25. The characteristic equation is

$$1 + KG(z) = 1 + \frac{K(z + 1)}{(z - 1)^2} = 0.$$

Let $z = \sigma$ and solve for K to obtain

$$K = -\frac{(\sigma - 1)^2}{\sigma + 1} = F(\sigma).$$

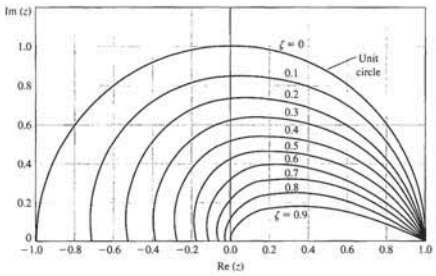

FIGURE 13.27
Curves of constant ζ on the z-plane.

The plot of these lines for constant ζ is shown in Figure 13.27 for a range of T. A common value of ζ for many design specifications is $\zeta = 1/\sqrt{2}$. Then we have $\sigma = -\omega$ and

$$z = e^{-\omega T}e^{j\omega T} = e^{-\omega T}\angle\theta,$$

where $\theta = \omega T$.

13.9 IMPLEMENTATION OF DIGITAL CONTROLLERS

We will consider the PID controller with an s-domain transfer function

$$\frac{U(s)}{X(s)} = G_c(s) = K_P + \frac{K_I}{s} + K_D s. \tag{13.54}$$

We can determine a digital implementation of this controller by using a discrete approximation for the derivative and integration. For the time derivative, we use the **backward difference rule**

$$u(kT) = \left.\frac{dx}{dt}\right|_{t=kT} = \frac{1}{T}(x(kT) - x[(k-1)T]). \tag{13.55}$$

The z-transform of Equation (13.55) is then

$$U(z) = \frac{1 - z^{-1}}{T}X(z) = \frac{z-1}{Tz}X(z).$$

The integration of $x(t)$ can be represented by the **forward-rectangular integration** at $t = kT$ as

$$u(kT) = u[(k-1)T] + Tx(kT), \tag{13.56}$$

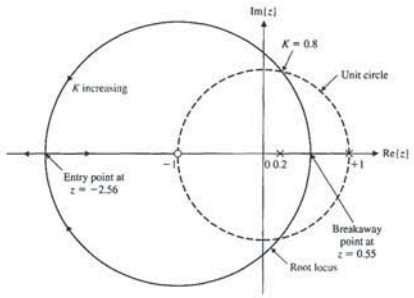

FIGURE 13.26
Root locus for Example 13.9.

for $K < 0.8$. If we select $K = 0.25$, we find that the step response has an overshoot of 20% and a settling time (with a 2% criterion) equal to 8.5 seconds.

If the system performance were inadequate, we would improve the root locus by selecting $a = 1$ and $b = -0.98$ so that

$$KG(z)D(z) = \frac{K(z+1)}{(z-1)(z+0.98)} \approx \frac{K}{z-1}.$$

Then the root locus would lie on the real axis of the z-plane. When $K = 1$, the root of the characteristic equation is at the origin, and $T(z) = 1/z = z^{-1}$. Then the response of the sampled system (at the sampling instants) is the input step delayed by one sampling period. ■

We can draw lines of constant ζ on the z-plane. The mapping between the s-plane and the z-plane is obtained by the relation $z = e^{sT}$. The lines of constant ζ on the s-plane are radial lines with

$$\frac{\sigma}{\omega} = -\tan\theta = -\tan(\sin^{-1}\zeta) = -\frac{\zeta}{\sqrt{1-\zeta^2}}.$$

Since $s = \sigma + j\omega$, we have

$$z = e^{\sigma T}e^{j\omega T},$$

where

$$\sigma = -\frac{\zeta}{\sqrt{1-\zeta^2}}\omega.$$

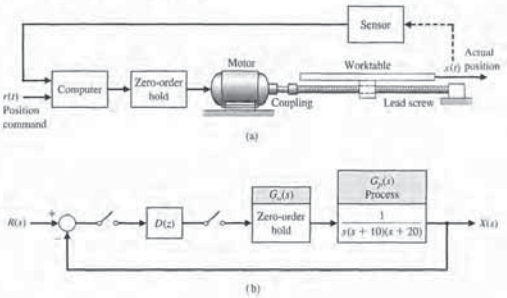

FIGURE 13.28
A table motion control system: (a) actuator and table; (b) block diagram.

To configure the system, we choose a power amplifier and motor so that the system is described by Figure 13.29. Obtaining the transfer function of the motor and power amplifier, we have

$$G_p(s) = \frac{1}{s(s+10)(s+20)}. \tag{13.59}$$

We will initially use a continuous system and design $G_c(s)$ as described in Section 13.8. We then obtain $D(z)$ from $G_c(s)$. First, we select the controller as a simple gain K in order to determine the response that can be achieved without a compensator. Plotting the root locus, we find that when $K = 700$, the dominant complex roots have a damping ratio of 0.707, and we expect a 5% overshoot. Then, using a simulation, we find that the overshoot is 5%, the rise time is 0.48 second, and the settling time (with a 2% criterion) is 1.12 seconds. These values are recorded as item 1 in Table 13.5.

The next step is to introduce a lead compensator, so that

$$G_c(s) = \frac{K(s+a)}{s+b}. \tag{13.60}$$

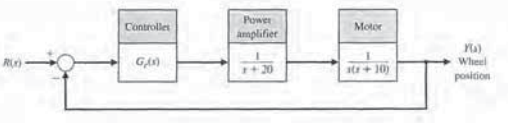

FIGURE 13.29
Model of the wheel control for a work table.

where $u(kT)$ is the output of the integrator at $t = kT$. The z-transform of Equation (13.56) is

$$U(z) = z^{-1}U(z) + TX(z),$$

and the transfer function is then

$$\frac{U(z)}{X(z)} = \frac{Tz}{z-1}.$$

Hence, the z-domain transfer function of the **PID controller** is

$$\boxed{G_c(z) = K_P + \frac{K_I T z}{z-1} + K_D\frac{z-1}{Tz}.} \tag{13.57}$$

The complete difference equation algorithm that provides the PID controller is obtained by adding the three terms to obtain [we use $x(kT) = x(k)$]

$$\begin{aligned} u(k) &= K_P x(k) + K_I[u(k-1) + Tx(k)] + (K_D/T)[x(k) - x(k-1)] \\ &= [K_P + K_I T + (K_D/T)]x(k) - K_D T x(k-1) + K_I u(k-1). \end{aligned} \tag{13.58}$$

Equation (13.58) can be implemented using a digital computer or microprocessor. Of course, we can obtain a PI or PD controller by setting an appropriate gain equal to zero.

13.10 DESIGN EXAMPLES

In this section we present two illustrative examples. In the first example, two controllers are designed to control the motor and lead screw of a movable worktable. Using a zero-order hold formulation, a proportional controller and a lead compensator are obtained and their performance compared. In the second example, a control system is designed to control an aircraft control surface as part of a fly-by-wire system. Using root locus methods, the design process focuses on the design of a digital controller to meet settling time and percent overshoot performance specifications.

EXAMPLE 13.10 Worktable motion control system

An important positioning system in manufacturing systems is a worktable motion control system. The system controls the motion of a worktable at a certain location [18]. We assume that the table is activated in each axis by a motor and lead screw, as shown in Figure 13.28(a). We consider the x-axis and examine the motion control for a feedback system, as shown in Figure 13.28(b). The goal is to obtain a fast response with a rapid rise time and settling time to a step command while not exceeding an overshoot of 5%.

The specifications are then (1) a percent overshoot equal to 5% and (2) a minimum settling time (with a 2% criterion) and rise time. Rise time is defined as the time to reach the magnitude of the command and is illustrated in Figure 5.7 by T_R.

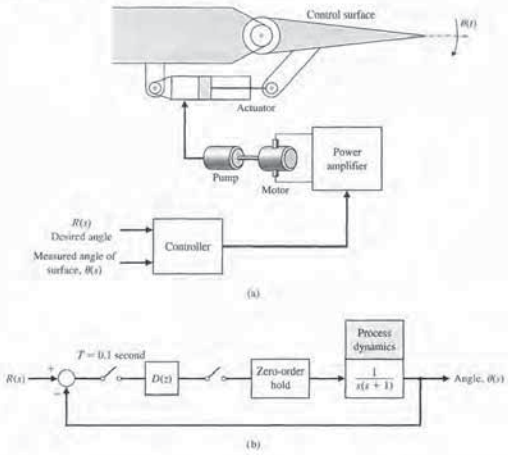

FIGURE 13.30
(a) Fly-by-wire aircraft control surface system and (b) block diagram. The sampling period is 0.1 second.

flight actuator system consists of a special type of DC motor, driven by a power amplifier, which drives a hydraulic pump that is connected to either side of a hydraulic cylinder. The piston of the hydraulic cylinder is directly connected to a control surface of an aircraft through some appropriate mechanical linkage, as shown in Figure 13.30. The elements of the design process emphasized in this example are highlighted in Figure 13.31.

The process model is given by

$$G_p(s) = \frac{1}{s(s+1)}. \tag{13.61}$$

The zero-order hold is modeled by

$$G_o(s) = \frac{1 - e^{-sT}}{s}. \tag{13.62}$$

Combining the process and the zero-order hold in series yields

$$G(s) = G_o(s)G_p(s) = \frac{1 - e^{-sT}}{s^2(s+1)}. \tag{13.63}$$

Table 13.5 Performance for Two Controllers

Compensator $G_c(s)$	K	Percent Overshoot	Settling Time (seconds)	Rise Time (seconds)
1. K	700	5.0	1.12	0.40
2. $K(s + 11)/(s + 62)$	8000	5.0	0.60	0.25

We will select the zero at $s = -11$ so that the complex roots near the origin dominate. Using the method of Section 10.5, we find that we require the pole at $s = -62$. Evaluating the gain at the roots, we find that $K = 8000$. Then the step response has a rise time of 0.25 second and a settling time (with a 2% criterion) of 0.60 second. This is an improved response, and we finalize this system as acceptable.

It now remains to select the sampling period and then use the method of Section 13.7 to obtain $D(z)$. The rise time of the compensated continuous system is 0.25 second. Then we require $T \ll T_R$ in order to obtain a system response predicted by the design of the continuous system. Let us select $T = 0.01$ s. We have

$$G_c(s) = \frac{8000(s + 11)}{s + 62}.$$

Then

$$D(z) = C\frac{z - A}{z - B},$$

where

$$A = e^{-11T} = 0.8958 \quad \text{and} \quad B = e^{-62T} = 0.5379.$$

We now have

$$C = K\frac{a(1 - B)}{b(1 - A)} = \frac{8000(11)(0.462)}{62(0.1042)} = 6293.$$

Using this $D(z)$, we expect a response very similar to that obtained for the continuous system model. ■

EXAMPLE 13.11 **Fly-by-wire aircraft control surface**

Increasing constraints on weight, performance, fuel consumption, and reliability created a need for a new type of flight control system known as fly-by-wire. This approach implies that particular system components are interconnected electrically rather than mechanically and that they operate under the supervision of a computer responsible for monitoring, controlling, and coordinating the tasks. The fly-by-wire principle allows for the implementation of totally digital and highly redundant control systems reaching a remarkable level of reliability and performance [19].

Operational characteristics of a flight control system depend on the dynamic stiffness of an actuator, which represents its ability to maintain the position of the control surface in spite of the disturbing effects of random external forces. One

We begin the design process by determining $G(z)$ from $G(s)$. Expanding $G(s)$ in Equation (13.63) in partial fractions yields

$$G(s) = (1 - e^{-sT})\left(\frac{1}{s^2} - \frac{1}{s} + \frac{1}{s+1}\right),$$

and

$$G(z) = Z\{G(s)\} = \frac{ze^{-T} - z + Tz + 1 - e^{-T} - Te^{-T}}{(z-1)(z-e^{-T})},$$

where $Z\{\cdot\}$ represents the z-transform. Choosing $T = 0.1$, we have

$$G(z) = \frac{0.004837z + 0.004679}{(z-1)(z-0.9048)}. \tag{13.64}$$

For a simple compensator, $D(z) = K$, the root locus is shown in Figure 13.32. For stability we require $K < 21$. Note that the stability region for discrete-time systems is inside the unit circle in the complex plane. Recall that for continuous-time systems, the stability region is the left half-plane.

Using an iterative approach we discover that as $K \to 21$, the step response is very oscillatory, and the percent overshoot is too large; conversely, as K gets smaller, the settling time gets too long, although the percent overshoot decreases. In any case the design specifications cannot be satisfied with a simple proportional controller, $D(z) = K$. We need to utilize a more sophisticated controller.

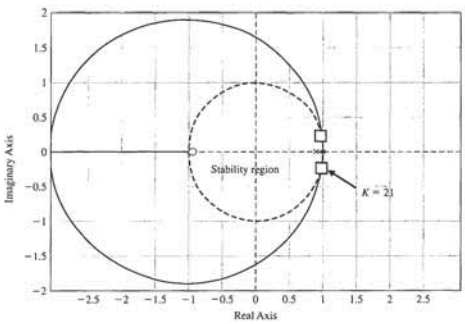

FIGURE 13.32
Root locus for $D(z) = K$.

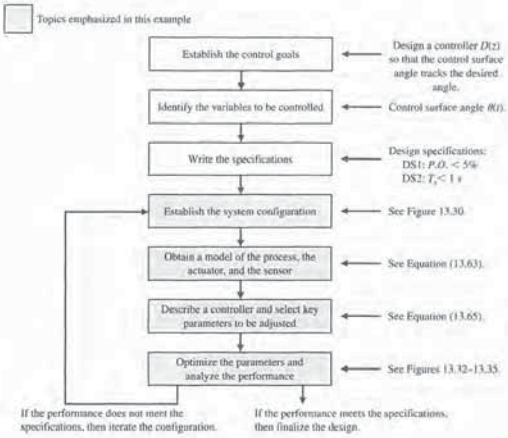

FIGURE 13.31
Elements of the control system design process emphasized in this fly-by-wire aircraft control surface example.

The control goal is to design a compensator, $D(z)$, so that the control surface angle $Y(s) = \theta(s)$ tracks the desired angle, denoted by $R(s)$. We state the control goal as

Control Goal

Design a controller $D(z)$ so that the control surface angle tracks the desired angle.

The variable to be controlled is the control surface angle $\theta(t)$:

Variable to Be Controlled

Control surface angle $\theta(t)$.

The design specifications are as follows:

Design Specifications

DS1 Percent overshoot less than 5% to a unit step input.

DS2 Settling time less than 1 second to a unit step input.

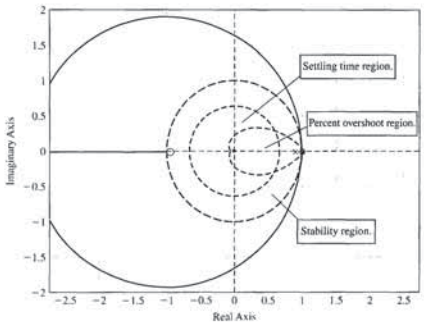

FIGURE 13.33
Root locus for $D(z) = K$ with the stability and performance regions shown.

than $\zeta \geq 0.69$. When $\zeta \geq 0.69$, the percent overshoot for a second-order system (with no zeros) will be less than 5%. The curves of constant ζ on the z-plane will define the region in the z-plane where we need to place the dominant z-plane poles to meet the percent overshoot specification.

The root locus in Figure 13.32 is repeated in Figure 13.33 with the stability and desired performance regions included. We can see that the root locus does not lie in the intersection of the stability and performance regions. The question is how to select the controller parameters K, a, and b so that the root locus lies in the desired regions.

One approach to the design is to choose a such that the pole of $G(z)$ at $z = 0.9048$ is cancelled. Then we must select b so that the root locus lies in the desired region. For example, when $a = -0.9048$ and $b = 0.25$, the compensated root locus appears as shown in Figure 13.34. The root locus lies inside the performance region, as desired.

A valid value of K is $K = 70$. Thus the compensator is

$$D(z) = 70\,\frac{z - 0.9048}{z + 0.25}.$$

The closed-loop step response is shown in Figure 13.35. Notice that the percent overshoot specification ($P.O. \leq 5\%$) is satisfied, and the system response settles in less than 10 samples (10 samples = 1 second because the sampling time is 0.1 second). ■

We have the freedom to select the controller type. As with control design for continuous-time systems, the choice of compensator is always a challenge and problem-dependent. Here we choose a compensator with the general structure

$$D(z) = K\frac{z - a}{z - b}. \tag{13.65}$$

Therefore, the key tuning parameters are the compensation parameters:

Select Key Tuning Parameters
K, a, and b.

For continuous systems we know that a design rule-of-thumb formula for the settling time is

$$T_s = \frac{4}{\zeta\omega_n},$$

where we use a 2% bound to define settling. This design rule-of-thumb is valid for second-order systems with no zeros. So to meet the T_s requirement, we want

$$-\mathrm{Re}(s_i) = \zeta\omega_n > \frac{4}{T_s}, \tag{13.66}$$

where s_i, $i = 1, 2$ are the dominant complex-conjugate poles. In the definition of the desired region of the z-plane for placing the dominant poles, we use the transform

$$z = e^{s_i T} = e^{\left(-\zeta\omega_n \pm j\omega_n\sqrt{(1-\zeta^2)}\right)T} = e^{-\zeta\omega_n T}e^{\pm j\omega_n T\sqrt{(1-\zeta^2)}}.$$

Computing the magnitude of z yields

$$r_o = |z| = e^{-\zeta\omega_n T}.$$

To meet the settling time specification, we need the z-plane poles to be inside the circle defined by

$$r_o = e^{-4T/T_s}, \tag{13.67}$$

where we have used the result in Equation (13.66).

Consider the settling time requirement $T_s < 1$ s. In our case $T = 0.1$ s. From Equation (13.67) we determine that the dominant z-plane poles should lie inside the circle defined by

$$r_o = e^{-0.4/1} = 0.67.$$

As shown previously we can draw lines of constant ζ on the z-plane. The lines of constant ζ on the s-plane are radial lines with

$$\sigma = -\omega\tan(\sin^{-1}\zeta) = -\frac{\zeta}{\sqrt{1-\zeta^2}}\omega.$$

Then, with $s = \sigma + j\omega$ and using the transform $z = e^{sT}$, we have

$$z = e^{-\sigma\omega T}e^{j\omega T}. \tag{13.68}$$

For a given ζ, we can plot $\mathrm{Re}(z)$ vs $\mathrm{Im}(z)$ for z given in Equation (13.68).

If we were working with a second-order transfer function in the s-domain, we would need to have the damping ratio associated with the dominant roots be greater

13.11 DIGITAL CONTROL SYSTEMS USING CONTROL DESIGN SOFTWARE

The process of designing and analyzing sampled-data systems is enhanced with the use of interactive computer tools. Many of the control design functions for continuous-time control design have equivalent counterparts for sampled-data systems. Discrete-time transfer function model objects are obtained with the tf function, similar to continuous time models discussed in Chapter 2. Figure 13.36 illustrates the use of tf. Model conversion can be accomplished with the functions c2d and d2c, shown in Figure 13.36. The function c2d converts continuous-time systems to discrete-time systems; the function d2c converts discrete-time systems to continuous-time systems. For example, consider the process transfer function

$$G_p(s) = \frac{1}{s(s+1)},$$

as shown in Figure 13.16. For a sampling period of $T = 1$ s, we know from Equation (13.16) that

$$G(z) = \frac{0.3678(z + 0.7189)}{(z - 1)(z - 0.3680)} = \frac{0.3679z + 0.2644}{z^2 - 1.368z + 0.3680}. \tag{13.69}$$

We can use an m-file script to obtain the $G(z)$, as shown in Figure 13.37.

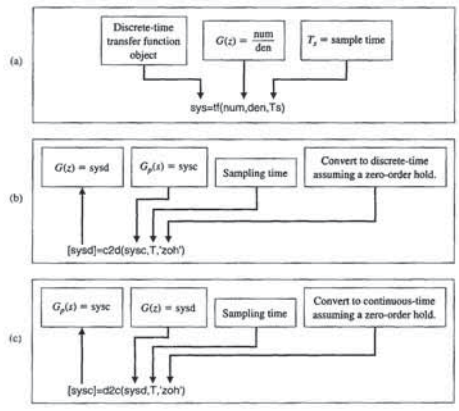

FIGURE 13.36
(a) The tf function. (b) The c2d function. (c) The d2c function.

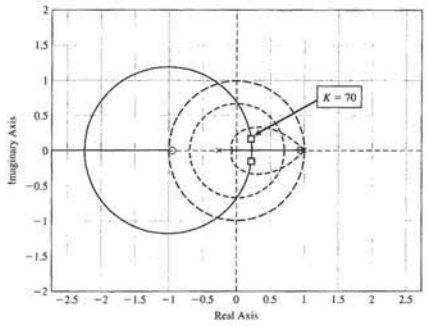

FIGURE 13.34
Compensated root locus.

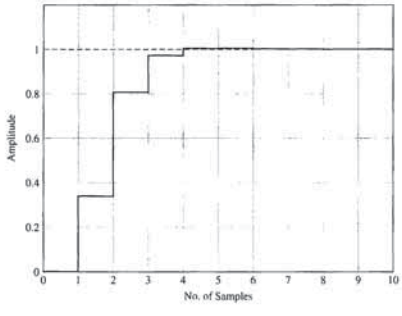

FIGURE 13.35
Closed-loop system step response.

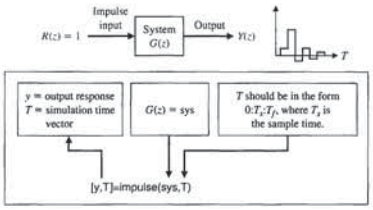

FIGURE 13.39
The **impulse** function generates the output $y(kT)$ for an impulse input.

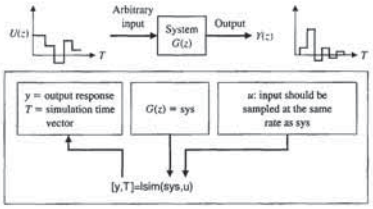

FIGURE 13.40
The **lsim** function generates the output $y(kT)$ for an arbitrary input.

using long division. We can compute the response $y(kT)$ using the step function, shown in Figure 13.38. With the closed-loop transfer function given by

$$\frac{Y(z)}{R(z)} = \frac{0.3678z + 0.2644}{z^2 - z + 0.6322},$$

the associated closed-loop step response is shown in Figure 13.41. The discrete step response shown in this figure is also shown in Figure 13.17. To determine the actual continuous response $y(t)$, we use the m-file script as shown in Figure 13.42. The zero-order hold is modeled by the transfer function

$$G_0(s) = \frac{1 - e^{-sT}}{s}.$$

In the m-file script in Figure 13.42, we approximate the e^{-sT} term using the pade function with a second-order approximation and a sampling time of 1 second.

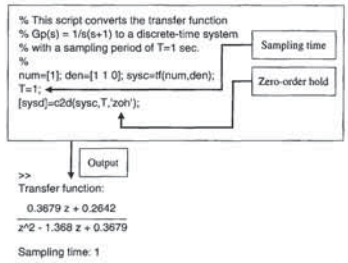

FIGURE 13.37
Using the **c2d** function to convert $G(s) = G_0(s)G_p(s)$ to $G(z)$.

The functions step, impulse, and lsim are used for simulation of sampled-data systems. The unit step response is generated by step. The step function format is shown in Figure 13.38. The unit impulse response is generated by the function impulse, and the response to an arbitrary input is obtained by the lsim function. The impulse and lsim functions are shown in Figures 13.39 and 13.40, respectively. These sampled-data system simulation functions operate in essentially the same manner as their counterparts for continuous-time (unsampled) systems. The output is $y(kT)$ and is shown as $y(kT)$ held constant for the period T.

We now consider again Example 13.4 and approach the problem of obtaining a step response without utilizing long division.

EXAMPLE 13.12 **Unit step response**

In Example 13.4, we considered the problem of computing the step response of a closed-loop sampled-data system. In that example, the response, $y(kT)$, was computed

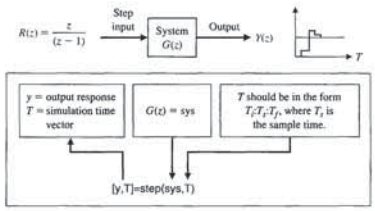

FIGURE 13.38
The **step** function generates the output $y(kT)$ for a step input.

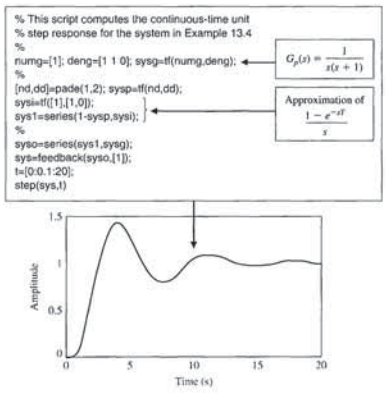

FIGURE 13.42 The continuous response $y(t)$ to a unit step for the system of Figure 13.16.

with the parameter K as a variable yet to be determined. When

$$G(z)D(z) = K\frac{0.3678(z + 0.7189)}{(z - 1)(z + 0.2400)}, \tag{13.70}$$

we have the problem in a form for which the root locus method is directly applicable. The rlocus function works for discrete-time systems in the same way as for continuous-time systems. Using a m-file script, the root locus associated with Equation (13.70) is easily generated, as shown in Figure 13.43. Remember that the stability region is defined by the unit circle in the complex plane. The function rlocfind can be used with the discrete-time system root locus in exactly the same way as for continuous-time systems to determine the value of the system gain associated with any point on the locus. Using rlocfind, we determine that $K = 4.639$ places the roots on the unit circle. ■

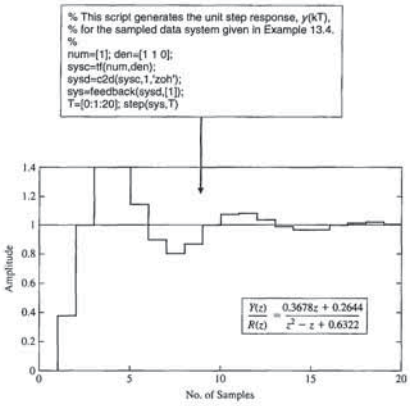

FIGURE 13.41
The discrete response, $y(kT)$, of a sampled second-order system to a unit step.

We then compute an approximation for $G_0(s)$ based on the Padé approximation of e^{-sT}. ■

The subject of digital computer compensation was discussed in Section 13.7. In the next example, we consider again the subject utilizing control design software.

EXAMPLE 13.13 **Root locus of a digital control system**

Recall from Equation (13.16) that the process was given by

$$G(z) = \frac{0.3678(z + 0.7189)}{(z - 1)(z - 0.3680)}.$$

The compensator is selected to be

$$D(z) = \frac{K(z - 0.3678)}{z + 0.2400},$$

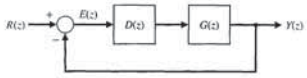

FIGURE 13.44
Feedback control system with a digital controller. Note that $G(z) = Z[G_0(s)G_p(s)]$.

we have

$$G_0(s)G_p(s) = \frac{1 - e^{-sT}}{s}\frac{5}{s(s + 20)}.$$

We note that for $s = 20$ and $T = 1$ ms, e^{-sT} is equal to 0.98. Then we see that the pole at $s = -20$ in Equation (13.71) has an insignificant effect. Therefore, we could approximate

$$G_p(s) \approx \frac{0.25}{s}.$$

Then we need

$$\begin{aligned} G(z) &= Z\left[\frac{1 - e^{-sT}}{s}\frac{0.25}{s}\right] \\ &= (1 - z^{-1})(0.25)Z\left[\frac{1}{s^2}\right] \\ &= (1 - z^{-1})(0.25)\frac{Tz}{(z - 1)^2} \\ &= \frac{0.25T}{z - 1} = \frac{0.25 \times 10^{-3}}{z - 1}. \end{aligned}$$

We need to select the digital controller $D(z)$ so that the desired response is achieved for a step input. If we set $D(z) = K$, then we have

$$D(z)G(z) = \frac{K(0.25 \times 10^{-3})}{z - 1}.$$

The root locus for this system is shown in Figure 13.45. When $K = 4000$,

$$D(z)G(z) = \frac{1}{z - 1}.$$

Therefore, the closed-loop transfer function is

$$T(z) = \frac{D(z)G(z)}{1 + D(z)G(z)} = \frac{1}{z}.$$

We expect a rapid response for the system. The percent overshoot to a step input is 0%, and the settling time is 2 ms.


```
% This script generates the root locus for
% the sampled data system
%
%     K(0.3678)(z+0.7189)
%     -------------------------------
%      (z-1)(z+0.2400)
%
num=[0.3678 0.2644]; den=[1.0000 -0.7600 -0.2400]; sys=tf(num,den);
rlocus(sys);hold on
x=[-1:0.1:1];y=sqrt(1-x.^2);
plot(x,y,'--',x,-y,'--')
```

Plot unit circle.

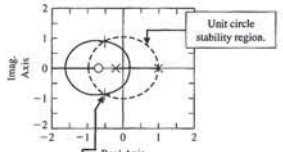

Unit circle stability region.

```
>>rlocfind(sys)
Select a point in the graphics window

selected_point =
 -0.4787 + 0.8530i

ans =
    4.6390
```

Determine K at the unit circle boundary.

$K = 4.639$

FIGURE 13.43
The **rlocus** function for sampled data systems.

13.12 SEQUENTIAL DESIGN EXAMPLE: DISK DRIVE READ SYSTEM

In this chapter, we will design a digital controller for the disk drive system. As the disk rotates, the sensor head reads the patterns used to provide the reference error information. This error information pattern is read intermittently as the head reads the stored data, and then the pattern in turn. Because the disk is rotating at a constant speed, the time T between position-error readings is a constant. This sampling period is typically 100 μs to 1 ms [20]. Thus, we have sampled error information. We may also use a digital controller, as shown in Figure 13.44, to achieve a satisfactory system response. In this section, we will design $D(z)$.

First, we determine

$$G(z) = Z[G_0(s)G_p(s)].$$

Since

$$G_p(s) = \frac{5}{s(s + 20)}, \tag{13.71}$$

In the following **True or False** and **Multiple Choice** problems, circle the correct answer.

1. A digital control system uses digital signals and a digital computer to control a process. *True or False*
2. The sampled signal is available only with limited precision. *True or False*
3. Root locus methods are not applicable to digital control system design and analysis. *True or False*
4. A sampled system is stable if all the poles of the closed-loop transfer function lie outside the unit circle of the z-plane. *True or False*
5. The z-transform is a conformal mapping from the s-plane to the z-plane by the relation $z = e^{sT}$. *True or False*
6. Consider the function in the s-domain

$$Y(s) = \frac{10}{s(s + 2)(s + 6)}.$$

Let T be the sampling time. Then, in the z-domain the function $Y(s)$ is

a. $Y(z) = \frac{5}{6}\frac{z}{z - 1} - \frac{5}{4}\frac{z}{z - e^{-2T}} + \frac{5}{12}\frac{z}{z - e^{-6T}}$

b. $Y(z) = \frac{5}{6}\frac{z}{z - 1} - \frac{5}{4}\frac{z}{z - e^{-6T}} + \frac{5}{12}\frac{z}{z - e^{-T}}$

c. $Y(z) = \frac{5}{6}\frac{z}{z - 1} - \frac{z}{z - e^{-6T}} + \frac{5}{12}\frac{z}{z - e^{-2T}}$

d. $Y(z) = \frac{1}{6}\frac{z}{z - 1} - \frac{z}{1 - e^{-2T}} + \frac{5}{6}\frac{z}{1 - e^{-6T}}$

7. The impulse response of a system is given by

$$Y(z) = \frac{z^3 + 2z^2 + 2}{z^3 - 25z^2 + 0.6z}.$$

Determine the values of $y(nT)$ at the first four sampling instants.

a. $y(0) = 1, y(T) = 27, y(2T) = 647, y(3T) = 660.05$

b. $y(0) = 0, y(T) = 27, y(2T) = 47, y(3T) = 60.05$

c. $y(0) = 1, y(T) = 27, y(2T) = 674.4, y(3T) = 16845.8$

d. $y(0) = 1, y(T) = 647, y(2T) = 47, y(3T) = 27$

8. Consider a sampled-data system with the closed-loop system transfer function

$$T(z) = K\frac{z^2 + 2z}{z^2 + 0.2z - 0.5}.$$

This system is:

a. Stable for all finite K.

b. Stable for $-0.5 < K < \infty$.

c. Unstable for all finite K.

d. Unstable for $-0.5 < K < \infty$.

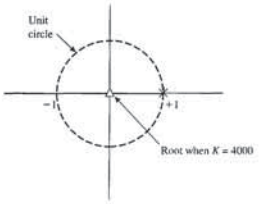

FIGURE 13.45
Root locus.

13.13 SUMMARY

The use of a digital computer as the compensation device for a closed-loop control system has grown during the past two decades as the price and reliability of computers have improved dramatically. A computer can be used to complete many calculations during the sampling interval T and to provide an output signal that is used to drive an actuator of a process. Computer control is used today for chemical processes, aircraft control, machine tools, and many common processes.

The z-transform can be used to analyze the stability and response of a sampled system and to design appropriate systems incorporating a computer. Computer control systems have become increasingly common as low-cost computers have become readily available.

SKILLS CHECK

In this section, we provide three sets of problems to test your knowledge: True or False, Multiple Choice, and Word Match. To obtain direct feedback, check your answers with the answer key provided at the conclusion of the end-of-chapter problems. Use the block diagram in Figure 13.46 as specified in the various problem statements.

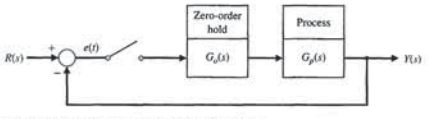

FIGURE 13.46 Block diagram for the Skills Check.

In Problems 13 and 14, consider the sampled data system with a zero-order hold where

$$G_p(s) = \frac{20}{s(s+9)}.$$

13. The closed-loop transfer function $T(z)$ of this system using a sampling period of $T = 0.5$ second is which of the following:

a. $T(z) = \dfrac{1.76z + 1.76}{z^2 + 2.76}$

b. $T(z) = \dfrac{0.87z + 0.23}{z^2 - 0.14z + 0.24}$

c. $T(z) = \dfrac{0.87z + 0.23}{z^2 - 1.01z + 0.011}$

d. $T(z) = \dfrac{0.92z + 0.46}{z^2 - 1.01z}$

14. The range of the sampling period T for which the closed-loop system is stable is:

a. $T \leq 1.12$

b. The system is stable for all $T > 0$.

c. $1.12 \leq T \leq 10$

d. $T \leq 4.23$

15. Consider a continuous-time system with the closed-loop transfer function

$$T(s) = \frac{s}{s^2 + 4s + 8}.$$

Using a zero-order hold on the inputs and a sampling period of $T = 0.02$ second, determine which of the following is the equivalent discrete-time closed-loop transfer function representation:

a. $T(z) = \dfrac{0.019z - 0.019}{z^2 + 2.76}$

b. $T(z) = \dfrac{0.87z + 0.23}{z^2 - 0.14z + 0.24}$

c. $T(z) = \dfrac{0.019z - 0.019}{z^2 - 1.9z + 0.9}$

d. $T(z) = \dfrac{0.043z - 0.02}{z^2 + 1.9231}$

In the following **Word Match** problems, match the term with the definition by writing the correct letter in the space provided.

a. Precision	A system where part of the system acts on sampled data (sampled variables).	_____
b. Digital computer compensator	The stable condition exists when all the poles of the closed-loop transfer function $T(z)$ are within the unit circle on the z-plane.	_____
c. z-plane	The plane with the vertical axis equal to the imaginary part of z and the horizontal axis equal to the real part of z.	_____
d. Backward difference rule	A control system using digital signals and a digital computer to control a process.	_____

9. The characteristic equation of a sampled system is

$$q(z) = z^2 + (2K - 1.75)z + 2.5 = 0,$$

where $K > 0$. The range of K for a stable system is:

a. $0 < K \leq 2.63$

b. $K \geq 2.63$

c. The system is stable for all $K > 0$.

d. The system is unstable for all $K > 0$.

10. Consider the unity feedback system in Figure 13.46, where

$$G_p(s) = \frac{K}{s(0.2s + 1)}$$

with the sampling time $T = 0.4$ second. The maximum value for K for a stable closed-loop system is which of the following:

a. $K = 7.25$

b. $K = 10.5$

c. Closed-loop system is stable for all finite K

d. Closed-loop system is unstable for all $K > 0$

In Problems 11 and 12, consider the sampled data system in Figure 13.46 where

$$G_p(s) = \frac{225}{s^2 + 225}.$$

11. The closed-loop transfer function $T(z)$ of this system with sampling at $T = 1$ second is

a. $T(z) = \dfrac{1.76z + 1.76}{z^2 + 3.279z + 2.76}$

b. $T(z) = \dfrac{z + 1.76}{z^2 + 2.76}$

c. $T(z) = \dfrac{1.76z + 1.76}{z^2 + 1.519z + 1}$

d. $T(z) = \dfrac{z}{z^2 + 1}$

12. The unit step response of the closed-loop system is:

a. $Y(z) = \dfrac{1.76z + 1.76}{z^2 + 3.279z + 2.76}$

b. $Y(z) = \dfrac{1.76z + 1.76}{z^3 + 2.279z^2 - 0.5194z - 2.76}$

c. $Y(z) = \dfrac{1.76z^2 + 1.76z}{z^3 + 2.279z^2 - 0.5194z - 2.76}$

d. $Y(z) = \dfrac{1.76z^2 + 1.76z}{2.279z^2 - 0.5194z - 2.76}$

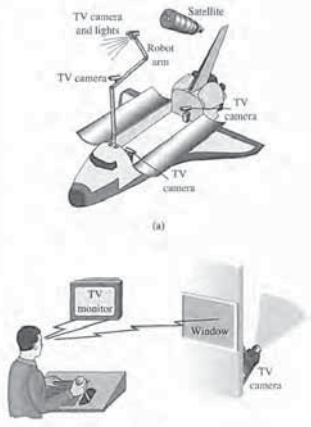

FIGURE E13.5
(a) Space shuttle and robotic arm. (b) Astronaut control of the arm.

E13.6 Computer control of a robot to spraypaint an automobile is shown by the system in Figure E13.6 [1]. The system is of the type shown in Figure 13.24, where

$$KG_p(s) = \frac{20}{s(s/2 + 1)},$$

and we want a phase margin of 45°. A compensator for this system was obtained in Section 10.8. Obtain the $D(z)$ required when $T = 0.001$ s.

E13.7 Find the response for the first four sampling instants for

$$Y(z) = \frac{z^3 + 2z^2 + 1}{z^3 - 1.5z^2 + 0.5z}.$$

Then find $y(0)$, $y(1)$, $y(2)$, and $y(3)$.

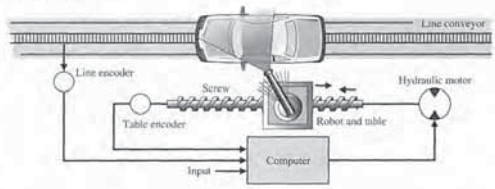

FIGURE E13.6
Automobile spraypaint system.

e. Minicomputer	Data obtained for the system variables only at discrete intervals.	_____
f. Sampled-data system	The period when all the numbers leave or enter the computer.	_____
g. Sampled data	A conformal mapping from the s-plane to the z -plane by the relation $z = e^{sT}$.	_____
h. Digital control system	The sampled signal available only with a limited precision.	_____
i. Microcomputer	A system that uses a digital computer as the compensator element.	_____
j. Forward rectangular integration	A computational method of approximating the time derivative of a function.	_____
k. Stability of a sampled-data system	A computational method of approximating the integration of a function.	_____
l. Amplitude quantization error	A small personal computer (PC) based on a microprocessor.	_____
m. PID controller	A stand-alone computer with size and performance between a microcomputer and a large mainframe.	_____
n. z-transform	A controller with three terms in which the output is the sum of a proportional term, an integral term, and a differentiating term.	_____
o. Sampling period	The degree of exactness or discrimination with which a quantity is stated.	_____
p. Zero-order hold	A mathematical model of a sample and data hold operation.	_____

EXERCISES

E13.1 State whether the following signals are discrete or continuous:

(a) Elevation contours on a map.
(b) Temperature in a room.
(c) Digital clock display.
(d) The score of a basketball game.
(e) The output of a loudspeaker.

E13.2 (a) Find the values $y(kT)$ when

$$Y(z) = \frac{z}{z^3 - 3z + 2}$$

for $k = 0$ to 4.

(b) Obtain a closed form of solution for $y(kT)$ as a function of k.

Answer: $y(0) = 0$, $y(T) = 1$, $y(2T) = 3$, $y(3T) = 7$, $y(4T) = 15$

E13.3 A system has a response $y(kT) = kT$ for $k \geq 0$. Find $Y(z)$ for this response.

Answer: $Y(z) = \dfrac{Tz}{(z-1)^2}$

E13.4 We have a function

$$Y(s) = \frac{5}{s(s+2)(s+10)}.$$

Using a partial fraction expansion of $Y(s)$ and Table 13.1, find $Y(z)$ when $T = 0.1$ s.

E13.5 The space shuttle, with its robotic arm, is shown in Figure E13.5(a). An astronaut controls the robotic arm and gripper by using a window and the TV cameras [9]. Discuss the use of digital control for this system and sketch a block diagram for the system, including a computer for display generation and control.

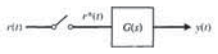

FIGURE P13.3 Sampling system.

P13.4 A closed-loop system has a hold circuit and process as shown in Figure 13.18. Determine $G(z)$ when $T = 1$ and

$$G_p(s) = \frac{2}{s+2}.$$

P13.5 For the system in Problem P13.4, let $r(t)$ be a unit step input and calculate the response of the system by synthetic division.

P13.6 For the output of the system in Problem P13.4, find the initial and final values of the output directly from $Y(z)$.

P13.7 A closed-loop system is shown in Figure 13.18. This system represents the pitch control of an aircraft. The process transfer function is $G_p(s) = K/[s(0.5s + 1)]$. Select a gain K and sampling period T so that the overshoot is limited to 0.3 for a unit step input and the steady-state error for a unit ramp input is less than 1.0.

P13.8 Consider the computer-compensated system shown in Figure 13.24 when $T = 1$ and

$$KG_p(s) = \frac{K}{s(s+10)}.$$

Select the parameters K and r of $D(z)$ when

$$D(z) = \frac{z - 0.3678}{z + r}.$$

Select within the range $1 < K < 2$ and $0 < r < 1$.

Determine the response of the compensated system and compare it with the uncompensated system.

P13.9 A suspended, mobile, remote-controlled system to bring three-dimensional mobility to professional NFL football is shown in Figure P13.9. The camera can be moved over the field as well as up and down. The motor control on each pulley is represented by Figure 13.18 with

$$G_p(s) = \frac{10}{s(s+1)(s/10+1)}.$$

We wish to achieve a phase margin of 45° using $G_c(s)$. Select a suitable crossover frequency and sampling period to obtain $D(z)$. Use the $G_c(s)$-to-$D(z)$ conversion method.

P13.10 Consider a system as shown in Figure 13.15 with a zero-order hold, a process

$$G_p(s) = \frac{1}{s(s+10)},$$

and $T = 0.1$ s.

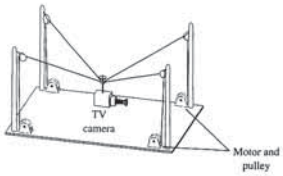

FIGURE P13.9 Mobile camera for football field.

(a) Let $D(z) = K$ and determine the transfer function $G(z)D(z)$. (b) Determine the characteristic equation of the closed-loop system. (c) Calculate the maximum value of K for a stable system. (d) Determine K such that the overshoot is less than 30%. (e) Calculate the closed-loop transfer function $T(z)$ for K of part (d) and plot the step response. (f) Determine the location of the closed-loop roots and the overshoot if K is one-half of the value determined in part (c). (g) Plot the step response for the K of part (f).

P13.11 (a) For the system described in Problem P13.10, design a lag compensator $G_c(s)$ using the methods of Chapter 10 to achieve an overshoot less than 30% and a steady-state error less than 0.01 for a ramp input. Assume a continuous nonsampled system with $G_p(s)$.

(b) Determine a suitable $D(z)$ to satisfy the requirements of part (a) with a sampling period $T = 0.1$ s. Assume a zero-order hold and sampler, and use the $G_c(s)$-to-$D(z)$ conversion method.

(c) Plot the step response of the system with the continuous-time compensator $G_c(s)$ of part (a) and of the digital system with the $D(z)$ of part (b). Compare the results.

(d) Repeat part (b) for $T = 0.01$ s and then repeat part (c).

(e) Plot the ramp response for $D(z)$ with $T = 0.1$ s and compare it with the continuous-system response.

P13.12 The transfer function of a plant and a zero-order hold (Figure 13.18) is

$$G(z) = \frac{K(z+0.5)}{z(z-1)}.$$

(a) Plot the root locus. (b) Determine the range of gain K for a stable system.

E13.8 Determine whether the closed-loop system with $T(z)$ is stable when

$$T(z) = \frac{z}{z^2 + 0.2z - 1.0}.$$

Answer: unstable

E13.9 (a) Determine $y(kT)$ for $k = 0$ to 3 when

$$Y(z) = \frac{z+1}{z^2-1}.$$

(b) Determine the closed form solution for $y(kT)$ as a function of k.

E13.10 A system has $G(z)$ as described by Equation (13.34) with $T = 0.01$ s and $\tau = 0.008$ s. (a) Find K so that the overshoot is less than 40%. (b) Determine the steady-state error in response to a unit ramp input. (c) Determine K to minimize the integral squared error.

E13.11 A system has a process transfer function

$$G_p(s) = \frac{100}{s^2 + 100}.$$

(a) Determine $G(z)$ for $G_p(s)$ preceded by a zero-order hold with $T = 0.05$ s. (b) Determine whether the digital system is stable. (c) Plot the impulse response of $G(z)$ for the first 15 samples. (d) Plot the response for a sine wave input with the same frequency as the natural frequency of the system.

E13.12 Find the z-transform of

$$X(s) = \frac{s+1}{s^2 + 5s + 6}$$

when the sampling period is 1 second.

E13.13 The characteristic equation of a sampled system is

$$z^2 + (K-4)z + 0.8 = 0.$$

Find the range of K so that the system is stable.

Answer: $2.2 < K < 5.8$

E13.14 A unity feedback system, as shown in Figure 13.18, has a plant

$$G_p(s) = \frac{K}{s(s+3)},$$

with $T = 0.5$. Determine whether the system is stable when $K = 5$. Determine the maximum value of K for stability.

E13.15 Consider the open-loop sampled-data system shown in Figure E13.15. Determine the transfer function $G(z)$ when the sampling time is $T = 1$ s.

E13.16 Consider the open-loop sampled-data system shown in Figure E13.16. Determine the transfer function $G(z)$ and when the sampling time $T = 0.5$ s.

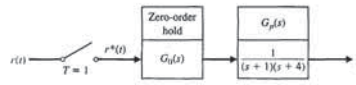

FIGURE E13.15 An open-loop sampled-data system with sampling time $T = 1$ s.

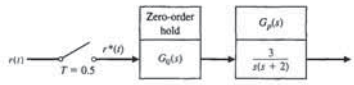

FIGURE E13.16 An open-loop sampled-data system with sampling time $T = 0.5$ s.

PROBLEMS

P13.1 The input to a sampler is $r(t) = \sin(\omega t)$, where $\omega = 1/\pi$. Plot the input to the sampler and the output $r^*(t)$ for the first 2 seconds when $T = 0.25$ s.

P13.2 The input to a sampler is $r(t) = \sin(\omega t)$, where $\omega = 1/\pi$. The output of the sampler enters a zero-order hold, as shown in Figure 13.7. Plot the output of the hold circuit $p(t)$ for the first 2 seconds when $T = 0.25$ s.

P13.3 A unit ramp $r(t) = t, t > 0$, is used as an input to a process where $G(s) = 1/(s+1)$, as shown in Figure P13.3. Determine the output $y(kT)$ for the first four sampling instants.

that represents an integral controller. Determine $G(z)D(z)$ for $T = 30$ ms, and plot the root locus. Select an appropriate gain K and plot the step response.

AP13.3 A system of the form shown in Figure 13.15 has $D(z) = K$ and

$$G_p(s) = \frac{12}{s(s+12)}.$$

When $T = 0.05$, find a suitable K for a rapid step response with an overshoot less than 10%.

AP13.4 A system of the form shown in Figure 13.18 has

$$G_p(s) = \frac{10}{s+1}.$$

Determine the range of sampling period T for which the system is stable. Select a sampling period T so that the system is stable and provides a rapid response.

AP13.5 Consider the closed-loop sampled-data system shown in Figure AP13.5. Determine the acceptable range of the parameter K for closed-loop stability.

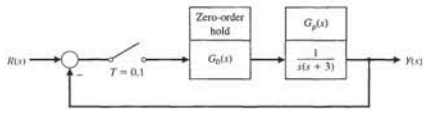

FIGURE AP13.5 A closed-loop sampled-data system with sampling time $T = 0.1$ s.

DESIGN PROBLEMS

CDP13.1 Design a digital controller for the system using the second-order model of the motor-capstan-slide as described in CDP2.1 and CDP4.1. Use a sampling period of $T = 1$ ms and select a suitable $D(z)$ for the system shown in Figure 13.15. Determine the response of the designed system to a step input $r(t)$.

DP13.1 A temperature system, as shown in Figure 13.15, has a process transfer function

$$G_p(s) = \frac{0.8}{3s+1}$$

and a sampling period T of 0.5 second.

(a) Using $D(z) = K$, select a gain K so that the system is stable. (b) The system may be slow and overdamped, and thus we seek to design a lead network using the method of Section 10.5. Determine a suitable controller $G_c(s)$ and then calculate $D(z)$. (c) Verify the design obtained in part (b) by plotting the step response of the system for the selected $D(z)$.

DP13.2 A disk drive read-write head-positioning system has a system as shown in Figure 13.15 [11]. The process transfer function is

$$G_p(s) = \frac{9}{s^2 + 0.85s + 788}.$$

Accurate control using a digital compensator is required. Let $T = 10$ ms and design a compensator, $D(z)$, using (a) the $G_c(s)$-to-$D(z)$ conversion method and (b) the root locus method.

DP13.3 Vehicle traction control, which includes antiskid braking and antispin acceleration, can enhance vehicle performance and handling. The objective of this control is to maximize tire traction by preventing the wheels from locking during braking and from spinning during acceleration.

Wheel slip, the difference between the vehicle speed and the wheel speed (normalized by the vehicle speed for braking and the wheel speed for acceleration), is chosen as the controlled variable for most of the traction-control algorithm because of its strong influence on the tractive force between the tire and the road [17].

A model for one wheel is shown in Figure DP13.3 when y is the wheel slip. The goal is to minimize the slip when a disturbance occurs due to road conditions. Design a controller $D(z)$ so that the ζ of the system is $1/\sqrt{2}$, and determine the resulting K. Assume $T = 0.1$ s. Plot the resulting step response, and find the overshoot and settling time (with a 2% criterion).

P13.13 The space station orientation controller described in Exercise E7.6 is implemented with a sampler and hold and has the transfer function (Figure 13.18)

$$G(z) = \frac{K(z^2 + 1.1206z - 0.0364)}{z^3 - 1.7358z^2 + 0.8711z - 0.1353}.$$

(a) Plot the root locus. (b) Determine the value of K so that two of the roots of the characteristic equation are equal. (c) Determine all the roots of the characteristic equation for the gain of part (b).

P13.14 A sampled-data system with a sampling period $T = 0.05$s (Figure 13.18) is

$$G(z) = \frac{K(z^3 + 10.3614z^2 + 9.758z + 0.8353)}{z^4 - 3.7123z^3 + 5.1644z^2 - 3.195z + 0.7408}.$$

(a) Plot the root locus. (b) Determine K when the two real poles break away from the real axis. (c) Calculate the maximum K for stability.

P13.15 A closed-loop system with a sampler and hold, as shown in Figure 13.18, has a process transfer function

$$G_p(s) = \frac{20}{s-5}.$$

Calculate and plot $y(kT)$ for $0 \le T \le 0.6$ when $T = 0.1$ s. The input signal is a unit step.

P13.16 A closed-loop system as shown in Figure 13.18 has

$$G_p(s) = \frac{1}{s(s+3)}.$$

Calculate and plot $y(kT)$ for $0 \le k \le 8$ when $T = 1$ s and the input is a unit step.

P13.17 A closed-loop system, as shown in Figure 13.18, has

$$G_p(s) = \frac{K}{s(s+0.75)}$$

and $T = 1$ s. Plot the root locus for $K \ge 0$, and determine the gain K that results in the two roots of the characteristic equation on the z-circle (at the stability limit).

P13.18 A unity feedback system, as shown in Figure 13.18, has

$$G_p(s) = \frac{K}{s(s+1)}.$$

If the system is continuous ($T = 0$), then $K = 1$ yields a step response with an overshoot of 16% and a settling time (with a 2% criterion) of 8 seconds. Plot the response for $0 \le T \le 1.2$, varying T by increments of 0.2 when $K = 1$. Complete a table recording overshoot and settling time versus T.

ADVANCED PROBLEMS

AP13.1 A closed-loop system, as shown in Figure 13.18, has a process

$$G_p(s) = \frac{K(1+as)}{s^2},$$

where a is adjustable to achieve a suitable response. Plot the root locus when $a = 10$. Determine the range of K for stability when $T = 1$ s.

AP13.2 A manufacturer uses an adhesive to form a seam along the edge of the material, as shown in Figure AP13.2. It is critical that the glue be applied evenly to avoid flaws; however, the speed at which the material passes beneath the dispensing head is not constant. The glue needs to be dispensed at a rate proportional to the varying speed of the material. The controller adjusts the valve that dispenses the glue [12].

The system can be represented by the block diagram shown in Figure 13.15, where $G_p(s) = 2/(0.03s + 1)$ with a zero-order hold $G_h(s)$. Use a controller

$$D(z) = \frac{KT}{1 - z^{-1}} = \frac{KTz}{z-1}$$

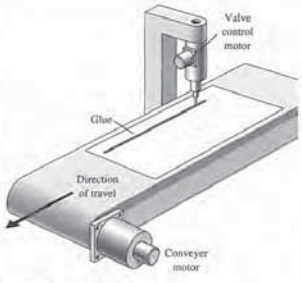

FIGURE AP13.2 A glue control system.

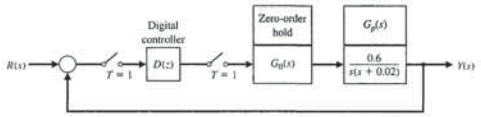

FIGURE DP13.6
A closed-loop sampled-data system with sampling time $T = 1$ s.

COMPUTER PROBLEMS

CP13.1 Develop an m-file to plot the unit step response of the system

$$G(z) = \frac{0.2145z + 0.1609}{z^2 - 0.75z + 0.125}.$$

Verify graphically that the steady-state value of the output is 1.

CP13.2 Convert the following continuous-time transfer functions to sampled-data systems using the c2d function. Assume a sample period of 1 second and a zero-order hold $G_0(s)$.

(a) $G_p(s) = \frac{1}{s}$

(b) $G_p(s) = \frac{s}{s^2 + 2}$

(c) $G_p(s) = \frac{s + 4}{s + 3}$

(d) $G_p(s) = \frac{1}{s(s + 8)}$

CP13.3 The closed-loop transfer function of a sampled-data system is given by

$$T(z) = \frac{Y(z)}{R(z)} = \frac{1.7(z + 0.46)}{z^2 + z + 0.5}.$$

(a) Compute the unit step response of the system using the step function. (b) Determine the continuous-time transfer function equivalent of $T(z)$ using the d2c function and assume a sampling period of $T = 0.1$ s. (c) Compute the unit step response of the continuous (nonsampled) system using the step function, and compare the plot with part (a).

CP13.4 Plot the root locus for the system

$$G(z)D(z) = K\frac{z}{z^2 - z + 0.45}.$$

Find the range of K for stability.

CP13.5 Consider the feedback system in Figure CP13.5. Obtain the root locus and determine the range of K for stability.

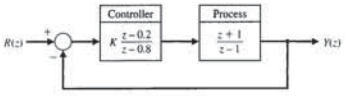

FIGURE CP13.5
Control system with a digital controller.

CP13.6 Consider the sampled data system with the loop transfer function

$$G(z)D(z) = K\frac{z^2 + 3z + 3.75}{z^2 - 0.2z - 1.9}.$$

(a) Plot the root locus using the rlocus function.
(b) From the root locus, determine the range of K for stability. Use the rlocfind function.

CP13.7 An industrial grinding process is given by the transfer function [15]

$$G_p(s) = \frac{10}{s(s + 5)}.$$

The objective is to use a digital computer to improve the performance, where the transfer function of the computer is represented by $D(z)$. The design specifications are (1) phase margin greater than 45°, and (2) settling time (with a 2% criterion) less than 1 second.

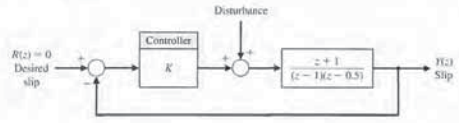

FIGURE DP13.3
Vehicle traction control system.

DP13.4 A machine-tool system has the form shown in Figure 13.28 with [10]

$$G_p(s) = \frac{0.1}{s(s + 0.1)}.$$

The sampling rate is chosen as $T = 1$ s. We desire the step response to have an overshoot of 16% or less and a settling time (with a 2% criterion) of 12 seconds or less. Also, the error to a unit ramp input, $r(t) = t$, must be less than or equal to 1. Design a $D(z)$ to achieve these specifications.

DP13.5 Plastic extrusion is a well-established method widely used in the polymer processing industry [12]. Such extruders typically consist of a large barrel divided into several temperature zones, with a hopper at one end and a die at the other. Polymer is fed into the barrel in raw and solid form from the hopper and is pushed forward by a powerful screw. Simultaneously, it is gradually heated while passing through the various temperature zones set in gradually increasing temperatures. The heat produced by the heaters in the barrel, together with the heat released from the friction between the raw polymer and the surfaces of the barrel and the screw, eventually causes the melting of the polymer, which is then pushed by the screw out from the die, to be processed further for various purposes.

The output variables are the outflow from the die and the polymer temperature. The main controlling variable is the screw speed, since the response of the process to it is rapid.

The control system for the output polymer temperature is shown in Figure DP13.5. Select a gain K and a sampling period T to obtain a step overshoot of 10% while reducing the steady-state error for a ramp input.

DP13.6 A sampled-data system closed-loop block diagram is shown in Figure DP13.6. Design $D(z)$ to such that the closed-loop system response to a unit step response has a percent overshoot $P.O. \leq 12\%$ and a settling time $T_s \leq 20$ s.

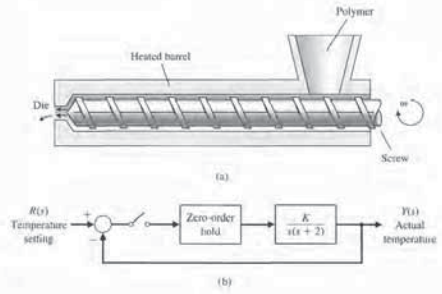

FIGURE DP13.5
Control system for an extruder.

APPENDIX A MATLAB Basics

A.1 INTRODUCTION

MATLAB is an interactive program for scientific and engineering calculations. The MATLAB family of programs includes the base program plus a variety of **toolboxes**, a collection of special files called *m-files* that extend the functionality of the base program [1–8]. Together, the base program plus the *Control System Toolbox* provide the capability to use MATLAB for control system design and analysis. Whenever MATLAB is referenced in this book, it means the base program plus the *Control System Toolbox*.

Most of the statements, functions, and commands are computer-platform-independent. Regardless of what particular computer system you use, your interaction with MATLAB is basically the same. This appendix concentrates on this computer platform–independent interaction. A typical session will utilize a variety of objects that allow you to interact with the program: (1) statements and variables, (2) matrices, (3) graphics, and (4) scripts. MATLAB interprets and acts on input in the form of one or more of these objects. The goal in this appendix is to introduce each of the four objects in preparation for our ultimate goal of using MATLAB for control system design and analysis.

The manner in which MATLAB interacts with a specific computer system is computer-platform-dependent. Examples of computer-dependent functions include installation, the file structure, hard-copy generation of the graphics, the invoking and exiting of a session, and memory allocation. Questions related to platform-dependent issues are not addressed here. This does not mean that they are not important, but rather that there are better sources of information such as the MATLAB *User's Guide* or the local resident expert.

The remainder of this appendix consists of four sections corresponding to the four objects already listed. In the first section, we present the basics of **statements** and **variables**. Following that is the subject of **matrices**. The third section presents an introduction to **graphics**, and the fourth section is a discussion on the important topic of **scripts** and **m-files**. All the figures in this appendix can be constructed using the m-files found at the MCS website.

A.2 STATEMENTS AND VARIABLES

Statements have the form shown in Figure A.1. MATLAB uses the assignment so that equals ("=") implies the assignment of the expression to the variable. The command

(a) Design a controller

$$G_c(s) = K\frac{s + a}{s + b}$$

to meet the design specifications. (b) Assuming a sampling time of $T = 0.02$ s, convert $G_c(s)$ to $D(z)$. (c) Simulate the continuous-time, closed-loop system with a unit step input. (d) Simulate the sampled-data, closed-loop system with a unit step input. (e) Compare the results in parts (c) and (d) and comment.

ANSWERS TO SKILLS CHECK

True or False: (1) True; (2) True; (3) False; (4) False; (5) True

Multiple Choice: (6) a; (7) c; (8) a; (9) d; (10) a; (11) a; (12) c; (13) b; (14) a; (15) c

Word Match (in order, top to bottom): f, k, c, h, g, o, n, l, b, d, j, i, e, m, a, p

TERMS AND CONCEPTS

Amplitude quantization error The sampled signal available only with a limited precision. The error between the actual signal and the sampled signal.

Backward difference rule A computational method of approximating the time derivative of a function given by $\dot{x}(kT) \approx \frac{x(kT) - x((k-1)T)}{T}$, where $t = kT$, T is the sample time, and $k = 1, 2, \ldots$.

Digital computer compensator A system that uses a digital computer as the compensator element.

Digital control system A control system using digital signals and a digital computer to control a process.

Forward rectangular integration A computational method of approximating the integration of a function given by $x(kT) \approx x((k-1)T) + T\dot{x}((k-1)T)$, where $t = kT$, T is the sample time, and $k = 1, 2, \ldots$.

Microcomputer A small personal computer (PC) based on a microprocessor.

Minicomputer A stand-alone computer with size and performance between a microcomputer and a large mainframe. The term is not commonly used today, and computers in this class are now often known as mid-range servers.

PID controller A controller with three terms in which the output is the sum of a proportional term, an integrating term, and a differentiating term, with an adjustable gain for each term, given by

$$G_c(z) = K_1 + \frac{K_2 T s}{z - 1} + K_3\frac{z - 1}{Tz}.$$

Precision The degree of exactness or discrimination with which a quantity is stated.

Sampled data Data obtained for the system variables only at discrete intervals. Data obtained once every sampling period.

Sampled-data system A system where part of the system acts on sampled data (sampled variables).

Sampling period The period when all the numbers leave or enter the computer. The period for which the sampled variable is held constant.

Stability of a sampled-data system The stable condition exists when all the poles of the closed-loop transfer function $T(z)$ are within the unit circle on the z-plane.

z-plane The plane with the vertical axis equal to the imaginary part of z and the horizontal axis equal to the real part of z.

z-transform A conformal mapping from the s-plane to the z-plane by the relation $z = e^{sT}$. A transform from the s-domain to the z-domain.

Zero-order hold A mathematical model of a sample and data hold operation whose input–output transfer function is represented by $G_0(s) = \frac{1 - e^{-sT}}{s}$.

Table A.2 Common Mathematical Functions

sin(x)	Sine	acoth(x)	Inverse hyperbolic cotangent
sinh(x)	Hyperbolic sine	exp(x)	Exponential
asin(x)	Inverse sine	log(x)	Natural logarithm
asinh(x)	Inverse hyperbolic sine	log10(x)	Common (base 10) logarithm
cos(x)	Cosine	log2(x)	Base 2 logarithm and dissect floating point number
cosh(x)	Hyperbolic cosine	pow2(x)	Base 2 power and scale floating point number
acos(x)	Inverse cosine	sqrt(x)	Square root
acosh(x)	Inverse hyperbolic cosine	nextpow2(x)	Next higher power of 2
tan(x)	Tangent	abs(x)	Absolute value
tanh(x)	Hyperbolic tangent	angle(x)	Phase angle
atan(x)	Inverse tangent	complex(x,y)	Construct complex data from real and imaginary parts
atan2(y,x)	Four quadrant inverse tangent	conj(x)	Complex conjugate
atanh(x)	Inverse hyperbolic tangent	imag(x)	Complex imaginary part
sec(x)	Secant	real(x)	Complex real part
sech(x)	Hyperbolic secant	unwrap(x)	Unwrap phase angle
asec(x)	Inverse secant	isreal(x)	True for real array
asech(x)	Inverse hyperbolic secant	cplxpair(x)	Sort numbers into complex conjugate pairs
csc(x)	Cosecant	fix(x)	Round towards zero
csch(x)	Hyperbolic cosecant	floor(x)	Round towards minus infinity
acsc(x)	Inverse cosecant	ceil(x)	Round towards plus infinity
acsch(x)	Inverse hyperbolic cosecant	round(x)	Round towards nearest integer
cot(x)	Cotangent	mod(x,y)	Modulus (signed remainder after division)
coth(x)	Hyperbolic cotangent	rem(x,y)	Remainder after division
acot(x)	Inverse cotangent		

Variable names begin with a letter and are followed by any number of letters and numbers (including underscores). Keep the name length to N characters, since MATLAB remembers only the first N characters, where N = namelengthmax. It is a good practice to use variable names that describe the quantity they represent. For example, we might use the variable name *vel* to represent the quantity *aircraft velocity*. Generally, we do not use extremely long variable names even though they may be legal MATLAB names.

Since MATLAB is **case sensitive**, the variables *M* and *m* are not the same. By **case**, we mean upper- and lowercase, as illustrated in Figure A.5. The variables *M* and *m* are recognized as different quantities.

MATLAB has several predefined variables, including *pi*, *Inf*, *NaN*, *i*, and *j*. Three examples are shown in Figure A.6. *NaN* stands for *Not-a-Number* and results from undefined operations. *Inf* represents $+\infty$, and *pi* represents π. The variable $i = \sqrt{-1}$ is used to represent complex numbers. The variable $j = \sqrt{-1}$ can be used for complex arithmetic by those who prefer it over *i*. These predefined variables can be inadvertently overwritten. Of course, they can also be purposely overwritten in order to free the variable name for other uses. For instance, you might want to use *i* as an integer and reserve *j* for complex arithmetic. Be safe and leave these predefined variables alone, as

FIGURE A.5 Variables are case sensitive.

```
>>M=[1 2];
>>m=[3 5 7];
```


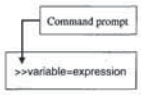

FIGURE A.1 MATLAB statement form.

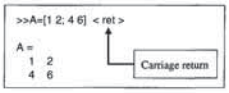

FIGURE A.2 Entering and displaying a matrix **A**.

prompt is two right arrows, " >> ." A typical statement is shown in Figure A.2, where we are entering a 2×2 matrix to which we attach the variable name **A**. The statement is executed after the carriage return (or enter key) is pressed. The carriage return is not explicitly denoted in the remaining examples in this appendix.

The matrix **A** is automatically displayed after the statement is executed following the carriage return. If the statement is followed by a semicolon (;), the output matrix **A** is suppressed, as seen in Figure A.3. The assignment of the variable **A** has been carried out even though the output is suppressed by the semicolon. It is often the case that your MATLAB sessions will include intermediate calculations for which the output is of little interest. Use the semicolon whenever you have a need to reduce the amount of output. Output management has the added benefit of increasing the execution speed of the calculations since displaying screen output takes time.

The usual mathematical operators can be used in expressions. The common operators are shown in Table A.1. The order of the arithmetic operations can be altered by using parentheses.

The example in Figure A.4 illustrates that MATLAB can be used in a "calculator" mode. When the variable name and "=" are omitted from an expression, the result is assigned to the generic variable *ans*. MATLAB has available most of the trigonometric and elementary math functions of a common scientific calculator. Type help elfun at the command prompt to view a complete list of available trigonometric and elementary math functions; the more common ones are summarized in Table A.2.

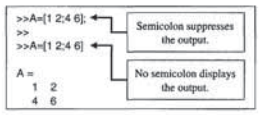

FIGURE A.3 Using semicolons to suppress the output.

Table A.1 Mathematical Operators

+	Addition
−	Subtraction
*	Multiplication
/	Division
^	Power

FIGURE A.4 Using the calculator mode.

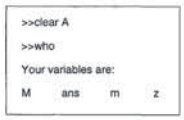

FIGURE A.9 Removing the matrix **A** from the workspace.

Computations in MATLAB are performed in **double precision**. However, the screen output can be displayed in several formats. The default output format contains four digits past the decimal point for nonintegers. This can be changed by using the format function shown in Figure A.10. Once a particular format has been specified, it remains in effect until altered by a different format input. The output format does not affect internal MATLAB computations. On the other hand, the number of digits displayed does not necessarily reflect the number of significant digits of the number. This is problem-dependent, and only the user can know the true accuracy of the numbers input and displayed by MATLAB. Other display formats (not shown in Figure A.10) include format long g (best of fixed or floating point format with 14 digits after the decimal point), format short g (same as format long g but with 4 digits after the decimal point), format hex (hexadecimal format), format bank (fixed format for dollars and cents), format rat (ratio of small integers) and format (same as format short).

Since MATLAB is case sensitive, the functions who and WHO are not the same functions. The first function, who, is a built-in function, and typing who lists the variables in the workspace. On the other hand, typing the uppercase WHO results in the error message shown in Figure A.11. Case sensitivity applies to all functions.

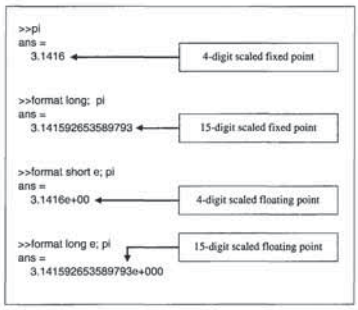

FIGURE A.10 Output format control illustrates the four forms of output.

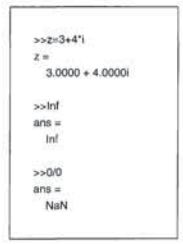

FIGURE A.6 Three predefined variables *i*, *Inf*, and *NaN*.

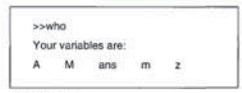

FIGURE A.7 Using the **who** function to display variables.

there are plenty of alternative names that can be used. Predefined variables can be reset to their default values by using clear *name* (e.g., clear *pi*).

The matrix **A** and the variable *ans*, in Figures A.3 and A.4, respectively, are stored in the **workspace**. Variables in the workspace are automatically saved for later use in your session. The who function gives a list of the variables in the workspace, as shown in Figure A.7. MATLAB has a host of built-in functions. Refer to the MATLAB *User's Guide* for a complete list or use the MATLAB help browser. Each function will be described as the need arises.

The whos function lists the variables in the workspace and gives additional information regarding variable dimension, type, and memory allocation. Figure A.8 gives an example of the whos function. The memory allocation information given by the whos function can be interpreted as follows: Each element of the 2×2 matrix **A** requires 8 bytes of memory for a total of 32 bytes, the 1×1 variable *ans* requires 8 bytes, and so forth. All the variables in the workspace use a total of 96 bytes.

Variables can be removed from the workspace with the clear function. Using the function clear, by itself, removes all items (variables and functions) from the workspace; clear variables removes all variables from the workspace; clear *name1 name2* . . . removes the variables *name1*, *name2*, and so forth. The procedure for removing the matrix **A** from the workspace is shown in Figure A.9.

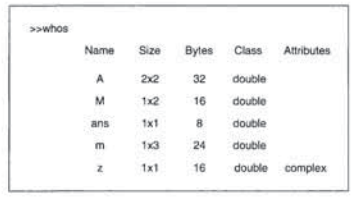

FIGURE A.8 Using the **whos** function to display variables.

No dimension statements or type statements are necessary when using matrices; memory is allocated automatically. Notice in the example in Figure A.12 that the size of the matrix **A** is automatically adjusted when the input matrix is redefined. Also notice that the matrix elements can contain trigonometric and elementary math functions, as well as complex numbers.

The important basic matrix operations are addition and subtraction, multiplication, transpose, powers, and the so-called array operations, which are element-to-element operations. The mathematical operators given in Table A.1 apply to matrices. We will not discuss matrix division, but be aware that MATLAB has a left- and right-matrix division capability.

Matrix operations require that the matrix dimensions be compatible. For matrix addition and subtraction, this means that the matrices must have the same dimensions. If **A** is an $n \times m$ matrix and **B** is a $p \times r$ matrix, then $\mathbf{A} \pm \mathbf{B}$ is permitted only if $n = p$ and $m = r$. Matrix multiplication, given by **A** * **B**, is permitted only if $m = p$. Matrix-vector multiplication is a special case of matrix multiplication. Suppose **b** is a vector of length p. Multiplication of the vector **b** by the matrix **A**, where **A** is an $n \times m$ matrix, is allowed if $m = p$. Thus, **y** = **A** * **b** is the $n \times 1$ vector solution of **A** * **b**. Examples of three basic matrix-vector operations are given in Figure A.13.

The matrix transpose is formed with the apostrophe ('). We can use the matrix transpose and multiplication operation to create a vector **inner product** in the following manner. Suppose **w** and **v** are $m \times 1$ vectors. Then the inner product (also known as the dot product) is given by **w**' * **v**. The inner product of two vectors is a scalar. The **outer product** of two vectors can similarly be computed as **w** * **v**'. The outer product of two $m \times 1$ vectors is an $m \times m$ matrix of rank 1. Examples of inner and outer products are given in Figure A.14.

The basic matrix operations can be modified for element-by-element operations by preceding the operator with a period. The modified matrix operations are known

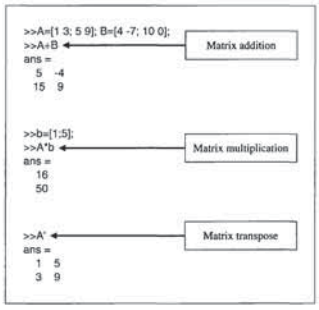

FIGURE A.13 Three basic matrix operations: addition, multiplication, and transpose.

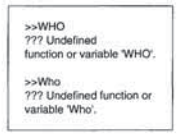

FIGURE A.11 Function names are case sensitive.

A.3 MATRICES

MATLAB is short for **matrix laboratory**. Although we will not emphasize the matrix routines underlying our calculations, we will learn how to use the interactive capability to assist us in the control system design and analysis. We begin by introducing the basic concepts associated with manipulating matrices and vectors.

The basic computational unit is the matrix. Vectors and scalars can be viewed as special cases of matrices. A typical matrix expression is enclosed in square brackets, [·]. The column elements are separated by blanks or commas, and the rows are separated by semicolons or carriage returns. Suppose we want to input the matrix

$$\mathbf{A} = \begin{bmatrix} 1 & -4j & \sqrt{2} \\ \log(-1) & \sin(\pi/2) & \cos(\pi/3) \\ \text{asin}(0.8) & \text{acos}(0.8) & \exp(0.8) \end{bmatrix}.$$

One way to input **A** is shown in Figure A.12. The input style in Figure A.12 is not unique.

Matrices can be input across multiple lines by using a carriage return following the semicolon or in place of the semicolon. This practice is useful for entering large matrices. Different combinations of spaces and commas can be used to separate the columns, and different combinations of semicolons and carriage returns can be used to separate the rows, as illustrated in Figure A.12.

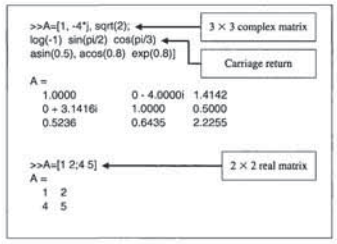

FIGURE A.12 Complex and real matrix input with automatic dimension and type adjustment.

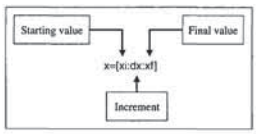

FIGURE A.16 The colon notation.

Before proceeding to the important topic of graphics, we need to introduce the notion of **subscripting using colon notation**. The colon notation, shown in Figure A.16, allows us to generate a row vector containing the numbers from a given starting value, x_i, to a final value, x_f, with a specified increment, dx.

We can easily generate vectors using the colon notation, and as we shall soon see, this is quite useful for developing ***x*-*y* plots**. Suppose our objective is to generate a plot of $y = x \sin(x)$ versus x for $x = 0, 0.1, 0.2, \ldots, 1.0$. Our first step is to generate a table of x-y data. We can generate a vector containing the values of x at which the values of $y(x)$ are desired using the colon notation, as illustrated in Figure A.17. Given the desired x vector, the vector $y(x)$ is computed using the multiplication array operation. Creating a plot of $y = x \sin(x)$ versus x is a simple step once the table of x-y data is generated.

A.4 GRAPHICS

Graphics plays an important role in both the design and analysis of control systems. An important component of an **interactive** control system design and analysis tool is an effective graphical capability. A complete solution to the control system design and analysis will eventually require a detailed look at a multitude of data types in many formats. The objective of this section is to acquaint the reader with the basic

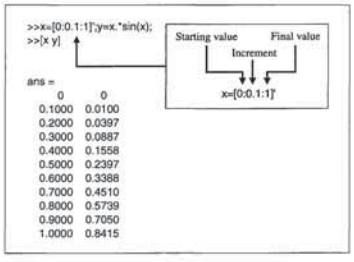

FIGURE A.17 Generating vectors using the colon notation.

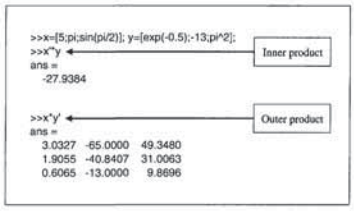

FIGURE A.14 Inner and outer products of two vectors.

Table A.3 Mathematical Array Operators

+	Addition
−	Subtraction
.*	Multiplication
./	Division
.^	Power

as **array operations**. The commonly used array operators are given in Table A.3. Matrix addition and subtraction are already element-by-element operations and do not require the additional period preceding the operator. However, array multiplication, division, and power do require the preceding dot, as shown in Table A.3.

Consider **A** and **B** as 2×2 matrices given by

$$\mathbf{A} = \begin{bmatrix} a_{11} & a_{12} \\ a_{21} & a_{22} \end{bmatrix}, \quad \mathbf{B} = \begin{bmatrix} b_{11} & b_{12} \\ b_{21} & b_{22} \end{bmatrix}.$$

Then, using the array multiplication operator, we have

$$\mathbf{A} .* \mathbf{B} = \begin{bmatrix} a_{11}b_{11} & a_{12}b_{12} \\ a_{21}b_{21} & a_{22}b_{22} \end{bmatrix}.$$

The elements of **A**.* **B** are the products of the corresponding elements of **A** and **B**. A numerical example of two array operations is given in Figure A.15.

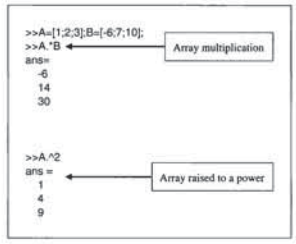

FIGURE A.15 Array operations.

Table A.6 Commands for Line Types for Customized Plots

-	Solid line
--	Dashed line
:	Dotted line
-.	Dashdot line

chosen unless specified by the user. The use of the text function and the changing of line types are illustrated in Figure A.19.

The other graphics functions—loglog, semilogx, and semilogy—are used in a fashion similar to that of plot. To obtain an x-y plot where the x-axis is a linear scale and the y-axis is a $\log_{10}$ scale, you would use the semilogy function in place of the plot function. The customizing features listed in Table A.5 can also be utilized with the loglog, semilogx, and semilogy functions.

The graph display can be subdivided into smaller subwindows. The function subplot(m,n,p) subdivides the graph display into an $m \times n$ grid of smaller subwindows. The integer p specifies the window, numbered left to right, top to bottom, as illustrated in Figure A.20, where the graphics window is subdivided into four subwindows.

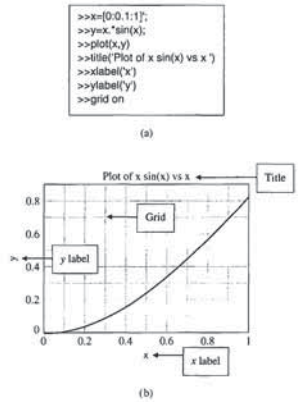

FIGURE A.18 (a) MATLAB commands. (b) A basic x-y plot of x sin(x) versus x.

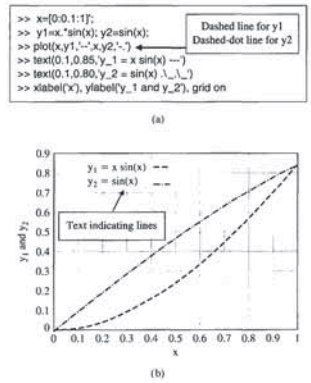

FIGURE A.19 (a) MATLAB commands. (b) A basic x-y plot with multiple lines.

Table A.4 Plot Formats

plot(x,y)	Plots the vector **x** versus the vector **y**.
semilogx(x,y)	Plots the vector **x** versus the vector **y**. The x-axis is $\log_{10}$; the y-axis is linear.
semilogy(x,y)	Plots the vector **x** versus the vector **y**. The x-axis is linear; the y-axis is $\log_{10}$.
loglog(x,y)	Plots the vector **x** versus the vector **y**. Creates a plot with $\log_{10}$ scales on both axes.

x-y plotting capability of MATLAB. More advanced graphics topics are addressed in the chapter sections on MATLAB.

MATLAB uses a **graph display** to present plots. The graph display is activated automatically when a plot is generated using any function that generates a plot (e.g., the plot function). The plot function opens a graph display, called a **FIGURE** window. You can also create a new figure window with the figure function. Multiple figure windows can exist in a single MATLAB session; the function figure (n) makes n the current figure. The plot in the graph display is cleared by the clf function at the command prompt. The shg function brings the current figure window forward.

There are two basic groups of graphics functions. The first group, shown in Table A.4, specifies the type of plot. The list of available plot types includes the x-y plot, semilog plots, and log plots. The second group of functions, shown in Table A.5, allows us to customize the plots by adding titles, axis labels, and text to the plots and to change the scales and display multiple plots in subwindows.

The standard x-y plot is created using the plot function. The x-y data in Figure A.17 are plotted using the plot function, as shown in Figure A.18. The axis scales and line types are automatically chosen. The axes are labeled with the xlabel and ylabel functions; the title is applied with the title function. The legend function puts a legend on the current figure. A grid can be placed on the plot by using the grid on function. A basic x-y plot is generated with the combination of functions plot, legend, xlabel, ylabel, title, and grid on.

Multiple lines can be placed on the graph by using the plot function with multiple arguments, as shown in Figure A.19. The default line types can also be altered. The available line types are shown in Table A.6. The line types will be automatically

Table A.5 Functions for Customized Plots

title('text')	Puts 'text' at the top of the plot
legend (string1, string2,...)	Puts a legend on current plot using specified strings as labels
xlabel('text')	Labels the x-axis with 'text'
ylabel('text')	Labels the y-axis with 'text'
text(p1,p2, 'text')	Adds 'text' to location (p1,p2), where (p1,p2) is in units from the current plot
subplot	Subdivides the graphics window
grid on	Adds grid lines to the current figure
grid off	Removes grid lines from the current figure
grid	Toggles the grid state

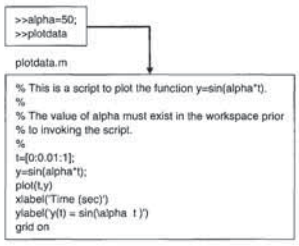

FIGURE A.21 A simple script to plot the function $y(t) = \sin \alpha t$.

shown in Figure A.21, then input a value of α at the command prompt, placing α in the workspace. Then we execute the script by typing in plotdata at the command prompt; the script plotdata.m will use the most recent value of α in the workspace. After executing the script, we can enter another value of α at the command prompt and execute the script again.

Your scripts should be well documented with **comments**, which begin with a %. Put a **header** in the script; make sure the header includes several descriptive comments regarding the function of the script, and then use the help function to display the header comments and describe the script to the user, as illustrated in Figure A.22.

Use plotdata.m to develop an interactive capability with α as a variable, as shown in Figure A.23. At the command prompt, input a value of $\alpha = 10$ followed by the script filename, which in this case is plotdata. The graph of $y(t) = \sin \alpha t$ is automatically generated. You can now go back to the command prompt, enter a value of $\alpha = 50$, and run the script again to obtain the updated plot.

A limited subset of TeX[1] characters are available to allow you to annotate plots with symbols and mathematical characters. Table A.7 shows the available symbols. Figure A.21 illustrates the use of '\alpha' to generate the α character in the y-axis label. The '\' character preceeds all TeX sequences. Also, you can modify the characters with the following modifiers:

- \bf—bold font
- \it—italics font
- \rm—normal font
- \fontname—specify the name of the font family to use
- \fontsize—specify the font size
- \color—specify color for succeeding characters

[1]TeX is a trademark of the American Mathematical Society.

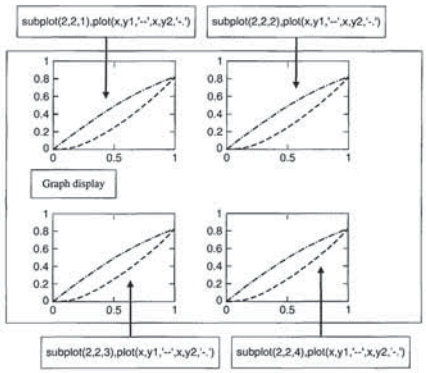

FIGURE A.20 Using **subplot** to create a 2×2 partition of the graph display.

A.5 SCRIPTS

Up to this point, all of our interaction with MATLAB has been at the command prompt. We entered statements and functions at the command prompt, and MATLAB interpreted our input and took the appropriate action. This is the preferable mode of operation whenever the work sessions are short and nonrepetitive. However, the real power of MATLAB for control system design and analysis derives from its ability to execute a long sequence of commands stored in a file. These files are called **m-files**, since the filename has the form *filename.m*. A **script** is one type of m-file. The *Control System Toolbox* is a collection of m-files designed specifically for control applications. In addition to the preexisting m-files delivered with MATLAB and the toolboxes, we can develop our own scripts for our applications. Scripts are ordinary ASCII text files and are created using a text editor.

A script is a sequence of ordinary statements and functions used at the command prompt level. A script is invoked at the command prompt level by typing in the filename or by using the pull-down menu. Scripts can also invoke other scripts. When the script is invoked, MATLAB executes the statements and functions in the file without waiting for input at the command prompt. The script operates on variables in the workspace.

Suppose we want to plot the function $y(t) = \sin \alpha t$, where α is a variable that we want to vary. Using a text editor, we write a script that we call plotdata.m, as

Table A.7 TeX Symbols and Mathematics Characters

Character Sequence	Symbol	Character Sequence	Symbol	Character Sequence	Symbol
\alpha	α	\upsilon	υ	\sim	~
\beta	β	\phi	φ	\leq	≤
\gamma	γ	\chi	χ	\infty	∞
\delta	δ	\psi	ψ	\clubsuit	♣
\epsilon	ϵ	\omega	ω	\diamondsuit	♦
\zeta	ζ	\Gamma	Γ	\heartsuit	♥
\eta	η	\Delta	Δ	\spadesuit	♠
\theta	θ	\Theta	Θ	\leftrightarrow	↔
\vartheta	ϑ	\Lambda	Λ	\leftarrow	←
\iota	ι	\Xi	Θ	\uparrow	↑
\kappa	κ	\Pi	Π	\rightarrow	→
\lambda	λ	\Sigma	Σ	\downarrow	↓
\mu	μ	\Upsilon	Υ	\circ	∘
\nu	ν	\Phi	Φ	\pm	±
\xi	ξ	\Psi	Ψ	\geq	≥
\pi	π	\Omega	Ω	\propto	∝
\rho	ρ	\forall	∀	\partial	∂
\sigma	σ	\exists	∃	\bullet	·
\varsigma	ζ	\ni	∍	\div	÷
\tau	τ	\cong	≅	\neq	≠
\equiv	≡	\approx	≈	\aleph	ℵ
\Im	ℑ	\Re	ℜ	\wp	℘
\otimes	⊗	\oplus	⊕	\oslash	∅
\cap	∩	\cup	∪	\supseteq	⊇
\supset	⊃	\subseteq	⊆	\subset	⊂
\int	∫	\in	∈	\o	o


```
>>help plotdata

   This is a script to plot the function y=sin(alpha*t).

   The value of alpha must exist in the workspace prior
   to invoking the script.
```

FIGURE A.22 Using the **help** function.

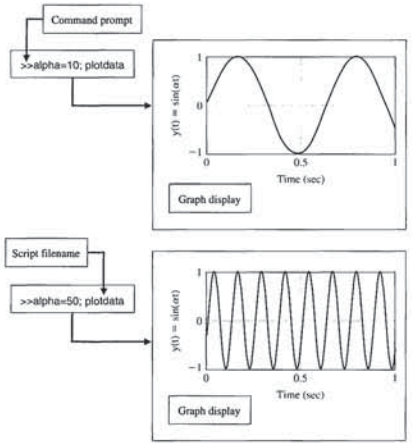

FIGURE A.23 An interactive session using a script to plot the function $y(t) = \sin \alpha t$.

Subscripts and superscripts are obtained with "_" and "^", respectively. For example, ylabel('y_1 and y_2') generates the y-axis label shown in Figure A.19.

The graphics capability of MATLAB extends beyond the introductory material presented here. A table of MATLAB functions used in this book is provided in Table A.8.

Table A.8 *Continued*

Function Name	Function Description
NaN	Representation for Not-a-Number
ngrid	Draws grid lines on a Nichols chart
nichols	Computes a Nichols frequency response plot
num2str	Converts numbers to strings
nyquist	Calculates the Nyquist frequency response
obsv	Computes the observability matrix
ones	Generates a matrix of integers where all the integers are 1
pade	Computes an nth-order Padé approximation to a time delay
parallel	Computes a parallel system connection
plot	Generates a linear plot
pole	Computes the poles of a system
poly	Computes a polynomial from roots
polyval	Evaluates a polynomial
printsys	Prints state variable and transfer function representations of linear systems in a pretty form
pzmap	Plots the pole–zero map of a linear system
rank	Calculates the rank of a matrix
real	Computes the real part of a complex number
residue	Computes a partial fraction expansion
rlocfind	Finds the gain associated with a given set of roots on a root locus plot
rlocus	Computes the root locus
roots	Determines the roots of a polynomial
semilogx	Generates an x-y plot using semilog scales with the x-axis $\log_{10}$ and the y-axis linear
semilogy	Generates an x-y plot using semilog scales with the y-axis $\log_{10}$ and the x-axis linear
series	Computes a series system connection
shg	Shows graph window
sin	Computes the sine
sqrt	Computes the square root
ss	Creates a state-space model object
step	Calculates the unit step response of a system
subplot	Splits the graph window into subwindows
tan	Computes the tangent
text	Adds text to the current graph
title	Adds a title to the current graph
tf	Creates a transfer function model object
who	Lists the variables currently in memory
whos	Lists the current variables and sizes
xlabel	Adds a label to the x-axis of the current graph
ylabel	Adds a label to the y-axis of the current graph
zero	Computes the zeros of a system
zeros	Generates a matrix of zeros

Table A.8 MATLAB Functions

Function Name	Function Description
abs	Computes the absolute value
acos	Computes the arccosine
ans	Variable created for expressions
asin	Computes the arcsine
atan	Computes the arctangent (2 quadrant)
atan2	Computes the arctangent (4 quadrant)
axis	Specifies the manual axis scaling on plots
bode	Generates Bode frequency response plots
c2d	Converts a continuous-time state variable system representation to a discrete-time system representation
clear	Clears the workspace
clf	Clears the graph window
conj	Computes the complex conjugate
conv	Multiplies two polynomials (convolution)
cos	Computes the cosine
ctrb	Computes the controllability matrix
diary	Saves the session in a disk file
d2c	Converts a discrete-time state variable system representation to a continuous-time system representation
eig	Computes the eigenvalues and eigenvectors
end	Terminates control structures
exp	Computes the exponential with base e
expm	Computes the matrix exponential with base e
eye	Generates an identity matrix
feedback	Computes the feedback interconnection of two systems
for	Generates a loop
format	Sets the output display format
grid on	Adds a grid to the current graph
help	Prints a list of HELP topics
hold on	Holds the current graph on the screen
i	$\sqrt{-1}$
imag	Computes the imaginary part of a complex number
impulse	Computes the unit impulse response of a system
inf	Represents infinity
j	$\sqrt{-1}$
legend	Puts a legend on the current plot
linspace	Generates linearly spaced vectors
load	Loads variables saved in a file
log	Computes the natural logarithm
log10	Computes the logarithm base 10
loglog	Generates log-log plots
logspace	Generates logarithmically spaced vectors
lsim	Computes the time response of a system to an arbitrary input and initial conditions
margin	Computes the gain margin, phase margin, and associated crossover frequencies from frequency response data
max	Determines the maximum value
mesh	Creates three-dimensional mesh surfaces
meshgrid	Generates arrays for use with the mesh function
min	Determines the minimum value
minreal	Transfer function pole–zero cancellation

Table A.8 continued

References

Chapter 1

1. O. Mayr, *The Origins of Feedback Control*, MIT Press, Cambridge, Mass., 1970.
2. O. Mayr, "The Origins of Feedback Control," *Scientific American*, Vol. 223, No. 4, October 1970, pp. 110–118.
3. O. Mayr, *Feedback Mechanisms in the Historical Collections of the National Museum of History and Technology*, Smithsonian Institution Press, Washington, D. C., 1971.
4. E. P. Popov, *The Dynamics of Automatic Control Systems*, Gostekhizdat, Moscow, 1956; Addison-Wesley, Reading, Mass., 1962.
5. J. C. Maxwell, "On Governors," *Proc. of the Royal Society of London*, 16, 1868, in *Selected Papers on Mathematical Trends in Control Theory*, Dover, New York, 1964, pp. 270–283.
6. I. A. Vyshnegradskii, "On Controllers of Direct Action," *Izv. SPB Tekhnolog. Inst.*, 1877.
7. H. W. Bode, "Feedback—The History of an Idea," in *Selected Papers on Mathematical Trends in Control Theory*, Dover, New York, 1964, pp. 106–123.
8. H. S. Black, "Inventing the Negative Feedback Amplifier," *IEEE Spectrum*, December 1977, pp. 55–60.
9. J. E. Brittain, *Turning Points in American Electrical History*, IEEE Press, New York, 1977, Sect. II-E.
10. W. S. Levine, *The Control Handbook*, CRC Press, Boca Raton, Fla., 1996.
11. G. Newton, L. Gould, and J. Kaiser, *Analytical Design of Linear Feedback Controls*, John Wiley & Sons, New York, 1957.
12. M. D. Fagen, *A History of Engineering and Science on the Bell Systems*, Bell Telephone Laboratories, 1978, Chapter 3.
13. G. Zorpette, "Parkinson's Gun Director," *IEEE Spectrum*, April 1989, p. 43.
14. R. C. Dorf and A. Kusiak, *Handbook of Automation and Manufacturing*, John Wiley & Sons, New York, 1994.
15. W. D. Rasmussen, "The Mechanization of Agriculture," *Scientific American*, September 1982, pp. 26–37.
16. M. M. Gupta, *Intelligent Control*, IEEE Press, Piscataway, N. J., 1995.
17. A. G. Ulsoy, "Control of Machining Processes," *Journal of Dynamic Systems*, ASME, June 1993, pp. 301–307.
18. M. P. Groover, *Fundamentals of Modern Manufacturing*, Prentice Hall, Englewood Cliffs, N. J., 1996.
19. R. T. O'Brien, "Vertical Lateral Control for Automated Highway Systems," *IEEE Transactions on Control Systems Technology*, May 1996, pp. 266–273.
20. J. G. Kassakian, "Automotive Electrical Systems circa 2005," *IEEE Spectrum*, August 1996, pp. 22–27.
21. P. M. Moretti and L. V. Divone, "Modern Windmills," *Scientific American*, June 1986, pp. 110–118.
22. B. Preising and T. C. Hsia, "Robots in Medicine," *IEEE Engineering in Medicine and Biology*, June 1991, pp. 13–22.
23. R. C. Dorf and J. Unmack, "A Time-Domain Model of the Heart Rate Control System," *Proceedings of the San Diego Symposium for Biomedical Engineering*, 1965, pp. 43–47.
24. R. C. Dorf, *Electrical Engineering Handbook*, 2nd ed., CRC Press, Boca Raton, Fla., 1998.
25. R. C. Dorf, *Introduction to Computers and Computer Science*, 3rd ed., Boyd and Fraser, San Francisco, 1982, Chapters 13, 14.
26. K. Sutton, "Productivity," in *Encyclopedia of Engineering*, McGraw-Hill, New York, pp. 947–948.
27. R. C. Dorf, *The Encyclopedia of Robotics*, John Wiley & Sons, New York, 1988.
28. R. C. Dorf, *Robotics and Automated Manufacturing*, Reston Publishing, Reston, Va., 1983.
29. S. S. Hacisalihzade, "Control Engineering and Therapeutic Drug Delivery," *IEEE Control Systems*, June 1989, pp. 44–46.
30. E. R. Carson and T. Deutsch, "A Spectrum of Approaches for Controlling Diabetes," *IEEE Control Systems*, December 1992, pp. 25–30.
31. J. R. Sankey and H. Kaufman, "Robust Considerations of a Drug Infusion System," *Proceedings of the American Control Conference*, San Francisco, Calif., June 1993, pp. 1689–1695.
32. W. S. Levine, *The Control Handbook*, CRC Press, Boca Raton, Fla., 1996.

MATLAB BASICS: PROBLEMS

A.1 Consider the two matrices

$$A = \begin{bmatrix} 4 & 2\pi \\ 6j & 10 + \sqrt{2}j \end{bmatrix}$$

$$B = \begin{bmatrix} 6j & -13\pi \\ \pi & 16 \end{bmatrix}.$$

Using MATLAB, compute the following:

(a) $A + B$ (b) AB
(c) A^2 (d) A'
(e) B^{-1} (f) $B'A'$
(g) $A^2 + B^2 - AB$

A.2 Consider the following set of linear algebraic equations:

$$5x + 6y + 10z = 4,$$
$$-3x + 14z = 10,$$
$$-7y + 21z = 0.$$

Determine the values of x, y, and z so that the set of algebraic equations is satisfied. (*Hint:* Write the equations in matrix vector form.)

A.3 Generate a plot of

$$y(x) = e^{-0.5x} \sin \omega x,$$

where $\omega = 10$ rad/s, and $0 \le x \le 10$. Utilize the colon notation to generate the x vector in increments of 0.1.

A.4 Develop a MATLAB script to plot the function

$$y(x) = \frac{4}{\pi}\cos \omega x + \frac{4}{9\pi}\cos 3\omega x.$$

where ω is a variable input at the command prompt. Label the x-axis with *time (sec)* and the y-axis with $y(x) = (4/\pi) * \cos(\omega x) + (4/9\pi) * \cos(3\omega x)$. Include a descriptive header in the script, and verify that the help function will display the header. Choose $\omega = 1, 3, 10$ rad/s and test the script.

A.5 Consider the function

$$y(x) = 10 + 5e^{-x}\cos(\omega x + 0.5).$$

Develop a script to co-plot $y(x)$ for the three values of $\omega = 1, 3, 10$ rad/s with $0 \le x \le 5$ seconds. The final plot should have the following attributes:

Title	$y(x) = 10 + 5\exp(-x) * \cos(\omega x + 0.5)$
x-axis label	Time (sec)
y-axis label	$y(x)$
Line type	$\omega = 1$: solid line
	$\omega = 3$: dashed line
	$\omega = 10$: dotted line
Grid	grid on

71. D. Tomkinson and J. Horne, *Mechatronics Engineering*, McGraw-Hill, New York, 1996.
72. H. Kobayashi, Guest Editorial, *IEEE/ASME Transactions on Mechatronics*, Vol. 2, No. 4, 1997, p. 217.
73. D. S. Bernstein, "What Makes Some Control Problems Hard?" *IEEE Control Systems Magazine*, August 2002, pp. 8–19.
74. S. Douglas, "No Pilot Required," *Popular Science*, June 2001, pp. 40–44.
75. O. Zerbinati, "A Direct Methanol Fuel Cell," *Journal of Chemical Education*, Vol. 79, No. 7, July 2002, p. 829.
76. D. Basmadjian, *Mathematical Modeling of Physical Systems: An Introduction*, Oxford University Press, New York, N.Y., 2003.
77. D. W. Boyd, *Systems Analysis and Modeling: A Macro-to-Micro Approach with Multidisciplinary Applications*, Academic Press, San Diego, CA, 2001.
78. F. Bullo and A. D. Lewis, *Geometric Control of Mechanical Systems: Modeling, Analysis, and Design for Simple Mechanical Control Systems*, Springer Verlag, New York, N.Y., 2004.
79. P. D. Cha, J. J. Rosenberg, and C. L. Dym, *Fundamentals of Modeling and Analyzing Engineering Systems*, Cambridge University Press, Cambridge, United Kingdom, 2000.
80. P. H. Zipfel, *Modeling and Simulation of Aerospace Vehicle Dynamics*, AIAA Education Series, American Institute of Aeronautics & Astronautics, Inc., Reston, Virginia, 2001.
81. D. Hristu-Varsakelis and W. S. Levin, eds., *Handbook of Networked and Embedded Control Systems*, Series: Control Engineering Series, Birkhäuser, Boston, MA, 2005.
82. See the website http://www.gps.gov.
83. B. W. Parkinson and J. J. Spilker, eds., *Global Positioning System: Theory & Applications*, Vol. 1 & 2, Progress in Astronautics and Aeronautics, AIAA, 1996.
84. E. D. Kaplan and C. Hegarty, eds., *Understanding GPS: Principles and Applications*, 2nd ed., Artech House Publishers, Norwood, Mass., 2005.
85. B. Hofmann-Wellenhof, H. Lichtenegger, and E. Wasle, *GNSS-Global navigation Satellite Systems*, Springer-Verlag, Vienna, Austria, 2008.
86. M. A. Abraham and N. Nguyen, "Green Engineering: Defining the Principles," *Environmental Progress*, Vol. 22, No. 4, American Institute of Chemical Engineers, 2003, pp. 233–236.
87. "National Electric Delivery Technologies Roadmap: Transforming the Grid to Revolutionize Electric Power in North America," U.S. Department of Energy, Office of Electric Transmission and Distribution, 2004.
88. D. T. Allen and D. R. Shonnard, *Green Engineering: Environmentally Conscious Design of Chemical Processes*, Prentice Hall, N. J., 2001.
89. "The Modern Grid Strategy: Moving Towards the Smart Grid," U.S. Department of Energy, Office of Electricity Delivery and Energy Reliability, http://www.netl.doe.gov/moderngrid/.
90. "Smart Grid System Report," U.S. Department of Energy, July 2009, http://www.oe.energy.gov/DocumentsandMedia/SGSRMain_090707_lowres.pdf.
91. Climate Group, "SMART 2020: Enabling the Low Carbon Economy in the Information Age," A report by the Climate Group on behalf of the Global eSustainability Initiative, published by Creative Commons, 2008.
92. J. Machowski, J. Bialek, and J. Bumby, *Power System Dynamics: Stability and Control*, 2nd ed., John Wiley & Sons, Ltd, West Sussex, United Kingdom, 2008.
93. R. H. Bishop, ed., *Mechatronics Handbook*, 2nd ed., CRC Press, 2007.
94. See http://www.burjdubai.com/
95. R. Roberts, "Control of high-rise high-speed elevators," *Proceedings of the American Control Conference*, Philadelphia, Pa., 1998, pp. 3440–3444.
96. N. L. Doh, C. Kim, and W. K. Chung, "A Practical Path Planner for the Robotic Vacuum Cleaner in Rectilinear Environments," *IEEE Transactions on Consumer Electronics*, Vol. 53, No. 2, 2007, pp. 519–527.
97. S. C. Lin and C. C. Tsai, "Development of a Self-Balancing Human Transportation Vehicle for the Teaching of Feedback Control," *IEEE Transactions on Education*, Vol. 52, No. 1, 2009, pp. 157–168.
98. K. Li, E. B. Kosmatopoulos, P. A. Ioannou, and H. Ryaciotaki-Boussalis, "Large Segmented Telescopes: Centralized, Decentralized and Overlapping Control Designs," *IEEE Control Systems Magazine*, October 2000.
99. A. Cavalcanti, "Assembly Automation with Evolutionary Nanorobots and Sensor-Based Control Applied to Nanomedicine," *IEEE Transactions on Nanotechnology*, Vol. 2, No. 2, 2003, pp. 82–87.

Chapter 2

1. R. C. Dorf, *Electric Circuits*, 4th ed., John Wiley & Sons, New York, 1999.
2. I. Cochin, *Analysis and Design of Dynamic Systems*, Addison-Wesley Publishing Co., Reading, Mass., 1997.

33. D. Auslander and C. J. Kempf, *Mechatronics*, Prentice Hall, Englewood Cliffs, N. J., 1996.
34. "Things that Go Bump in Your Flight," *The Economist*, July 3, 1999, pp. 69–70.
35. P. J. Brancazio, "Science and the Game of Baseball," *Science Digest*, July 1984, pp. 66–70.
36. C. Klomp, et al., "Development of an Autonomous Cow-Milking Robot Control System," *IEEE Control Systems*, October 1990, pp. 11–19.
37. M. B. Tischler et al., "Flight Control of a Helicopter," *IEEE Control Systems*, August 1999, pp. 22–32.
38. G. B. Gordon and J. C. Roark, "ORCA: An Optimized Robot for Chemical Analysis," *Hewlett-Packard Journal*, June 1993, pp. 6–19.
39. K. Hollenback, "Destabilizing Effects of Muscular Contraction in Human-Machine Interaction," *Proceedings of the American Control Conference*, San Francisco, Calif., 1993, pp. 736–740.
40. L. Scivicco and B. Siciliano, *Modeling and Control of Robot Manipulators*, McGraw-Hill, New York, 1996.
41. O. Mayr, "Adam Smith and the Concept of the Feedback System," *Technology and Culture*, Vol. 12, No. 1, January 1971, pp. 1–22.
42. A. Goldsmith, "Autofocus Cameras," *Popular Science*, March 1988, pp. 70–72.
43. R. Johansson, *System Modeling and Identification*, Prentice Hall, Englewood Cliffs, N. J., 1993.
44. M. DiChristina, "Telescope Tune-Up," *Popular Science*, September 1999, pp. 66–68.
45. K. Capek, *Rossum's Universal Robots*, English version by P. Selver and N. Playfair, Doubleday, Page, New York, 1923.
46. D. Hancock, "Prototyping the Hubble Fix," *IEEE Spectrum*, October 1993, pp. 34–39.
47. A. K. Naj, "Engineers Want New Buildings to Behave Like Human Beings," *Wall Street Journal*, January 20, 1994, p. B1.
48. E. H. Maslen, et al., "Feedback Control Applications in Artifical Hearts," *IEEE Control Systems*, December 1998, pp. 26–30.
49. M. DiChristina, "What's Next for Hubble?" *Popular Science*, March 1998, pp. 56–59.
50. K. G. Ashar, *Magnetic Disk Drive Technology*, IEEE Press, Piscataway, N. J., 1997.
51. T. Coughlin, "2010 Could Be Great Year for Hard Disk Drives," Analysis published at quicktake.morningstar.com, http://www.glgroup.com/News/2010-could-be-great-year-for-hard-disk-drives-46098.html.
52. R. Stone, "Putting a Human Face on a New Breed of Robot," *Science*, October 11, 1996, p. 182.
53. P. I. Ro, "Nanometric Motion Control of a Traction Drive," *ASME Dynamic Systems and Control*, Vol. 55.2, 1994, pp. 879–883.
54. K. C. Cheok, "A Smart Automatic Windshield Wiper," *IEEE Control Systems Magazine*, December 1996, pp. 28–34.
55. D. Dooling, "Transportation," *IEEE Spectrum*, January 1996, pp. 82–86.
56. G. Norris, "Boeing's Seventh Wonder," *IEEE Spectrum*, October 1995, pp. 20–23.
57. D. Hughes, "Fly-by-Wire 777 Keeps Traditional Cockpit," *Aviation Week & Space Technology*, McGraw-Hill Publication, May 1, 1995, pp. 42–48.
58. R. Reck, "Design Engineering," *Aerospace America*, American Institute of Aeronautics and Astronautics, December 1994, p. 74.
59. C. Rist, "Angling for Momentum," *Discover*, September 1999, p. 37.
60. S. J. Elliott, "Down With Noise," *IEEE Spectrum*, June 1999, pp. 54–62.
61. W. Ailor, "Controlling Space Traffic," *AIAA Aerospace America*, November 1999, pp. 34–38.
62. "Seagate Outlines the Future of Storage," An interview with Jim Christico, 2006, http://www.hardwarezone.com/articles/view.php?cid=1&id=1805&pg=2.
63. G. F. Hughes, "Wise Drives," *IEEE Spectrum*, August 2002, pp. 37–41.
64. R. H. Bishop, *The Mechatronics Handbook*, 2nd ed., CRC Press, Inc., Boca Raton, Fla., 2007.
65. N. Kyura and H. Oho, "Mechatronics—An Industrial Perspective," *IEEE/ASME Transactions on Mechatronics*, Vol. 1, No. 1, 1996, pp. 10–15.
66. T. Mori, "Mecha-tronics," *Yasakawa Internal Trademark Application Memo 21.131.01*, July 12, 1969.
67. F. Harshama, M. Tomizuka, and T. Fukuda, "Mechatronics—What is it, Why, and How?—An Editorial," *IEEE/ASME Transactions on Mechatronics*, Vol. 1, No. 1, 1996, pp. 1–4.
68. D. M. Auslander and C. J. Kempf, *Mechatronics: Mechanical System Interfacing*, Prentice Hall, Upper Saddle River, N. J., 1996.
69. D. Shetty and R. A. Kolk, *Mechatronic System Design*, PWS Publishing Company, Boston, Mass., 1997.
70. W. Bolton, *Mechatronics: Electrical Control Systems in Mechanical and Electrical Engineering*, 2nd ed., Addison Wesley Longman, Harlow, England, 1999.

3. J. W. Nilsson, *Electric Circuits*, 5th ed., Addison-Wesley, Reading, Mass., 1996.
4. E. W. Kamen and B. S. Heck, *Fundamentals of Signals and Systems Using MATLAB*, Prentice Hall, Upper Saddle River, N. J., 1997.
5. F. Raven, *Automatic Control Engineering*, 3rd ed., McGraw-Hill, New York, 1994.
6. S. Y. Nof, *Handbook of Industrial Robotics*, John Wiley & Sons, New York, 1999.
7. R. R. Kadiyala, "A Toolbox for Approximate Linearization of Nonlinear Systems," *IEEE Control Systems*, April 1993, pp. 47–56.
8. R. Smith and R. Dorf, *Circuits, Devices and Systems*, 5th ed., John Wiley & Sons, New York, 1992.
9. Y. M. Pulyer, *Electromagnetic Devices for Motion Control*, Springer-Verlag, New York, 1992.
10. B. C. Kuo, *Automatic Control Systems*, 5th ed., Prentice Hall, Englewood Cliffs, N. J., 1996.
11. F. E. Udwadia, *Analytical Dynamics*, Cambridge Univ. Press, New York, 1996.
12. R. C. Dorf, *Electrical Engineering Handbook*, 2nd ed., CRC Press, Boca Raton, Fla., 1998.
13. S. M. Ross, *Simulation*, 2nd ed., Academic Press, Orlando, Fla., 1996.
14. G. B. Gordon, "ORCA: Optimized Robot for Chemical Analysis," *Hewlett-Packard Journal*, June 1993, pp. 6–19.
15. P. E. Sarachik, *Principles of Linear Systems*, Cambridge Univ. Press, New York, 1997.
16. S. Bennett, "Nicholas Minorsky and the Automatic Steering of Ships," *IEEE Control Systems*, November 1984, pp. 10–15.
17. P. Gawthorp, *Metamodeling: Bond Graphs and Dynamic Systems*, Prentice Hall, Englewood Cliffs, N. J., 1996.
18. C. M. Close and D. K. Frederick, *Modeling and Analysis of Dynamic Systems*, 2nd ed., Houghton Mifflin, Boston, 1995.
19. H. S. Black, "Stabilized Feed-Back Amplifiers," *Electrical Engineering*, 53, January 1934, pp. 114–120. Also in *Turning Points in American History*, J. E. Brittain, ed., IEEE Press, New York, 1977, pp. 359–361.
20. P. L. Corke, *Visual Control of Robots*, John Wiley & Sons, New York, 1997.
21. W. J. Rugh, *Linear System Theory*, 2nd ed., Prentice Hall, Englewood Cliffs, N. J., 1997.
22. S. Pannu and H. Kazerooni, "Control for a Walking Robot," *IEEE Control Systems*, February 1996, pp. 20–25.
23. K. Ogata, *Modern Control Engineering*, 3rd ed., Prentice Hall, Upper Saddle River, N. J., 1997.
24. S. P. Parker, *Encyclopedia of Engineering*, 2nd ed., McGraw-Hill, New York, 1993.
25. G. T. Pope, "Living-Room Levitation," *Discover*, June 1993, p. 24.
26. G. Rowell and D. Wormley, *System Dynamics*, Prentice Hall, Upper Saddle River, N. J., 1997.
27. R. H. Bishop, *The Mechatronics Handbook*, 2nd ed., CRC Press, Inc., Boca Raton, Fla., 2007.
28. C. N. Dorny, *Understanding Dynamic Systems: Approaches to Modeling, Analysis, and Design*, Prentice-Hall, Englewood Cliffs, New Jersey, 1993.
29. T. D. Burton, *Introduction to Dynamic Systems Analysis*, McGraw-Hill, Inc., New York, 1994.
30. K. Ogata, *System Dynamics*, 4th ed., Prentice-Hall, Englewood Cliffs, New Jersey, 2003.
31. J. D. Anderson, *Fundamentals of Aerodynamics*, 4th ed., McGraw-Hill, Inc., New York, 2005.
32. G. Emanuel, *Gasdynamics Theory and Applications*, AIAA Education Series, New York, 1986.
33. A. M. Kuethe and C-Y. Chow, *Foundations of Aerodynamics: Bases of Aerodynamic Design*, 5th ed., John Wiley & Sons, New York, 1997.
34. M. A. S. Masoum, H. Dehbonei, and E. F. Fuchs, "Theoretical and Experimental Analyses of Photovoltaic Systems with Voltage- and Current-Based Maximum Power-Point Tracking," *IEEE Transactions on Energy Conversion*, Vol. 17, No. 4, 2002, pp. 514–522.
35. M. G. Wanzeller, R. N. C. Alves, J. V. da Fonseca Neto, and W. A. dos Santos Fonseca, "Current Control Loop for Tracking of Maximum Power Point Supplied for Photovoltaic Array," *IEEE Transactions on Instrumentation And Measurement*, Vol. 53, No. 4, 2004, pp. 1304–1310.
36. G. M. S. Azevedo, M. C. Cavalcanti, K. C. Oliveira, F. A. S. Neves, and Z. D. Lins, "Comparative Evaluation of Maximum Power Point Tracking Methods for Photovoltaic Systems," *ASME Journal of Solar Energy Engineering*, Vol. 131, 2009.
37. W. Xiao, W. G. Dunford, and A. Capel, "A Novel Modeling Method for Photovoltaic Cells," *35th Annual IEEE Power Electronics Specialists Conference*, Aachen, Germany, 2004, pp. 1950–1956.
38. M. Uzunoglu, O.C. Onar, M.S. Alam, "Modeling, Control and Simulation of a PV/FC/UC Based Hybrid Power Generation System for Stand-Alone Applications," *Renewable Energy*, Vol. 34, Elsevier Ltd., 2009, pp. 509–520.
39. N. Hamrouni and A. Cherif, "Modelling and Control of a Grid Connected Photovoltaic System," *International Journal of Electrical and Power*

Engineering, Vol. 1, No. 3, Medwell Journals, 2007, pp. 307–313.
40. N. Kakimoto, S. Takayama, H. Satoh, and K. Nakamura, "Power Modulation of Photovoltaic Generator for Frequency Control of Power System," *IEEE Transactions on Energy Conversion*, Vol. 24, No. 4, 2009, pp. 943–949.
41. S. J. Chiang, H.-J. Shieh, and M.-C. Chen, "Modeling and Control of PV Charger System with SEPIC Converter," *IEEE Transactions on Industrial Electronics*, Vol. 56, No. 11, 2009, pp. 4344–4353.
42. M. Castilla, J. Miret, J. Matas, L. G. de Vicuña, and J. M. Guerrero, "Control Design Guidelines for Single-Phase Grid-Connected Photovoltaic Inverters with Damped Resonant Harmonic Compensators," *IEEE Transactions on Industrial Electronics*, Vol. 56, No. 11, 2009, pp. 4492–4501.

Chapter 3

1. R. C. Dorf, *Electric Circuits*, 3rd ed., John Wiley & Sons, New York, 1997.
2. W. J. Rugh, *Linear System Theory*, 2nd ed., Prentice Hall, Englewood Cliffs, N. J., 1996.
3. H. Kajiwara, et al., "LPV Techniques for Control of an Inverted Pendulum," *IEEE Control Systems*, February 1999, pp. 44–47.
4. R. C. Dorf, *Encyclopedia of Robotics*, John Wiley & Sons, New York, 1988.
5. A. V. Oppenheim, et al., *Signals and Systems*, Prentice Hall, Englewood Cliffs, N. J., 1996.
6. J. L. Stein, "Modeling and State Estimator Design Issues for Model Based Monitoring Systems," *Journal of Dynamic Systems*, ASME, June 1993, pp. 318–326.
7. I. Cochin, *Analysis and Design of Dynamic Systems*, Addison-Wesley, Reading, Mass., 1997.
8. R. C. Dorf, *Electrical Engineering Handbook*, CRC Press, Boca Raton, Fla., 1993.
9. Y. M. Pulyer, *Electromagnetic Devices for Motion Control*, Springer-Verlag, New York, 1992.
10. C. M. Close and D. K. Frederick, *Modeling and Analysis of Dynamic Systems*, 2nd ed., Houghton Mifflin, Boston, 1995.
11. R. C. Durbeck, "Computer Output Printer Technologies," in *Electrical Engineering Handbook*, R. C. Dorf, ed., CRC Press, Boca Raton, Fla., 1998, pp. 1958–1975.
12. B. Wie, et al., "New Approach to Attitude/Momentum Control for the Space Station," *AIAA Journal of Guidance, Control, and Dynamics*, Vol. 12, No. 5, 1989, pp. 714–722.
13. H. Ramirez, "Feedback Controlled Landing Maneuvers," *IEEE Transactions on Automatic Control*, April 1992, pp. 518–523.
14. C. A. Canudas De Wit, *Theory of Robot Control*, Springer-Verlag, New York, 1996.
15. R. R. Kadiyala, "A Toolbox for Approximate Linearization of Nonlinear Systems," *IEEE Control Systems*, April 1993, pp. 47–56.
16. B. C. Crandall, *Nanotechnology*, MIT Press, Cambridge, Mass., 1996.
17. W. Leventon, "Mountain Bike Suspension Allows Easy Adjustment," *Design News*, July 19, 1993, pp. 75–77.
18. A. Cavallo, et al., *Using* MATLAB, SIMULINK, *and Control System Toolbox*, Prentice Hall, Englewood Cliffs, N. J., 1996.
19. G. E. Carlson, *Signal and Linear System Analysis*, John Wiley & Sons, New York, 1998.
20. D. Cho, "Magnetic Levitation Systems," *IEEE Control Systems*, February 1993, pp. 42–48.
21. W. J. Palm, *Modeling, Analysis, Control of Dynamic Systems*, 2nd ed., John Wiley & Sons, New York, 2000.
22. H. Kazerooni, "Human Extenders," *Journal of Dynamic Systems*, ASME, June 1993, pp. 281–290.
23. C. N. Dorny, *Understanding Dynamic Systems*, Prentice Hall, Englewood Cliffs, N. J., 1993.
24. Chen, Chi-Tsing, *Linear System Theory and Design*, 3rd ed., Oxford Univ. Press, New York, 1998.
25. M. Kaplan, *Modern Spacecraft Dynamics and Control*, John Wiley and Sons, New York, 1976.
26. J. Wertz, ed., *Spacecraft Attitude Determination and Control*, Kluwer Academic Publishers, Dordrecht, The Netherlands, 1978 (reprinted in 1990).
27. W. E. Wiesel, *Spaceflight Dynamics*, McGraw-Hill, New York, 1989.
28. B. Wie, K. W. Byun, V. W. Warren, D. Geller, D. Long and J. Sunkel, "New Approach to Attitude/Momentum Control for the Space Station," *AIAA Journal Guidance, Control, and Dynamics*, Vol. 12, No. 5, 1989, pp. 714–722.
29. L. R. Bishop, R. H. Bishop, and K. L. Lindsay, "Proposed CMG Momentum Management Scheme for Space Station," *AIAA Guidance Navigation and Controls Conference Proceedings*, Vol. 2, No. 87-2528, 1987, pp. 1229–1236.
30. H. H. Woo, H. D. Morgan, and E. T. Falangas, "Momentum Management and Attitude Control Design for a Space Station," *AIAA Journal of Guidance, Control, and Dynamics*, Vol. 11, No. 1, 1988, pp. 19–25.

31. J. W. Sunkel and L. S. Shieh, "An Optimal Momentum Management Controller for the Space Station," *AIAA Journal of Guidance, Control, and Dynamics*, Vol. 13, No. 4, 1990, pp. 659–668.
32. V. W. Warren, B. Wie, and D. Geller, "Periodic-Disturbance Accommodating Control of the Space Station," *AIAA Journal of Guidance, Control, and Dynamics*, Vol. 13, No. 6, 1990, pp. 984–992.
33. B. Wie, A. Hu, and R. Singh, "Multi-Body Interaction Effects on Space Station Attitude Control and Momentum Management," *AIAA Journal of Guidance, Control, and Dynamics*, Vol. 13, No. 6, 1990, pp. 993–999.
34. J. W. Sunkel and L. S. Shieh, "Multistage Design of an Optimal Momentum Management Controller for the Space Station," *AIAA Journal of Guidance, Control, and Dynamics*, Vol. 14, No. 3, 1991, pp. 492–502.
35. K. W. Byun, B. Wie, D. Geller, and J. Sunkel, "Robust H_∞ Control Design for the Space Station with Structured Parameter Uncertainty," *AIAA Journal of Guidance, Control, and Dynamics*, Vol. 14, No. 6, 1991, pp. 1115–1122.
36. E. Elgersma, G. Stein, M. Jackson, and J. Yeichner, "Robust Controllers for Space Station Momentum Management," *IEEE Control Systems Magazine*, Vol. 12, No. 2, October 1992, pp. 14–22.
37. G. J. Balas, A. K. Packard, and J. T. Harduvel, "Application of μ-Synthesis Technique to Momentum Management and Attitude Control of the Space Station," *Proceedings of 1991 AIAA Guidance, Navigation, and Control Conference*, New Orleans, Louisiana, pp. 565–575.
38. Rhee and J. L. Speyer, "Robust Momentum Management and Attitude Control System for the Space Station," *AIAA Journal of Guidance, Control, and Dynamics*, Vol. 15, No. 2, 1992, pp. 342–351.
39. T. F. Burns and H. Flashner, "Adaptive Control Applied to Momentum Unloading Using the Low Earth Orbital Environment," *AIAA Journal of Guidance, Control, and Dynamics*, Vol. 15, No. 2, 1992, pp. 325–333.
40. X. M. Zhao, L. S. Shieh, J. W. Sunkel, and Z. Z. Yuan, "Self-Tuning Control of Attitude and Momentum Management for the Space Station," *AIAA Journal of Guidance, Control, and Dynamics*, Vol. 15, No. 1, 1992, pp. 17–27.
41. G. Parlos and J. W. Sunkel, "Adaptive Attitude Control and Momentum Management for Large-Angle Spacecraft Maneuvers," *AIAA Journal of Guidance, Control, and Dynamics*, Vol. 15, No. 4, 1992, pp. 1018–1028.
42. R. H. Bishop, S. J. Paynter, and J. W. Sunkel, "Adaptive Control of Space Station with Control Moment Gyros," *IEEE Control Systems Magazine*, Vol. 12, No. 2, October 1992, pp. 23–28.
43. S. R. Vadali and H. S. Oh, "Space Station Attitude Control and Momentum Management: A Nonlinear Look," *AIAA Journal of Guidance, Control, and Dynamics*, Vol. 15, No. 3, 1992, pp. 577–586.
44. S. N. Singh and T. C. Bossart, "Feedback Linearization and Nonlinear Ultimate Boundedness Control of the Space Station Using CMG," *AIAA Guidance Navigation and Controls Conference Proceedings*, Vol. 1, No. 90-3354-CP, 1990, pp. 369–376.
45. S. N. Singh and T. C. Bossart, "Invertibility of Map, Zero Dynamics and Nonlinear Control of Space Station," *AIAA Guidance Navigation and Controls Conference Proceedings*, Vol. 1, No. 91-2663-CP, 1991, pp. 576–584.
46. S. N. Singh and A. Iyer, "Nonlinear Regulation of Space Station: A Geometric Approach," *AIAA Journal of Guidance, Control, and Dynamics*, Vol. 17, No. 2, 1994, pp. 242–249.
47. J. J. Sheen and R. H. Bishop, "Spacecraft Nonlinear Control," *The Journal of Astronautical Sciences*, Vol. 42, No. 3, 1994, pp. 361–377.
48. J. Dzielski, E. Bergmann, J. Paradiso, D. Rowell, and D. Wormley, "Approach to Control Moment Gyroscope Steering Using Feedback Linearization," *AIAA Journal of Guidance, Control, and Dynamics*, Vol. 14, No. 1, 1991, pp. 96–106.
49. J. J. Sheen and R. H. Bishop, "Adaptive Nonlinear Control of Spacecraft," *The Journal of Astronautical Sciences*, Vol. 42, No. 4, 1994, pp. 451–472.
50. S. N. Singh and T. C. Bossart, "Exact Feedback Linearization and Control of Space Station Using CMG," *IEEE Transactions on Automatic Control*, Vol. Ac-38, No. 1, 1993, pp. 184–187.

Chapter 4

1. R. C. Dorf, *Electrical Engineering Handbook*, 2nd ed., CRC Press, Boca Raton, Fla., 1998.
2. R. C. Dorf, *Electric Circuits*, 3rd ed., John Wiley & Sons, New York, 1996.
3. C. E. Rohrs, J. L. Melsa, and D. Schultz, *Linear Control Systems*, McGraw-Hill, New York, 1993.
4. P. E. Sarachik, *Principles of Linear Systems*, Cambridge Univ. Press, New York, 1997.
5. B. K. Bose, *Power Electronics and Variable Frequency Drives*, IEEE Press, Piscataway, N. J., 1997.

6. J. C. Nelson, *Operational Amplifier Circuits*, Butterworth, New York, 1995.
7. *Motomatic Speed Control*, Electro-Craft Corp., Hopkins, Minn., 1999.
8. M. W. Spong et al., *Robot Control Dynamics, Motion Planning and Analysis*, IEEE Press, New York, 1993.
9. R. C. Dorf, *Encyclopedia of Robotics*, John Wiley & Sons, New York, 1988.
10. D. J. Bak, "Dancer Arm Feedback Regulates Tension Control," *Design News*, April 6, 1987, pp. 132–133.
11. "The Smart Projector Demystified," *Science Digest*, May 1985, p. 76.
12. J. M. Maciejowski, *Multivariable Feedback Design*, Addison-Wesley, Wokingham, England, 1989.
13. L. Fortuna and G. Muscato, "A Roll Stabilization System for a Monohull Ship," *IEEE Transactions on Control Systems Technology*, January 1996, pp. 18–28.
14. C. N. Dorny, *Understanding Dynamic Systems*, Prentice Hall, Englewood Cliffs, N. J., 1993.
15. D. W. Clarke, "Sensor, Actuator, and Loop Validation," *IEEE Control Systems*, August 1995, pp. 39–45.
16. S. P. Parker, *Encyclopedia of Engineering*, 2nd ed., McGraw-Hill, New York, 1993.
17. M. S. Markow, "An Automated Laser System for Eye Surgery," *IEEE Engineering in Medicine and Biology*, December 1989, pp. 24–29.
18. M. Eslami, *Theory of Sensitivity in Dynamic Systems*, Springer-Verlag, New York, 1994.
19. Y. M. Pulyer, *Electromagnetic Devices for Motion Control*, Springer-Verlag, New York, 1992.
20. J. R. Layne, "Control for Cargo Ship Steering," *IEEE Control Systems*, December 1993, pp. 23–33.
21. S. Begley, "Greetings From Mars," *Newsweek*, July 14, 1997, pp. 23–29.
22. M. Carroll, "Assault on the Red Planet," *Popular Science*, January 1997, pp. 44–49.
23. The American Medical Association, *Home Medical Encyclopedia*, vol. 1, Random House, New York, 1989, pp. 104–106.
24. J. B. Slate, L. C. Sheppard, V. C. Rideout, and E. H. Blackstone, "Closed-loop Nitroprusside Infusion: Modeling and Control Theory for Clinical Applications," *Proceedings IEEE International Symposium on Circuits and Systems*, 1980, pp. 482–488.
25. B. C. McInnis and L. Z. Deng, "Automatic Control of Blood Pressures with Multiple Drug Inputs," *Annals of Biomedical Engineering*, vol. 13, 1985, pp. 217–225.
26. R. Meier, J. Nieuwland, A. M. Zbinden, and S. S. Hacisalihzade, "Fuzzy Logic Control of Blood Pressure During Anesthesia," *IEEE Control Systems*, December 1992, pp. 12–17.
27. L. C. Sheppard, "Computer Control of the Infusion of Vasoactive Drugs," *Proceedings IEEE International Symposium on Circuits and Systems*, 1980, pp. 469–473.
28. S. Lee, "Intelligent Sensing and Control for Advanced Teleoperation," *IEEE Control Systems*, June 1993, pp. 19–28.
29. L. L. Cone, "Skycam: An Aerial Robotic Camera System," *Byte*, October 1985, pp. 122–128.

Chapter 5

1. C. M. Close and D. K. Frederick, *Modeling and Analysis of Dynamic Systems*, 2nd ed., Houghton Mifflin, Boston, 1993.
2. R. C. Dorf, *Electric Circuits*, 3rd ed., John Wiley & Sons, New York, 1996.
3. B. K. Bose, *Power Electronics and Variable Frequency Drives*, IEEE Press, Piscataway, N. J., 1997.
4. P. R. Clement, "A Note on Third-Order Linear Systems," *IRE Transactions on Automatic Control*, June 1960, p. 151.
5. R. N. Clark, *Introduction to Automatic Control Systems*, John Wiley & Sons, New York, 1962, pp. 115–124.
6. D. Graham and R. C. Lathrop, "The Synthesis of Optimum Response: Criteria and Standard Forms, Part 2," *Trans. of the AIEE* 72, November 1953, pp. 273–288.
7. R. C. Dorf, *Encyclopedia of Robotics*, John Wiley & Sons, New York, 1988.
8. L. E. Ryan, "Control of an Impact Printer Hammer," *ASME Journal of Dynamic Systems*, March 1990, pp. 69–75.
9. E. J. Davison, "A Method for Simplifying Linear Dynamic Systems," *IEEE Transactions on Automatic Control*, January 1966, pp. 93–101.
10. R. C. Dorf, *Electrical Engineering Handbook*, CRC Press, Boca Raton, Fla., 1998.
11. A. G. Ulsoy, "Control of Machining Processes," *ASME Journal of Dynamic Systems*, June 1993, pp. 301–310.
12. I. Cochin, *Analysis and Design of Dynamic Systems*, Addison-Wesley, Reading, Mass., 1997.
13. W. J. Rugh, *Linear System Theory*, 2nd ed., Prentice Hall, Englewood Cliffs, N.J., 1997.

14. W. J. Book, "Controlled Motion in an Elastic World," *Journal of Dynamic Systems*, June 1993, pp. 252–260.
15. C. E. Rohrs, J. L. Melsa, and D. Schultz, *Linear Control Systems*, McGraw-Hill, New York, 1993.
16. S. Lee, "Intelligent Sensing and Control for Advanced Teleoperation," *IEEE Control Systems*, June 1993, pp. 19–28.
17. T. J. Lueck, "Amtrack Unveils Its Bullet to Boston," *New York Times*, March 10, 1999, p. B2.
18. M. DiChristina, "Telescope Tune-Up," *Popular Science*, September 1999, pp. 66–68.
19. M. Hutton and M. Rabins, "Simplification of Higher-Order Mechanical Systems Using the Routh Approximation," *Journal of Dynamic Systems*, ASME, December 1975, pp. 383–392.
20. E. W. Kamen and B. S. Heck, *Fundamentals of Signals and Systems Using MATLAB*, Prentice Hall, Upper Saddle River, N. J., 1997.
21. M. DiChristina, "What's Next for Hubble?" *Popular Science*, March 1998, pp. 56–59.
22. Aaron Edsinger-Gonzales and Jeff Weber, "Domo: A Force Sensing Humanoid Robot for Manipulation Research," *Proceedings of the IEEE/RSJ International Conference on Humanoid Robotics*, 2004.
23. Aaron Edsinger-Gonzales, "Design of a Compliant and Force Sensing Hand for a Humanoid Robot," *Proceedings of the International Conference on Intelligent Manipulation and Grasping*, 2004.
24. B. L. Stevens and F. L. Lewis, *Aircraft Control and Simulation*, 2nd ed., John Wiley & Sons, New York, 2003.
25. B. Etkin and L. D. Reid, *Dynamics of Flight*, 3rd ed., John Wiley & Sons, New York, 1996.
26. G. E. Cooper and R. P. Harper, Jr., "The Use of Pilot Rating in the Evaluation of Aircraft Handling Qualities," NASA TN D-5153, 1969 (see also http://flighttest.navair.navy.mil/unrestricted/ch.pdf).
27. USAF, "Flying Qualities of Piloted Vehicles," USAF Spec., MIL-F-8785C, 1980.
28. H. Paraci and M. Jamshidi, *Design and Implementation of Intelligent Manufacturing Systems*, Prentice Hall, Upper Saddle River, N. J., 1997.

Chapter 6

1. R. C. Dorf, *Electrical Engineering Handbook*, 2nd ed., CRC Press, Boca Raton, Fla., 1998.
2. R. C. Dorf, *Electric Circuits*, 3rd ed., John Wiley & Sons, New York, 1996.
3. W. J. Palm, *Modeling, Analysis and Control*, 2nd ed., John Wiley & Sons, New York, 2000.
4. W. J. Rugh, *Linear System Theory*, 2nd ed., Prentice Hall, Englewood Cliffs, N. J., 1997.
5. F. B. Farquharson, "Aerodynamic Stability of Suspension Bridges, with Special Reference to the Tacoma Narrows Bridge," *Bulletin 116, Part I*, The Engineering Experiment Station, University of Washington, 1950.
6. A. Hurwitz, "On the Conditions under which an Equation Has Only Roots with Negative Real Parts," *Mathematische Annalen* 46, 1895, pp. 273–284. Also in *Selected Papers on Mathematical Trends in Control Theory*, Dover, New York, 1964, pp. 70–82.
7. E. J. Routh, *Dynamics of a System of Rigid Bodies*, Macmillan, New York, 1892.
8. G. G. Wang, "Design of Turning Control for a Tracked Vehicle," *IEEE Control Systems*, April 1990, pp. 122–125.
9. N. Mohan, *Power Electronics*, John Wiley & Sons, New York, 1995.
10. *World Robotics 2003–Statistics, Market Analysis, Forecasts, Case Studies, and Profitability of Robot Investment*, U. N. Economic Commission, ISBN No. 92-1-101059-4, 2003.
11. R. C. Dorf and A. Kusiak, *Handbook of Manufacturing and Automation*, John Wiley & Sons, New York, 1994.
12. A. N. Michel, "Stability: The Common Thread in the Evolution of Control," *IEEE Control Systems*, June 1996, pp. 50–60.
13. S. P. Parker, *Encyclopedia of Engineering*, 2nd ed., McGraw-Hill, New York, 1933.
14. J. Levine, et al., "Control of Magnetic Bearings," *IEEE Transactions on Control Systems Technology*, September 1996, pp. 524–544.
15. F. S. Ho, "Traffic Flow Modeling and Control," *IEEE Control Systems*, October 1996, pp. 16–24.
16. D. W. Freeman, "Jump-Jet Airliner," *Popular Mechanics*, June 1993, pp. 38–40.
17. B. Sweetman, "Venture Star–21st-Century Space Shuttle," *Popular Science*, October 1996, pp. 43–47.
18. S. Lee, "Intelligent Sensing and Control for Advanced Teleoperation," *IEEE Control Systems*, June 1993, pp. 19–28.
19. "Uplifting," *The Economist*, July 10, 1993, p. 79.
20. R. N. Clark, "The Routh-Hurwitz Stability Criterion, Revisited," *IEEE Control Systems*, June 1992, pp. 119–120.
21. Gregory Mone, "5 Paths to the Walking, Talking, Pie-Baking Humanoid Robot," *Popular Science*, September 2006.

22. L. Hatvani, "Adaptive Control: Stabilization," *Applied Control*, edited by Spyros G. Tzafestas, Marcel Decker, New York, 1993, pp. 273–287.
23. H. Kazerooni, "Human Extenders," *Journal of Dynamic Systems*, ASME, 1993, pp. 281–290.

Chapter 7

1. W. R. Evans, "Graphical Analysis of Control Systems," *Transactions of the AIEE*, 67, 1948, pp. 547–551. Also in G. J. Thaler, ed., *Automatic Control*, Dowden, Hutchinson, and Ross, Stroudsburg, Pa., 1974, pp. 417–421.
2. W. R. Evans, "Control System Synthesis by Root Locus Method," *Transactions of the AIEE*, 69, 1950, pp. 1–4. Also in *Automatic Control*, G. J. Thaler, ed., Dowden, Hutchinson, and Ross, Stroudsburg, Pa., 1974, pp. 423–425.
3. W. R. Evans, *Control System Dynamics*, McGraw-Hill, New York, 1954.
4. R. C. Dorf, *Electrical Engineering Handbook*, 2nd ed., CRC Press, Boca Raton, Fla., 1998.
5. J. G. Goldberg, *Automatic Controls*, Allyn and Bacon, Boston, 1965.
6. R. C. Dorf, *The Encyclopedia of Robotics*, John Wiley & Sons, New York, 1988.
7. H. Ur, "Root Locus Properties and Sensitivity Relations in Control Systems," *I.R.E. Trans. on Automatic Control*, January 1960, pp. 57–65.
8. T. R. Kurfess and M. L. Nagurka, "Understanding the Root Locus Using Gain Plots," *IEEE Control Systems*, August 1991, pp. 37–40.
9. T. R. Kurfess and M. L. Nagurka, "Foundations of Classical Control Theory," *The Franklin Institute*, Vol. 330, No. 2, 1993, pp. 213–227.
10. "Webb Automatic Guided Carts," Jervis B. Webb Company, http://www.jervisbwebb.com/, 2008.
11. D. K. Lindner, *Introduction to Signals and Systems*, McGraw-Hill, New York, 1999.
12. S. Ashley, "Putting a Suspension through Its Paces," *Mechanical Engineering*, April 1993, pp. 56–57.
13. B. K. Bose, *Modern Power Electronics*, IEEE Press, New York, 1992.
14. P. Varaiya, "Smart Cars on Smart Roads," *IEEE Transactions on Automatic Control*, February 1993, pp. 195–207.
15. S. Bermana, E. Schechtmana and Y. Edana, "Evaluation of Automatic Guided Vehicle Systems," *Robotics and Computer-Integrated Manufacturing*, Vol. 25, No. 3, 2009, pp. 522–528.
16. B. Sweetman, "21st Century SST," *Popular Science*, April 1998, pp. 56–60.
17. L. V. Merritt, "Tape Transport Head Positioning Servo Using Positive Feedback," *Motion*, April 1993, pp. 19–22.
18. G. E. Young and K. N. Reid, "Control of Moving Webs," *Journal of Dynamic Systems*, ASME, June 1993, pp. 309–316.
19. S. P. Parker, *Encyclopedia of Engineering*, 2nd ed., McGraw-Hill, New York, 1993.
20. A. J. Calise and R. T. Rysdyk, "Nonlinear Adaptive Flight Control Using Neural Networks," *IEEE Control Systems*, December 1998, pp. 14–23.
21. T. B. Sheridan, *Telerobotics, Automation and Control*, MIT Press, Cambridge, Mass., 1992.
22. L. W. Couch, *Digital and Analog Communication Systems*, 5th ed., Macmillan, New York, 1997.
23. D. Hrovat, "Applications of Optimal Control to Automotive Suspension Design," *Journal of Dynamic Systems*, ASME, June 1993, pp. 328–342.
24. T. J. Lueck, "Amtrak Unveils Its Bullet to Boston," *New York Times*, March 10, 1999.
25. M. van de Panne, "A Controller for the Dynamic Walk of a Biped," *Proceedings of the Conference on Decision and Control*, IEEE, December 1992, pp. 2668–2673.
26. R. C. Dorf, *Electric Circuits*, 3rd ed., John Wiley & Sons, New York, 1996.
27. S. Begley, "Mission to Mars," *Newsweek*, September 23, 1996, pp. 52–58.
28. W. J. Cook, "The International Space Station Takes Shape," *US News and World Report*, December 7, 1998, pp. 56–59.
29. "Batwings and Dragonflies," *The Economist*, July 2002, pp. 66–67.
30. "Global Automotive Electronics with Special Focus on OEMs Market Report," *Business Wire*, http://www.pcb007.com/, December 3, 2009.
31. J. G. Kassakian, H.-C. Wolf, J. M. Miller, and C. J. Hurton, "Automotive Electrical Systems Circa 2005," Vol. 33, No. 8, *IEEE Spectrum*, August, 1996, pp. 22–27.
32. M. B. Barron and W. F. Powers, "The Role of Electronic Controls for Future Automotive Mechatronic Systems," *IEEE/ASME Transactions on Mechatronics*, Vol. 1, No. 1, 1996, pp. 80–88.
33. *Wind Energy—The Facts*, European Wind Energy Association, http://windfacts.eu/, 2009.
34. P. D. Sclavounos, E. N. Wayman, S. Butterfield, J. Jonkman, and W. Musial, "Floating Wind Turbine Concepts," *European Wind Energy Association Conference (EWAC)*, Athens, Greece, 2006.

10. J. J. Gribble, "Systems with Time Delay," *IEEE Control Systems*, February 1993, pp. 54–55.
11. C. N. Dorny, *Understanding Dynamic Systems*, Prentice Hall, Englewood Cliffs, N. J., 1993.
12. R. C. Dorf, *Electric Circuits*, 3rd ed., John Wiley & Sons, New York, 1996.
13. J. Yan and S. E. Salcudean, "Teleoperation Controller Design," *IEEE Transactions on Control Systems Technology*, May 1996, pp. 244–247.
14. K. K. Chew, "Control of Errors in Disk Drive Systems," *IEEE Control Systems*, January 1990, pp. 16–19.
15. R. C. Dorf, *The Encyclopedia of Robotics*, John Wiley & Sons, New York, 1988.
16. D. W. Freeman, "Jump-Jet Airliner," *Popular Mechanics*, June 1993, pp. 38–40.
17. F. D. Norvelle, *Electrohydraulic Control Systems*, Prentice Hall, Upper Saddle River, N. J., 2000.
18. B. K. Bose, *Power Electronics and Variable Frequency Drives*, IEEE Press, Piscataway, N. J., 1997.
19. C. S. Bonaventura and K. W. Lilly, "A Constrained Motion Algorithm for the Shuttle Remote Manipulator System," *IEEE Control Systems*, October 1995, pp. 6–16.
20. A. T. Bahill and L. Stark, "The Trajectories of Saccadic Eye Movements," *Scientific American*, January 1979, pp. 108–117.
21. A. G. Ulsoy, "Control of Machining Processes," ASME, *Journal of Dynamic Systems*, June 1993, pp. 301–310.
22. C. E. Rohrs, J. L. Melsa, and D. Schultz, *Linear Control Systems*, McGraw-Hill, New York, 1993.
23. J. L. Jones and A. M. Flynn, *Mobile Robots*, A. K. Peters Publishing, New York, 1993.
24. D. A. Linkens, "Adaptive and Intelligent Control in Anesthesia," *IEEE Control Systems*, December 1992, pp. 6–10.
25. R. H. Bishop, "Adaptive Control of Space Station with Control Moment Gyros," *IEEE Control Systems*, October 1992, pp. 23–27.
26. J. B. Song, "Application of Adaptive Control to Arc Welding Processes," *Proceedings of the American Control Conference*, IEEE, June 1993, pp. 1751–1755.
27. X. G. Wang, "Estimation in Paper Machine Control," *IEEE Control Systems*, August 1993, pp. 34–43.
28. R. Patton, "Mag Lift," *Scientific American*, October 1993, pp. 108–109.
29. P. Ferreira, "Concerning the Nyquist Plots of Rational Functions of Nonzero Type," *IEEE Transaction on Education*, Vol. 42, No. 3, 1999, pp. 228–229.
30. J. Pretolve, "Stereo Vision," *Industrial Robot*, Vol. 21, No. 2, 1994, pp. 24–31.
31. M. W. Spong and M. Vidyasagar, *Robot Dynamics and Control*, John Wiley & Sons, New York, 1989.
32. L. Y. Pao and K. E. Johnson, "A Tutorial on the Dynamics and Control of Wind Turbines and Wind Farms," *Proceedings of the American Control Conference*, St. Louis, MO, 2009, pp. 2076–2089.
33. G. K. Klute, U. Tsach, and D. Geselowitz, "An Optimal Controller for an Electric Ventricular Assist Device: Theory, Implementation, and Testing," *IEEE Transactions of Biomedical Engineering*, Vol. 39, No. 4, 1992, pp. 394–403.

Chapter 10

1. R. C. Dorf, *Electrical Engineering Handbook*, 2nd ed., CRC Press, Boca Raton, Fla., 1998.
2. Z. Gajic and M. Lelic, *Modern Control System Engineering*, Prentice Hall, Englewood Cliffs, N. J., 1996.
3. K. S. Yeung, et al., "A Non-trial and Error Method for Lag-Lead Compensator Design," *IEEE Transactions on Education*, February 1998, pp. 76–80.
4. W. R. Wakeland, "Bode Compensator Design," *IEEE Transactions on Automatic Control*, October 1976, pp. 771–773.
5. J. R. Mitchell, "Comments on Bode Compensator Design," *IEEE Transactions on Automatic Control*, October 1977, pp. 869–870.
6. S. T. Van Voorhis, "Digital Control of Measurement Graphics," *Hewlett-Packard Journal*, January 1986, pp. 24–26.
7. R. H. Bishop, "Adaptive Control of Space Station with Control Moment Gyros," *IEEE Control Systems*, October 1992, pp. 23–27.
8. C. L. Phillips, "Analytical Bode Design of Controllers," *IEEE Transactions on Education*, February 1985, pp. 43–44.
9. R. C. Garcia and B. S. Heck, "Enhancing Classical Controls Education via Interactive Design," *IEEE Control Systems*, June 1999, pp. 77–82.
10. J. D. Powell, N. P. Fekete, and C-F. Chang, "Observer-Based Air-Fuel Ratio Control," *IEEE Control Systems*, October 1998, p. 72.
11. T. B. Sheridan, *Telerobotics, Automation and Control*, MIT Press, Cambridge, Mass., 1992.
12. R. C. Dorf, *The Encyclopedia of Robotics*, John Wiley & Sons, New York, 1988.
13. R. L. Wells, "Control of a Flexible Robot Arm," *IEEE Control Systems*, January 1990, pp. 9–15.
14. H. Kazerooni, "Human Extenders," *Journal of Dynamic Systems*, ASME, June 1993, pp. 281–290.

35. I. Munteanu, A. I. Bratcu, N. A. Cutululis, and E. Ceanga, *Optimal Control of Wind Energy Systems*, Springer-Verlag, London, 2008.
36. F. G. Martin, *The Art of Robotics*, Prentice Hall, Upper Saddle River, N. J., 1999.

Chapter 8

1. R. C. Dorf, *Electrical Engineering Handbook*, 2nd ed., CRC Press, Boca Raton, Fla., 1998.
2. I. Cochin and H. J. Plass, *Analysis and Design of Dynamic Systems*, John Wiley & Sons, New York, 1997.
3. R. C. Dorf, *Electric Circuits*, 3rd ed., John Wiley & Sons, New York, 1996.
4. H. W. Bode, "Relations Between Attenuation and Phase in Feedback Amplifier Design," *Bell System Tech. J.*, July 1940, pp. 421–454. Also in *Automatic Control: Classical Linear Theory*, G. J. Thaler, ed., Dowden, Hutchinson, and Ross, Stroudsburg, Pa., 1974, pp. 145–178.
5. M. D. Fagen, *A History of Engineering and Science in the Bell System*, Bell Telephone Laboratories, Murray Hill, N.J., 1978, Chapter 3.
6. D. K. Lindner, *Introduction to Signals and Systems*, McGraw-Hill, New York., 1999.
7. R. C. Dorf and A. Kusiak, *Handbook of Manufacturing and Automation*, John Wiley & Sons, New York, 1994.
8. R. C. Dorf, *The Encyclopedia of Robotics*, John Wiley & Sons, New York, 1988.
9. T. B. Sheridan, *Telerobotics, Automation and Control*, MIT Press, Cambridge, Mass., 1992.
10. J. L. Jones and A. M. Flynn, *Mobile Robots*, A. K. Peters Publishing, New York, 1993.
11. D. McLean, *Automatic Flight Control Systems*, Prentice Hall, Englewood Cliffs, N. J., 1990.
12. G. Leitman, "Aircraft Control Under Conditions of Windshear," *Proceedings of IEEE Conference on Decision and Control*, December 1990, pp. 747–749.
13. S. Lee, "Intelligent Sensing and Control for Advanced Teleoperation," *IEEE Control Systems*, June 1993, pp. 19–28.
14. R. A. Hess, "A Control Theoretic Model of Driver Steering Behavior," *IEEE Control Systems*, August 1990, pp. 3–8.
15. J. Winters, "Personal Trains," *Discover*, July 1999, pp. 32–33.
16. J. Ackermann and W. Sienel, "Robust Yaw Damping of Cars with Front and Rear Wheel Steering," *IEEE Transactions on Control Systems Technology*, March 1993, pp. 15–20.
17. L. V. Merritt, "Differential Drive Film Transport," *Motion*, June 1993, pp. 12–21.
18. S. Ashley, "Putting a Suspension through Its Paces," *Mechanical Engineering*, April 1993, pp. 56–57.
19. D. A. Linkens, "Anaesthesia Simulators," *Computing and Control Engineering Journal*, IEEE, April 1993, pp. 55–62.
20. J. R. Layne, "Control for Cargo Ship Steering," *IEEE Control Systems*, December 1993, pp. 58–64.
21. A. Titli, "Three Control Approaches for the Design of Car Semi-active Suspension," *IEEE Proceedings of Conference on Decision and Control*, December 1993, pp. 2962–2963.
22. H. H. Ottesen, "Future Servo Technologies for Hard Disk Drives," *Journal of the Magnetics Society of Japan*, Vol. 18, 1994, pp. 31–36.
23. D. Leonard, "Ambler Ramblin," *Ad Astra*, Vol. 2, No. 7, July–August 1990, pp. 7–9.
24. M. G. Wanzeller, R. N. C. Alves, J. V. da Fonseca Neto, and W. A. dos Santos Fonseca, "Current Control Loop for Tracking of Maximum Power Point Supplied for Photovoltaic Array," *IEEE Transactions on Instrumentation And Measurement*, Vol. 53, No. 4, 2004, pp. 1304–1310.

Chapter 9

1. H. Nyquist, "Regeneration Theory," *Bell Systems Tech. J.*, January 1932, pp. 126–147. Also in *Automatic Control: Classical Linear Theory*, G. J. Thaler, ed., Dowden, Hutchinson, and Ross, Stroudsburg, Pa., 1932, pp. 105–126.
2. M. D. Fagen, *A History of Engineering and Science in the Bell System*, Bell Telephone Laboratories, Inc., Murray Hill, N. J., 1978, Chapter 5.
3. H. M. James, N. B. Nichols, and R. S. Phillips, *Theory of Servomechanisms*, McGraw-Hill, New York, 1947.
4. W. J. Rugh, *Linear System Theory*, 2nd ed., Prentice Hall, Englewood Cliffs, N. J., 1996.
5. D. A. Linkens, *CAD for Control Systems*, Marcel Dekker, New York, 1993.
6. A. Cavallo, *Using MATLAB, SIMULINK, and Control System Toolbox*, Prentice Hall, Englewood Cliffs, N. J., 1996.
7. R. C. Dorf, *Electrical Engineering Handbook*, 2nd ed., CRC Press, Boca Raton, Fla., 1998.
8. D. Sbarbaro-Hofer, "Control of a Steel Rolling Mill," *IEEE Control Systems*, June 1993, pp. 69–75.
9. R. C. Dorf and A. Kusiak, *Handbook of Manufacturing and Automation*, John Wiley & Sons, New York, 1994.

24. Rama K. Yedavalli, "Robust Control Design for Aerospace Applications," *IEEE Transactions of Aerospace and Electronic Systems*, Vol. 25, No. 3, 1989, pp. 314–324.
25. Bryan L. Jones and Robert H. Bishop, "H_2 Optimal Halo Orbit Guidance," *Journal of Guidance, Control, and Dynamics, AIAA*, Vol. 16, No. 6, 1993, pp. 1118–1124.
26. D. G. Luenberger, "Observing the State of a Linear System," *IEEE Transactions on Military Electronics*, 1964, pp. 74–80.
27. G. F. Franklin, J. D. Powell, and A. Emami-Naeini, *Feedback Control of Dynamic Systems*, 4th ed., Prentice Hall, Upper Saddle River, N. J., 2002.
28. R. E. Kalman, "Mathematical description of linear dynamical systems," *SIAM J. Control*, Vol. 1, 1963, pp. 152–192.
29. R. E. Kalman, "A New Approach to Linear Filtering and Prediction Problems," *Journal of Basic Engineering*, 1960, pp. 35–45.
30. R. E. Kalman and R. S. Bucy, "New Results in Linear Filtering and Prediction Theory," Transactions of the American Society of Mechanical Engineering, Series D, *Journal of Basic Engineering*, 1961, pp. 95–108.
31. B. Cipra, "Engineers Look to Kalman Filtering for Guidance," *SIAM News*, Vol. 26, No. 5, August 1993.
32. R. H. Battin, "Theodore von Karman Lecture: Some Funny Things Happened on the Way to the Moon," 27th Aerospace Sciences Meeting, Reno, Nevada, AIAA-89-0861, 1989.
33. R. G. Brown and P. Y. C. Hwang, *Introduction to Random Signal Analysis and Kalman Filtering with Matlab Exercises and Solutions*, John Wiley and Sons, Inc., 1996.
34. M. S. Grewal, and A. P. Andrews, *Kalman Filtering: Theory and Practice Using MATLAB, 2nd ed.*, Wiley-Interscience, 2001.

Chapter 12

1. R. C. Dorf, *The Encyclopedia of Robotics*, John Wiley & Sons, New York, 1988.
2. R. C. Dorf, *Electrical Engineering Handbook*, 2nd ed., CRC Press, Boca Raton, Fla., 1998.
3. R. S. Sanchez-Pena and M. Sznaier, *Robust Systems Theory and Applications*, John Wiley & Sons, New York, 1998.
4. G. Zames, "Input-Output Feedback Stability and Robustness," *IEEE Control Systems*, June 1996, pp. 61–66.
5. K. Zhou and J. C. Doyle, *Essentials of Robust Control*, Prentice Hall, Upper Saddle River, N. J., 1998.
6. C. M. Close and D. K. Frederick, *Modeling and Analysis of Dynamic Systems*, 2nd ed., Houghton Mifflin, Boston, 1993.
7. A. Charara, "Nonlinear Control of a Magnetic Levitation System," *IEEE Transactions on Control System Technology*, September 1996, pp. 513–523.
8. J. Yen, *Fuzzy Logic: Intelligence and Control*, Prentice Hall, Upper Saddle River, N. J., 1998.
9. X. G. Wang, "Estimation in Paper Machine Control," *IEEE Control Systems*, August 1993, pp. 34–43.
10. D. Sbarbaro-Hofer, "Control of a Steel Rolling Mill," *IEEE Control Systems*, June 1993, pp. 69–75.
11. N. Mohan, *Power Electronics*, John Wiley & Sons, New York, 1995.
12. J. M. Weiss, "The TGV Comes to Texas," *Europe*, March 1993, pp. 18–20.
13. S. Lee, "Intelligent Sensing and Control for Advanced Teleoperation," *IEEE Control Systems*, June 1993, pp. 19–28.
14. J. V. Wait and L. P. Huelsman, *Operational Amplifier Theory*, 2nd ed., McGraw-Hill, New York, 1992.
15. F. G. Martin, *The Art of Robotics*, Prentice Hall, Upper Saddle River, N. J., 1999.
16. R. Shoureshi, "Intelligent Control Systems," *Journal of Dynamic Systems*, June 1993, pp. 392–400.
17. A. Butar and R. Sales, "Control for MagLev Vehicles," *IEEE Control Systems*, August 1998, pp. 18–25.
18. H. Paraci and M. Jamshidi, *Design and Implementation of Intelligent Manufacturing Systems*, Prentice Hall, Upper Saddle River, N. J., 1997.
19. B. Johnstone, "Japan's Friendly Robots," *Technology Review*, June 1999, pp. 66–69.
20. W. J. Grantham and T. L. Vincent, *Modern Control Systems Analysis and Design*, John Wiley & Sons, New York, 1993.
21. K. Capek, *Rossum's Universal Robots*, English edition by P. Selver and N. Playfair, Doubleday, Page, New York, 1923.
22. H. Kazerooni, "Human Extenders," *Journal of Dynamic Systems*, ASME, June 1993, pp. 281–290.
23. C. Lapiska, "Flight Simulation," *Aerospace America*, August 1993, pp. 14–17.
24. D. E. Bossert, "A Root-Locus Analysis of Quantitative Feedback Theory," *Proceedings of the American Control Conference*, June 1993, pp. 1698–1705.
25. J. A. Gutierrez and M. Rabins, "A Computer Loop-shaping Algorithm for Controllers," *Proceedings of the American Control Conference*, June 1993, pp. 1711–1715.

15. R. C. Dorf and A. Kusiak, *Handbook of Manufacturing and Automation*, John Wiley & Sons, New York, 1994.
16. F. M. Ham, S. Greeley, and B. Henniges, "Active Vibration Suppression for the Mast Flight System," *IEEE Control System Magazine*, Vol. 9, No. 1, 1989, pp. 85–90.
17. K. Pfeiffer and R. Isermann, "Driver Simulation in Dynamical Engine Test Stands," *Proceedings of the American Control Conference*, IEEE, 1993, pp. 721–725.
18. A. G. Ulsoy, "Control of Machining Processes," ASME, *Journal of Dynamic Systems*, June 1993, pp. 301–310.
19. B. K. Bose, *Modern Power Electronics*, IEEE Press, New York, 1992.
20. F. G. Martin, *The Art of Robotics*, Prentice Hall, Upper Saddle River, N. J., 1999.
21. J. M. Weiss, "The TGV Comes to Texas," *Europe*, March 1993, pp. 18–20.
22. H. Kazerooni, "A Controller Design Framework for Telerobotic Systems," *IEEE Transactions on Control Systems Technology*, March 1993, pp. 50–62.
23. W. H. Zhu, "Industrial Manipulators," *IEEE Control Systems*, April 1999, pp. 24–28.
24. E. W. Kamen and B. S. Heck, *Fundamentals of Signals and Systems Using MATLAB*, Prentice Hall, Upper Saddle River, N. J., 1997.
25. C. T. Chen, *Analog and Digital Control Systems Design*, Oxford Univ. Press, New York, 1996.
26. M. J. Sidi, *Spacecraft Dynamics and Control*, Cambridge Univ. Press, New York, 1997.
27. A. Arenas, et al., "Angular Velocity Control for a Windmill Radiometer," *IEEE Transactions on Education*, May 1999, pp. 147–152.
28. M. Berenguel, et al., "Temperature Control of a Solar Furnace," *IEEE Control Systems*, February 1999, pp. 8–19.
29. A. H. Moore, "The Shipping News: Fast Ferries," *Fortune*, December 6, 1999, pp. 240–249.
30. M. P. Dinca, M. Gheorghe, and P. Galvin, "Design of a PID Controller for a PCR Micro Reactor," *IEEE Transactions on Education*, Vol. 52, No. 1, 2009, pp. 117–124.

Chapter 11

1. R. C. Dorf, *Electrical Engineering Handbook*, 2nd ed., CRC Press, Boca Raton, Fla., 1998.
2. G. Goodwin, S. Graebe, and M. Salgado, *Control System Design*, Prentice Hall, Saddle River, N.J., 2001.
3. A. E. Bryson, "Optimal Control," *IEEE Control Systems*, June 1996, pp. 26–33.
4. J. Farrell, "Using Learning Techniques to Accommodate Unanticipated Faults," *IEEE Control Systems*, June 1993, pp. 40–48.
5. M. Jamshidi, *Design of Intelligent Manufacturing Systems*, Prentice Hall, Upper Saddle River, N. J., 1998.
6. M. Bodson, "High Performance Control of a Permanent Magnet Stepper Motor," *IEEE Transactions on Control Systems Technology*, March 1993, pp. 5–14.
7. G. W. Van der Linden, "Control of an Inverted Pendulum," *IEEE Control Systems*, August 1993, pp. 44–50.
8. W. J. Book, "Controlled Motion in an Elastic World," *Journal of Dynamic Systems*, June 1993, pp. 252–260.
9. E. W. Kamen, *Introduction to Industrial Control*, Academic Press, San Diego, 1999.
10. M. Jamshidi, *Large-Scale Systems*, Prentice Hall, Upper Saddle River, N. J., 1997.
11. W. J. Rugh, *Linear System Theory*, 2nd ed., Prentice Hall, Englewood Cliffs, N. J., 1996.
12. J. B. Burl, *Linear Optimal Control*, Prentice Hall, Upper Saddle River, N. J., 1999.
13. D. Hrovat, "Applications of Optimal Control to Automotive Suspension Design," *Journal of Dynamic Systems*, ASME, June 1993, pp. 328–342.
14. R. H. Bishop, "Adaptive Control of Space Station with Control Moment Gyros," *IEEE Control Systems*, October 1992, pp. 23–27.
15. R. C. Dorf, *Encyclopedia of Robotics*, John Wiley & Sons, New York, 1988.
16. T. B. Sheridan, *Telerobotics, Automation and Control*, MIT Press, Cambridge, Mass., 1992.
17. R. C. Dorf and A. Kusiak, *Handbook of Manufacturing and Automation*, John Wiley & Sons, New York, 1994.
18. C. T. Chen, *Linear System Theory and Design*, 3rd ed., Oxford University Press, New York, 1999.
19. F. L. Chernousko, *State Estimation for Dynamic Systems*, CRC Press, Boca Raton, Fla., 1993.
20. M. A. Gottschalk, "Dino-Adventure Duels Jurassic Park," *Design News*, August 16, 1993, pp. 52–58.
21. Y. Z. Tsypkin, "Robust Internal Model Control," *Journal of Dynamic Systems*, ASME, June 1993, pp. 419–425.
22. J. D. Irwin, *The Industrial Electronics Handbook*, CRC Press, Boca Raton, Fla., 1997.
23. J. K. Pieper, "Control of a Coupled-Drive Apparatus," *IEE Proceedings*, March 1993, pp. 70–79.

26. J. W. Song, "Synthesis of Compensators in Linear Uncertain Plants," *Proceedings of the Conference on Decision and Control*, December 1992, pp. 2882–2883.
27. M. Gottschalk, "Part Surgeon–Part Robot," *Design News*, June 7, 1993, pp. 68–75.
28. S. Jayasuriya, "Frequency Domain Design for Robust Performance Under Uncertainties," *Journal of Dynamic Systems*, June 1993, pp. 439–450.
29. L. S. Shieh, "Control of Uncertain Systems," *IEE Proceedings*, March 1993, pp. 99–110.
30. M. van de Panne, "A Controller for the Dynamic Walk of a Biped," *Proceedings of the Conference on Decision and Control*, IEEE, December 1992, pp. 2668–2673.
31. S. Bennett, "The Development of the PID Controller," *IEEE Control Systems*, December 1993, pp. 58–64.
32. J. C. Doyle, A. B. Francis, and A. R. Tannenbaum, *Feedback Control Theory*, Macmillan, New York, 1992.

Chapter 13

1. R. C. Dorf, *The Encyclopedia of Robotics*, John Wiley & Sons, New York, 1988.
2. C. L. Phillips and H. T. Nagle, *Digital Control Systems*, Prentice Hall, Englewood Cliffs, N. J., 1995.
3. G. F. Franklin, et al., *Digital Control of Dynamic Systems*, 2nd ed., Prentice Hall, Upper Saddle River, N.J., 1998.
4. S. H. Zak, "Ripple-Free Deadbeat Control," *IEEE Control Systems*, August 1993, pp. 51–56.
5. C. Lapiska, "Flight Simulation," *Aerospace America*, August 1993, pp. 14–17.
6. F. G. Martin, *The Art of Robotics*, Prentice Hall, Upper Saddle River, N. J., 1999.
7. D. Raviv and E. W. Djaja, "Discretized Controllers," *IEEE Control Systems*, June 1999, pp. 52–58.
8. R. C. Dorf, *Elecirical Engineering Handbook*, 2nd ed., CRC Press, Boca Raton, Fla., 1998.
9. T. M. Foley, "Engineering the Space Station," *Aerospace America*, October 1996, pp. 26–32.
10. A. G. Ulsoy, "Control of Machining Processes," ASME, *Journal of Dynamic Systems*, June 1993, pp. 301–310.
11. K. J. Astrom, *Computer-Controlled Systems*, Prentice Hall, Upper Saddle River, N. J., 1997.
12. R. C. Dorf and A. Kusiak, *Handbook of Manufacturing and Automation*, John Wiley & Sons, New York, 1994.
13. L. W. Couch, *Digital and Analog Communication Systems*, 5th ed., Macmillan, New York, 1995.
14. K. S. Yeung and H. M. Lai, "A Reformation of the Nyquist Criterion for Discrete Systems," *IEEE Transactions on Education*, February 1988, pp. 32–34.
15. T. R. Kurfess, "Predictive Control of a Robotic Grinding System," *Journal of Engineering for Industry*, ASME, November 1992, pp. 412–420.
16. D. M. Auslander, *Mechatronics*, Prentice Hall, Englewood Cliffs, N. J., 1996.
17. R. Shoureshi, "Intelligent Control Systems," *Journal of Dynamic Systems*, June 1993, pp. 392–400.
18. D. J. Leo, "Control of a Flexible Frame in Slewing," *Proceedings of American Control Conference*, 1992, pp. 2535–2540.
19. V. Skormin, "On-Line Diagnostics of a Self-Contained Flight Actuator," *IEEE Transactions on Aerospace and Electronic Systems*, January 1994, pp. 130–141.
20. H. H. Ottesen, "Future Servo Technologies for Hard Disk Drives," *J. of the Magnetics Society of Japan*, Vol. 18, 1994, pp. 31–36.

Appendix A

1. A. Gilat, MATLAB: *An Introduction with Applications*, 3rd ed., Wiley and Sons, N. J., 2008.
2. D. Hanselman and B. Littlefield, *Mastering MATLAB 7*, The MATLAB Curriculum Series, Prentice Hall, Upper Saddle River, N. J., 2004.
3. R. Pratap, *Getting Started with MATLAB 7*, Oxford University Press, New York, 2005.
4. *The Student Edition of MATLAB 7 User's Guide*, The Mathworks, Inc., Prentice Hall, Upper Saddle River, N. J., 2007.
5. D. J. Higham and N. J. Higham, *MATLAB Guide*, SIAM, Society for Industrial and Applied Mathematics, 2005.
6. W. J. Palm III, *Introduction to MATLAB 7 for Engineers*, McGraw-Hill, Boston, 2003.
7. T. A. Davis and K. Sigmon, *MATLAB Primer 7e*, Chapman and Hall/CRC, Boca Raton, FL, 2004.
8. D. M. Etter, *Engineering Problem Solving with MATLAB*, 3rd ed., Prentice Hall, Upper Saddle River, N. J., 2006.

Index

Selected Tables and Formulas for Design

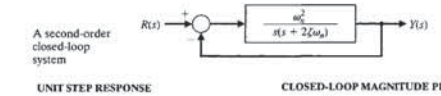

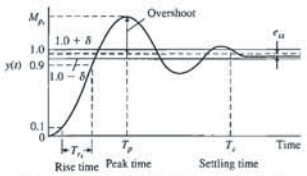

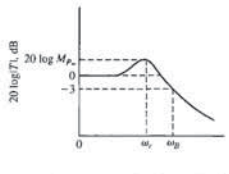

- ❑ Settling time (to within 2% of the final value)

$$T_s = \frac{4}{\zeta\omega_n}$$

- ❑ Maximum magnitude ($\zeta \leq 0.7$)

$$M_{p_w} = \frac{1}{2\zeta\sqrt{1-\zeta^2}}$$

- ❑ Percent overshoot

$$M_p = 1 + e^{-\zeta\pi/\sqrt{1-\zeta^2}} \quad \text{and} \quad P.O. = 100e^{-\pi\zeta/\sqrt{1-\zeta^2}}$$

- ❑ Time-to-peak

$$T_p = \frac{\pi}{\omega_n\sqrt{1-\zeta^2}}$$

- ❑ Resonant frequency ($\zeta \leq 0.7$)

$$\omega_r = \omega_n\sqrt{1-2\zeta^2}$$

- ❑ Rise time (time to rise from 10% to 90% of final value)

$$T_{r_1} = \frac{2.16\zeta + 0.60}{\omega_n} \quad (0.3 \leq \zeta \leq 0.8)$$

- ❑ Bandwidth ($0.3 \leq \zeta \leq 0.8$)

$$\omega_B = (-1.196\zeta + 1.85)\omega_n$$

PID Controller:

$$G_c(s) = K_P + K_D s + \frac{K_1}{s} = \frac{(s+z_1)(s+z_2)}{s}$$

Design Process

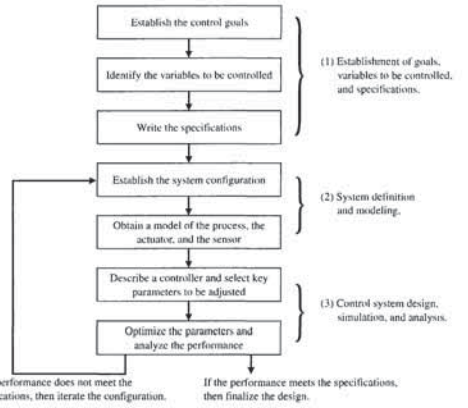

EXAMPLES